FINAL REPORT

Flow-population Models for Tracking Non-stationary Changes in Riparian and Aquatic Ecosystems

SERDP Project RC-2511

JANUARY 2020

David Lytle
Oregon State University

Distribution Statement A
This document has been cleared for public release

SERDP
DOD ▪ EPA ▪ DOE

Page Intentionally Left Blank

This report was prepared under contract to the Department of Defense Strategic Environmental Research and Development Program (SERDP). The publication of this report does not indicate endorsement by the Department of Defense, nor should the contents be construed as reflecting the official policy or position of the Department of Defense. Reference herein to any specific commercial product, process, or service by trade name, trademark, manufacturer, or otherwise, does not necessarily constitute or imply its endorsement, recommendation, or favoring by the Department of Defense.

Page Intentionally Left Blank

REPORT DOCUMENTATION PAGE

Form Approved
OMB No. 0704-0188

The public reporting burden for this collection of information is estimated to average 1 hour per response, including the time for reviewing instructions, searching existing data sources, gathering and maintaining the data needed, and completing and reviewing the collection of information. Send comments regarding this burden estimate or any other aspect of this collection of information, including suggestions for reducing the burden, to Department of Defense, Washington Headquarters Services, Directorate for Information Operations and Reports (0704-0188), 1215 Jefferson Davis Highway, Suite 1204, Arlington, VA 22202-4302. Respondents should be aware that notwithstanding any other provision of law, no person shall be subject to any penalty for failing to comply with a collection of information if it does not display a currently valid OMB control number.
PLEASE DO NOT RETURN YOUR FORM TO THE ABOVE ADDRESS.

1. REPORT DATE *(DD-MM-YYYY)*
01/29/2020

2. REPORT TYPE
SERDP Final Report

3. DATES COVERED *(From - To)*
5/12/2015 - 5/12/2020

4. TITLE AND SUBTITLE
Flow-population Models for Tracking Non-stationary Changes in Riparian and Aquatic Ecosystems

5a. CONTRACT NUMBER
15-C-0009

5b. GRANT NUMBER

5c. PROGRAM ELEMENT NUMBER

6. AUTHOR(S)
Dr. David A. Lytle, Oregon State University
Dr. Julian D. Olden, University of Washington
Dr. David M. Merritt, US Forest Service

5d. PROJECT NUMBER
RC-2511

5e. TASK NUMBER

5f. WORK UNIT NUMBER

7. PERFORMING ORGANIZATION NAME(S) AND ADDRESS(ES)
Oregon State University
3029 Cordley Hall, OSU Zoology
Corvallis, OR 97331

8. PERFORMING ORGANIZATION REPORT NUMBER
RC-2511

9. SPONSORING/MONITORING AGENCY NAME(S) AND ADDRESS(ES)
Strategic Environmental Research and Development Program
4800 Mark Center Drive, Suite 17D03
Alexandria, VA 22350-3605

10. SPONSOR/MONITOR'S ACRONYM(S)
SERDP

11. SPONSOR/MONITOR'S REPORT NUMBER(S)
RC-2511

12. DISTRIBUTION/AVAILABILITY STATEMENT
DISTRIBUTION STATEMENT A. Approved for public release: distribution unlimited.

13. SUPPLEMENTARY NOTES

14. ABSTRACT Climate change is expected to alter temperature and precipitation patterns on military lands throughout the western U.S., and this will alter the timing, frequency, and magnitude of flood and drought events. These changes in streamflow regime will directly affect populations of aquatic organisms (fish, aquatic invertebrates, riparian vegetation) and indirectly affect stream-dependent birds, reptiles, and mammals, including federally threatened and endangered species and other at-risk species. Although climate models as drivers of hydrologic models are becoming increasingly sophisticated in their ability to enable forecasting changes in streamflow regime at small spatial scales (e.g., <144 km2), current species population models do not accommodate the non-stationary effects that shifting flow regimes can exert on population trajectories and viability. Thus, a critical gap remains between our ability to model how climate change will alter streamflow regimes and our ability to predict how these changes will impact management-sensitive aquatic and riparian organisms. The objective of this proposal is to fill this knowledge gap by designing, testing, and implementing flow-population models that integrate nonstationary low regime dynamics with quantitative population models to forecast potential impacts on aquatic and riparian taxa.

15. SUBJECT TERMS
Biodiversity, climate change, aquatic ecosystems, population modeling, nonstationarity, flow regime, flow-population modeling, matrix population models, network theory, sensitivity analysis

16. SECURITY CLASSIFICATION OF:			17. LIMITATION OF ABSTRACT	18. NUMBER OF PAGES	19a. NAME OF RESPONSIBLE PERSON
a. REPORT	b. ABSTRACT	c. THIS PAGE			David Lytle
UNCLASS	UNCLASS	UNCLASS	UNCLASS	178	19b. TELEPHONE NUMBER *(Include area code)* 541-737-1068

Page Intentionally Left Blank

Table of Contents

List of tables iii

List of figures iv

List of acronyms vii

Keywords vii

Acknowledgements vii

Abstract viii

1 Task 1: Initial site visits with base managers 1

2 Task 2: Develop core flow-population models 2

2.1 Linking river flow regimes to riparian plant guilds: a community-wide modeling approach 2

2.1.1 Summary 2

2.1.2 Introduction 3

2.1.3 Methods 4

2.1.4 Results 11

2.1.5 Discussion 16

2.1.6 Acknowledgments 20

2.1.7 References 20

2.2 Modeling the effect of drought on fish communities in a changing climate 24

2.2.1 Introduction 24

2.2.2 Methods 26

2.2.3 Results 33

2.2.4 References 37

2.3 High mortality and enhanced recovery: modeling the countervailing effects of disturbance on insect population dynamics 41

2.3.1 Summary 41

2.3.2 Introduction 41

2.3.3 Methods 42

2.3.4 Results 48

2.3.5 Discussion 53

2.3.6 Acknowledgements 56

2.3.7 References 57

3 Task 3: Obtain data for model parameterization 61

3.1 Base-specific data from managers and from fieldwork 61

3.1.1 Camp Pendleton 61

3.1.2 Santa Margarita Ecological Reserve 64

3.1.3 Fort Hunter Liggett 68

3.1.4 Los Padres National Forest 73

3.1.5 Piñon Canyon Manouver Site - Comanche National Grassland 76

3.2 Vital rate estimation 79

3.2.1 Xeroriparian shrub and hydroriparian tree 79

3.2.2 Aquatic invertebrates 83

4 Task 4: Forecast ecological effects of changing flow regimes 86

4.1 Hydraulic and Variable Infiltration Capacity modeling....86
4.1.1 Hydrograph scenarios....86
4.1.2 Hydraulic modeling: Camp Pendleton....96
4.1.3 Hydraulic modeling: Fort Hunter Liggett....101
4.1.4 Hydraulic modeling: Comanche National Grasslands....107
4.1.5 Literature Cited....112
4.2 Simulated and retrospective hydrograph scenarios: flow regime alteration degrades ecological networks in riparian ecosystems....114
4.2.1 Summary....114
4.2.2 Introduction....114
4.2.3 Methods....118
4.2.4 Results and Discussion....121
4.2.5 Conclusions....127
4.2.6 Acknowledgements....128
4.2.7 References....129
4.3 Synthesis: Cross-taxon analysis of riparian vegetation, fish, and invertebrates....133
4.3.1 Summary....133
4.3.2 Introduction....133
4.3.3 Methods....134
4.3.4 Results and discussion....137
4.3.5 Acknowledgements....142
4.3.6 References....142

5 Task 5: Technology transfer....147
5.1 Web tools....147
5.2 Guild occurrence maps....147
5.3 Professional summary: Managing rivers for resilience....158
5.3.1 Introduction....158
5.3.2 Model process....158
5.3.3 Obstacles to implementation....160
5.3.4 Next steps....161
5.3.5 References....162

6 Task 6: Submit technical reports to SERDP....164
6.1 Interim report....164
6.2 Final report....164
6.3 Web tools....164

List of tables

Table 2.1.1 Stage-specific parameter values for hydroriparian tree (HT), xeroriparian shrub (XS), hydroriparian shrub (HS), mesoriparian meadow (MM), and desert shrub (DS). 9
Table 2.2.1 Life history traits of study species. 27
Table 2.2.2 Sources of vital rate information....27
Table 2.2.3 Modifier values based on flow-ecology relationships in literature. 28
Table 2.2.4 Flow-ecology relationship. Directionality of response to generalized flow attributes reported in the literature. 28
Table 2.2.5 Length-weight relationships. 30
Table 2.2.6 Literature-derived values of important life history information. 30
Table 2.2.7 Vital rates of seven study species. 31

Table 2.3.1 Model parameters and variables for flooding scenarios with default values for target taxa. 45
Table 2.3.2 Flooding scenario model predictions and observed averages and standard errors for relative population size of the three taxa. 52
Table 3.1.1 Site descriptions for seven sites visited in April, 2016 along the Santa Margarita River through Camp Pendleton Marine Corps Base and the Santa Margarita Ecological Reserve.62
Table 3.1.2 Vegetation species list for the Santa Margarita River through Camp Pendleton Marine Corps Base and the Santa Margarita Ecological Reserve. 63
Table 3.1.3 Site descriptions for seven sites visited in April, 2016 along the Santa Margarita River through Camp Pendleton Marine Corps Base and the Santa Margarita Ecological Reserve.64
Table 3.1.4 Vegetation species list for the Santa Margarita River through the Santa Margarita Ecological Reserve. 66
Table 3.1.5 Summary of fish species and number of individuals captured at each location. 68
Table 3.1.6 Site descriptions for ten sites visited in April, 2016 along the San Antonio River (top five sites) and the Nacimiento River (bottom five sites) through Los Padres National Forest and Fort Hunter Liggett. 68
Table 3.1.7 Vegetation species list for the Nacimiento and San Antonio Rivers through Fort Hunter Liggett. 71
Table 3.1.8 Summary of species and number of individuals captured at each location on the Nacimiento River. 72
Table 3.1.9 Summary of species and number of individuals captured at each location on the San Antonio River. 72
Table 3.1.10 Site descriptions for ten sites visited in April, 2016 along the San Antonio River (top five sites) and the Nacimiento River (bottom five sites) through Los Padres National Forest and Fort Hunter Liggett. 73
Table 3.1.11 Vegetation species list for the Nacimiento and San Antonio Rivers through Fort Hunter Liggett. 75
Table 3.1.12 Site descriptions for six sites visited in July, 2016 along the Purgatoire River through Comanche National Grassland. 76
Table 3.1.13 Vegetation species list for the Purgatoire River Study Sites. 78
Table 3.2.1 Parameter values used for life-table calculations and resulting estimated intrinsic rates of population increase. 83
Table 4.1.1 Species list for plots sampled in April 2017 at the Fallbrook bridge study site. 99
Table 4.1.2 Species with the most cover in vegetation plots in the Fallbrook Bridge site sampled in April 2017. 100
Table 4.1.3 Species list for plots sampled in June 2017 at the San Antonio Landfill study site. ..105
Table 4.1.4 Species with the most cover in vegetation plots in the San Antonio Landfill site sampled in June 2017. 106
Table 4.1.5 Species list for the Purgatoire River Study Sites. 111
Table 4.1.6 Species with the most cover in vegetation plots in the Gage site sampled in July 2016. 111
Table 4.2.1 Glossary of important terms used in the paper. 115
Table 5.2.1 Description of riparian plant – streamflow response guilds from cluster analyses on plant stream-flow response trait values. 150

List of figures

Figure 2.1.1 Life cycle diagrams for hydroriparian tree (top) and xeroriparian shrub (bottom). 8

Figure 2.1.2 Effect of increasing drought frequency on abundances of the five vegetation guilds (top panel) and bare substrates (bottom panel), starting at natural flow regime drought frequency (0.20). 12
Figure 2.1.3 Comparison of model and empirical data. 13
Figure 2.1.4 Effect of flood timing on hydroriparian tree and xeroriparian shrub dominance on the floodplain. 14
Figure 2.1.5 Multi-guild sensitivity analysis showing the community-wide effects of changing vital rates for flood mortality, drought mortality, and baseline transition probability. 15
Figure 2.1.6 Sensitivity networks depicting the community-wide effects of altering flood susceptibility (S_{ij}) under natural flow regime conditions (left) and a 75% increase in drought frequency (right). 16
Figure 2.2.1 Population level model projections for each species compared to observed data from long-term surveys on the Verde River. 35
Figure 2.2.2 Community level correspondence between long-term surveys and model projections. 36
Figure 2.2.3 Average relative abundance of native and non-native species by flow-type year over 1,000 iterations of model runs. 36
Figure 2.2.4 Effect of changing biomass carrying capacity on changes in relative abundance. 37
Figure 2.3.1 Flood-population response surfaces for three taxa with contrasting life histories after a single flood event. 49
Figure 2.3.2 Plot of population size 50 days after a flood for a species whose habitat is enhanced by floods at different combinations of r and h. r is interpreted as a measure of resilience, and h as an inverse measure of resistance. 50
Figure 2.3.3 Relationship between flood frequency and cumulative flood magnitude for mayflies, dragonflies, and ostracods at 20 and 100 d post-flood. 51
Figure 2.3.4 Relationship between fire return interval (ranging from 1 to 20 years) and relative population size (Nt) for a tropical savanna grass. 53
Figure 3.1.1 Field site locations for April, 2016 sampling along the Santa Margarita River through Camp Pendleton and the Santa Margarita Ecological Reserve. 63
Figure 3.1.2 Field site locations for April, 2016 sampling along the Santa Margarita River through Camp Pendleton and the Santa Margarita Ecological Reserve. 66
Figure 3.1.3 Field sampling sites visited in April, 2016 along the San Antonio and Nacimiento Rivers through Los Padres National Forest and Fort Hunter Liggett. 70
Figure 3.1.4 Field sampling sites visited in April 2016 along the San Antonio and Nacimiento Rivers through Los Padres National Forest and Fort Hunter Liggett. 74
Figure 3.1.5 Field sampling sites visited in July, 2016 along the Purgatoire River through Comanche National Grasslands. 77
Figure 4.1.1 Mean and median (light and dark blue lines) daily flow statistics calculated from the USGS observed historical stream gage record for the San Antonio River, near Lockwood, CA, water years 1965-2018. 88
Figure 4.1.2 Mean and median (light and dark blue lines) daily flow statistics calculated from the USGS observed historical stream gage record for the Santa Margarita River, near Fallbrook, CA, water years 1990-2018. 89
Figure 4.1.3 Time series of Palmer Drought Severity Index (PDSI, left axis) for central coastal California 1965-2018 superimposed on the stream flow record for the San Antonio River near Lockwood, California (Discharge, cms, right axis). 90
Figure 4.1.4 Time series of Palmer Drought Severity Index (left axis) for southern coast of California 1989-2018 superimposed on the stream flow record for the Santa Margarita River near Fallbrook, California (Discharge, cms, right axis). 91
Figure 4.1.5 Daily mean discharge (cms) over time for the San Antonio River, California 92

Figure 4.1.6 Daily mean discharge (cms) over time for Santa Margarita River, Fallbrook, California....93
Figure 4.1.7 Flow duration curves for the historical stream gage record (water years 1965-2018) for the San Antonio River 94
Figure 4.1.8 Flow duration curves for the historical stream gage record (water years 1990-2018) for the Santa Margarita River near Fallbrook, California 95
Figure 4.1.9 Field site locations from 2016 sampling along the Santa Margarita River through Camp Pendleton and the Santa Margarita Ecological Reserve....96
Figure 4.1.10 Surveyed floodplain topography overlain on satellite imagery of the Santa Margarita River near Fallbrook Bridge, California....98
Figure 4.1.11 Cluster analysis ordination plot, grouping species into riparian functional plant guilds depicted by symbols. 99
Figure 4.1.12 Photos of trait sampling and vegetation plot sampling of species on the Santa Margarita River, CA, April 2017....101
Figure 4.1.13 Field site locations from 2016 along the San Antonio and Nacimiento Rivers through Los Padres National Forest and Fort Hunter Liggett....103
Figure 4.1.14 Surveyed floodplain topography overlain on satellite imagery of the San Antonio River at the Landfill site....104
Figure 4.1.15 Cluster analysis ordination plot, grouping species into riparian functional plant guilds depicted by symbols. 107
Figure 4.1.16 Field sampling sites visited in July, 2016 along the Purgatoire River through Comanche National Grasslands....109
Figure 4.1.17 Surveyed floodplain topography overlain on satellite imagery of the Purgatoire River near the USGS Gage at Rock Crossing....110
Figure 4.2.1 Conceptual diagram outlining the workflow used in the analysis from data collection to projection....118
Figure 4.2.2 Examination of riparian plant networks across a spectrum of possible flow regime futures....122
Figure 4.2.3 Summary metrics of full ecological networks spanning the spectrum of flow extremes from extreme drought to flood....123
Figure 4.2.4 Degree (number of links connected to the node) of each network node in relation to flow-state....126
Figure 4.3.1 The modeled ecosystem components and flow regimes. 137
Figure 4.3.2 Results of simulations for target and non-target taxa, both within and among ecosystem components....138
Figure 4.3.3 The ecosystem-wide effects of designer and natural flow regimes. 139
Figure 5.2.1 The location of the San Antonio River in Central Coastal California....148
Figure 5.2.2 Mean trait values of seven functional traits for each of 16 riparian plant streamflow-response guilds for coastal California Rivers. 149
Figure 5.2.3 Inundation map from 2-dimensional hydraulic modeling of the San Antonio River, California....151
Figure 5.2.4 Probability of occurrence for five example guilds on the San Antonio River, California, across a gradient of flow exceedance probability (x-axis) from upland dry areas (left side) to wetter, frequently flooded areas by the river bank (right side). 152
Figure 5.2.5 Hydric trees - Guild distribution models projected on to the floodplain of the San Antonio River, Fort Hunter Ligget, California....153
Figure 5.2.6 Hydric mesic shrubs - Guild distribution models projected on to the floodplain of the San Antonio River, Fort Hunter Ligget, California 154
Figure 5.2.7 Hydric perennial herbs - Guild distribution models projected on to the floodplain of the San Antonio River, Fort Hunter Ligget, California....155

Figure 5.2.8 Hydric annual deep-root herbs - Guild distribution models projected on to the floodplain of the San Antonio River, Fort Hunter Ligget, California.....156
Figure 5.2.9 Mesic annual herbs - Guild distribution models projected on to the floodplain of the San Antonio River, Fort Hunter Ligget, California. 157

List of acronyms

BLM: Bureau of Land Management
DFC: Desert Fishes Council
DoD: Department of Defense
EPA: Environmental Protection Agency
EPT: Ephemeroptera, Plecoptera, Coleoptera
ESA: Ecological Society of America; also Endangered Species Act
GCM: Global Circulation Model
GIS: Geographic Information System
IPCC: Intergovernmental Panel on Climate Change
MSI: Madrean Sky Island
NAWS: Naval Air Weapons Station
NOAA: National Oceanic and Atmospheric Association
NWR: National Wildlife Refuge
OCH: Odonata, Coleoptera, Hemiptera
SFS: Society for Freshwater Science
SWAT: Soil Water Assessment Tool
USDA: United States Department of Agriculture
USGS: United States Geological Survey
USFS: United States Forest Service
VIC: variable infiltration capacity

Keywords
Biodiversity, climate change, aquatic ecosystems, population modeling, nonstationarity, flow regime, flow-population modeling, matrix population models, network theory, sensitivity analysis

Acknowledgements
We thank the base managers and natural resources staff at Camp Pendleton, Fort Hunter Liggett, Fort Huachuca, and Piñon Canyon Maneuver Site for assistance with field work and data collection.

Abstract

Objectives.

Climate change is expected to alter temperature and precipitation patterns on military lands throughout the western U.S., and this will alter the timing, frequency, and magnitude of flood and drought events. These changes in streamflow regime will directly affect populations of aquatic organisms (fish, aquatic invertebrates, riparian vegetation) and indirectly affect stream-dependent birds, reptiles, and mammals, including federally threatened and endangered species and other at-risk species. Although climate models as drivers of hydrologic models are becoming increasingly sophisticated in their ability to enable forecasting changes in streamflow regime at small spatial scales (e.g., <144 km^2), current species population models do not accommodate the non-stationary effects that shifting flow regimes can exert on population trajectories and viability. Thus, a critical gap remains between our ability to model how climate change will alter streamflow regimes and our ability to predict how these changes will impact management-sensitive aquatic and riparian organisms. The objective of this proposal is to fill this knowledge gap by designing, testing, and implementing flow-population models that integrate non-stationary flow regime dynamics with quantitative population models to forecast potential impacts on aquatic and riparian taxa.

Technical Approach.

This project will combine the: (1) development of novel flow-population models for riparian vegetation, fish, and aquatic invertebrates; (2) parameterization of model vital rates using longterm datasets from military and other lands; (3) and implementation of models to forecast how changing climate regimes will affect aquatic populations across a suite of western U.S. military installations. Objective 1 will build flow-population models that are suitable for capturing the non-stationary, stochastic dynamics that flow regimes exert on populations. Importantly, a "flow-response guild" approach will be followed, in which groups of species that share similar responses to flow regime attributes will be modeled. Objective 2 involves the parameterization of models using data from aridland military installations and other long-term sites. This data-intensive objective will enable testing of model predictions and calibration of models so they directly apply to groups of species occurring on aridland Department of Defense installations. Objective 3 uses the modeling approach to forecast the ecological effects of changing streamflow regimes. This objective will explore future climate change scenarios and their effects on aquatic and riparian organisms.

Benefits.

The proposed research will provide a critical link between landscape-level climate predictions and population responses of organisms. This link will enable researchers and managers to anticipate how climate-driven changes to precipitation will change current distributions of aquatic and riparian organisms. The project also will produce ready-to-

use web-based tools for managers that will enable them to explore the consequences of proposed management actions on relevant flow-response guilds, without requiring direct mastery of the underlying mathematical models.

1 Task 1: Initial site visits with base managers

Subtasks:

1. Site visit – Camp Pendleton, CA (DoD)
2. Site visit – Santa Margarita Ecological Reserve, CA (State)
3. Site visit – Cleveland National Forest, CA (USFS)
4. Site visit – Fort Hunter Liggett, CA (DoD)
5. Site visit – Los Padres National Forest, CA (USFS)
6. Site visit – Piñon Canyon Maneuver Site, CO (DoD)
7. Site visit – Comanche National Grasslands, CO (USFS)

The PIs completed site visits with base managers and adjacent National Forest lands with the goals of identifying viable study sites and building working relationships with base and USFS personnel. Details on the sites, along with preliminary data, can be found in the individual site reports under Task 3.

2 Task 2: Develop core flow-population models

Subtasks:

1. Riparian vegetation
2. Fish
3. Aquatic invertebrates

Task 2 develops the core flow-population models that are used in further analysis. The riparian vegetation model has been published in *Ecological Applications* (Lytle et al. 2017), the aquatic invertebrate model has been published in *Ecology Letters* (McMullen et al. 2017), and the fish model has been published in *Ecosphere* (Rogosch et al. 2019).

2.1 Linking river flow regimes to riparian plant guilds: a community-wide modeling approach

2.1.1 Summary

Modeling riparian plant dynamics along rivers is complicated by the fact that plants have different edaphic and hydrologic requirements at different life-stages. With intensifying human demands for water and continued human alteration of rivers, there is a growing need for predicting responses of vegetation to flow alteration, including responses related to climate change and river flow management. We developed a coupled structured population model that combines stage-specific responses of plant guilds with specific attributes of river hydrologic regime. The model uses information on the vital rates of guilds as they relate to different hydrologic conditions (flood, drought, and baseflow), but deliberately omits biotic interactions from the structure ("interaction neutral"). Our intent was to: 1) consolidate key vital rates concerning plant population dynamics and to incorporate these data into a quantitative framework, 2) determine whether complex plant stand dynamics, including biotic interactions, can be predicted from basic vital rates and river hydrology, and 3) project how altered flow regimes might affect riparian communities. We illustrated the approach using five flow-response guilds that encompass much of the river floodplain community: hydroriparian tree, xeroriparian shrub, hydroriparian shrub, mesoriparian meadow, and desert shrub. We also developed novel network-based tools for predicting community-wide effects of climate-driven shifts and deliberately altered flow regimes.

The model recovered known patterns of hydroriparian tree vs. xeroriparian shrub dominance, including the relative proportion of these two guilds as a function of river flow modification. By simulating flow alteration scenarios ranging from increased drought to shifts in flood timing, the model predicted that mature hydroriparian forest should be most abundant near the observed natural flow regime. Multiguild sensitivity analysis identified substantial network connectivity (many connected nodes) and biotic linkage (strong pairwise connections between nodes) under

natural flow regime conditions. Both connectivity and linkage were substantially reduced under drought and other flow-alteration scenarios, suggesting that community structure is destabilized under such conditions. This structured population modeling approach provides a useful tool for understanding the community-wide effects of altered flow regimes due to climate change and management actions that influence river flow regime.

2.1.2 Introduction

In light of the widespread damming and regulation of most major rivers worldwide, there is a need to manage downstream flow regimes to support ecosystem integrity and functioning while concurrently meeting human water needs (Naiman et al. 2002, Nilsson et al. 2005, Poff et al. 2010, Olden et al. 2014). Flow regulation, and associated effects on water quality and sediment regimes, has induced particularly significant impacts on riverine riparian ecosystems. These include alteration of channel processes and form (Grams and Schmidt 2002, Gaeuman et al. 2005), shifts in riparian plant community composition (Merritt et al. 2010, Stromberg et al. 2012), declines of native-dominated riparian forests (Stromberg et al. 2007, Merritt and Poff 2010), and increased abundance of non-native and ruderal plant species along rivers (Ringold et al. 2008). In conjunction with increased extraction from rivers, climate change will likely have confounding or amplifying effects on riparian ecosystems (Ström et al. 2011, Palmer et al. 2009). In the western United States, most climate change projections suggest less winter precipitation, less snowpack, earlier snowmelt runoff, and lower total discharge under the most likely greenhouse gas emission scenarios (Seager et al. 2013). Furthermore, the frequency and severity of drought is expected to increase in already arid parts of the North America (Dai 2011), resulting in demonstrable impacts on riverine biota (Jaeger et al. 2014).

In the western U.S., the introduced Eurasian shrub tamarisk and its hybrids (primarily *Tamarix ramosissima* and *T. chinensis*) have become widespread in dryland stream riparian zones (Friedman et al. 2005). During the same time period during which tamarisk shrublands became prevalent along western North American rivers, native cottonwood (*Populus deltoides*) dominated forests declined precipitously (Rood and Mahoney 1990). Because cottonwood-dominated riparian forests are among the most species rich riparian ecosystems in western North America, their decline is a major conservation concern (Poff et al. 2007). At present, cottonwood forests form the most extensive deciduous forests in arid parts of western North America, and empirical data and population modeling indicate that cottonwood population structure is governed by characteristics of the streamflow regime (Lytle and Merritt 2004). Even moderate alterations to streamflow regime can produce dramatic shifts in dominant riparian species and alter the physiognomy and functioning of riparian communities (Dixon & Turner 2006, Stromberg et al. 2007, Merritt and Poff 2010).

Riparian flow response guilds are non-taxonomic groups of species that have similar morphological and physiological trait syndromes and as a consequence, the species in these guilds respond to water availability and fluvial disturbance in similar ways (Merritt et al. 2010). Grouping species based upon convergent adaptations facilitates modeling and transferability of

models from one system to the next (McGill et al. 2006), even across regions, enabling predictions of guild distributions under a range of possible climate scenarios and flow regimes (Rivaes et al. 2014). Using data obtained from field studies, historical aerial photos of vegetation plots, and other sources, we specify the vital rates of each guild (survivorship, growth, fecundity) as they relate to the abiotic environment (primarily floods and droughts). The guild approach allows us to leverage these site- and species-specific datasets to make inferences that are relevant to other ecological systems.

The interaction-neutral modeling approach we utilize here deliberately omits direct biotic interactions between guilds. Between-guild interactions such as competition are instead obtained *post hoc* via sensitivity and elasticity analysis, as explained below. An interaction-neutral approach allows us to reveal biotic interactions (e.g., pairwise competition, keystone status) from the model structure, via the manifestation of different guild's collective life histories within a dynamic, disturbance-prone floodplain environment. Thus, our modeling approach is neutral with respect to biotic interactions, because these are deliberately omitted, but strongly niche-based with respect to autecology, because these are specified in the vital rates. This interaction-neutral approach lies firmly in the middle of a continuum bounded at one end by neutral biodiversity models, which specify nothing of individual species' biology (Hubbell 2001), and at the other end by food web models that specify *a priori* pairwise species interactions (Williams and Martinez 2000). An advantage of the interaction-neutral approach is that it requires little or no prior knowledge of pairwise competition or interaction coefficients. A disadvantage is that it requires a detailed empirical understanding of each species or guild's relationship to its abiotic environment as specified by vital rates.

In this paper we first develop a general model that can be extended to any number of riparian plant species or guilds occurring on a river floodplain. We then parameterize the model for five guilds that represent a wide range of functional vegetation types present throughout western North American dryland rivers and aridland streams worldwide (Aguiar et al. 2013, Stromberg & Merritt 2015): hydroriparian tree, xeroriparian shrub, hydroriparian shrub, mesoriparian meadow, and desert shrub. We use this framework to explore flow scenarios relevant to conservation and management of riparian ecosystems. We then develop new network-based tools derived from sensitivity and elasticity analysis that can be used to identify keystone species (high number of network connections) and important interactions (strong pairwise connectivity) under a variety of environmental contexts.

2.1.3 Methods

2.1.3.1 General model structure

Our model expands on a previous single-species version (Lytle and Merritt 2004) by allowing multiple guilds of species that share similar vital rates to simultaneously occupy a dynamic floodplain zone. Each guild j is described by a stage-based matrix $\mathbf{N}_j(t+1) = \mathbf{A}_j(t)\mathbf{N}_j(t)$, where $\mathbf{N}_j(t)$ is a vector containing stage abundances and $\mathbf{A}_j(t)$ is a set of transition matrices that

fluctuate according to variation in the hydrograph (Caswell 2001). Thus, the population dynamics of each guild are determined primarily by how their vital rates (mortality, fecundity, self-thinning) are affected by annual cycles of flooding and drought.

This modeling approach can work equally well with species or guilds, but for generality to dryland riparian ecosystems worldwide, we modeled five guilds representing key life history types. The hydroriparian tree guild (typified by *Populus fremontii* in the southwestern U.S.A.) is characterized by long-lived, flood-adapted species that depend on freshly-scoured bare substrates for recruitment. The xeroriparian shrub guild (e.g., *Tamarix ramosissima, T. chinensis,* and hybrids) is characterized by species that have a life history structure similar to hydroriparian tree but with deeper roots and shorter stems, and thus lower drought mortality rates, shorter age to maturity, and a larger time window of fecundity. Hydroriparian shrub (e.g., *Salix exigua*) is a guild that represents active-floodplain specialist shrubs and small trees that have high resilience to flooding and recruit aggressively following floods, but are prone to mortality during drought years. Mesoriparian meadow is a guild of perennial grasses and forbs, such as slender wheatgrass (*Elymus trachycaulus*), Canada wild rye (*Elymus canadensis*) and horseweed (*Conyza canadensis*), that recruit during flood years and whose adults are moderately tolerant of flooding and drought. Desert shrub is a guild of primarily upland, drought tolerant shrubs, such as big sage (*Artemisia tridentata*), which continue to recruit and grow during drought years but suffer high mortality from floods (Dalgleish et al. 2011).

The model quantifies floodplain dynamics at the reach scale. The total potential floodplain habitat, K, represents the size of the river reach. Within K, floods, droughts, and senescence may remove individuals according to their vital rates, thereby creating space for new recruitment. The model assumes that the total floodplain habitat K remains constant across years, although river meandering changes the type and proportion of specific habitats across years. As with Lytle and Merritt (2004) the approach is not spatially explicit, in that we do not keep track of the location of individual plants. Rather, spatial structure is implicit in the manner that vital rates interact with population structure. For example, the empirically-measured mortality rate of hydroriparian tree seedlings due to flooding tends to be high, which is due to the fact that young hydroriparian trees usually occur near the active channel on point bars that experience dynamic scouring and burial (Cooper et al. 1999, Manners et al. 2015). Older hydroriparian trees experience lower mortality, partly due to their position on higher terraces away from the active channel, as active channels abandon surfaces as a result of channel migration. Importantly, we obtain vital rates empirically from field studies of existing stands observed over time (see below and online Appendix S1). Community dynamics arise directly from the interaction of each guild's vital rates with particular sequences of flooding and drought. The spatially-implicit structure of our modeling approach facilitates the exploration of population dynamics generally, without depending on a particular landscape or spatial arrangement of stream channels, fluvial surfaces, or vegetation. The space occupied by any particular guild-stage (K_{ij}) and its population size (N_{ij}) are proportional to each other via self-thinning rates (b_{ij}) derived from stage-specific stem densities. This allows both the number of individuals and the floodplain area (m^2) occupied by

each class to be estimated over time. See Lytle & Merritt (2004) for a detailed explanation of how spatial position in the floodplain is implicitly incorporated into this modeling approach.

2.1.3.2 Recruitment

Recruitment for hydroriparian tree and xeroriparian shrub conforms to the "recruitment box model" for riparian plants (Mahoney and Rood 1998). For these two guilds, recruitment takes place only in years that meet the following conditions: a scouring flood occurs, at least part of the receding limb of the hydrograph occurs during the period of seed release, and at least one seed-producing tree is present in the river reach. In years that meet these requirements, the degree of recruitment success is determined by availability of bare substrates (created by mortality of existing vegetation during the flood), rate of hydrograph decline, and the degree to which flooding is synchronized with seed set. Because this is a multi-guild model, recruitment is potentially affected by all guilds occupying the riparian zone, so this interdependence is incorporated into the recruitment function $F_j(t)$. For a guild j, the upper limit on recruitment is determined by the total area of bare substrates that become available following the flood. This upper limit is modified by the rate of hydrograph stage decline for each guild, $g_j(h)$, and the proportion of post-flood days that occur during seed set, $p_j(h)$, so that:

$$F_j(t+1) = \left(K - \sum_{j=1}^{n} \sum_{i=2}^{m} K_{ij}(t+1)\right) * \; p_j(h) g_j(h) \qquad \text{Eq. 1}$$

where $K_{ij}(t+1)$ is the space that will be occupied by the ith stage of the jth guild following a flood. There is a total of n guilds each with m stages, and K is the total space available to all riparian guilds within the reach. Eq. 1 introduces generalized density dependence into the model because the recruitment success of any given guild is affected by the aggregate density of all individuals on the landscape.

We assume that reproduction is independent of the number of reproductive adults present (i.e., one reproducing individual can potentially seed the entire reach). This is achieved by assigning reproduction directly during matrix projection, conditional on at least one reproductive adult being present prior to the flood at time t. The hydrograph stage decline function, $g_j(h)$, varies between 1 (complete establishment) and 0 (complete failure) and depends on the rate of post-flood hydrograph stage decline h (cm/d). $g_j(h)$ is also 0 in years with no flood. The timing function $p_j(h)$ gives the proportion of all possible recruitment days (that is, days on which the hydrograph is declining post-flood) that occur in tandem with seed set. Stage decline rate for the receding limb of the hydrograph for each year of gage record was calculated by linking discharge to stage (rating curve) from two staff gages from our study site on the Yampa River. These functions allow us to examine more precisely how within-year timing of floods affects population dynamics of guilds (Stella et al. 2010). Hydroriparian shrub and mesoriparian meadow reproduction only occur in flood years and depends on the total amount of unoccupied space (Eq. 1). For these guilds we did not assume a particular dependence on the rate or timing of flood stage decline (p=1, g=1 in flood years and 0 otherwise), but this could be added in cases

where these within-season dynamics are understood. Conversely, desert shrub recruitment occurs only in drought years in unoccupied space or space made available by mortality of other stages and guilds.

Guilds do not compete directly in the model, in the sense that they do not directly alter one another's survival probability or fecundity. Competition occurs indirectly because each guild occupies some portion of K, the total amount of riparian habitat available to all guilds within a given reach, and K is bounded by the size of the riparian zone. Guilds may affect each other's population dynamics by occupying space that might otherwise be available for new recruitment. For example, the mature stages of one guild may experience low mortality from flooding; because of this population-dynamic inertia, space that might otherwise be scoured by floods and colonized by seedlings of other guilds is unavailable. This is a form of competition, since the recruitment of any given guild is affected by the abundances of all guilds on the landscape. It is important to note that Eq. 1 makes no assumptions about the strength or direction of pairwise biotic interactions, and only posits that bare space for recruitment is a finite quantity. This way of modeling seedling recruitment is analogous to the lottery model for reef fish recruitment (Sale 1977).

Overseeding is also permitted in our modeling approach (Eq. 1), where seedlings of multiple guilds can occupy the same space, at least initially. This assumption allows us to avoid specifying direct competition at the seedling stage, since initial seed germination in the model is strictly a function of the hydrograph and a guild's vital rates and is not affected by the presence or absence of seeds from other guilds.

2.1.3.3 Incorporating flow regime dynamics

The life cycle of each guild was divided into discrete stages (N_{ij}), with transition probabilities corresponding to the probability of surviving within a stage (P_{ij}) or surviving to the next stage (G_{ij}) in successive years (Figure 2.1.1). Transition probabilities varied depending on whether a given year had a flood, a drought, or neither, so that $G_{ij} = (1 - S_{ij}) * (1 - D_{ij}) * b_{ij} * a_{ij}$, where S_{ij} is flood mortality given that a flood year occurs, D_{ij} is drought mortality given that a drought year occurs, b_{ij} is a self-thinning rate, and a_{ij} is the baseline probability of transitioning to the next stage apart from flood and drought mortality. Similarly, the probability of remaining in a stage class was $P_{ij} = (1 - S_{ij}) * (1 - D_{ij}) * (1 - a_{ij})$.

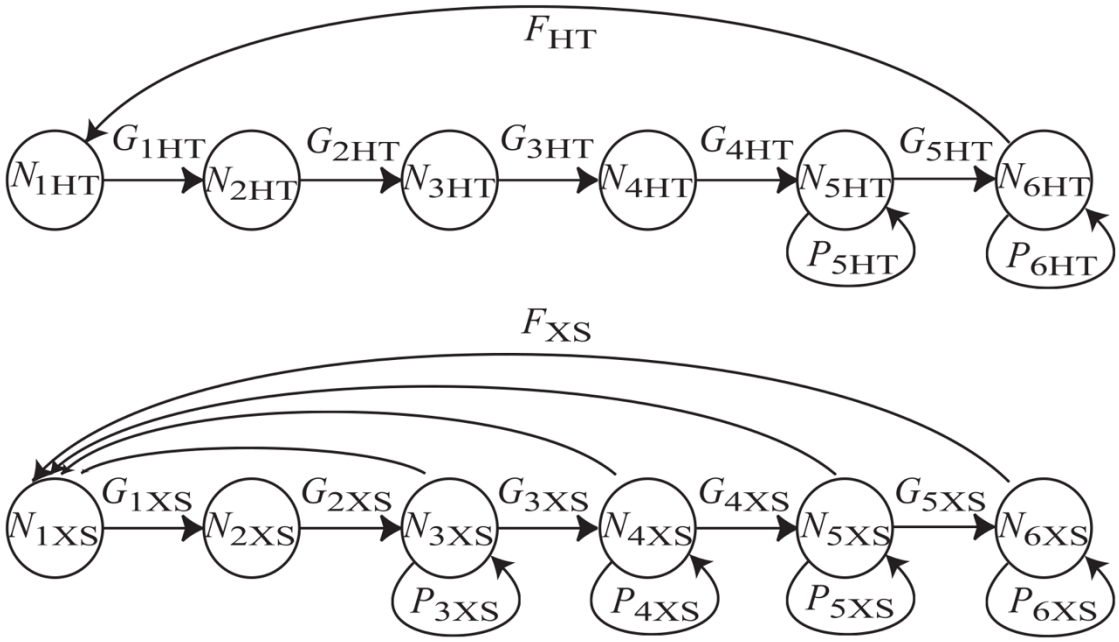

Figure 2.1.1 Life cycle diagrams for hydroriparian tree (top) and xeroriparian shrub (bottom).For hydroriparian tree, stage 1 represents seedlings, stages 2 through 4 are two to four year-olds, respectively, stage 5 represents subadult trees (5 to 10 year-olds), and stage 6 represents reproductive adults. *N* is abundance, *G* is the probability of transition to the next stage, *P* is the probability of remaining in that stage, and *F* is fecundity. For xeroriparian shrub, stage 1 represents seedlings, stage 2 contains second-year plants, stage 3 represents 3-6 year-olds, stage 4 are 7-15 year-olds, stage 5 are 16-30 year-olds, and stage 6 contains all older trees. Xeroriparian shrub reproduction occurs in stages 3 through 6. General life cycle diagrams are similar for hydroriparian shrub, mesoriparian meadow, and desert shrub guilds.

2.1.3.4 Vital rate estimation

Vital rates form the core of this modeling effort, so information was obtained from a variety of sources georeferenced to the Colorado River Basin, USA (Table 2.1.1). Hydroriparian tree and xeroriparian shrub have been well-studied, so we estimated stage-specific values for flood mortality, drought mortality, baseline transition probability, self-thinning, and other rates from existing studies (online Appendix S1). Vital rates for the hydroriparian shrub, mesoriparian meadow, and desert shrub guilds are less established from field studies, so we estimated relative values based on known life-history tradeoffs in each group. Hydroriparian shrub is adapted to the high shear associated with flows that occur near the active river channel, but its relatively shallow rooting structure gives it a disadvantage during droughts (Francis et al. 2005, Douhovnikoff et al. 2005). Therefore, we assumed flood mortality and drought survivorship rates half those of hydroriparian tree. We also assumed that the baseline transition probability in the final stage (a_{iHS}, which can be interpreted as the senescence rate apart from flooding or drought mortality) is greater than that of hydroriparian tree to reflect a shorter lifespan, and allowed reproduction in 3 year-olds and older. Mesoriparian meadow exhibits the opposite life-history syndrome as hydroriparian shrub. During early life stages this guild is more prone to mortality from flooding than hydroriparian tree, but exhibits some degree of drought tolerance once established. Therefore, we halved the flood survivorship of mesoriparian meadow relative to

hydroriparian tree during stages 1-3 and again halved the drought mortality of hydroriparian tree during stages 4-6. Desert shrub is an upland guild that has high drought tolerance but low resistance to flooding (Schlaepfer et al. 2012), so we assigned it half the flood survivorship and drought mortality of hydroriparian tree for all stages.

Table 2.1.1 Stage-specific parameter values for hydroriparian tree (HT), xeroriparian shrub (XS), hydroriparian shrub (HS), mesoriparian meadow (MM), and desert shrub (DS). Parameter symbols are as follows: q is stem density (individuals·m^{-2}), b is self-thinning rate, S is flood mortality in a flood year, D is drought mortality in a drought year, a is baseline transition probability. Column headers refer to guild stages.

	1	2	3	4	5	6
q_{iHT}	350	10	1.0	0.91	0.6	0.12
b_{iHT}	0.029	0.10	0.91	0.66	0.20	-
S_{iHT}	0.97	0.33	0.22	0.19	0.073	0.02
D_{iHT}	0.49	0.16	0.083	0.05	0.01	0.01
a_{iHT}	1	1	1	1	0.17	0.03
q_{iXS}	400	29	4.5	1.4	1.3	1.3
b_{iXS}	0.07	0.16	0.31	0.93	1.00	-
S_{iXS}	0.9	0.55	0.25	0.05	0.01	0.01
D_{iXS}	0.5	0.15	0.05	0.025	0.025	0.025
a_{iXS}	1	1	0.25	0.11	0.07	0.05
q_{iHS}	350	35	1	1	1	1
b_{iHS}	0.10	0.030	1	1	1	-
S_{iHS}	0.49	0.17	0.11	0.10	0.04	0.01
D_{iHS}	0.75	0.58	0.54	0.53	0.51	0.51
a_{iHS}	1	1	1	1	0.17	0.01
q_{iMM}	350	35	1	1	1	1
b_{iMM}	0.10	0.030	1	1	1	-
S_{iMM}	0.99	0.67	0.61	0.19	0.073	0.02
D_{iMM}	0.49	0.16	0.083	0.025	0.005	0.005
a_{iMM}	1	1	1	1	0.17	0.03
q_{iDS}	350	35	1	1	1	1
b_{iDS}	0.10	0.030	1	1	1	-
S_{iDS}	0.99	0.67	0.61	0.60	0.54	0.51
D_{iDS}	0.24	0.08	0.042	0.025	0.005	0.005
a_{iDS}	1	1	1	1	0.17	0.03

2.1.3.5 Model projection

We used 83 years of hydrograph data from the free-flowing Yampa River near Maybell, Colorado, U.S.A. (1916-1999; U.S. Geological Survey gage number 09251000). Based on river geomorphology, years when peak discharge exceeded 280 m^{3}s^{-1} during the timing of seedset were considered flood years, and years in which flows failed to exceed 210 m^{3}s^{-1} were drought years (based on known thresholds for drought mortality; Cooper et al. 1999). Years falling in between these thresholds were considered non-event years, for a total of 55% flood years, 20% drought years, and 25% non-event years under natural flow regime conditions. These threshold values are specific to the Yampa River, and appropriate thresholds would need to be determined to apply the model to other rivers systems. Matrix projection was accomplished in annual time

steps. To project the model forward in time, a year was drawn at random from the time series and the corresponding flow metrics were calculated for that year (flood decline rate, timing, and whether it was a flood, drought or non-event year). In flood or drought years, all guilds would be subject to flood or drought mortality, respectively, in addition to baseline transition probabilities.

2.1.3.6 Management and climate scenarios

To simulate the effect of altered flow regimes on population dynamics, the model was projected forward under a variety of relevant hydrograph scenarios by altering the frequency of year-types in the Maybell gauge dataset. Vital rates were held constant across all scenarios (i.e., our goal was to simulate ecological rather than evolutionary dynamics), but hydrograph parameters were allowed to vary across an array of flow regime scenarios. To simulate increased flood (or drought) frequency, we successively changed two of the 83 gauge years so that eventually all of them became flood (or drought) years (42 iterations in total). At each iteration, the model was projected forward a large number of years (10,000 years in most scenarios), the first 500 years were discarded as burn-in, and population sizes were averaged over the time series. To simulate flow homogenization due to damming, we successively changed year types, starting at natural flow regime frequency, until all of them became non-event years. To simulate the effects of climate change, we iteratively changed the timing of all flood peaks to occur earlier or later in the year.

2.1.3.7 Model performance

We evaluated model performance by analyzing the sensitivity and elasticity of individual vital rates to perturbations, and by comparing our modeled results to empirical field data. Sensitivities and elasticities were estimated using the iterated sensitivity and elasticity analysis described in Lytle & Merritt (2004). For this computationally-intensive exercise, we changed a given vital rate by increments of 0.01 in the vicinity of its actual value, projected the model forward, and recorded population sizes at each increment as described above. At each increment, this was repeated independently up to 1000 times to achieve stable convergence on mean values. Sensitivity was calculated as the slope of the average population size (N_{ij}) regressed against the vital rate, which is analogous to taking the partial derivative of population size with respect to the vital rate of interest (Lytle & Merritt 2004). Elasticity was also calculated as the slope of this regression on a logarithmic scale. Only sensitivities and elasticities with $R^2>0.3$ were retained for further analysis and interpretation. Because this is a multi-guild model, we also calculated cross-guild sensitivities and elasticities, which quantify how changing any single vital rate in a particular guild affects the population dynamics of all other guilds in the system. Furthermore, as sensitivities and elasticities can change in the context of different hydrologic regimes, we repeated this entire exercise using the natural flow regime hydrograph (20% drought years) as well as an increased-drought hydrograph (75% drought years). We used these cross-guild sensitivities to create sensitivity networks, which can be used to quantify the effect of one guild on the entire community within the context of any given flow regime. We compared our modeled results to empirical data reported by Merritt & Poff (2010), which examined the relative dominance of established cottonwood vs. tamarisk stems across 13 western U.S. rivers that

differed in degree of flow modification. To keep results parallel with the original study, which focused on established cottonwood and tamarisk stems in the active floodplain, we made the comparison with established hydroriparian tree and xeroriparian shrub stems (5-10 and 7-15 year-olds, respectively).

2.1.4 Results

Our model recovered some well-documented riparian dynamics and also produced some less-intuitive and more informative findings. Despite the fact that competitive interactions were not defined in our model parameterization, the trade-offs between life history attributes and relationships to flow implicitly captured a spectrum of community dynamics. Model projections were ergodic under all flow regime scenarios tested, with populations fluctuating about a quasi-equilibrium after only 30-50 years regardless of initial population sizes. All populations followed strong boom-bust dynamics driven by sequences of flood or drought year types. This was especially evident in seedling stages, which often experienced large pulses in recruitment followed by high mortality in subsequent years.

Simulations of increasing drought frequency demonstrated strong effects on the relative dominance of the five flow-response guilds (Figure 2.1.2). Hydroriparian shrub and hydroriparian tree were the two most dominant guilds on the landscape under natural flow regime conditions (drought frequency = 0.2), but hydroriparian shrub abundance declined in direct proportion to increasing drought. Hydroriparian tree, xeroriparian shrub, and mesoriparian meadow were each negatively correlated with hydroriparian shrub abundance, with slight increases in area occupied as the drought frequency approached approximately 0.5. At higher drought frequencies (>0.8) hydroriparian shrub and mesoriparian meadow were absent from the floodplain, which became increasing dominated by desert shrub and a higher percentage of bare, unvegetated ground. Rates of change also differed by guild. While hydroriparian shrub showed a near-linear decrease in abundance with increasing drought, desert shrub increased exponentially. Both hydroriparian tree and xeroriparian shrub exhibited a threshold response, with abundances constant or slightly increasing until high drought frequencies were reached, in which case abundances of both guilds decreased sharply.

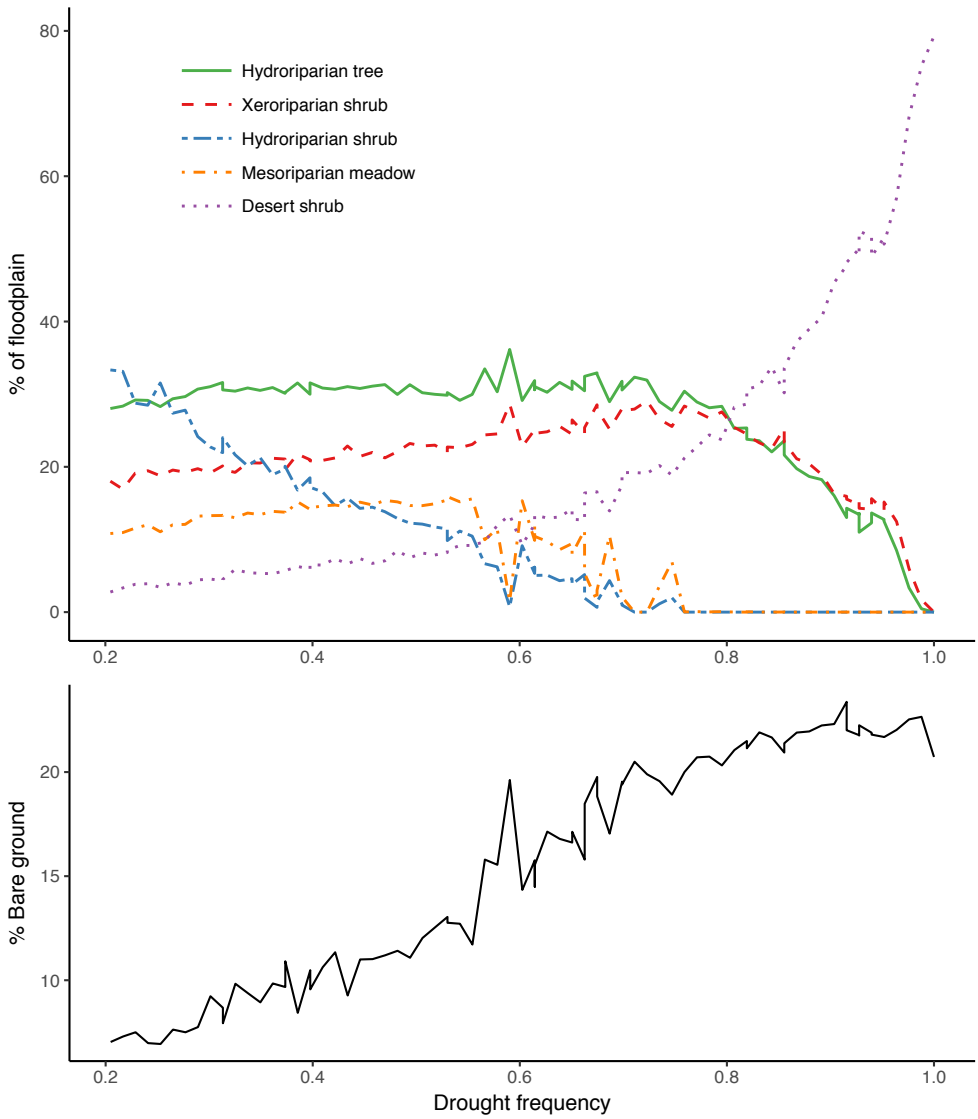

Figure 2.1.2 Effect of increasing drought frequency on abundances of the five vegetation guilds (top panel) and bare substrates (bottom panel), starting at natural flow regime drought frequency (0.20).

The model accurately represented some well-documented patterns of xeroriparian shrub and hydroriparian tree abundance, which have somewhat similar life histories and vital rates, particularly in early life-stages. In a flow homogenization scenario, where we increased the frequency of non-event years (no drought or flood), the model predicted an increase in the relative dominance of xeroriparian shrub over hydroriparian tree (Figure 2.1.3). This modeling result parallels empirical results obtained by Merritt and Poff (2010) from 13 rivers in the western U.S.A. that differed in their degrees of flow modification. The model also demonstrated an increase in the relative coverage of xeroriparian shrub vs. hydroriparian tree with increasing drought frequency. Thus, the model appears able to parlay differences in measured vital rates between these two guilds into meaningful predictions about abundances on the landscape.

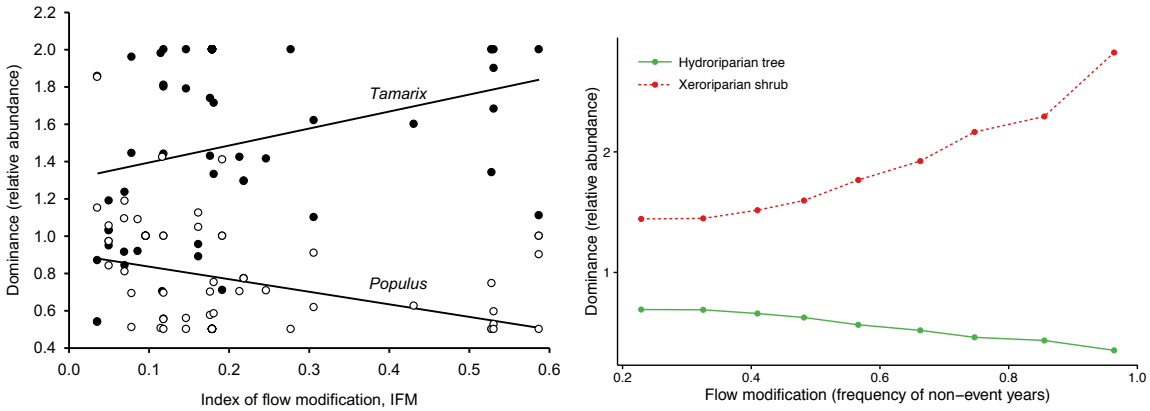

Figure 2.1.3 Comparison of model and empirical data. Left panel: figure from Merritt & Poff (2010) showing the relative dominance of hydroriparian tree vs. xeroriparian shrub in 13 western U.S.A. rivers experiencing varying degrees of flow modification. The *Tamarix* line shows the ratio of established xeroriparian shrub/hydroriparian tree, while the *Populus* line shows the reciprocal (hydroriparian tree/xeroriparian shrub). Right panel: model output showing relative dominance of established hydroriparian tree and xeroriparian shrub stems (5-10 and 7-15 year-olds, respectively) under increasing degrees of flow homogenization (elimination of floods and droughts to increase the frequency of non-event years).

Under a climate-change scenario represented altered flood timing, average coverage of hydroriparian tree increased with earlier floods, and then demonstrated a decline (Figure 2.1.4). Xeroriparian shrub illustrated the opposite effect, with earlier floods causing a reduction in abundance and later floods producing an increase. The relative difference between the two was maximized under flow regimes occurring approximately 20 days earlier than current natural flow regime conditions.

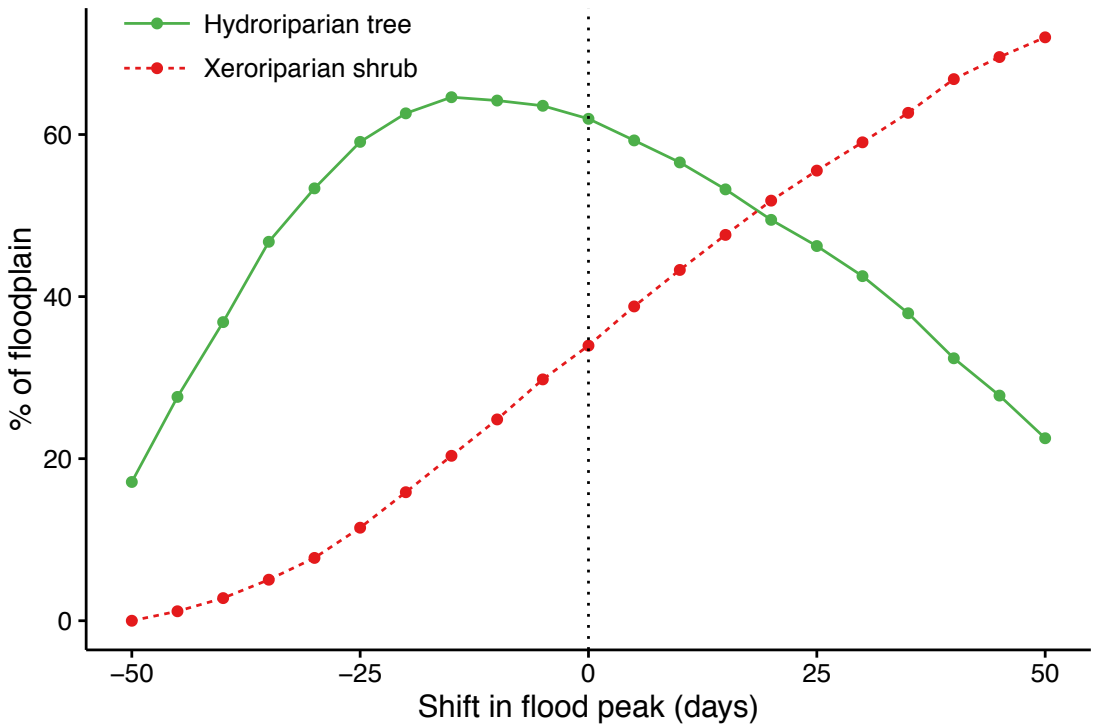

Figure 2.1.4 Effect of flood timing on hydroriparian tree and xeroriparian shrub dominance on the floodplain. Negative numbers indicate a shift to earlier flood peaks, positive numbers to later flood peaks. Hydroriparian tree was more abundant with slightly earlier flood peaks, but all other shifts in flood timing favored xeroriparian shrub.

Multi-guild sensitivity analysis revealed that population dynamics were strongly dependent on vital rates both within a single guild and across the entire community (Figure 2.1.5). All guilds except desert shrub showed negative within-guild responses to changes in vital rates, reflecting the fact that increased susceptibility to any given source of mortality should produce a reduction in population size. Changes in one guild's vital rates also produced significant positive responses across the community. For example, changing hydroriparian tree's susceptibility to flooding (S_{6HT}, left column in Figure 2.1.5) produced a marked increase in xeroriparian shrub, hydroriparian shrub, and mesoriparian meadow populations. Thus, even though pairwise guild interactions were not specified in the model, apparent biotic interactions such as competitive release arose from the interaction of individual guild's vital rates with the abiotic environment. These community-wide effects were most strongly apparent in hydroriparian tree, but xeroriparian shrub, hydroriparian shrub, and mesoriparian meadow also had significant effects on other guilds in the community. Desert shrub was the only guild that did not appear to directly affect the population dynamics of other members of the riparian community.

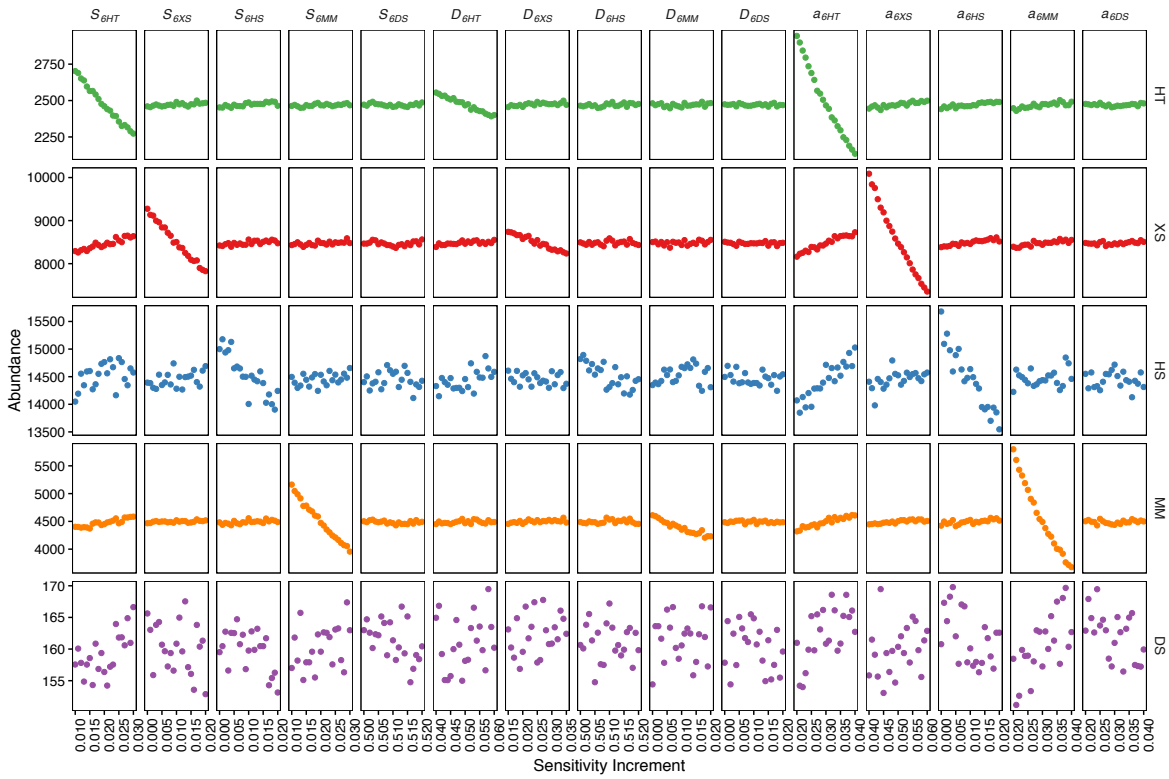

Figure 2.1.5 Multi-guild sensitivity analysis showing the community-wide effects of changing vital rates for flood mortality, drought mortality, and baseline transition probability. Column headers depict the relevant vital rate, and guild responses (total individuals occupying the river reach *K*) are shown in the row margins. Only responses of stage 6 of each guild are shown here for brevity.

We used sensitivity networks to visualize these complex guild interactions arising from the model. Sensitivity networks depict the direction and strength of each interaction in graphical format. Here, we show two such networks, one produced by calculating sensitivities under natural flow regime conditions (i.e., years drawn at random from the U.S.G.S. streamflow gauge data, which has a drought-year frequency of 20%) and another depicting a drought scenario, where the number of drought years was increased to 75% (Figure 2.1.6). Each node corresponds to a particular life stage within each guild, and the size of the node depicts the relative dominance (areal coverage as a percentage of the floodplain) on the landscape. The thickness of the line connecting two nodes depicts the strength of interaction. There were strong linkages among life stages within each guild (lines along outer circle), reflecting the fact that a change to a vital rate in one stage had strong effects on abundances of other stages. More importantly, there were many linkages that crossed from one guild to another, demonstrating that a change in a vital rate had a strong impact on the abundance of other guild life-stages. This was most evident under natural flow regime conditions, where the overall graph density (ratio of number of linkages to total number of possible linkages) was 0.27. In this scenario, mature hydroriparian tree (stage 6) exhibited the highest dominance on the landscape, and also had a strong keystone effect on other guilds due to its high connectance to other guilds (26 nodes). Hydroriparian tree also had a

strong pairwise interaction with hydroriparian shrub populations, particularly hydroriparian shrub seedlings and stage 5 individuals.

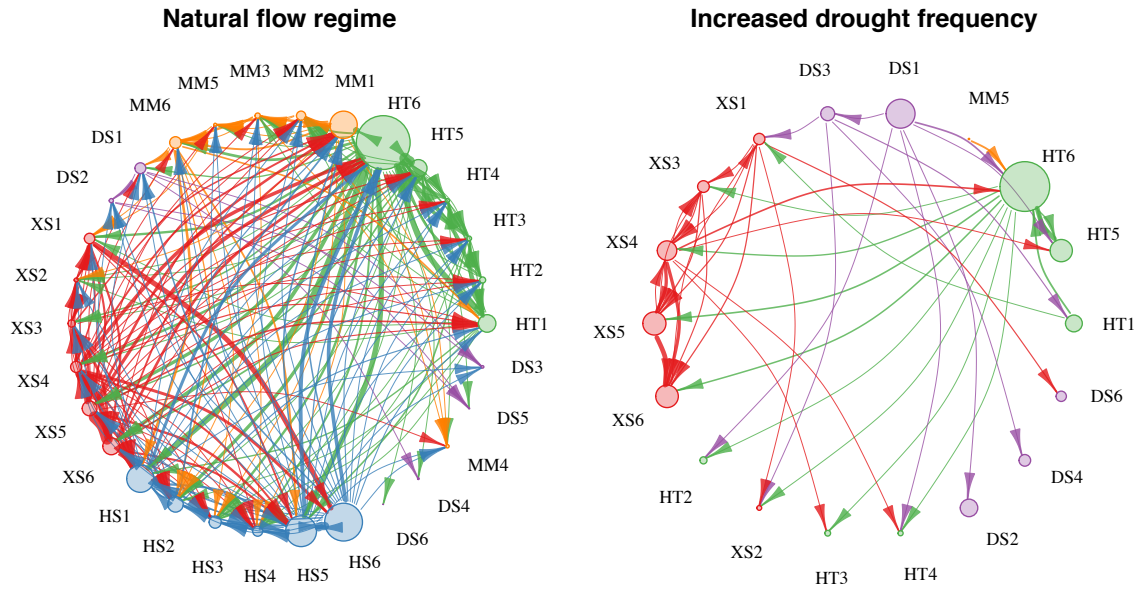

Figure 2.1.6 Sensitivity networks depicting the community-wide effects of altering flood susceptibility (S_{ij}) under natural flow regime conditions (left) and a 75% increase in drought frequency (right). Circle diameter depicts the areal dominance of each stage class and line thickness denotes strength of correlation (only linkages with R^2>0.3 are shown). Under natural flow regime conditions the community network was saturated with linkages, and mature hydroriparian tree and hydroriparian shrub were dominant keystone guilds with high connectivity. Under the drought scenario the community network was sparse, and although hydroriparian tree retained some presence on the landscape, xeroriparian shrub and desert shrub had increased in dominance.

By contrast, the drought-affected community network exhibited much sparser connectivity and weaker pairwise interactions (Figure 2.1.6, right panel). The graph density was only 0.14, and many life stages did not have any significant connectivity to the network at all (nodes with no connections were excluded from Figure 2.1.6). Although adult hydroriparian tree still retained dominance under this altered flow scenario (connectance out = 9), hydroriparian shrub and mesoriparian meadow were effectively absent from the community and xeroriparian shrub increased in relative dominance. The strength of most pairwise interactions (e.g., between HT6 and XS6) was also substantially reduced.

2.1.5 Discussion

Floods and droughts exert an influence on both mortality and fecundity in riparian plant communities. Floods and the hydraulics associated with high flows govern shear stress, scouring, and sediment transport and deposition, all of which can cause mortality to varying degrees especially in the vulnerable seedling stages (Kui & Stella 2016). Although areas nearer the channel afford resources such as moisture, these same areas are subjected to the highest frequency and intensity of disturbance, a significant trade-off for plants (Tockner and Stanford

2002, Manners et al. 2015). This was observable in the measured vital rates, where seedling flood mortality rates always exceeded those of adults, and in the strong boom-bust dynamics we observed during model runs. On the other hand, floods are a necessary driver of recruitment in all riparian guilds except desert shrub (for which recruitment is inhibited by flooding). Under extremely flood-reduced scenarios in the model, recruitment of these guilds was highly limited by the recurrence of floods. These opposing processes create highly-fluctuating populations dynamics that can obscure longer-term trends in relative guild abundances and make it difficult to predict when large cohorts of individuals will recruit into mature stages.

In this effort we obtained stage-specific mortality rates that describe how guilds respond to flood, drought, and non-event year types. We also obtained fecundity estimates as a function of the timing and recession rate of flood events. In the context of our stochastic stage-structured model, these vital rates give us a way to understand the trajectory of population dynamics under a variety of novel flow regimes, including simulations of drought, changes in flood timing, and flow homogenization due to damming. Thus, the structured population model described here allows for a rich exploration of information implicit in well-measured vital rates, and facilitates the exploration of how organisms interact with the environment in complex ways, resulting in landscape-level population dynamics that play out over multiple years. This full-community approach complements other riparian modeling efforts that focus on specific stage-classes such as seedlings (Dixon & Turner 2006) or on the population dynamics of single species (Lytle & Merritt 2004, Harper et al. 2011).

The model recovered some patterns of riparian vegetation distribution as a function of hydrology that have been observed in other studies. By simulating the loss of flood and drought events that results from dam-induced flow homogenization (Poff et al. 2007), the model predicted an increased dominance of xeroriparian shrub at the expense of hydroriparian tree abundance. This result mirrors the empirical patterns of cottonwood vs. xeroriparian shrub (*Tamarix*) dominance observed in surveys of aridland rivers in the western United States, where *Tamarix* dominance increased as a function of flow modification (Merritt and Poff 2010). In this case, tamarisk possesses greater drought tolerance and longer period of seed release that allow it to increase proportionately under modified flow regimes, even though it does not entirely replace cottonwood (Glen & Nagler 2005). The results from this kind of analysis could be used to guide flow management prescriptions where the goal is to favor a desired riparian vegetation (such as native cottonwood-dominated) over another type (such as nonnative *Tamarix*). Our results also paralleled those of Rivaes et al. (2014) which found that future drying climate scenarios led to simplifications of the plant communities and dominance of established woodlands, mature woodlands and upland forests in sites in Spain and Portugal, with the strongest impacts on younger and more water-dependent stages. Further, higher prevalence of xeric, non-flood adapted species in riparian areas is an indication of terrestrialization, wherein riparian areas become more similar to adjacent uplands and lose their uniquely riparian characteristics (Catford et al. 2014).

Our model also revealed riparian vegetation patterns that were less intuitive. The model predicted that a shift in flood timing toward earlier peaks, as is projected under most climate warming scenarios, might produce an initial increase in hydroriparian tree abundance on the landscape. However, beyond a threshold of approximately 20d, the model predicted a sharp decline in this vegetation type. Under these more extreme climate change scenarios, the relative abundance of xeroriparian shubs such as tamarisk are predicted to increase with respect to hydroriparian trees such as cottonwood, even though the absolute abundance of both guilds decreases. Note that although flood timing was varied in this simulation, dates of seed set were held constant. Climate change could cause these events to change as growing degree-days and the onset of spring shift earlier in the season (Parmesan 2007). It is still unknown whether climate-driven shifts in plant flowering phenology will keep pace with climate-driven shifts in peak streamflow timing, however our results suggest that if there is a temporal decoupling of seed set and peak stream flow there will be dramatic shifts in relative abundance of important riparian plants (e.g. Stella et al. 2006). Although not specifically addressed in this analysis, it is possible to use this modeling framework to examine the simultaneous effects of multiple hydrologic stressors (shifts in flood timing, increases in drought frequency, decreases in recruitment floods) on riparian vegetation dynamics.

Our modeling approach deliberately omitted pairwise competition between guilds, yet we were able to discover important species interactions via multi-guild sensitivity analysis. In the model structure each guild was specified as an independent matrix of vital rates, with one exception: fecundity of each guild was modeled as a function of the combined abundances of all guilds occupying the landscape. Although recruitment of all seedlings was suppressed at high aggregate densities, the model contained no assumptions about the strength or direction (with respect to guild identity) of this effect. Sensitivity analysis, however, revealed numerous strong interactions between specific guild stages that were not explicitly modeled. There were particularly strong inverse relationships between mature stage classes of hydroriparian tree and all other guilds in the community; when hydroriparian tree decreased due to a vital rate change, other members of the community responded by increasing in abundance. Interestingly, these biotic interactions changed depending on the flow regime. Network analysis showed that many of the strong among-guild interactions that occurred under natural flow regime conditions were weakened under increased-drought scenarios. The lesson here is that while vital rates can be considered a fundamental attribute of a species' or guild's collective biology, species interactions may be highly context-dependent, especially in environments as dynamic and stochastic as riverine floodplains.

The ability of the model to project realistic population dynamics depends largely on the robustness of the measured vital rates. For hydroriparian tree and xeroriparian shrub, vital rates were obtained from detailed analyses of aerial photographic time series, from long-term transect monitoring data, and from a wealth of edaphic and hydrologic studies pertaining to these well-studied guilds. For the hydroriparian shrub, mesoriparian meadow, and desert shrub guilds we relied largely on generalized vital rates that were specified relative to those of hydroriparian tree

and xeroriparian shrub. Thus, more empirical work needs to be done before we can make specific, reliable predictions for these groups. While the vital rates obtained for this study were derived largely from field studies, burial-scour experiments in artificial flumes show promise for obtaining some vital rates, at least for earlier stage classes (Kui et al. 2014). The effect of variability in vital rates, and how this affects model output, is another consideration that can be explored with methods such as global sensitivity analysis (Harper et al. 2011). It is also important to note that although we modeled these five particular guilds, the general modeling structure can incorporate other species or guilds with different life histories and degrees of tolerance to flooding or drought.

In order to generalize this modeling approach we must also consider how it applies to other river systems. Our hydrograph data were based on the undammed Yampa River in Colorado, U.S.A. To apply this method to other river systems, the threshold values for flood and drought would need to be determined from geomorphological data, gage records, or other information. In other river systems, it will not always be straightforward to identify the relevant flow thresholds, especially where long-term vegetation data are not available. Differences in substrate type, valley form, sources of water other than streamflow (precipitation and lateral groundwater) and other factors will affect how a given rate of discharge causes mortality. Thus, the threshold functions for what constitutes a flood or a drought need to be carefully calibrated for each system modeled. In the Yampa River, having three year-type categories (flood, drought, neither) appears sufficient for describing riparian vegetation dynamics. In other river systems, however, other mortality thresholds beyond the three used here may be needed, especially in systems that experience extreme-magnitude events that cause disproportionate mortality. Mathematically, the model can also accommodate the situation where a single year contains both a flood and a drought (i.e., when the S_{ij}'s and D_{ij}'s are both non-zero). Alternatively, the special situation of a combined flood-drought year could be specified as its own year-type with corresponding vital rates particular to that situation. Rivers with highly modified floodplain geomorphologies could also present a unique modelling challenge, especially rivers that have experienced reduced channel mobility or bed incision due to damming or other human modifications, as the amount of floodplain habitat K, could be changing over time.

Practitioners require defensible methods and actionable science for prescribing environmental flows to ensure functioning riverine ecosystems. Projections of the effects of alternative river flow management scenarios in riverscapes can serve to inform this process and facilitate cost-benefit analyses of alternative flow prescriptions. Static models that ignore stage-specific responses to river flows will tend to produce hydrographs that accommodate adults, but may fail to include flows that support recruitment, seedling establishment, and the changing flow requirements of the full complement of age classes. Our ability to balance human and ecosystem needs for fresh water requires models that reflect more than a single species or cover type, but capture interactions between multiple vegetation types across multiple life stages. The model presented here is a step towards modeling multiple guilds with shared life history traits to

determine the outcomes of climate change and management scenarios on riparian forest ecosystems.

2.1.6 Acknowledgments

Thanks to Kate Boersma, Mike Bogan, Emily Hartfield-Kirk, Laura McMullen, Haley Ohms, Max Smith, John Stella, and three anonymous reviewers for useful feedback and comments on an earlier version of this manuscript. Funding was provided in part by the U.S. Department of Defense (SERDP RC-2511) and the U.S. Department of Agriculture Forest Service.

2.1.7 References

Aguiar, F. C., J. O. Cerdeira, M. J. Martins, and M. T. Ferreira. 2013. Riparian forests of Southwest Europe: are functional trait and species composition assemblages constrained by environment? Journal of Vegetation Science 24: 628-638.

Caswell, H., ed. 2001. Matrix Population Models: Construction, Analysis, and Interpretation. Sunderland, MA, USA, Sinauer Associates, Inc.

Catford, J. A., W. K. Morris, P. A. Vesk, C. J. Gippel, B. J. Downes, and J. Diez. 2014. Species and environmental characteristics point to flow regulation and drought as drivers of riparian plant invasion. Diversity and Distributions 20:1084-1096.

Cooper, D. J., D. M. Merritt, D. C. Andersen and R. A. Chimner. 1999. Factors controlling the establishment of Fremont cottonwood seedlings on the upper Green River, U.S.A. Regulated Rivers: Research and Management 15: 419-440.

Dai, A. 2011. Drought under global warming: a review. WIREs Climate Change 2: 45–65.

Dalgleish, H. J., D. N. Koons, M. B. Hooten, C. A. Moffet, P. B. Adler. 2011. Climate influences the demography of three dominant sagebrush steppe plants. Ecology 92: 75–85.

Dixon, M. D., and M. G. Turner. 2006. Simulated recruitment of riparian trees and shrubs under natural and regulated flow regimes on the Wisconsin River, USA. River Research and Applications 22:1057–1083.

Friedman, J. M., G. T. Auble, P. B. Shafroth, M. L. Scott, M. F. Merigliano, M. D. Preehling and E. K. Griffin. 2005. Dominance of non-native riparian trees in western USA. Biological Invasions 7: 747-751.

Gaeuman, D., J. C. Schmidt and P. R. Wilcock. 2005. Complex channel responses to changes in stream flow and sediment supply on the lower Duchesne River, Utah. Geomorphology 64: 185-206.

Glenn, E.P. and P.L. Nagler. 2005. Comparative ecophysiology of *Tamarix ramosissima* and native trees in western US riparian zones. Journal of Arid Environments 61(3): 419-446.

Grams, P. E. and J. C. Schmidt. 2002. Streamfow regulation and multi-level flood plain formation: channel narrowing on the aggrading Green River in the eastern Unita Mountains, Colorado and Utah. Geomorphology 44: 337-360.

Harper, E. B., J. C. Stella, and A. K. Fremier. 2011. Global sensitivity analysis for complex ecological models: a case study of riparian cottonwood population dynamics. Ecological Applications 21: 1225–1240.

Hubbell, S.P. 2001. The Unified Neutral Theory of Biodiversity and Biogeography. Princeton University Press, Princeton, NJ.

Jaeger, K.L., Olden, J.D., and N.A. Pelland. 2014. Climate change poised to threaten hydrologic connectivity and endemic fishes in dryland streams. Proceedings of the National Academy of Sciences, USA 111: 13894-13899.

Kui, L., J. C. Stella, A. Lightbody, and A. C. Wilcox. 2014. Ecogeomorphic feedbacks and flood loss of riparian tree seedlings in meandering channel experiments. Water Resources Research 50:9366–9384.

Kui, L., and J. C. Stella. 2016. Fluvial sediment burial increases mortality of young riparian trees but induces compensatory growth response in survivors. Forest Ecology and Management 366:32–40.

Lytle, D. A. and D. M. Merritt. 2004. Hydrologic regimes and riparian forests: a structured population model for cottonwood. Ecology 85: 2493-2503.

Mahoney, J. M. and S. B. Rood. 1998. Streamflow requirements for cottonwood seedling recruitment-an integrative model. Wetlands 18: 634-645.

Manners, R. B., A. C. Wilcox, L. Kui, A. F. Lightbody, J. C. Stella, and L. S. Sklar. 2015. When do plants modify fluvial processes? Plant-hydraulic interactions under variable flow and sediment supply rates. Journal of Geophysical Research: Earth Surface 120:325–345.

McGill, B.J., B.J. Enquist, E. Weiher and M. Westoby. 2006. Rebuilding community ecology from functional traits. Trends in Ecology & Evolution 21(4):178-185.

Merritt, D. M. and N. L. Poff. 2010. Shifting dominance of riparian *Populus* and *Tamarix* along gradients of flow alteration in western North American rivers. Ecological Applications 20: 135-152.

Merritt, D. M., M. L. Scott, N. L. Poff, G. T. Auble and D. A. Lytle. 2010. Theory, methods and tools for determining environmental flows for riparian vegetation: riparian vegetation-flow response guilds. Freshwater Biology 551: 206-225.

Naiman, R. J., S. E. Bunn, C. Nilsson, G. E. Petts, G. Pinay and L. C. Thompson. 2002. Legitimizing fluvial ecosystems as users of water: an overview. Environmental Management 30: 455-467.

Nilsson, C., C. A. Reidy, M. Dynesius and C. Revenga. 2005. Fragmentation and flow regulation of the world's large river systems. Science 308: 405-408.

Olden, J. D., C. P. Konrad, T. S. Melis, M. J. Kennard, M. C. Freeman, M. C. Mims, E. N. Bray, K. B. Gido, N. P. Hemphill, D. A. Lytle, L. E. McMullen, M. Pyron, C. T. Robinson, J. C. Schmidt, and J. G. Williams 2014. Are large-scale flow experiments informing the science and management of freshwater ecosystems? Frontiers in Ecology and the Environment 12: 176-185.

Palmer, M.A., D.P. Lettenmaier, N.L. Poff, S.L. Postel, B. Richter, R. Warner. 2009. Climate change and river ecosystems: protection and adaptation options. Environmental Management 44: 1053–68.

Parmesan, C. 2007. Influences of species, latitudes and methodologies on estimates of phenological response to global warming. Global Change Biology 13: 1860-1872.

Poff, N. L., J. D. Olden, D. M. Merritt and D. M. Pepin. 2007. Homogenization of regional river dynamics by dams and global biodiversity implications. Proceedings Of The National Academy Of Sciences 104: 5732–5737.

Poff, N. L., B. D. Richter, A. H. Arthington, S. E. Bunn, R. J. Naiman, E. Kendy, M. Acreman, C. Apse, B. P. Bledsoe, M. C. Freeman, J. Henriksen, R. B. Jacobson, J. G. Kennen, D. M. Merritt, J. H. O'Keeffe, J. D. Olden, K. Rogers, R. E. Tharme and A. Warner. 2010. The ecological limits of hydrologic alteration (ELOHA): a new framework for developing regional environmental flow standards. Freshwater Biology 55: 147-170.

Ringold, P. L., T. K. Magee and D. V. Peck. 2008. Twelve invasive plant taxa in U.S. western riparian ecosystems. Journal of the North American Benthological Society 27: 949-966.

Rivaes, R. P., P. M. Rodriguez-Gonzalez, M. T. Ferreira, A. N. Pinheiro, E. Politti, G. Egger, A. Garcia-Arias, and F. Frances. 2014. Modeling the evolution of riparian woodlands facing climate change in three European rivers with contrasting flow regimes. PLoS ONE 9: e110200. doi:10.1371/journal.pone.0110200

Rood, S. B. and J. M. Mahoney. 1990. Collapse of riparian Poplar forests downstream from dams in western prairies: Probable causes and prospects for mitigation. Environmental Management 14: 451-464.

Sale, P. 1977. Maintenance of high diversity in coral reef fish communities. The American Naturalist 111: 337-359.

Schlaepfer, D. R., W. K. Lauenroth, and J. B. Bradford. 2012. Ecohydrological niche of sagebrush ecosystems. Ecohydrology 5: 453–466.

Seager, R., M. F. Ting, C. H. Li, N. Naik, B. Cook, J. Nakamura, and H. B. Liu. 2013. Projections of declining surface-water availability for the southwestern United States. Nature Climate Change 3: 482-486.

Stella, J. C., J. J. Battles, B. K. Orr, and J. R. McBride. 2006. Synchrony of seed dispersal, hydrology and local climate in a semi-arid river reach in California. Ecosystems 9: 1200-1214.

Stella, J. C., J. J. Battles, J. R. McBride, and B. K. Orr. 2010. Riparian seedling mortality from simulated water table recession, and the design of sustainable flow regimes on regulated rivers. Restoration Ecology 18:284–294.

Ström, L., R. Jansson, C. Nilsson, M. E. Johansson and S. Xiong. 2011. Hydrologic effects on riparian vegetation in a boreal river: an experiment testing climate change predictions. Global Change Biology 17: 254-267.

Stromberg, J. C., S. J. Lite, R. Marler, C. Paradzick, P. B. Shafroth, D. Shorrock, J. M. White and M. S. White. 2007. Altered stream-flow regimes and invasive plant species: the *Tamarix* case. Global Ecology and Biogeography 16: 381-393.

Stromberg, J. C., P. B. Shafroth and A. F. Hazelton. 2012. Legacies of flood reduction on a dryland river. River Research and Applications 28: 143–159.

Stromberg, J. C. and D. M. Merritt. 2015. Riparian plant guilds of ephemeral, intermittent and perennial rivers. Freshwater Biology 61:1259-1275.

Tockner, K., and J. A. Stanford. 2002. Riverine flood plains: present state and future trends. Environmental Conservation 29: 308-330.

Williams, R. J. and N. D. Martinez. 2000. Simple rules yield complex food webs. Nature 404: 180-183.

2.2 Modeling the effect of drought on fish communities in a changing climate

2.2.1 Introduction

Novel species assemblages, referring to local communities comprised of new species combinations that differ from historical compositions, are increasingly widespread across the world (Hobbs et al. 2009). It is well recognized that human activities leading to the emergence of novel assemblages do not occur from a random reshuffling of species; rather, community shifts are the result of heterogeneous rates of species losses and gains over time and space (Zavaleta et al. 2009, Dirzo et al. 2014, Moore and Olden 2017). Species invasions are a primary contributor to novel assemblages, where changes in species composition and not systematic reductions in species richness are unfolding at unprecedented rates (Dornelas et al. 2014). Novel assemblages may emerge as a factor of environmental changes, the invasion of non-native species, or both. Understanding how climate change will affect novel assemblages is important because the combination of climate and invasion may interact synergistically, adding to the challenge of controlling invasive species in order to maintain native species biodiversity (Hobbs et al. 2009). Communities will not respond to changes in climate trends or variability as a collective unit. The species that make up an assemblage have unique biological and behavior adaptations with respect to the changing environmental conditions, resulting in different responses. So, understanding individual species dynamics is a precursor to understanding higher levels of organization like assemblages. Given mounting threats from continued climate change, projecting community assembly responses into the future has emerged as a primary research challenge (Williams and Jackson 2007).

Recent decades have witnessed considerable advances in modeling assemblage responses to climate change. Initial efforts focused on using multivariate approaches to model assemblage-level variability in species composition (Ferrier and Guisan 2006). Later, multi-response models (Olden et al. 2006) and the aggregation of outputs from multiple species models were advanced (Brown et al. 2011); the latter of which has become increasingly common in both species distribution and demographic models (e.g. Yen et al. 2013, James et al. 2017). Despite only limited application to predict species responses under climate change, demographic models are advantageous because of their flexibility as a heuristic framework (e.g. Keith et al. 2008, van de Pol et al. 2010, Yen et al. 2013). Demographic models utilize the wealth of knowledge regarding autecology of a species, such as rates of birth, growth, fecundity, and mortality (i.e. vital rates) of individuals, to determine population structure over time. Causal mechanisms can be incorporated into these models by varying vital rates as a function of environmental variability (i.e., stochasticity) and species density-dependence (Caswell 2001). Unlike species distribution models, which largely rely on combining many single species analyses to understand community change, demographic approaches can model an entire assemblage by using density-dependent relationships with a set carrying capacity. In fact, demographic approaches have demonstrated a striking ability to recover realistic patterns of community dynamics (Lytle et al. 2017, Tonkin et al. 2017).

Demographic models may have particular utility in freshwater ecosystems where novel species assemblages are rapidly emerging in response to a multitude of human threats (Olden et al. 2010, Craig et al. 2017). The southwestern United States is a flashpoint for this conservation challenge. Widespread dam construction, flow diversions and water abstraction for growing human populations have significantly altered the environmental conditions in the region, creating conditions that threaten native species persistence and promote the proliferation of nonnative fishes (Minckley and Deacon 1968, Olden et al. 2006, Pool and Olden 2012).

With human demands on water resources compounded with changes in precipitation regimes, native fishes are now vulnerable to multiple stressors (Christensen et al. 2004, Seager et al. 2013, Udall and Overpeck 2017, Solander et al. 2017). Making inferences about population and community responses to climate change in already altered and threatened ecosystems is one of the greatest challenges facing freshwaters in general and arid rivers in particular (e.g., (Murphy et al. 2015). In the Southwestern U.S., native fishes are adapted to extreme hydrologic events including mega droughts, but their response to current and future changes in the flow regime will be affected by the current dynamics with non-native fishes and water regulations (Minckley and Deacon 1991, Minckley et al. 2003).

In the southwestern U.S. unregulated watersheds facilitate the coexistence of native and non-native species through periodic disturbances (i.e. floods and droughts) and high flow variability ((Matthews and Heins 1988, Propst et al. 2008, Pool et al. 2010). Native and non-native fishes have physical and behavioral adaptations to periodic disturbances particular to their system of origin. For example, the reproductive timing of many native fish occurs after high spring discharge when clean spawning substrate and off-channel habitat for young-of-year is most available (Brouder 2001, Gido and Propst 2012). By contrast, nonnative fishes are adapted to reproduce in stable low-flow conditions during the summer (Olden et al. 2006, Gido et al. 2013). Streams regulated by dams have reduced flow variability and, consequently, the fish assemblages within them have become dominated by non-native fishes. In unregulated rivers, high monsoonal discharge events disrupt non-native reproduction by scouring nests, interrupting spawning, or flushing young-of-year downstream (Gido et al. 2013). Although the timing and magnitude of flood events are detrimental to non-natives, low-flow drought events are unlikely to be deleterious. Non-native fishes in these systems come from the Great Plains, so they are adapted to stream drying and have behavioral and physiological characteristics to withstand periods of low-flow conditions (Matthews and Heins 1988, Dodds et al. 2004).

The current trend in the flow regime is toward an increasing occurrence and severity of low-flow anomalies and decreasing occurrence and magnitude of high flow anomalies, which could mean that native species persistence is at risk even in unregulated streams (Ruhi et al. 2015, Ruhi et al. 2016). Rivers that remain unregulated by large dams are perhaps the last remaining strong holds for native species persistence, thus providing the opportunity to gain insight into the dynamics and drivers of novel species assembly. Here, we examine a novel fish assemblage in the Verde

River as an exemplar for how hydrologic change has shaped the dynamics of native and non-native fishes. The Verde River, one of only a small number of federally designated Wild and Scenic Rivers in the United States, is large perennial flowing river and a regional conservation hub for protecting native species (Averitt et al. 1994, Turner and List 2007), thus allowing us to leverage multi-decadal time series of hydrology and fish surveys to compare model inference to empirical observations. Our goal was to advance a mechanistic model that predicts fish population and community responses to changing hydrologic regimes through time according to specific life history attributes and flow-ecology relationships of native and nonnative species. Then, populations were coupled together into a multispecies framework through density-dependent relationships. Once we built the model, we compared population projections under the historic flow record to a long-term fish monitoring dataset to examine the correspondence between our model and the empirically collected data. Finally, we examined how years with different flow events influenced native and non-native dominance in the community to project community dynamics under the changing flow regime. Our research uses fundamental species biology and autecology relationships with the environment to build mechanistic models that can be used as a heuristic framework to explore community dynamics of native and non-native species in a changing flow regime.

2.2.2 Methods

The Verde River, a semi-arid tributary of the Lower Colorado River, drains over 17,000 km^2 of central Arizona. The perennial mainstem river runs approximately 270 km through private, state, tribal and United States Forest Service lands, originating in the Big Chino Wash (elevation = 1325 m) and flowing to its confluence with the Salt River north of Phoenix, AZ (elevation = 402 m). Our study region included the unregulated upper Verde River mainstem, where development is primarily limited to livestock grazing and reductions in baseflows as a result of groundwater withdrawals. Hydrology in the upper Verde River mainstem is characterised by relatively steady, spring-fed base flow, with high-flow events that vary in magnitude and timing among years in response to storm runoff.

Highly valued for its natural beauty and management priorities, the Verde River is a focal point for the conservation of highly endemic native fishes (Averitt et al. 1994, Turner and List 2007). At least twelve fish species were native to the system, but the fish assemblage is changing rapidly, and only five native species have been observed since 1997 (Rinne 2005). By contrast, numerous nonnative fishes are present in the Verde system, including several species of centrarchids, ictalurid catfishes and minnows (Rinne 2005). Fish community composition of the Verde River varies widely among years, but nonnative fish have generally outnumbered natives for the past two decades. Management Fish population fluctuations follow natural rhythms of high and low flows because the river is not regulated by any major dam. The Verde River has been the focus of detailed monitoring efforts both with respect to fish communities and hydrologic conditions. The Upper Verde, between old highway 89 and Perkinsville, AZ, is particularly data rich, including water discharge data (flow record) from a USGS gage

(09503700) (1964 – present), long-term fish monitoring surveys (1994 – 2008; Stefferud and Rinne 1995, Neary et al. 2012), and estimates of fish biomass (2012; Gibson et al. 2015).

Table 2.2.1 Life history traits of study species.

SppCode	Species name	Common name	Status	Life-history
AMNA	*Ameiurus natalis*	Yellow bullhead	Non-native	Equilibrium
CACL	*Catostomus clarki*	Desert sucker	Native	Opportunistic
CAIN	*Catostomus insignis*	Sonora sucker	Native	Periodic
CYLU	*Cyprinella lutrensis*	Red shiner	Non-native	Opportunistic
GIRO	*Gila robusta*	Roundtail chub	Native	Opportunistic
LECY	*Lepomis cyanellus*	Green sunfish	Non-native	Equilibrium
MIDO	*Micropterus dolomieu*	Smallmouth bass	Non-native	Equilibrium

Our study examined the seven most common fish species in the Verde River where population fluctuations follow natural rhythms of high and low flows. In the model, we populated a 1 km reach with the biomass of seven commonly co-occurring and abundant native and non-native fishes in the Upper Verde. The seven species represented the suite of life history traits and body size ranges of resident native and non-native fishes in the Verde River (Table 2.2.1). Each species has unique adaptations and eco-evolutionary traits of reproduction and survival in response to flow regimes (Olden et al. 2006, Mims and Olden 2012). Representing multiple species with a variety of life history traits was important to explore changes in assemblage dynamics under non-stationary flow regimes. The unique biological traits of each species related to reproduction, growth, and survival were gathered from the literature, preferentially from sources who collected information in the southwest (Table 2.2.2). We also gathered information about relationships between flow and species responses from research conducted in the Verde and elsewhere in the Colorado River Basin (CRB). Then, we used the fundamental species biology, flow-ecology relationships and the flow record to construct the community dynamic model.

Table 2.2.2 Sources of vital rate information.

Species Code	Vital Rate Sources
CACL	Ivanyi et al. 1995, Minckley 1973, Klein et al. 2017, McAda and Wydoski 1983, Propst et al. 2001, Carothers and Minckley 1980, McCall 1980
GIRO	Brouder et al. 2000, Brouder 2001, 2005, Brouder et al. 2006, USFWS 2015
LECY	Carlander 1977, Kaya and Hesler 1972, Mannes and Jester 1980, Delp et al. 2000, Quist and Guy 2001
CAIN	Kennedy and Kucera 1978, Hinck et al. 2006, Bowron 2008, Begley 2017, Mendoza 2016, Minckley 1973, Minckley and Marsh 2009, Frimpong and Angermeier 2009
MIDO	Minckley 1973, Smith et al. 2005, Blazer et al. 2012, Lawrence et al. 2015, Knotek and Orth 1998, Robertson and Winemiller 2001, Dauwalter and Fisher 2007, Jackson et al. 2008, Humston et al. 2015

CYLU	Franssen et al. 2007, Herrington and DeVries 2008, Marsh-Matthews 2002, Brewer et al. 2008, Brewere et al. 2006, Quist et al. 2001, Marsh-Matthews et al. 2001, Matthews et al. 2002, Gale 1986, Yildrim and Peters 2006
AMNA	Langlois 1936, Murie et al. 2009, Copp et al. 2016

2.2.2.1 Flow-ecology relationships

The flow regime affects two key life stages for understanding population structure and dynamics: juvenile survival and recruitment, and adult survival so that they may live to reproduce (Schlosser 1985). We used values which we call modifiers to affect the baseline mortality for each species according to literature based relationships between major flow or cease-to-flow events and abundance. In the model, modifier values are applied to transitions between stages in the matrix at each time step according to flow classification for each year in the flow record (Table 2.2.3). For example, juvenile survival and recruitment is most affected by the magnitude and timing of high flow events in Roundtail Chub (*Gila robusta* -- GIRO) and Smallmouth Bass (*Micropterus dolomieu* -- MIDO). High flow events in the spring decrease the mortality of juvenile GIRO, while high flow events in the summer increase mortality of juvenile MIDO (Brouder 2001, Smith et al. 2005). Adult survival is most affected by extended low-flow events. Low-flow events reduce survival when reaches are reduced to isolated pools where fish may experience more intra and interspecific interactions in crowded spaces over limited resources and/or suffer from degrading water quality conditions as temperatures rise and oxygen is depleted (Lake 2003). The magnitude of these modifiers is set to reduce or increase mortality by a factor related to trends and effect sizes documented in studies from the CRB, and occasionally from other watersheds for non-native species if otherwise unavailable (Table 2.2.4).

Table 2.2.3 Modifier values based on flow-ecology relationships in literature.

Stage	YearType	CACL	GIRO	LECY	CAIN	MIDO	CYLU	AMNA
S1	SP_HF	0.1	0.1	1	0.1	1	1	1
S1	SU_HF	1	1	2	1	2	1.5	2
S1	SP_MF	0.2	0.2	1	0.2	1	1	1
S1	NE	1	1	0.1	1	0.1	0.3	0.1
S1	DR	2	2	0.2	2	0.2	0.2	0.2
S2, S3	SP_HF	1	1	1	1	1	1	1
S2, S3	SU_HF	1	1	1	1	1	1.5	1
S2, S3	SP_MF	1	1	1	1	1	1	1
S2, S3	NE	1	1	0.2	1	1	0.3	0.1
S2, S3	DR	3	3	1	3	1.5	0.2	1

Abbreviations for flow year type (HF = high flood, MF = medium flood, NE = non-event, DR = drought). S1 = YOY, S2 = sub-adult, size at first maturity, S3 = average adult size in population

Table 2.2.4 Flow-ecology relationship. Directionality of response to generalized flow attributes reported in the literature.

Flow Attribute	(+ / -)	Species	Response	Sources

high flows (spring)	+	*Catostomus sp.*, *Gila sp.*	abundance/density	Propst and Gido 2004, Propst et al. 2008, Stefferud et al. 2011, Gido et al. 2013, Ruhi et al. 2015
high spring flows	+	*Gila robusta*	recruitment	Brouder 2001
high flows (summer, spring, or number of events)	-	*Ameiurus sp., Cyprinella lutrensis, Lepomis cyanellus, Micropterus sp.*	abundance/density	Minckley and Meffe 1987, Propst et al. 2008, Gido et al. 2013, Ruhi et al. 2015
high summer flows	-	*Micropterus dolomieu*	recruitment	Smith et al. 2005
low flows (constant baseflow)	+	*Ameiurus sp., Cyprinella lutrensis, Lepomis cyanellus, Micropterus sp.*	abundance/density	Propst and Gido 2004, Propst et al. 2008, Gido et al. 2013, Ruhi et al. 2015
low flows	-	*Catostomus sp., Gila sp.*	abundance/density	Stefferud and Stefferud 1997, Propst et al. 2008, Stefferud et al. 2011, Gido et al. 2013, Ruhi et al. 2015

2.2.2.2 Flow data

Each time-step in the model represents a water year belonging to one of six categories. The flow year types were defined using discharge thresholds that typify flood years based on recurrence intervals, and drought years on the duration of baseflow. Historic discharge values from the Upper Verde came from USGS gage (09503700) near Paulden, AZ using water year (1 Oct – 30 Sep) over the period of 1964 – 2017. High spring flood years, were water years in which the maximum of late winter/early spring discharge (1 Jan – 30 Apr) exceeded 700 cfs, which is about a 4 yr recurrence interval (following Brouder 2001, Neary et al. 2012). Medium spring flood years had a maximum discharge that exceeded 220 cfs, about a 2.5 yr recurrence interval, a bankfull flow (Haney et al. 2008 report). Monsoon season summer floods (1 May – 30 Sep) exceeded a maximum discharge of 200 cfs, about a 4 yr recurrence interval for that time of year. Drought years were categorized by the absence of floods and where low flow conditions lasted a duration of 40 or more days (exceeding the 75th percentile of low-flow duration). Low flow conditions were defined as flows less than the 25th percentile of flows (following (Bêche et al. 2009)). A nonevent year occurred by default if years were otherwise not defined by flood or drought. A year type with both high spring flood and summer flood was possible, all other year types were mutually exclusive. This results in six possible flow-year types: drought, non-event, medium spring flood, high spring flood, summer flood, and spring/summer flood.

2.2.2.3 Population Projection Matrix, Model building, Vital rates

We modeled all seven species populations simultaneously to represent the community of a one kilometer reach. The foundation of the model is a stage structured population model for each species, which has been modified to incorporate environmental variability and density-dependent relationship (Caswell 2001 book). The model had several assumptions about carrying capacity and vital rates. First, we assumed that the carrying capacity of the reach was limited by the amount of biomass that could be sustained. Carrying capacity, *K*, was set to the average total biomass found in a 1 km reach from surveys in nine replicate 100 m sampling sites in the Upper Verde in 2012 (Gibson et al. 2015). We chose to use average total biomass because some reaches will naturally be more or less productive and suitable for fishes than others. Population growth was limited by a density-dependent function in the reproductive term (fecundity, *F*) so that fish could not spawn if total biomass in the reach was greater than or equal to K (see below). Second, baseline mortality was the same for all life stages within a species excepting the egg and larval phase. The combination of egg and larval mortality was calculated as part of fecundity so that the starting population of adults reproduced enough offspring to equal their replacement after stage 1 and stage 2 baseline mortality was taken into account. Third, we assumed that all fishes surviving a stage had sufficient growth to transition to the next life stage. Fourth, all fishes had a 1:1 sex ratio, and the life cycle could be completed in a 1 km reach for all species.

Table 2.2.5 Length-weight relationships.

	Length-Weight (W = aL^b)		Source
	a	b	
CACL	9.76E-06	3.038	Gibson et al. 2015 (unpublished data)
IRO	7.89E-06	3.022	Brouder 2000
ECY	3.31E-05	3.356	Mannes and Jester 1980
CAIN	9.61E-06	3.022	Gibson unpublished data
MIDO	1.16E-06	3.02	Lawrence et al. 2015
CYLU	5.75E-06	3.16	Franssen et al. 2007
AMNA	7.03E-06	2.92	Gibson et al. 2015 (unpublished data)

Each fish species had three life stages. The first stage represents juveniles, the second stage represents sub-adults at the length of first maturity, and the third stage represents adults at the average length of mature individuals from samples in the Upper Verde River (unpublished data from study Gibson et al. 2015). Individuals in each stage of the model occupied biomass calculated from length-weight relationships (Table 2.2.5) on literature reported relationships or from length-weight relationships in samples from the Upper Verde River (Table 2.2.2, Table 2.2.6). Vital rates for each stage of each species, or closely related congeners, were derived from the literature (Table 2.2.2, Table 2.2.7).

Table 2.2.6 Literature-derived values of important life history information.

	CACL	GIRO	LECY	CAIN	MIDO	CYLU	AMNA
ClutchSize (eggs)	450 - 2,772	7,267 - 26,903	2,000	2,500 - 60,000	2,000 - 5,000	131 - 1,661	1,251 - 6,820
Clutches/Season	1	1	1	1	1	2 +	1

LengthYOY_S1 (mm)	68	101	45	152	70	25	99
LengthMaturity_S2 (mm)	92	181	65	282	200	30	200
LengthAdult_S3 (mm)	180	237	87	360	222	53	218
AgeMaturity (yrs)	2	2	2	3	3	1	3
AgeMax (yrs)	8	7	5	8	6	3	7

Table 2.2.7 Vital rates of seven study species.

Parameter	CACL	GIRO	LECY	CAIN	MIDO	CYLU	AMNA
GSI	0.08	0.06	0.1	0.14	0.07	0.11	0.06
a_S1, S2	1	1	1	1	1	1	1
a_S3	0.167	0.2	0.333	0.167	0.25	1	0.2
den_Sel	894	1000	667	345	484	2123	533
den_S1	0.278	0.111	0.856	0.027	0.231	6.645	0.070
den_S2	0.113	0.019	0.249	0.004	0.010	3.735	0.009
den_S3	0.014	0.008	0.094	0.002	0.007	0.618	0.007
Mort_Sel	0.999154	0.999409	0.991380	0.999869	0.999367	0.988550	0.998945
Mort_S1, S2, S3	0.29	0.31	0.43	0.212	0.188	0.32	0.356
biom_S1, S2 start	0	0	0	0	0	0	0
biom_S3 start	5115	2293	190	33026	4583	301	1082

Species biomass, rather than species abundances (although the values were interchangeable using the weight of individuals for each species at each stage) were the currency for the model framework such that for each species:

$$\begin{pmatrix} biom1 \\ biom2 \\ biom3 \end{pmatrix}_{t+1} = \begin{pmatrix} F1 & F2 & F3 \\ G1 & 0 & 0 \\ 0 & G2 & P3 \end{pmatrix} \times \begin{pmatrix} biom1 \\ biom2 \\ biom3 \end{pmatrix}_{t}$$

Where *biom* is the biomass (g) of the species at the corresponding life stage. Fecundity (F) is linearly density dependent

$$f(x) = \begin{cases} F_{ij}, & \sum_{i=1}^{n} Biom_{ij} \leq K \\ 0, & otherwise \end{cases}$$

$$F_{ij} = a_i \times (K - \textstyle\sum_{i=1}^{n} Biom_{ij}) \times K^{-1} \times den_{iSel} \times den_{iS1}^{-1}$$

$$a_i = 0.5 \times GSI_i \times (1 - M_{iSel})$$

where $i = 1, 2, \ldots, n$ was an index representing species in the community at stage j, GSI was the Gonadal Somatic Index, M_{Sel} was the mortality of the egg and larval stage, and $Biom_{ij}$ was the

biomass of species *i* at stage *j*. The density of species i at stage j used to transition from one stage to another, to account for changes in biomass as fish grow such that:

$$den_{ij} = individuals \times grams^{-1}$$

and egg density of each species den_{iSel} was calculated as:

$$den_{iSel} = ClutchSize \times (Weight \times GSI)^{-1}$$

where *ClutchSize* was literature reported values of nest clutch size or the number of mature eggs in ripe individuals, and *Weight* is the adult biomass estimated using length-weight relationship (Table 2.2.6). If total lengths and clutch sizes were not linked for specific individuals in the reference study, egg density was estimated from the means of reported values.

Species began spawning at the stage that corresponded to the age of first reproduction (*AgeMaturity;* Table 2.2.6). All fish spawned at stage 3, some spawned at stage 2, and red shiner spawned in the first life stage. Therefore in each species matrix, the number of fecundity (F) terms corresponded to the number of life stages the species spawned in, determined by age of maturity, and was 0 in the matrix otherwise.

The probability of growing and surviving so that biomass transitions from stage 1 to stage 2 and stage 2 to stage 3, respectively are:

$$G1 = a_{S1,S2} \times den_{iS1} \times den_{iS2}^{-1} \times (1 - (M_{S1,S2,S3} \times mod_{ijk}))$$

$$G2 = a_{S1,S2} \times den_{iS2} \times den_{iS3}^{-1} \times (1 - (M_{S1,S2,S3} \times mod_{ijk}))$$

Survival is one minus mortality ($M_{S1,S2,S3}$) modified by a multiplier mod_{ijk} for species i at stage j for flow year k (Table 2.2.3).

The probability of surviving and remaining in the adult stage was related to the lifespan of each species:

$$P3 = (1 - (M_{S1,S2,S3} \times mod_{ijk})) \times (1 - a_{iS3})$$

$$and\ a_{iS3} = (AgeMax - 2)^{-1}$$

Such that senescence a_{iS3} is related to the maximum age of species i after accounting for the first two life stages of the model. At the end of each model run, biomass output was converted to abundances for subsequent data analysis and interpretation.

We ran 1,000 iterations of the model with different starting population sizes (seeds) to account for priority effects that would be present from metacommunity dynamics in a 1 km reach. Seeds for each species were derived from a negative binomial distribution with lambda and the dispersion parameter (k) calculated from the mean and variance in relative abundance of the long term Verde dataset for seven sites and 15 years of data (n = 105). These values were then converted from relative abundance to relative biomass to seed the model.

2.2.2.4 Comparisons to long-term dataset and projections beyond

We compared our model to long-term fish surveys from seven sites in the Upper Verde River from 1994 – 2008 (Stefferud and Rinne 1995, Rinne et al. 1998, Rinne 2012 p 180-232). We wanted to compare population level responses for each species before making inferences about community dynamics. The sum of stage 2 and 3 model relative abundances were compared with survey relative abundances. We reasoned the sum of stage 2 and 3 abundances would be directly comparable to survey data because these stages are most likely to be sampled with electrofishing methods due to its size bias (Sigler and Sigler 1990 book, (Peterson et al. 2004)). We chose relative abundance over absolute abundance because we were interested in the proportions of species in the community and actual abundance could not be estimated for the count data in the long-term surveys due to missing information about survey effort. Relative abundances between model outputs and survey data were compared using spearman rank correlations to measure the strength of the association between the two datasets. We also calculated the root mean square error (RMSE) to examine the average difference between model predictions and observed data for relative abundance of each species. Then, we examined entire community correlations from 1994 to 2008.

Next, we combined native and non-native species to compare to examine their relative dominance in the community through time, projected up to 2017. We wanted to know if individual species responses to the flow regime could be recovered in community dynamics related to the flow record of flow-year types. First, we examined the relative abundance of native and non-native species for the six flow-year types to look at the average response from all model runs through the flow-record. Then, we examined changes in frequency of flow-year types to see what events, if any were driving any changes in the dominance of native and non-native species.

2.2.2.5 Evaluating model uncertainty/ Sensitivity Analysis

We evaluated the effect of the size of the biomass carrying capacity on species dynamics. We started with the average biomass as the carrying capacity, and then varied the carrying capacity by 10% increments in either direction, up to 40%, and examined responses in the relative abundance of species.

2.2.3 Results

2.2.3.1 Correlations between observed data and model projections

The population level correlations between long-term fish surveys (1994 – 2008) and projections varied by species (Figure 2.2.1). Three species had strong (0.5 – 1.0), one had (0.3 – 0.5), and

three species had small correlations between observed survey relative abundances and model projections. Prediction errors, measured by root mean square error (RMSE), varied from 0.02 to 0.25 (Figure 2.2.1). The highest error was for Red Shiner (*Cyprinella lutrensis*), a small-bodied non-native species. When community level correlations were examined by year, 13 of 15 years had strong relationships between observed data and model projections (Figure 2.2.2). The 2002 data was excluded from the analysis because only two of the seven long-term sites were surveyed in that year. The smallest correlations occurred between 1999 and 2005. For the period in the flow record after 2008, the model projects a shift from a native dominant assemblage to a non-native dominant assemblage (Figure 2.2.2).

2.2.3.2 Flow-year type

When community composition was examined by flow-year type, on average, drought years had higher proportion of non-native species than for any other flow-year (Figure 2.2.3). All five major drought events occurred between 2000 – 2017, with none occurring before. Somewhat overlapping this time frame, between 1996 and 2004, neither high nor medium spring flood events occurred. The influence of droughts combined with many consecutive years without spring floods negatively affected native fish populations.

2.2.3.3 Uncertainty/Sensitivity

The fish assemblage was somewhat sensitive to changes in biomass carrying capacity. Increasing carrying capacity had less of an effect on the relative abundance of species in the assemblage then decreasing carrying capacity (Figure 2.2.4). Non-native red shiners were most sensitive to changes in carrying capacity with positive correlations between their relative abundance and the amount of available biomass.

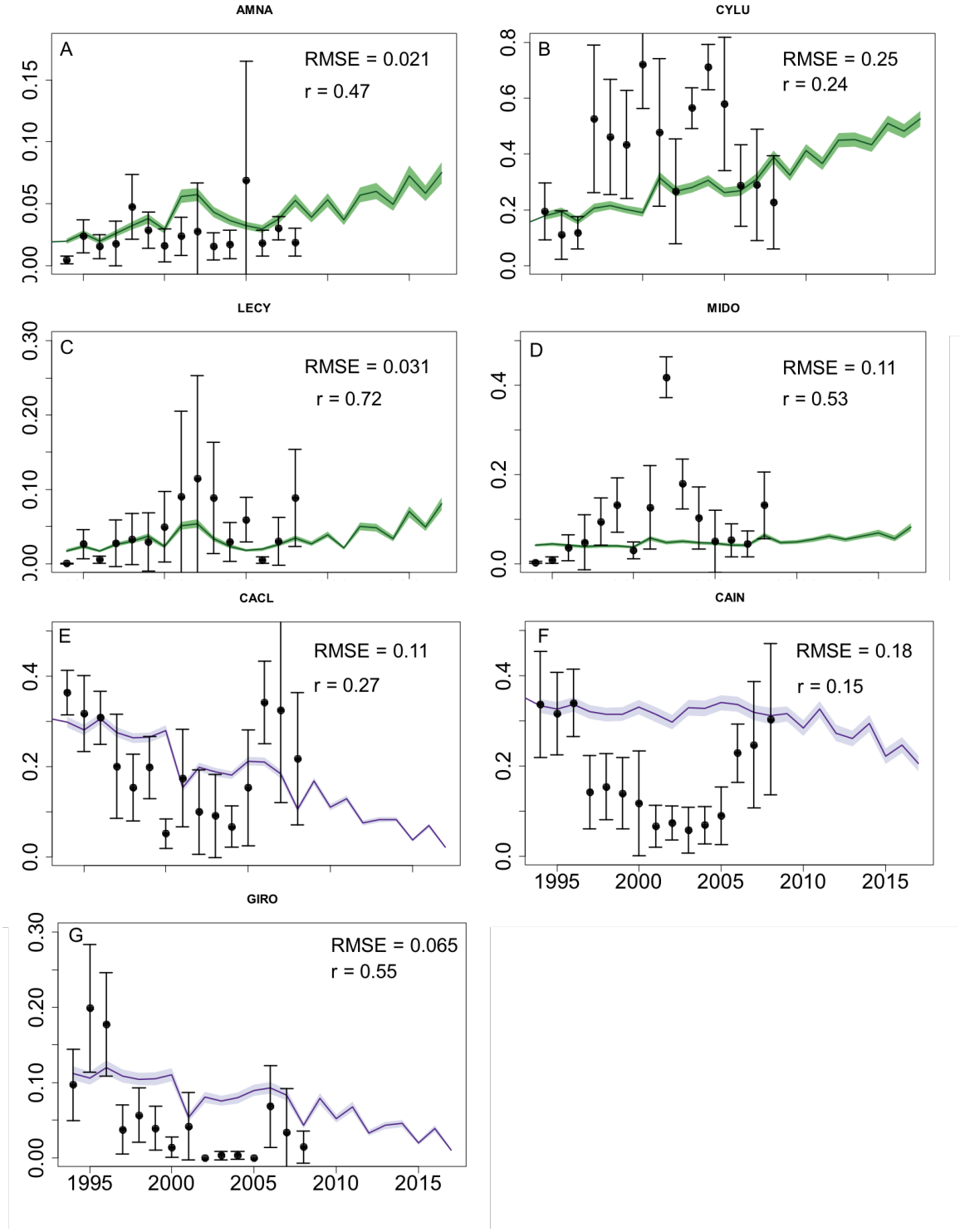

Figure 2.2.1 Population level model projections for each species compared to observed data from long-term surveys on the Verde River. Observed survey data are shown as points +- 2SE. Model data are solid line with polygon for 95% CI for all model iterations. Non-native species are green (A – D). Native species are purple (E-G). Each species is indicated by a four letter code corresponding to the first two letters of the genus and species names. Root mean squared error (RMSE) and spearman rank correlations (r) values indicate an estimate of model error, and correlation between model and observed data, respectively.

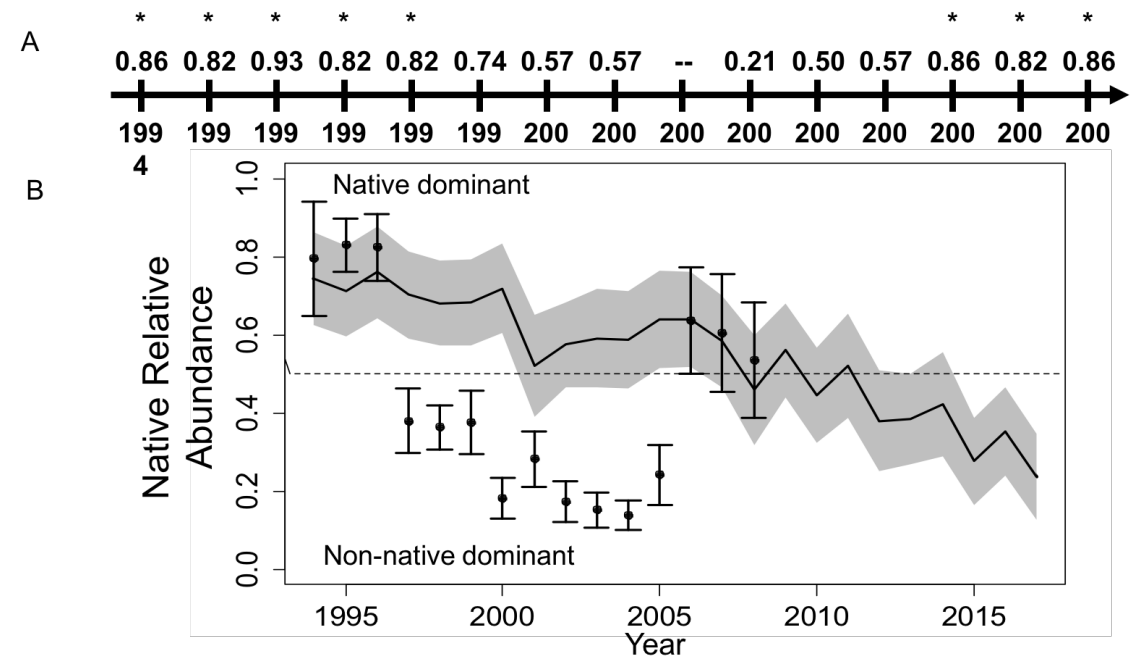

Figure 2.2.2 Community level correspondence between long-term surveys and model projections. Spearman rank correlation for observed and model data from 1994 – 2008 (A). Asterisks indicate significant monotonic relationship. Shift in projected dominance of native species through time (B). Observed survey data are shown as points +- 2SE. Model data are solid black line with grey 95% CI for all model iterations.

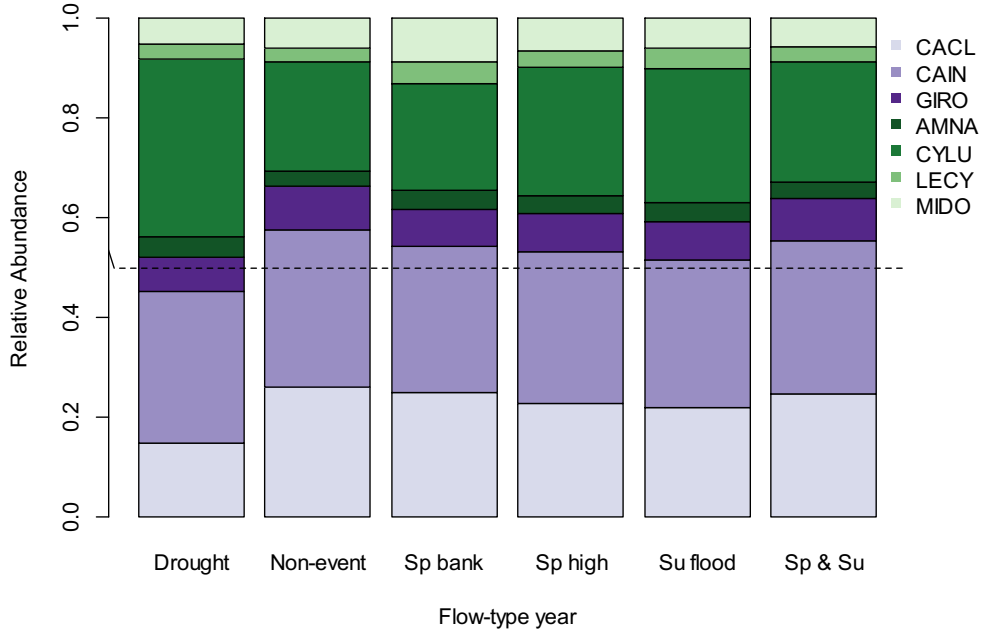

Figure 2.2.3 Average relative abundance of native and non-native species by flow-type year over 1,000 iterations of model runs. Non-natives in green shades, natives in purple shades. Each species is indicated by a four letter code corresponding to the first two letters of the genus and species names. Flow-year type explained in detail in the text.

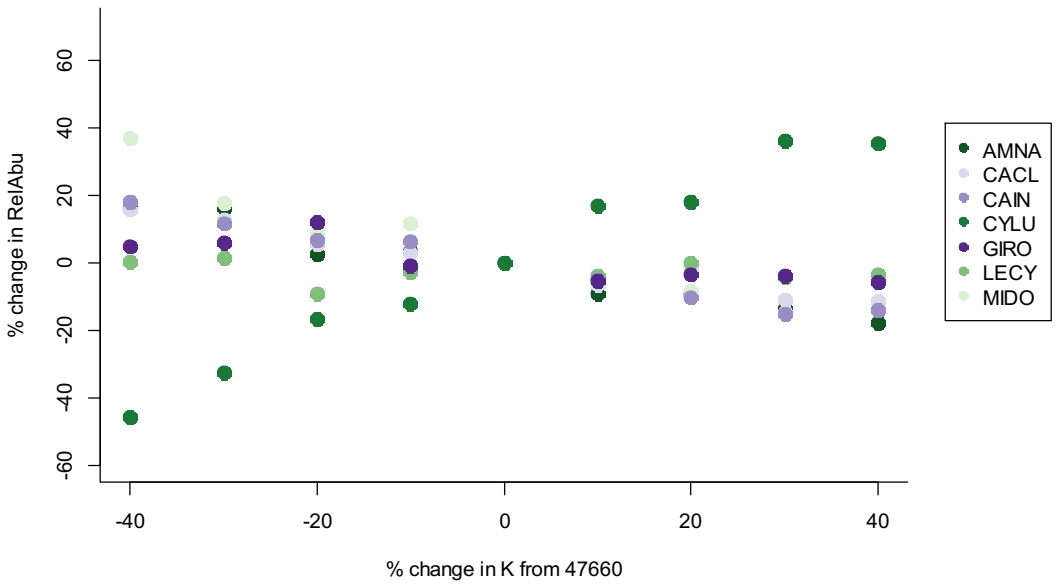

Figure 2.2.4 Effect of changing biomass carrying capacity on changes in relative abundance. Non-natives in green shades, natives in purple shades. Each species is indicated by a four letter code corresponding to the first two letters of the genus and species names.

2.2.4 References

Crossman, E. J., and B. C. Cudmore. 1999. Summary of fishes intentionally introduced in North America, 99–111. In Nonindigenous freshwater organisms, vectors, biology, and impacts.

Neary, Daniel G.; Medina, Alvin L.; Rinne, John N., eds. 2012. Synthesis of Upper Verde River research and monitoring 1993-2008. Gen. Tech. Rep. RMRS-GTR-291. Fort Collins, CO: U.S. Department of Agriculture, Forest Service, Rocky Mountain Research Station. 296 p.

Stubben, C.J. and Milligan, B.G. 2007. Estimating and Analyzing Demographic Models Using the popbio Package in R. Journal of Statistical Software 22:11.

Averitt, E., F. Steiner, R. A. Yabes, and D. Patten. 1994. An assessment of the Verde River Corridor Project in Arizona. Landscape and Urban Planning 28:161–178.

Brouder, M. J. 2001. Effects of Flooding on Recruitment of Roundtail Chub, Gila robusta, in a Southwestern River. The Southwestern Naturalist 46:302–310.

Brown, C. J., D. S. Schoeman, W. J. Sydeman, K. Brander, L. B. Buckley, M. Burrows, C. M. Duarte, P. J. Moore, J. M. Pandolfi, E. Poloczanska, W. Venables, and A. J. Richardson. 2011. Quantitative approaches in climate change ecology. Global Change Biology 17:3697–3713.

Christensen, N. S., A. W. Wood, N. Voisin, D. P. Lettenmaier, and R. N. Palmer. 2004. The Effects of Climate Change on the Hydrology and Water Resources of the Colorado River Basin. Climatic Change 62:337–363.

Dodds, W. K., K. Gido, M. R. Whiles, K. M. Fritz, and W. J. Matthews. 2004. Life on the Edge: The Ecology of Great Plains Prairie Streams. BioScience 54:205–216.

Ferrier, S., and A. Guisan. 2006. Spatial Modelling of Biodiversity at the Community Level. Journal of Applied Ecology 43:393–404.

Gibson, P. P., J. D. Olden, and M. W. O'Neill. 2015. Beaver dams shift desert fish assemblages toward dominance by non-native species (Verde River, Arizona, USA). Ecology of Freshwater Fish 24:355–372.

Gido, K. B., and D. L. Propst. 2012. Long-Term Dynamics of Native and Nonnative Fishes in the San Juan River, New Mexico and Utah, under a Partially Managed Flow Regime. Transactions of the American Fisheries Society 141:645–659.

Gido, K. B., D. L. Propst, J. D. Olden, K. R. Bestgen, and J. Rosenfeld. 2013. Multidecadal responses of native and introduced fishes to natural and altered flow regimes in the American Southwest. Canadian Journal of Fisheries and Aquatic Sciences 70:554–564.

Gozlan, R. E., J. R. Britton, I. Cowx, and G. H. Copp. 2010. Current knowledge on non-native freshwater fish introductions. Journal of Fish Biology 76:751–786.

Hobbs, R. J., E. Higgs, and J. A. Harris. 2009. Novel ecosystems: implications for conservation and restoration. Trends in Ecology & Evolution 24:599–605.

James, C. S., A. E. Reside, J. VanDerWal, R. G. Pearson, D. Burrows, S. J. Capon, T. D. Harwood, L. Hodgson, and N. J. Waltham. 2017. Sink or swim? Potential for high faunal turnover in Australian rivers under climate change. Journal of Biogeography 44:489–501.

Keith, D. A., H. R. Akçakaya, W. Thuiller, G. F. Midgley, R. G. Pearson, S. J. Phillips, H. M. Regan, M. B. Araújo, and T. G. Rebelo. 2008. Predicting extinction risks under climate change: coupling stochastic population models with dynamic bioclimatic habitat models. Biology Letters 4:560–563.

Lake, P. S. 2003. Ecological effects of perturbation by drought in flowing waters. Freshwater Biology 48:1161–1172.

Lytle, D. A., D. M. Merritt, J. D. Tonkin, J. D. Olden, and L. V. Reynolds. 2017. Linking river flow regimes to riparian plant guilds: a community-wide modeling approach. Ecological Applications 27:1338–1350.

Lytle, D. A., and N. L. Poff. 2004. Adaptation to natural flow regimes. Trends in Ecology & Evolution 19:94–100.

Matthews, W. J., and D. C. Heins, editors. 1988. Community and Evolutionary Ecology of North American Stream Fishes. 1st edition. University of Oklahoma Press, Norman.

Mims, M. C., and J. D. Olden. 2012. Life history theory predicts fish assemblage response to hydrologic regimes. Ecology 93:35–45.

Mims, M. C., and J. D. Olden. 2013. Fish assemblages respond to altered flow regimes via ecological filtering of life history strategies. Freshwater Biology 58:50–62.

Minckley, W. L., and J. E. Deacon, editors. 1991. Battle Against Extinction: Native Fish Management in the American West.

Minckley, W. L., P. C. Marsh, J. E. Deacon, T. E. Dowling, P. W. Hedrick, W. J. Matthews, and G. Mueller. 2003. A Conservation Plan for Native Fishes of the Lower Colorado River. BioScience 53:219–234.

Murphy, A. L., A. Pavlova, R. Thompson, J. Davis, and P. Sunnucks. 2015. Swimming through sand: connectivity of aquatic fauna in deserts. Ecology and Evolution 5:5252–5264.

Olden, J. D. 2003. A Species-Specific Approach to Modeling Biological Communities and Its Potential for Conservation. Conservation Biology 17:854–863.

Olden, J. D., N. L. Poff, and K. R. Bestgen. 2006. Life-History Strategies Predict Fish Invasions and Extirpations in the Colorado River Basin. Ecological Monographs 76:25–40.

Peterson, J. T., R. F. Thurow, and J. W. Guzevich. 2004. An evaluation of multipass electrofishing for estimating the abundance of stream-dwelling salmonids. Transactions of the American Fisheries Society. 133(2): 462-475:462–475.

van de Pol, M., Y. Vindenes, B.-E. Sæther, S. Engen, B. J. Ens, K. Oosterbeek, and J. M. Tinbergen. 2010. Effects of climate change and variability on population dynamics in a long-lived shorebird. Ecology 91:1192–1204.

Pool, T. K., J. D. Olden, J. B. Whittier, and C. P. Paukert. 2010. Environmental drivers of fish functional diversity and composition in the Lower Colorado River Basin. Canadian Journal of Fisheries and Aquatic Sciences 67:1791–1807.

Propst, D. L., K. B. Gido, and J. A. Stefferud. 2008. Natural Flow Regimes, Nonnative Fishes, and Native Fish Persistence in Arid-Land River Systems. Ecological Applications 18:1236–1252.

Rinne, J. N., J. A. Stefferud, A. Clark, and P. Sponholtz. 1998. Fish Community Structure in the Verde River, Arizona, 1974-1997. Hydrology and Water Resources in Arizona and the Southwest.

Schlosser, I. J. 1985. Flow Regime, Juvenile Abundance, and the Assemblage Structure of Stream Fishes. Ecology 66:1484–1490.

Seager, R., M. Ting, C. Li, N. Naik, B. Cook, J. Nakamura, and H. Liu. 2013. Projections of declining surface-water availability for the southwestern United States. Nature Climate Change 3:482–486.

Smith, S. M., J. S. Odenkirk, and S. J. Reeser. 2005. Smallmouth Bass Recruitment Variability and Its Relation to Stream Discharge in Three Virginia Rivers. North American Journal of Fisheries Management 25:1112–1121.

Solander, K. C., K. E. Bennett, and R. S. Middleton. 2017. Shifts in historical streamflow extremes in the Colorado River Basin. Journal of Hydrology: Regional Studies 12:363–377.

Stefferud, J. A., and J. N. Rinne. 1995. Sustainability of Fishes in Desert River: Preliminary Observations on the Roles of Streamflow and Introduced Fishes. Hydrology and Water Resources in Arizona and the Southwest.

Tonkin, J. D., D. M. Merritt, J. D. Olden, L. V. Reynolds, and D. A. Lytle. 2017. Flow regime alteration degrades ecological networks in riparian ecosystems. Nature Ecology & Evolution:1.

Turner, D. S., and M. D. List. 2007. Habitat mapping and conservation analysis to identify critical streams for Arizona's native fish. Aquatic Conservation: Marine and Freshwater Ecosystems 17:737–748.

Udall, B., and J. Overpeck. 2017. The twenty-first century Colorado River hot drought and implications for the future. Water Resources Research 53:2404–2418.

Williams, J. W., and S. T. Jackson. 2007. Novel climates, no-analog communities, and ecological surprises. Frontiers in Ecology and the Environment 5:475–482.

Winemiller, K. O., and K. A. Rose. 1992. Patterns of Life-History Diversification in North American Fishes: implications for Population Regulation. Canadian Journal of Fisheries and Aquatic Sciences 49:2196–2218.

Yen, J. D. L., N. R. Bond, W. Shenton, D. A. Spring, and R. Mac Nally. 2013. Identifying effective water-management strategies in variable climates using population dynamics models. Journal of Applied Ecology 50:691–701.

2.3 High mortality and enhanced recovery: modeling the countervailing effects of disturbance on insect population dynamics

2.3.1 Summary

Disturbances cause high mortality in populations while simultaneously enhancing population growth by improving habitats. These countervailing effects make it difficult to predict population dynamics following disturbance events. To address this challenge, we derived a novel form of the logistic growth equation that permits time-varying carrying capacity and growth rate. We combined this equation with concepts drawn from disturbance ecology to create a general model for population dynamics in disturbance-prone systems. A river flooding example using three insect species (a fast life-cycle mayfly, a slow life-cycle dragonfly, and an ostracod) found optimal tradeoffs between disturbance frequency vs. magnitude and a close fit to empirical data in 62% of cases. A savanna fire analysis identified fire frequencies of 3-4 years that maximized population size of a perennial grass. The model shows promise for predicting population dynamics after multiple disturbance events and for management of river flows and fire regimes.

2.3.2 Introduction

Understanding the effects of disturbance on population dynamics is critical for predicting species abundance and persistence over time. On the one hand, disturbances such as floods, fires, and extreme rainfall events impose high mortality via movement of substrates, destruction of habitat, and direct trauma. On the other hand, disturbances may positively affect population growth by regenerating physical habitats, enhancing food resources, and maintaining physical linkages between adjacent habitats such as rivers and their floodplains (Junk et al. 1989; Power et al. 1996; Effenberger et al. 2006). These countervailing disturbance effects – immediate mortality vs. enhanced population growth – create complex population dynamics that are challenging to predict. Adding to these complexities, successional processes can ameliorate the effects of disturbances over time. For example, disturbances such as grassland fires or riverine floods can provide fresh substrates for recruitment, increased nutrients, and removal of nuisance algae or necromass, but these benefits eventually diminish over time.

Population-dynamic models are essential for the management and conservation of many species, as well as for understanding their basic ecology and evolution. Prescribed fires are used to manage both vegetative and animal communities in terrestrial habitats (Pyke et al. 2010), and riverine flow prescriptions are used to manage populations of aquatic species in dammed rivers (Richter et al. 2006; Poff et al. 2010). Population models could, for example, help dam managers choose between allocating a fixed volume of water to more frequent, smaller flow events versus fewer, larger releases based on the population-level outcomes of each scenario (Richter et al. 2003). Population dynamics also drive evolutionary processes, and disturbance-mediated selective pressures may influence the evolution of life histories, behaviors and morphologies that allow individuals to escape or withstand disturbances (Holomuzki and Biggs 2000; Lytle 2001; Lytle and Poff 2004; Lytle et al. 2007). A strong quantitative linkage between disturbance events

and their population dynamic consequences could be used to examine fundamental ecological questions, such as the relationship between resistance (the ability of an organism to withstand disturbance) and resilience (the ability of a population to recover following disturbance) (Halpern 1988; Grimm & Fisher 1989; Nimmo et al. 2015). Thus, a disturbance-population model would provide a foundation for basic eco-evolutionary research as well as the conservation of ecosystems.

Our goal is to first derive a basic disturbance model that captures the fundamental dynamics of population growth, disturbance mortality, and disturbance-mediated changes to carrying capacity in the context of logistic population growth. Our modeling approach is deliberately abiotic, in that we focus on how multiple species respond autecologically to environmental disturbance events. This interaction-neutral approach allows us to examine how the vital rates of individual species (growth rate, fecundity, survivorship) interact with disturbance regimes to produce population dynamics without relying on assumptions about among-species biotic interactions (Lytle et al. 2017). The mechanistic approach we take also allows a direct mapping between individual disturbance events and their population-level consequences, which allows the model to accommodate non-stationary disturbance regimes such as shifts due to climate change (Shenton et al. 2012; Yen et al. 2013; Bond et al. 2015; Lytle et al. 2017). We begin with the general framework of logistic population growth because of its economy of assumptions (initial population size, growth rate, carrying capacity) and then we relax assumptions to accommodate complex disturbance regimes that vary in magnitude, frequency, and timing. To our knowledge, this is the first time that a logistic population growth model has been applied to understand time-varying phenomena such as disturbance dynamics.

We use riverine flooding and savanna fire as case studies to explore the model. For the river example, we calibrate the model for three contrasting life histories that span a representative range of riverine aquatic invertebrates: a fast life-cycle mayfly that experiences high flood mortality but recovers rapidly post-disturbance; a slow life-cycle dragonfly that requires occasional flood events to provide cleanly-scoured habitat; and an ostracod seed shrimp that reproduces rapidly but favors non-flooding, still-water habitats. For the fire example, we calibrate the model based on the life history of a perennial grass inhabiting tropical savannas. We also use the model to explore the relationship between resistance and resilience to disturbance.

2.3.3 Methods

2.3.3.1 Model Description

The standard logistic equation expresses growth rate for a population of size N at time t, assuming a constant carrying capacity K and a constant maximal per-capita growth rate r:

$$\frac{dN}{dt}(t) = rN(t)\left(1 - \frac{N(t)}{K}\right),\ N(t_0) = N_0 \qquad (1)$$

This equation can be solved for population size $N(t)$ given an initial population size N_0.

A more general form of this equation assumes that instead of constants, the carrying capacity and maximal per-capita growth rate can fluctuate in time. Denoting these by $K(t)$ and $r(t)$, respectively, the equation becomes:

$$\frac{dN}{dt}(t) = r(t)N(t)\left(1 - \frac{N(t)}{K(t)}\right),\ N(t_0) = N_0 \tag{2}$$

Under rather general assumptions about the time-dependence of both $r(t)$ and $K(t)$, we present a novel time-varying solution for $N(t)$ (details in online Appendix A):

$$N(t) = \frac{\left(e^{\int_{t_0}^{t} r(\tau)d\tau}\right)N_0}{\left(\int_{t_0}^{t} \frac{r(\tau)}{K(\tau)} e^{\int_{t_0}^{\tau} r(s)ds} d\tau\right)N_0 + 1} \tag{3}$$

Eq. 3 provides a general framework for incorporating biological situations where r and K might vary through time due to external environmental forces such as changes in habitat quality, abrupt disturbances, or changes in the species' biology. N_0 is population size immediately following a disturbance event, and τ and s are integration variables which will disappear from the expression after the integrals have been evaluated, leading to a function that depends only on time t. While we examine some specific cases of Eq. 3 below, this novel derivation creates new opportunities for the study of population dynamics and deserves a more thorough exploration of its general dynamics elsewhere.

To explore the dynamics of time-varying changes in carrying capacity, we make the simplifying assumption that r is constant, so Eq. 3 reduces to

$$N(t) = \frac{e^{r(t-t_0)}N_0}{\left(\int_{t_0}^{t} \frac{e^{r(\tau-t_0)}r}{K(\tau)} d\tau\right)N_0 + 1} \tag{4}$$

Eq. 4 describes situations where external factors such as habitat quality might change through time, allowing K to fluctuate up or down. We are interested in the situation where pulse disturbance events cause mortality in populations while simultaneously changing K by either enhancing or reducing habitat quality. The general framework can accommodate disturbance such as flooding, fire, pest outbreaks, or drought events. We allow disturbance mortality to occur in proportion to the disturbance's magnitude Q according to a negative exponential function:

$$N_0 = N_z e^{-hQ} \tag{5}$$

where h is a shape parameter describing the relationship between disturbance magnitude and disturbance-induced mortality, and N_z is population size immediately prior to the disturbance event. A negative exponential form arises when individuals in the population have the same per-

capita risk of mortality. Larger values of Q imply more exposure to mortality risk, although there is always a finite possibility of survival even for large Q. Eq. 5 was chosen to be a continuous function here, but a threshold function could be used in cases where disturbance events below a minimum magnitude do not cause mortality.

We include alterations to the species' habitat (either improvement or degradation) by assuming that a disturbance of magnitude Q will alter carrying capacity immediately post-disturbance according to:

$$K_0 = K_{pre} + (K_d - K_{pre})Q_f \tag{6}$$

where K_d is the carrying capacity limit following a large disturbance event and K_{pre} is carrying capacity immediately prior to the event. K_0 will be larger than K_{pre} for species whose habitat is improved by disturbances and smaller than K_{pre} for species whose habitat is degraded by disturbances. Q_f is a function that determines the shape of the relationship between disturbance magnitude and carrying capacity. In the simple case where larger disturbances have a larger effect on K_0, Q_f can be defined as:

$$Q_f = \begin{cases} 0 \; if \; Q < Q_{min} \\ \frac{Q - Q_{min}}{a + (Q - Q_{min})} \; if \; Q \geq Q_{min} \end{cases} \tag{7}$$

where Q_{min} is the minimum event magnitude that can be considered a disturbance, and a is a positive constant. Note that Q_f takes values in the interval [0, 1] for all possible values of the disturbance magnitude Q, and that Q_f increases towards 1 as Q approaches infinity. In the case of flooding disturbances, Q_{min} could be the minimum river discharge volume required to cause movement of substrates on the river bottom. The parameter a is the half-saturation constant, which determines the magnitude at which a disturbance event causes an addition to or subtraction from the pre-disturbance carrying capacity of half the difference between the pre-disturbance carrying capacity and K_d.

We assume that over time, successional processes in the habitat will eventually return carrying capacity to some pre-disturbance baseline value, K_b. We include this successional process by assuming that in the absence of more disturbances, carrying capacity eventually reverts to K_b according to:

$$K(\tau) = K_b + (K_0 - K_b)e^{-g\tau} \tag{8}$$

The shape parameter g describes how rapidly carrying capacity returns to pre-disturbance levels. For the parameterizations we explore below, values of g near 0.01 allow carrying capacity to approach pre-disturbance levels within about a year following a large disturbance. The exponential shape of Eq. 8 causes disturbance effects on carrying capacity to start diminishing

immediately after the disturbance event and then gradually disappear as $K(\tau)$ approaches K_b. This is a convenient shape that has desirable properties (few parameters, smooth convergence), but other forms could be used if post-disturbance successional processes are well understood. Eq. 8 is concave-down when disturbances increase carrying capacity ($K_0 > K_b$) and concave up when disturbances decrease carrying capacity ($K_0 < K_b$).

The equations above can be used to study the effects of multiple, sequential disturbance events on carrying capacity and population size. When modeling sequential disturbances, we must keep track of the reduction in population size due to mortality and the change in carrying capacity due to successive disturbances. The pre-flood values N_z and K_{pre} can be calculated by evaluating Eq. (4) and Eq. (8) at each specific flood time. The post-flood values N_0 and K_0 can then be calculated by evaluating Eq. (5) and Eq. (6). These post-flood values can then re-initialize the population model in Eq. (4), and the carrying capacity model in Eq. (8), until the next disturbance occurs. A summary of descriptions and values for model parameters and values is found in Table 2.3.1.

2.3.3.2 Model performance

To explore model dynamics, we parameterized the model for three aquatic invertebrate taxa that span a diversity of life cycle types. Intrinsic rates of population increase were estimated using a modified life-table approach with values obtained from the literature (online Appendix B). Table 2.3.1 describes the symbols used for parameters and variables in the model, their units, and default values used for the three target taxa. Modeling was implemented in Mathematica 10.2 (Wolfram Research 2015) and R (R Core Team 2015).

Table 2.3.1 Model parameters and variables for flooding scenarios with default values for target taxa.

			Default values		
Symbol	Description	Units	mayfly	dragonfly	ostracod
t	Time	Days			
N_t	Population size at time t	Individuals			
N_z	Population size pre-disturbance	Individuals			
N_0	Population size post-disturbance	Individuals			
K	Realized carrying capacity[a]	Individuals	40	40	100
K_d	Carrying capacity limit following strong disturbance	Individuals	100	100	40
K_b	Carrying capacity baseline when disturbances are absent	Individuals	40	40	100
K_0	Immediate post-disturbance carrying capacity	Individuals			
K_{pre}	Immediate pre-disturbance carrying capacity	Individuals			

r	Intrinsic rate of population increase	Individuals · day^{-1}	0.23	0.08	0.16
Q	Peak disturbance magnitude	m^3 · s^{-1}			
$\boldsymbol{Q_f}$	Function that determines disturbance-magnitude/ carrying capacity relationship				
$\boldsymbol{Q_{min}}$	Minimum event magnitude that can be considered a disturbance	m^3 · s^{-1}	5	5	5
a	Half-saturation constant		100	100	100
h	Strength of disturbance-mortality relationship		0.02	0.01	0.05
g	Rate that *K* returns to pre-disturbance level		0.01	0.01	0.01

NOTE.- All parameters with units of individuals were rescaled to a maximum of 100. [a] *K* was set at the non-flood carrying capacity prior to the first flood event, but generally it changes as a function of flood magnitude and time.

Fast life-cycle, flood-adapted species were represented by the mayfly *Fallceon quilleri* (Ephemeroptera: Baetidae), which can develop from egg to adult stage in as few as 7 days in Arizona, U.S.A. (Gray 1981). This species reproduces continuously in warm-climate streams and recolonizes post-flood from upstream drift as well as from ovipositing aerial adults (Gray and Fisher 1981; Poff et al. 2006). In desert rivers, mayflies such as *Fallceon* benefit from flood-generated riffles and nutrient pulses that promote algal growth, so to reflect a strong positive flood enhancement we set the maximum possible carrying capacity (K_d) to 100 (a maximum population size of 100 allows us to interpret population size as a percentage) and the lowest possible carrying capacity (K_b) to 40 (absence of flooding limits populations to 40% of maximum possible). Carrying capacity after flood enhancements was assumed to diminish during succession, due to depletion of nutrient pulses and alteration of riffle habitats by encroaching riparian vegetation (Andersen and Shafroth 2010). Slow life-cycle, flood-adapted species were represented by the sanddragon dragonfly *Progomphus borealis* (Odonata: Gomphidae). Sanddragon larvae are large-bodied predators, and thus have a slower population growth rate compared to other aquatic invertebrates such as mayflies (Table 2.3.1). Sanddragons also possess behaviors for surviving flood displacement (Poff et al. 2006; Lytle et al. 2008), and this was included in the model by using a lower flood mortality rate (Table 2.3.1). This species is suited to open, sandy river channels that are created by flooding (K_d =100 and K_b =40 to reflect a positive flood enhancement). Species poorly adapted to flooding were represented by ostracod seed shrimp (Crustacea: Ostracoda). Ostracods are filter feeders that prefer slow-water habitats and can reach high numbers in rivers with large amounts of established edge vegetation or beaver dam impoundments (Shafroth et al. 2009). Because floods reduce both of these preferred habitats, we assumed that floods have a strong negative effect on habitat quality (K_d =40 and K_b =100). We calculated a medium population growth rate and assumed a high mortality from flooding due to their limited swimming and crawling abilities, and apparent lack of flood-related survival behaviors (Table 2.3.1, Poff et al. 2006).

We examined population dynamics of the three target taxa after a single disturbance event and also after multiple disturbance events with flood magnitudes ranging from 1-1000 cubic meters per second and flood frequencies of 1-10 floods per season, with floods occurring 5 days apart. We modeled how allocating a specified volume of water across a range of flood events (from 1 to 10 floods) affected population dynamics. This 'cumulative flood magnitude' is useful for understanding how population dynamics are differentially affected by multiple small disturbance events as opposed to fewer large events.

We also examined the sensitivity of population recovery (using Eq. 4) to changes in the values of r (intrinsic rate of population increase) and h (strength of flood-mortality relationship). These parameters can be interpreted as measures of resilience (the ability of a population to recover from a disturbance) and resistance (the ability to withstand disturbance; in this case h represents inverse resistance) to disturbance.

2.3.3.3 Comparison with empirical estimates

We compared model predictions to observed population sizes of the three target taxa groups after three prescribed flood events on the Bill Williams River, Arizona (U.S.A.). Methods for these experimental flow releases are described in Shafroth et al. (2010). We calibrated the model for predictions based on peak magnitudes of the prescribed floods at a U.S. Geological Survey discharge gauge (USGS gauge #9426000), the time post-flood that invertebrate sampling occurred, and the observed relative population sizes at the study sites prior to the flood event. Population sizes were measured at three points along the river: Alamo Dam (0 km downstream of gauge), Rankin Ranch (18 km below gauge), and Mineral Wash (48 km below gauge). We relativized population sizes and variances according to the mean of the top three values for site abundance obtained over the project duration.

2.3.3.4 Application to savanna fire ecology

To explore the generality of our approach, we applied the model to disturbance from fire in tropical grasslands. We parameterized the model based on the life cycle of *Andropogon semiberbis*, a perennial grass that occurs in seasonal savannas in tropical South America (Silva et al. 1989; Silva et al. 1990; Silva et al. 1991), living up to eight years and reaching sexual maturity at two (Franco & Silvertown 2004). While prone to both natural and anthropogenic fire mortality at the seedling stage, *A. semiberbis* is adapted to fire due to its ability to withstand fire in mature stage classes. We sourced values of fire-specific mortality from seedling survivorship experiments reported in Silva et al. (1989), and corrected to a single population-wide value that accounts for low mortality in adults (i.e. divided by three; $m = 0.26$). We employed a shape parameter (g) of 0.02 that ensured K returned to approximately 50% of its maximum value after three years (K ranged between 0 and 100). We sourced the intrinsic rate of population increase (r) from Silva et al. (1991), representing the realized r under fire regimes (0.2251). We varied fire return interval (frequency^{-1}) from annual to every 20 years, and assumed that fire magnitude remained constant across events. We forecasted population abundance for 50 years to ensure population cycles had stabilized.

2.3.4 Results

2.3.4.1 General model performance

Overall, our implementation of the flooding example produced many of the population dynamic patterns that are typical of species inhabiting flood-prone rivers, although individual responses varied substantially across life-history types. Figure 2.3.1 shows population response surfaces for the three aquatic invertebrates after a single flood event at different values of Q. For most values of Q, population size of mayflies rose sharply as the population recovered post-flood, but eventually began to decline as beneficial flood enhancements diminished over time. For mayflies, the optimal balance between flood mortality and flood enhancements occurred at Q=298 cms and t=47 days, although the population never exceeded 68% of the maximum expected population size for any Q-t combination. A similar pattern was evident for dragonflies, although slower population growth rates coupled with lower flood mortality produced a different optimum (N_t=60% at Q=236 cms, t=60 days). The low N_t values emphasize that at least for these two species, a single flood event is not sufficient to boost a population to the theoretical maximum attainable size under the parameterized values. In contrast to the flood-adapted species, ostracod populations remained at 100% of their maximum population size when no flood occurred (Q=0) but experienced a sharp decline even for small floods, although population recovery was usually evident between 150 and 200 days.

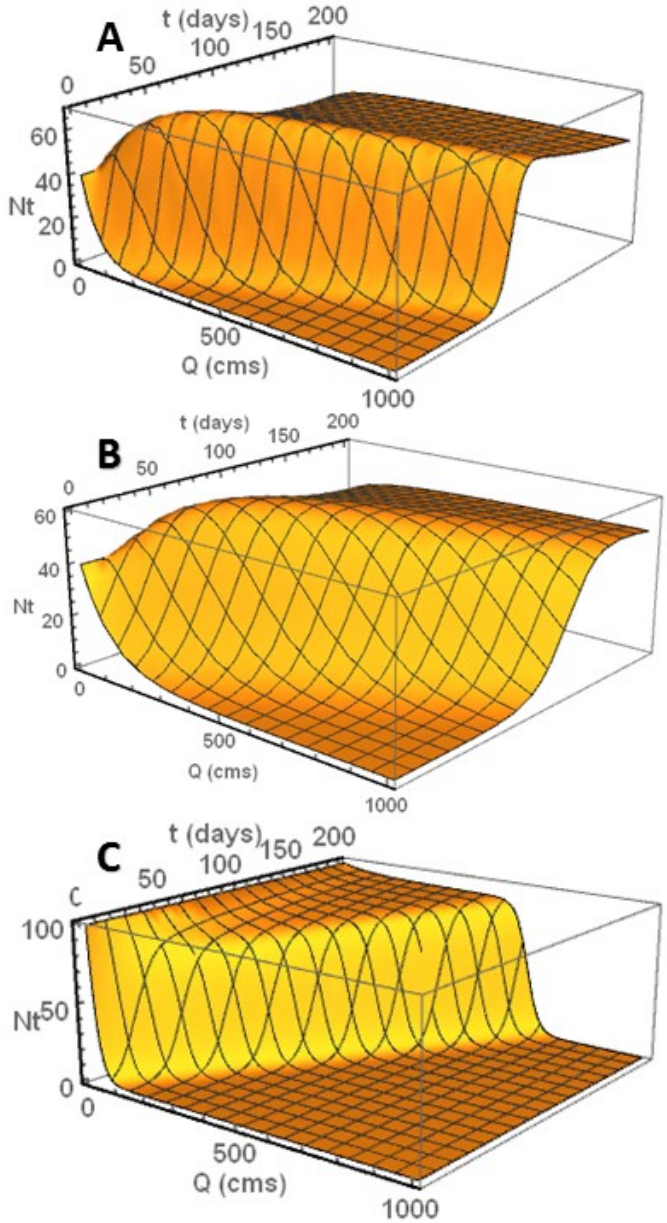

Figure 2.3.1 Flood-population response surfaces for three taxa with contrasting life histories after a single flood event. A) mayfly (*Fallceon quilleri*), B) dragonfly (*Progomphus borealis*), and C) ostracods (Ostracoda). Relative population size (N_t) vs. flood magnitude (Q) and time since flood event (t).

2.3.4.2 Resistance and resilience

Exploration of *r*-*h* parameter space revealed several notable features about the relationship between resistance and resilience under this model (Figure 2.3.2). First, there was a sharp jump from parameter combinations that allowed rapid population recovery over short timescales compared to parameter combinations that did not. Within a relatively narrow parameter space, a small change in *r* or *h* created a large shift in potential population recovery after flood events – evidence for a threshold effect. Secondly, the surface on either side of the threshold was a relatively flat plateau, indicating the existence of many *r*-*h* parameter combinations that led to

either strong or weak population response to disturbance. Parameter combinations on the surface of each plateau were numerically similar, in that they resulted in the nearly the same population sizes.

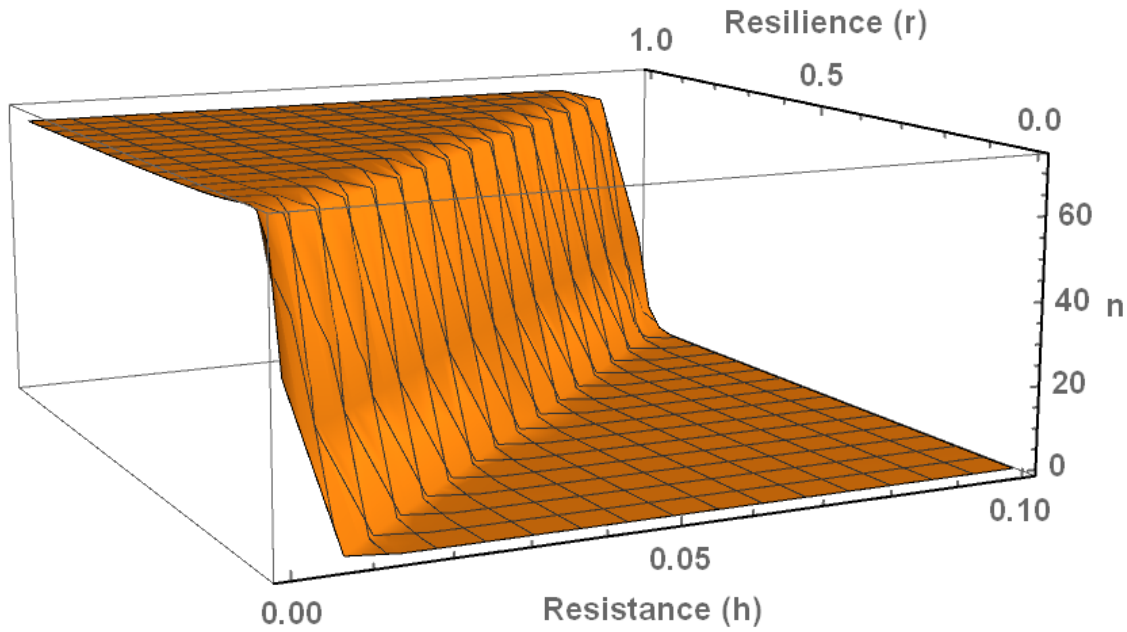

Figure 2.3.2 Plot of population size 50 days after a flood for a species whose habitat is enhanced by floods at different combinations of r and h. r is interpreted as a measure of resilience, and h as an inverse measure of resistance. Lower *h* denotes greater resistance. There is a resistance-resilience threshold beyond which the trait combination allows, or disallows, timely recovery from flooding. $K_d = 100$; $K_b = 40$; $Q = 500$; $t = 50$; $g = 0.01$; N_Z=40.

2.3.4.3 Multiple sequential disturbances

The modeled population-level consequences of multiple, sequential floods varied across taxa. Mayflies responded most favorably to floods, while dragonfly populations were the most resistant to disturbance. Ostracods were susceptible to large, sequential flood events with no evident recovery at 200 days following two sequential flood events. Differences were the most pronounced immediately following the series of disturbance events (20 d graphs in Figure 2.3.3). These differences became less pronounced as time since the disturbance events increased (100 d graphs in Figure 2.3.3).

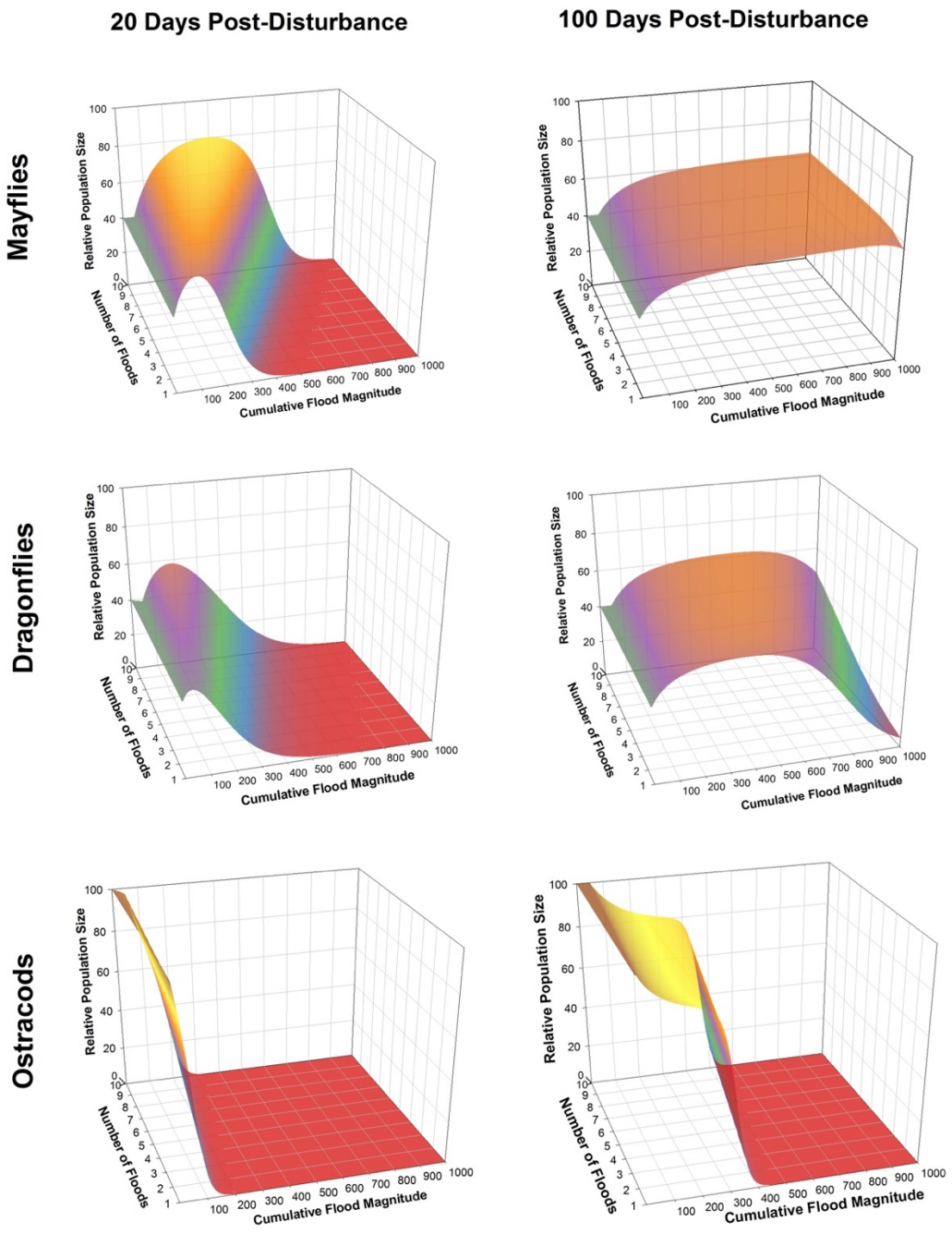

Figure 2.3.3 Relationship between flood frequency and cumulative flood magnitude for mayflies, dragonflies, and ostracods at 20 and 100 d post-flood. Cumulative flood magnitude represents the sum of all flood events, distributed across 1 to 10 individual flood events. Twenty days after the series of flood events both number of floods and cumulative flood magnitude had a large effect on relative population size, while after 100 days the effects were more homogeneous.

Mayflies experienced the greatest population increases after multiple mid-sized flood events. High population sizes were never reached after a single flood no matter the magnitude, indicating that mayfly populations likely respond positively to sequences of mid-sized, more frequent events. Maximum population sizes occurred 20 d after 10 small floods of 400 cms

magnitude. At 100 d post-disturbance, most of the benefits of flood disturbance had vanished, and population sizes had returned to baseline pre-disturbance values. Dragonflies responded positively to flooding on slower time scales, with the greatest population sizes occurring 100 d following any particular flooding sequence. Maximum population sizes occurred 100 d following 8-10 smaller floods of 400-700 cms cumulative magnitude. Thus, the slower growth dynamics of dragonflies caused flooding benefits to be realized much later in time than with mayflies. Ostracods numbers were maximized following no floods or very small floods. Even 100 days post-disturbance, ostracod populations were negatively impacted under all but the most benign flood scenarios. Ostracods populations were reduced the most severely by fewer, larger flood events.

Table 2.3.2 Flooding scenario model predictions and observed averages and standard errors for relative population size of the three taxa. M – mayflies (*Fallceon quilleri*), D – dragonflies (*Progomphus borealis*), and O – ostracods (Ostracoda) after three prescribed flood events on the Bill Williams River, Arizona. Sites: A – below Alamo Dam; R – Rankin Ranch; M – Mineral Wash confluence.

			Model prediction			Observed relative population size (mean ± SE)		
Flood magnitude (cms)	Days post-flood	Site	M	D	O	M	D	O
68.8	21-23	A	56	-	20	66±43	-	9±9
		R	59	12	-	52±23	17±13	-
		M	56	17	17	44±13	3±2*	0*
29.2	1-2	A	9	-	6	10±3	-	43±20
		R	18	41	53	9±5	29±17	9±6
		M	34	8	13	4±1*	5±3	37±12
	12-13	A	38	-	27	29±19	-	50±22
		R	44	46	53	16±4*	62±13	4±2*
		M	49	15	45	12±3*	14±4	17±11
64.85	1-3	A	0	_	1	0±0	-	3±1
		R	5	22	0	4±1	6±3*	1±1
		M	18	8	0	23±7	19±5	1±1
	16	A	9	-	9	0±0*	-	3±1*
		R	43	38	4	11±2*	5±2*	0±0*
		M	53	18	1	6±3*	41±33	2±1
	33-34	A	51	-	54	0±0*	-	3±1*
		R	56	51	39	28±4*	13±5*	14±11
		M	57	36	13	63±20	34±14	0±0*

NOTE: Values were rounded to the nearest integer.
*Cases where the model prediction did not fall within the 95% confidence interval of the observed relative population size.

2.3.4.4 Empirical model test

Overall, model predictions of relative population size fell within the 95% confidence intervals for observed population sizes 62% of the time (Table 2.3.2). The model differed in success at predicting relative population sizes among sampling sites on the river. The proportion of times

that model predictions fell within the 95% confidence intervals of the observed population sizes at Rankin Ranch was only 53%, while it was 67% at both Mineral Wash and Alamo. There were also taxonomic differences in success of the model at predicting relative population sizes. The model was most successful at predicting relative population sizes for dragonflies, where predictions fell within the 95% confidence intervals 67% of the time. The model was least successful for mayflies (56% of the time). Model success also differed among years. Model predictions fell within the 95% confidence intervals of the observed population sizes 75% of the time in 2006 and 2007 but only 50% of the time in 2008.

2.3.4.5 Savanna fire frequency

Population cycles of savanna grass fluctuated according to the specified fire frequency, but reached the highest average population size at fire return intervals of 3 to 4 years (Figure 2.3.4). A fire return interval of 1 year led to the population declining to zero, and above this populations maintained a stable cycle of population growth and decline attributable to either fire-induced mortality or carrying capacity decline. Fire mortality was the dominant cause of low population size for return intervals below 4 years, whereas carrying capacity became more important in scenarios with longer fire return intervals.

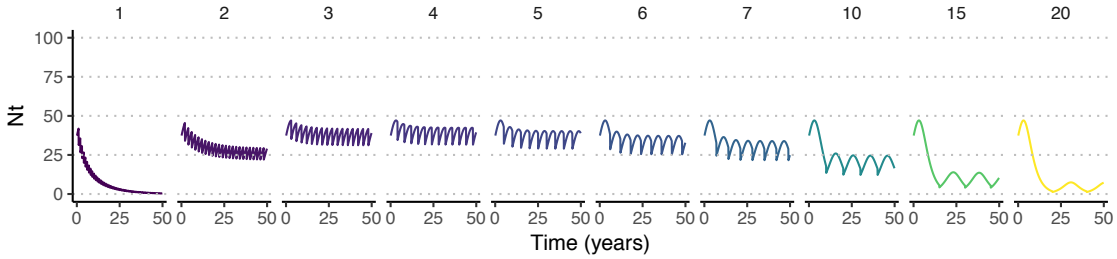

Figure 2.3.4 Relationship between fire return interval (ranging from 1 to 20 years) and relative population size (Nt) for a tropical savanna grass. The highest average population sizes were attained at return intervals of 3 to 4 years.

2.3.5 Discussion

The disturbance model we have presented unifies basic logistic population growth with fundamental concepts drawn from disturbance ecology. The model can be parameterized for any pulse disturbance (floods, fires, landslides) and, in principle, any species. The required information is an estimate of the species' intrinsic rate of population increase, expected mortality from disturbance, and knowledge of how disturbances would alter habitat in relation to the species' preference. In the model, disturbances affect two key variables related to logistic population growth, initial population size (N_0) and carrying capacity (K). To our knowledge, this is the first model to combine logistic growth models with general disturbance ecology. Stage-specific population models have been used to predict the effect of flooding on riparian plants (Lytle and Merritt 2004; Smith et al. 2005; Elderd and Doak 2006; Schleuning et al. 2008), spatially-explicit individual based models have been used to examine effects disturbance on demographic rates and habitats (Elderd and Nott 2007; Keith et al. 2008), and other models have predicted effects of disturbances such as fires at the community level while still considering

effects at the species level (He and Mladenoff 1999; Russell et al. 2009). Because population sizes and carrying capacities were represented in our model by scaling values to 100, the model results can be applied to any system as a percentage of the carrying capacity for a specific area of river habitat.

Our logistic disturbance model focuses on the abiotic effects of disturbances on population dynamics. Although biotic interactions between species certainly play a role in population dynamics (Wootton et al. 1996; Marks et al. 2000), it may not always be necessary to include these effects when considering abiotically-dominated ecosystems such as flood-prone rivers or fire-prone savannas (Moyle and Light 1996; Marchetti and Moyle 2001; Lepori and Hjerdt 2006; Hoffman et al. 2009). In principle, the single-species models presented here could be linked to examine biotic interactions and to predict community dynamics, as with Lytle et al. (2017). However, the abiotically-focused approach allows us to isolate the extent to which abiotic factors alone influence population dynamics (Death 2010), and the model can be used as a null that asks whether disturbance effects alone are sufficient for describing observed population dynamics in a system (Lytle and Merritt 2004, Lytle et al. 2017).

Aquatic taxa differed with respect to the size of a single flood that was most beneficial to their population levels, with smaller floods being more beneficial to dragonflies and mid-sized floods more beneficial to mayflies. Factors other than flood-induced mortality rates, such as flood alteration of habitat and differences in population life histories, appear to contribute to these results, highlighting the importance of incorporating these dynamics into modeling approaches. Not surprisingly, populations with faster growth rates such as mayflies reached maximum numbers after flood events more quickly than those with slower growth rates, such as dragonflies. Thus, it is important to consider the time scale of the species' population dynamics with respect to the time scale of disturbance dynamics (Townsend & Hildrew 1994; Tonkin et al. 2017).

The single-flood version of the model never allowed population levels to reach greater than 68% of maximum population size when looking at floods with magnitudes up to 1000 cms, suggesting that single flood events may not produce enough habitat enhancement to allow populations to reach maximum levels. Also, single flood events that might produce large enough enhancements to habitat often simultaneously produce great mortality, which hinders population recovery. Our modeling approach allows a close examination of this tradeoff between flood mortality and habitat enhancement, and the multi-disturbance version allows us to optimize population sizes across a wide distribution of disturbance frequencies and magnitudes.

Under the multi-flood model scenarios, populations eventually converged on similar relative abundances, regardless of the previous floods magnitudes (Figure 2.3.3). This pattern was more evident for fast lifecycle, flood adapted species (mayflies) than for species which are susceptible to flood events (ostracods). Mayflies were the least sensitive to differences in flood magnitude in the long run, while ostracods were the most sensitive. For ostracods, there was a sharp drop

within the cumulative flood magnitude- number of floods relationship, where certain combinations of floods (primarily large, less frequent floods) did not allow populations to recover after 100 days, while other combinations (smaller, more frequent floods) allowed populations to recover to levels near carrying capacity (Figure 2.3.3). For poorly flood adapted taxa such as ostracods, multiple smaller floods may have a lesser effect on abundances than fewer, larger floods. Overall, our model showed that many small disturbances are not always equivalent to one or a few larger events in relation to aquatic population dynamics, and that the optimum allocation of disturbance magnitude vs. frequency varies across taxa.

Our comparison of flooding model predictions to observed data found that about two thirds of the time, the model prediction fell within the 95% confidence interval of empirical data. In every case, the model predicted a higher abundance than what was observed from field data. The model was most successful at predicting post-flood relative population size for dragonflies, where predictions fell outside the 95% confidence intervals in only four cases. The model was least successful at predicting fast-lifecycle mayfly numbers. Floods of a given magnitude may cause greater mortality on these taxa than expected under the model assumptions, and it is also possible that recovery after flood events may be slower than the trajectory of modeled population growth, especially in rivers where temperature or food resources are highly variable. An alternative explanation, however, is that the empirical data themselves underestimated actual population sizes. In a meta-analysis of multiple flood studies, McMullen & Lytle (2012) found that aquatic invertebrate abundances are often underestimated following flood events, possibly due to invertebrates remaining hidden in deep substrates difficult to sample following floods. The difference in model success among river sites shows that the model may need to be fine-tuned to particular habitats, and the difference in model success among years may be due to seasonality or climate effects.

Our study sheds light on the interaction between resistance (*h*) and resilience (*r*). In our characterization of resistance and resilience, it appears that these traits in combination have a near-binary effect on population recovery, in contrast to finding a tradeoff between these two quantities (Miller & Chesson 2009; Nimmo et al. 2015). This is exhibited through certain combinations of *r*-*h* values allowing populations to recover to carrying capacity within a specified timeframe, and other combinations not allowing populations to recover within that timeframe. These findings suggest a binary relationship between resistance and resilience traits instead of a continuous relationship, and point to the existence of two distinct life-history syndromes - disturbance adapted vs. not disturbance-adapted. Ostracods, which often inhabit non-flooding habitats such as ponds, may fall into the group of species whose combination of *r*-*h* values does not allow the population to recover readily after severe flood events. Other aquatic invertebrate taxa that are favored during low-flow conditions may fall into this group as well (Sponseller et al. 2010). Crook et al. (2010) found a positive correlation between resistance and resilience in freshwater fish in a study examining drought, indicating that while some species may be very poor at responding to drought, others may thrive, which agrees with our finding of two distinct life history syndromes. The threshold-like reaction to disturbance events that we

observed in the model indicates that it is important to examine the qualities of resistance and resilience simultaneously, making predictions based on both factors. Because of this relationship, knowledge of a species' resistance and resilience traits in relation to disturbance events may allow determination of whether their populations will respond favorably or not to these events.

Application of the model to a fire-driven savanna ecosystem revealed that intermediate fire return intervals on the order of 3 to 4 years produced the greatest population sizes, although the fire cycle itself caused considerable population variability due to mortality from fire, reduction in carrying capacity, and subsequent recovery. The population crash during the annual fire regime contrasts with that found by Silva et al. (1991), which found a critical fire frequency of 0.85 for the species to persist. That is, under their scenario, fire is required at minimum every 1.2 years for this species to persist. The discrepancy may be attributable to parameters estimates rather than model structure. The variable r in the logistic growth model is the intrinsic rate of population increase, which is essentially the maximum growth rate that a population can achieve under ideal conditions. This value may differ considerably from realized values of r obtained under field conditions with factors that hinder population growth (limited food, predation, temperature, etc.). The value of r we used in the fire example may be an underestimate for the reasons noted above, thus contributing to the discrepancy. Furthermore, we used a single value for fire intensity in our model projection, but fire intensity could be lower with shorter return times due to lower fuel loads (Silva & Castro 1989). Although we could not find specific values from the literature to parameterize the model for different fire intensities, halving disturbance intensities at the 1-year return interval resulted in population persistence under that scenario, which is congruent with Silva et al. (1991).

2.3.5.1 Management applications

There is a strong need to produce scientific models that can predict the outcome of alternative management outcomes (Walters 1997). In the case of disturbance regime management, an important management question is the allocation of effort to frequent, smaller disturbance events vs. fewer, larger events. The modeling framework is clearly useful for addressing that issue. Invasive species are also one of the primary threats to ecosystems worldwide. While prescribed disturbances could be used to favor native over non-native taxa, few attempts have been made to model the population-level consequences of these disturbance regimes for a diverse array of affected taxa. A modeling approach such as ours could be a used to design disturbance regimes that achieve a particular conservation goal, such as maximizing population size for favored or endangered species and minimizing it for nuisance or invasive species.

2.3.6 Acknowledgements

Funding was provided by a U.S. Department of Defense grant (SERDP RC-2511) and a U.S. Fish & Wildlife Service grant to D.A.L., a U.S. National Science Foundation grant (DMS-1411853) to P.D. and a U.S. National Science Foundation Predoctoral Fellowship to L.E.M.

Helpful comments that resulted in substantial improvement to this manuscript were provided by Kate Boersma, Michael Bogan, Deb Finn, and four anonymous reviewers.

2.3.7 References

Andersen, D.C. and P.B. Shafroth. 2010. Beaver dams, hydrological thresholds, and controlled floods as a management tool in a desert riverine ecosystem, Bill Williams River, Arizona. Ecohydrology 3: 325-338.

Bond, N.R., S.R. Balcombe, D.A. Crook, J.C. Marshall, N. Menke, and J.S. Lobegeiger. 2015. Fish population persistence in hydrologically variable landscapes. Ecological Applications 25:901-913.

Crook, D.A., P. Reich, N.R. Bond, D. McMaster, J.D. Koehn, and P.S. Lake. 2010. Using biological information to support proactive strategies for managing freshwater fish during drought. Marine and Freshwater Research 61: 379-387.

Death, R.G. 2010. Disturbance and riverine benthic communities: what has it contributed to general ecological theory? River Research and Applications 26: 15-25.

Dole-Olivier, M.J., D.M.P. Galassi, P. Marmonier, and M.C.D. Chatelliers. 2000. The biology and ecology of lotic microcrustaceans. Freshwater Biology 44: 63-91.

Effenberger, M., G. Sailer, C.R. Townsend, and C.D. Matthaei. 2006. Local disturbance history and habitat parameters influence the microdistribution of stream invertebrates. Freshwater Biology 51: 312-332.

Elderd, B.D., and D.F. Doak. 2006. Comparing the direct and community-mediated effects of disturbance on plant population dynamics: flooding, herbivory and *Mimulus guttatus*. Journal of Ecology 94: 656-669.

Elderd, B.D. and M.P. Nott. 2007. Hydrology, habitat change and population demography: an individual-based model for the endangered Cape Sable seaside sparrow. Journal of Applied Ecology 45: 258-268.

Franco, M., and J. Silvertown. 2004. A comparative demography of plants based upon elasticities of vital rates. Ecology 85:531–538.

Gray, L.J. 1981. Species composition and life histories of aquatic insects in a lowland Sonoran Desert stream. The American Midland Naturalist 106: 229-242.

Gray, L.J. and S.G. Fisher. 2001. Postflood recolonization pathways of macroinvertebrates in a lowland Sonoran Desert stream. American Midland Naturalist 106: 249-257

Grimm, N.B. and S.G. Fisher. 1989. Stability of periphyton and macroinvertebrates to disturbance by flash floods in a desert stream. Journal of the North American Benthological Society 8: 293-307.

Halpern, C.B. 1988. Early successional pathways and the resistance and resilience of forest communities. Ecology 69: 1703-1715.

He, H.S., and D.J. Mladenoff. 1999. Spatially explicit and stochastic simulation of forest-landscape fire disturbance and succession. Ecology 80(1): 81-99.

Hoffman, W.A., R. Adasme, M. Haridasan, M.T. de Carvalho, E.L. Geiger, M.A.B. Pereira, S.G. Gotsch, and A.C. Franco. 2009. Tree topkill, not mortality, governs the dynamics of

savanna-forest boundaries under frequent fire in Central Brasil. Ecology 90(5): 1326-1337.

Holomuzki, J.R. and B.J.F. Biggs. 2000. Taxon-specific responses to high-flow disturbance in streams: implications for population persistence. Journal of the North American Benthological Society 19: 670-679.

Junk, W.J., P.B. Bayley, and R.E. Sparks. 1989. The flood pulse concept in river-floodplain systems. Pages 110-127 in D.P. Dodge, ed. Proceedings of the International Large River Symposium. Canadian Special Publication of Fisheries and Aquatic Scientists 106.

Keith, D.A., H.R. Akcakaya, W. Thuiller, G.F. Midgley, R.G. Pearson, S.J. Phillips, H.M. Regan, M.B. Araujo, and T.G. Rebelo. 2008. Predicting extinction risks under climate change: coupling stochastic population models with dynamic bioclimatic habitat models. Biology Letters 4: 5560-5563.

Lepori, F., and N. Hjerdt. 2006. Disturbance and aquatic biodiversity: reconciling contrasting views. BioScience 56: 809-818.

Lytle, D.A. 2001. Disturbance regimes and life history evolution. American Naturalist 157: 525-536.

Lytle, D.A. J.D. Olden, and L.E. McMullen. 2008. Drought-escape behaviors of aquatic insects may be adaptations to highly variable flow regimes characteristic of desert rivers. Southwestern Naturalist 53: 399-402.

Lytle, D.A. and D.M. Merritt. 2004. Hydrologic regimes and riparian forests: a structured population model for cottonwood. Ecology 85: 2493-2503.

Lytle, D.A., M.T. Bogan, and D.S. Finn. 2007. Evolution of aquatic insect behaviours across a gradient of disturbance predictability. Proceedings of the Royal Society B 275:453- 462.

Lytle, D.A. and N.L. Poff. 2004. Adaptation to natural flow regimes. Trends in Ecology and Evolution 19: 94-100.

Lytle, D.A., D.M. Merritt, J.D. Tonkin, J.D. Olden, and L.V. Reynolds. 2017. Linking river flow regimes to riparian plant guilds: a community-wide modeling approach. Ecological Applications 27: 1338-1350.

Marchetti, M.P. and P.B. Moyle. 2001. Effects of flow regime on fish assemblages in a regulated California stream. Ecological Applications 11: 530-539.

Marks, J.C., M.E. Power, and M.S. Parker. 2000. Flood disturbance, algal productivity, and interannual variation in food chain length. Oikos 90: 20-27.

McMullen, L. E., & D.A. Lytle. 2012. Quantifying invertebrate resistance to floods: a global-scale meta-analysis. Ecological Applications 22(8): 2164-2175.

Miller, A.D. and P. Chesson. 2009. Coexistence in disturbance-prone communities: how a resistance-resilience trade-off generates coexistence via the storage effect. The American Naturalist 173: E30-E43.

Moyle, P.B. and T. Light. 1996. Biological invasions of fresh water: empirical rules and assembly theory. Biological Conservation 78: 149-161.

Nimmo, D.G., R. Mac Nally, S.C. Cunningham, A. Haslem, and A.F. Bennett. 2015. Vive la résistance: reviving resistance for 21st century conservation. Trends in Ecology & Evolution, 30(9): 516-523.

Poff, N.L., B.D. Richter, A.H. Arthington, S.E. Bunn, R.J. Naiman, E. Kendy, M. Acreman, C. Apse, B.P. Bledsoe, M.C. Freeman, J. Henriksen, R.B. Jacobson, J.G. Kennen, D.M. Merritt, J.H. O'Keefe, J.D. Olden, K. Rogers, R.E. Tharme, and A. Warner. 2010. The ecological limits of hydrologic alteration (ELOHA): a new framework for developing regional environmental flow standards. Freshwater Biology 55: 147-170.

Poff, N.L., Olden, J.D., Vieira, N.K.M., Finn, D.S., Simmons, M.P., Kondratieff, B.C. 2006. Functional trait niches of North American lotic insects: traits-based ecological applications in light of phylogenetic relationships. Journal of the North American Benthological Society 25: 730-755.

Power, M.E., W.E. Dietrich, and J.C. Finlay. 1996. Dams and downstream aquatic biodiversity: potential food web consequences of hydrologic and geomorphic change. Environmental Management 20: 887-895.

Pyke, D.A., M.L. Brooks, and C. D'Antonio. 2010. Fire as a restoration tool: a decision framework for predicting the control or enhancement of plants using fire. Restoration Ecology 18(3): 274-284.

R Core Team. 2015. R: A language and environment for statistical computing.

Richter, B.D., R. Mathews, D.L. Harrison, and R. Wigington. 2003. Ecologically sustainable water management: managing river flows for ecological integrity. Ecological Applications 13: 206-224.

Richter, B.D., A.T. Warner, J.L. Meyer, and K. Lutz. 2006. A collaborative and adaptive process for developing environmental flow recommendations. River Research and Applications 22: 297-318.

Russell, R.E., J.A. Royle, V.A. Saab, J.F. Lehmkuhl, W.M. Block, and J.R. Sauer. 2009. Modeling the effects of environmental disturbance on wildlife communities: avian responses to prescribed fire. Ecological Applications 19(5): 1253-1263.

Schleuning, M., V. Huaman, and D. Matthies. 2008. Flooding and canopy dynamics shape the demography of a clonal Amazon understorey herb. Journal of Ecology 96: 1045-1055.

Shafroth, P.B., A.C. Wilcox, D.A. Lytle, J.T. Hickey, D.C. Andersen, V.B. Beauchamp, A. Hautzinger, L.E. McMullen, and A. Warner. 2010. Ecosystem effects of environmental flows: modeling and experimental floods in a dryland river. Freshwater Biology 55: 68-85.

Shenton, W., N.R. Bond, J.D.L. Yen, and R. MacNally. 2012. Putting the "ecology" into environmental flows: ecological dynamics and demographic modelling. Environmental Management 50:1-10.

Silva J.F. & F. Castro. 1989. Fire, growth and survivorship in a Neotropical savanna grass *Andropogon semiberbis* in Venezuela. Journal of Tropical Ecology 5: 387–400.

Silva J.F., H. Caswell, and J. Raventos. 1990. Fire and fire exclusion effects on the growth and survival of two savanna grasses. Acta Oecologica 11: 783.

Silva J.F., J. Raventos, H. Caswell, and M.C. Trevisan. 1991. Population responses to fire in a tropical savanna grass, *Andropogon semiberbis*: A matrix model approach. Journal of Ecology 79: 345–355.

Smith, M., H. Caswell, and P. Mettler-Cherry. 2005. Stochastic flood and precipitation regimes and the population dynamics pf a threatened floodplain plant. Ecological Applications 15(3): 1036-1052.

Sponseller, R.A., N.B. Grimm, A.J. Boulton, and J.L. Sabo. 2010. Responses of macroinvertebrate communities to long-term flow variability in a Sonoran Desert stream. Global Change Biology 16: 2891-2900.

Stromberg, J.C., V.B. Beauchamp, M.D. Dixon, S.J. Lite, and C. Paradzick. 2007. Importance of low-flow and high-flow characteristics to restoration of riparian vegetation along rivers in arid south-western United States. Freshwater Biology 52: 651-679.

Tonkin, J.D., M.T. Bogan, N. Bonada, B. Rios-Touma, and D.A. Lytle. 2017. Seasonality and predictability shape temporal species diversity. Ecology 98: 1201-1216.

Townsend, C.R. and A.G. Hildrew. 1994. Species traits in relation to a habitat templet for river systems. Freshwater Biology 31(3): 265-275.

Walters, C. 1997. Challenges in adaptive management of riparian and coastal ecosystems. Conservation Ecology [online] 1:1.

Wolfram Research, Inc., Mathematica, Version 10.2, Champaign, IL. 2015.

Wootton, J.T., M.S. Parker, and M.E. Power. 1996. Effects of disturbance on river food webs. Science 13: 1558-1561.

Yen, J.D.L., N.R. Bond, W. Shenton, D.A. Spring, and R. MacNally. 2013. Identifying effective water-management strategies in variable climates using population dynamics models. Journal of Applied Ecology 50:691-701.

3 Task 3: Obtain data for model parameterization

3.1 Base-specific data from managers and from fieldwork

3.1.1 Camp Pendleton

In April, 2016 we made preliminary visits to field sites on the Santa Margarita River (SMR) through Marine Corps Base Camp Pendleton (MCBCP). We also visited sites in the Santa Margarita Ecological Reserve (SMER) which is directly upstream from MCBCP on the SMR. We visited seven sites (Table 3.1.1, Figure 3.1.1) and surveyed plants to collect trait data including height, stem diameter, canopy cover and collected leaf and wood samples to determine specific leaf area, wood density, and Carbon13:Carbon12 ratios. We sampled trait data from 103 individual plants covering 57 different plant species on the floodplains and channel margins of the SMR (Table 3.1.2). Our seven field sites included three distinct geomorphic settings: low energy floodplains, medium energy confined, and narrow canyon reaches along the SMR (from our hydrogeomorphic valley classification (HGVC) mapping).

The Santa Margarita River forms where Temecula and Murrieta Creek join just west of the town of Temecula, and is regulated by several headwater dams upstream of where we sampled. The base flow of the River is also influenced by extractions for municipal use by the towns of Temecula and Fallbrook as well as groundwater extractions by Camp Pendleton. Despite streamflow regulation, the Santa Margarita River has an apparently healthy floodplain forest along most of its length, including many important native trees such as cottonwood, alder, several willow species, velvet ash, walnut, and sycamore. The Woodlot, Diversion and De Luz Crossing sites have been impacted by a recent fire, but we did not see evidence of recent grazing.

Since our field trip in April, we have conducted lab work in order to calculate leaf area, wood density, and Carbon13:Carbon12 (C13:C12) ratios for each of our samples. We are interested in C13:C12 ratio in plants because it is a useful measure of plant water use efficiency. We dried and weighed all wood and leaf samples. Once leaf samples were dried, we ground, homogenized and micro-weighed them to 2-3mg in preparation to send them to the University of California Davis Isotope lab for C13:C12 ratio analysis.

We are planning to collect detailed topographic surveys of the SMR floodplain at two chosen focal sites: the woodlot and county park sites (Table 3.1.1) in February, 2017. MCBCP is willing to share with us newly collected LiDAR data (flown in May, 2016) and the resulting high resolution elevation maps of the base. We will work from these elevation maps to tie in our own detailed surveys of the channel and floodplain. From these detailed surveys and high resolution

elevation maps, we will build 2-D hydraulic models which will be the foundation for our floodplain vegetation modeling under climate change scenarios.

Table 3.1.1 Site descriptions for seven sites visited in April, 2016 along the Santa Margarita River through Camp Pendleton Marine Corps Base and the Santa Margarita Ecological Reserve.

Site Name	Stream gage record	LiDAR	Hydrology	Valley type	Latitude	Longitude
Woodlot	1923-2016	YES	Intermittent	Low energy floodplain	33.307063	-117.356404
Diversion/Abandoned Hospital	1999-2001	YES	Perennial	Medium energy open	33.341700	-117.332082
Deluz crossing	NA	YES	Perennial	Medium energy open	33.362806	-117.320979
Navy	1989-2016	YES	Perennial	Medium energy open	33.390128	-117.279418
Fallbrook bridge	1989-2016	YES	Perennial	Medium energy open	33.396089	-117.262298
Fallbrook County park	1989-2016	YES	Perennial	Medium energy open	33.402432	-117.257133
Santa Margarita Ecological Reserve	1923-2016	No	Perennial	Gorge	33.455743	-117.171063

We are also planning to make a final field trip to Camp Pendleton in April, 2017 to do a detailed survey of floodplain vegetation in the woodlot and county park sites. We will then link the field-collected vegetation data to the topographic surveys and hydrologic models to produce floodplain vegetation maps under climate change scenarios.

Our goal is to create informed models of floodplain vegetation based on physical characteristics of the floodplain hydrology that can be used by base managers to understand how floodplain vegetation is expected to change under various climate change scenarios. Further, we seek to develop models that are applicable to other public lands in the Mediterranean, California Coastal Chaparral Forest and Shrub ecoregion, including U.S. Forest Service lands of the Cleveland National Forest. These models should help land managers develop vulnerability assessments and incorporate climate change into land management and forests plans.

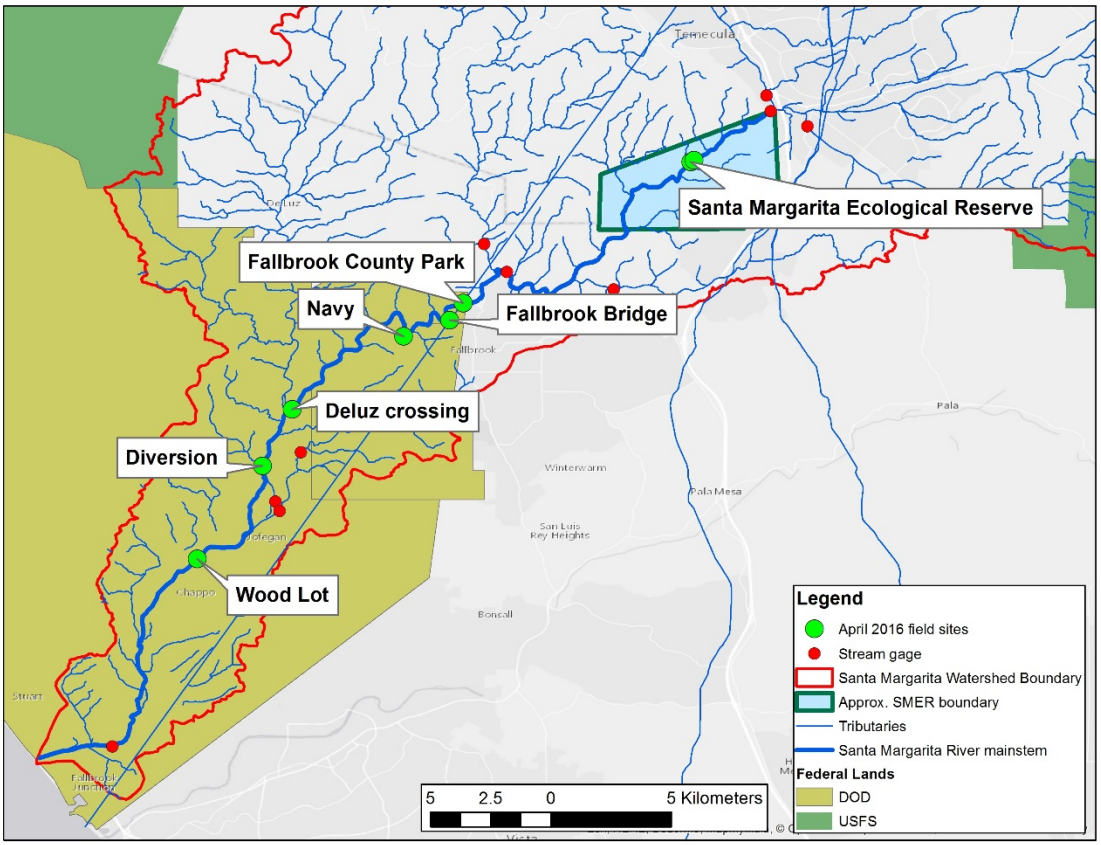

Figure 3.1.1 Field site locations for April, 2016 sampling along the Santa Margarita River through Camp Pendleton and the Santa Margarita Ecological Reserve.

Table 3.1.2 Vegetation species list for the Santa Margarita River through Camp Pendleton Marine Corps Base and the Santa Margarita Ecological Reserve.

Abronia umbellata	*Oenothera elata*
Alnus rhombifolia	*Phacelia ramosissima*
Amorpha californica	*Plantago lanceolata*
Anemopsis californica	*Plantago major*
Apocynum cannabinum	*Platanus racemosa*
Artemisia californica	*Polygonum lapathifolium*
Artemisia douglasiana	*Polypogon monspeliensis*
Artemisia dracunculus	*Populus balsamifera*
Arundo donax	*Populus fremontii*
Baccharis pilularis	*Pulicaria paludosa*
Baccharis salicifolia	*Quercus agrifolia*
Baccharis sarothroides	*Rosa californica*
Baccharis sergiloides	*Rubus ursinus*
Brickellia spp.	*Salix exigua*
Callistemon citrinus	*Salix gooddingii*
Eleocharis spp.	*Salix laevigata*
Epilobium spp.	*Salix lasiolepis*

Epipactis gigantea	*Salix lucida*
Equisetum hyemale	*Sambucus* spp.
Euthamia occidentalis	*Scirpus* spp.
Fraxinus velutina	*Solidago* spp.
Gnaphalium spp.	*Sonchus asper*
Juglans californica	*Symphoricarpos mollis*
Juncus balticus	*Tamarix ramosissima*
Ludwigia spp.	*Typha latifolia*
Malosma laurina	*Vicia* spp.
Melilotus spp.	*Vitis californica*
Mentha spp.	*Xanthium strumarium*
Mimulus guttatus	

3.1.2 Santa Margarita Ecological Reserve

In April, 2016 we made preliminary visits to field sites on the Santa Margarita River (SMR) through Marine Corps Base Camp Pendleton (MCBCP). We also visited sites in the Santa Margarita Ecological Reserve (SMER) which is directly upstream from MCBCP on the SMR. We visited seven sites (Table 3.1.3, Figure 3.1.2) and surveyed plants to collect trait data including height, stem diameter, canopy cover and collected leaf and wood samples to determine specific leaf area, wood density, and Carbon13:Carbon12 ratios. We sampled trait data from 103 individual plants covering 57 different plant species (37 species on the SMER) on the floodplains and channel margins of the SMR (Table 3.1.4). Our seven field sites included three distinct geomorphic settings: low energy floodplains, medium energy confined, and narrow canyon reaches along the SMR (from our hydrogeomorphic valley classification (HGVC) mapping).

The Santa Margarita River forms where Temecula and Murrieta Creek join just west of the town of Temecula, and is regulated by several headwater dams upstream of where we sampled. The base flow of the River is also influenced by extractions for municipal use by the towns of Temecula and Fallbrook as well as groundwater extractions by Camp Pendleton. Despite streamflow regulation, the Santa Margarita River has an apparently healthy floodplain forest along most of its length, including many important native trees such as cottonwood, alder, several willow species, velvet ash, walnut, and sycamore. The Woodlot, Diversion and De Luz Crossing sites have been impacted by a recent fire, but we did not see evidence of recent grazing.

Table 3.1.3 Site descriptions for seven sites visited in April, 2016 along the Santa Margarita River through Camp Pendleton Marine Corps Base and the Santa Margarita Ecological Reserve.

Site Name	Stream gage record	LiDAR	Hydrology	Valley type	Latitude	Longitude
Woodlot	1923-2016	YES	Intermittent	Low energy floodplain	33.307063	-117.356404

Diversion/Abandoned Hospital	1999-2001	YES	Perennial	Medium energy open	33.341700	-117.332082
Deluz crossing	NA	YES	Perennial	Medium energy open	33.362806	-117.320979
Navy	1989-2016	YES	Perennial	Medium energy open	33.390128	-117.279418
Fallbrook bridge	1989-2016	YES	Perennial	Medium energy open	33.396089	-117.262298
Fallbrook County park	1989-2016	YES	Perennial	Medium energy open	33.402432	-117.257133
Santa Margarita Ecological Reserve	1923-2016	No	Perennial	Gorge	33.455743	-117.171063

Since our field trip in April, we have conducted lab work in order to calculate leaf area, wood density, and Carbon13:Carbon12 (C13:C12) ratios for each of our samples. We are interested in C13:C12 ratio in plants because it is a useful measure of plant water use efficiency. We dried and weighed all wood and leaf samples. Once leaf samples were dried, we ground, homogenized and micro-weighed them to 2-3mg in preparation to send them to the University of California Davis Isotope lab for C13:C12 ratio analysis.

We are planning to collect detailed topographic surveys of the SMR floodplain at two chosen focal sites: the woodlot and county park sites (Table 3.1.3) in February, 2017. MCBCP is willing to share with us newly collected LiDAR data (flown in May, 2016) and the resulting high resolution elevation maps of the base. We will work from these elevation maps to tie in our own detailed surveys of the channel and floodplain. From these detailed surveys and high resolution elevation maps, we will build 2-D hydraulic models which will be the foundation for our floodplain vegetation modeling under climate change scenarios.

We are also planning to make a final field trip to Camp Pendleton in April, 2017 to do a detailed survey of floodplain vegetation in the woodlot and county park sites. We will then link the field-collected vegetation data to the topographic surveys and hydrologic models to produce floodplain vegetation maps under climate change scenarios.

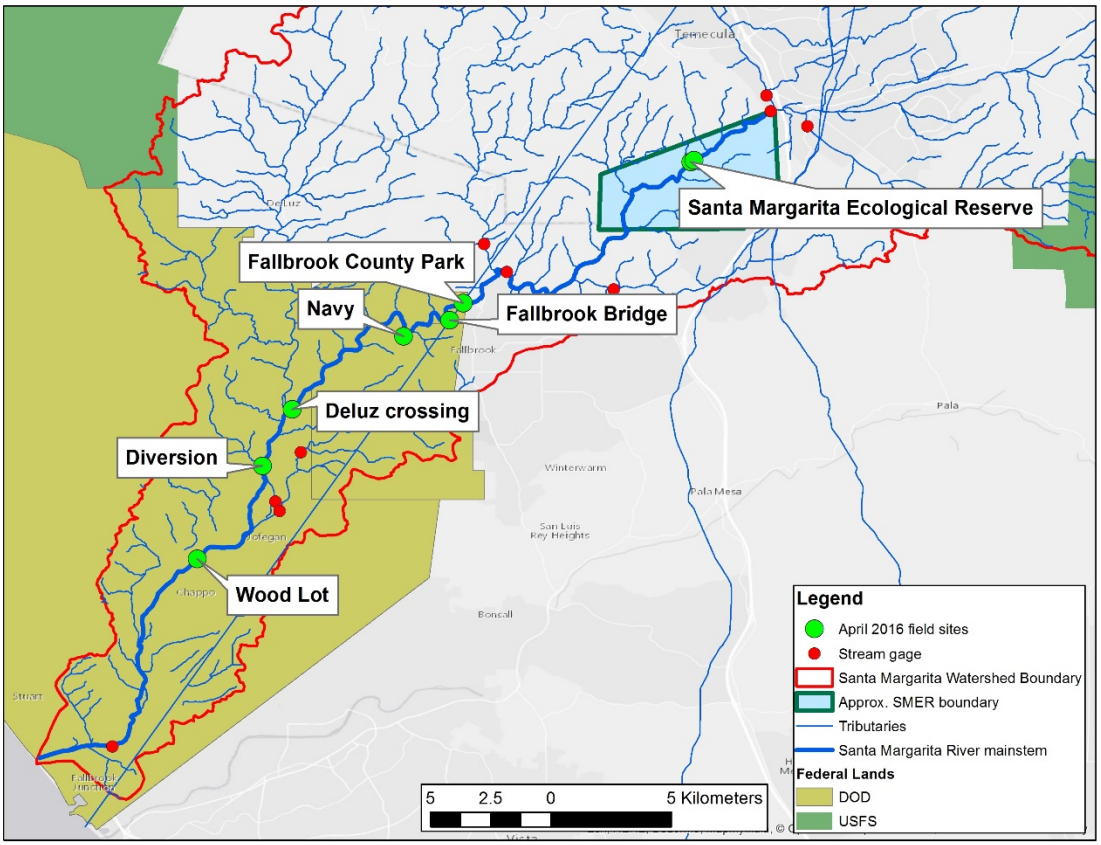

Figure 3.1.2 Field site locations for April, 2016 sampling along the Santa Margarita River through Camp Pendleton and the Santa Margarita Ecological Reserve.

Our goal is to create informed models of floodplain vegetation based on physical characteristics of the floodplain hydrology that can be used by base managers to understand how floodplain vegetation is expected to change under various climate change scenarios. Further, we seek to develop models that are applicable to other public lands in the Mediterranean, California Coastal Chaparral Forest and Shrub ecoregion, including U.S. Forest Service lands of the Cleveland National Forest. These models should help land managers develop vulnerability assessments and incorporate climate change into land management and forests plans.

Table 3.1.4 Vegetation species list for the Santa Margarita River through the Santa Margarita Ecological Reserve.

Alnus rhombifolia
Abronia umbellata
Amorpha californica
Anemopsis californica
Apocynum cannabinum
Artemisia californica
Arundo donax
Baccharis emorii
Brickellia spp

Eleocharis spp
Epipactis gigantea
Equisetum hyemale
Euthamia occidentalis
Fraxinus velutina
Juglans californica
Juncus balticus
Melilotus spp.
Oenothera elata
Polygonium lapathifolium
Phacelia ramosissima
Plantago lanceolata
Polypogon monspeliensis
Populus fremontii
Populus trichocarpa
Pulicaria paludosa
Rosa californica
Rubus ursinus
Salix gooddingii
Salix laevegata
Salix lucida
Schoenoplectus spp.
Sonchus asper
Symphoriocarpos millis
Tamarix ramosissima
Callistemon spp.
Vicia sativa
Vitus californica

Fish - We employed two-pass electrofishing for three reaches of the river at two sites on the Santa Margarita Reserve. We used a Smith Root L-24 Backpack Electrofishing Unit with a standard anode (25 cm diameter ring attached to a 2m pole) and cathode (3.2m wire cable) following the protocols recommended by the U.S. Fish and Wildlife (U.S. Fish and Wildlife Service. 2000. Principles and Techniques of Electrofishing). For each reach, a 100 m stretch of the river was blocked at the upstream and downstream ends with 5-mm bar mesh block nets unless there was a riffle that would prevent easy passage out of the sampling reach. The operator and two dip-netters electrofished from the downstream end of the site and, using short, intermittent pulses, moved upstream in a zigzag fashion. Fish were immediately placed in 5-gallon buckets (equipped with an aerator) containing fresh river water stationed at the river bank in the shade, where possible, thus ensuring the same environmental parameters (e.g., temperature, oxygen) as the natural habitat of the fish. All collected fish were identified and enumerated, measured for total length (mm) and biomass (g) and then released back into the river.

A total of four fish species and 91 individuals were captured and released on the Santa Margarita Reserve using backpack electrofishing (Table 3.1.5). All of the species were non-natives, no natives were captured in the river at or above the road crossing.

Table 3.1.5 Summary of fish species and number of individuals captured at each location.

Common name	Species	Below Crossing	Above Crossing	Upstream
Black bullhead	*Ameiurus melas*	1	3	2
Green sunfish	*Lepomis cyanellus*	11	23	21
Redeye bass	*Micropterus coosae*	13	13	3
Largemouth bass	*Micropterus salmoides*			1

3.1.3 Fort Hunter Liggett

In April, 2016 we visited field sites along the Nacimiento and San Antonio Rivers through Fort Hunter Liggett (FHL) and adjacent Los Padres National Forest (LPNF). We visited ten sites (Figure 3.1.3, Table 3.1.6) and surveyed plants to collect trait data including plant height, stem diameter, canopy cover. We also collected leaf and wood samples to determine specific leaf area, wood density, and Carbon13:Carbon12 ratios. We sampled trait data from 96 individual plants covering 55 different plant species on the floodplains and channel margins of the Nacimiento and San Antonio Rivers (Table 3.1.7). Our ten field sites included three distinct geomorphic settings: low energy floodplains, medium energy confined, and medium energy open reaches along the Nacimiento and San Antonio Rivers (from our hydrogeomorphic valley classification (HGVC) mapping).

Table 3.1.6 Site descriptions for ten sites visited in April, 2016 along the San Antonio River (top five sites) and the Nacimiento River (bottom five sites) through Los Padres National Forest and Fort Hunter Liggett.

Site Name	Stream gage record	LiDAR	Hydrology	Valley type	Latitude	Longitude
North Fork San Antonio	NA	No*	Perennial	Medium energy confined	36.064836	-121.388849
Merle Ranch	NA	Yes	Perennial	Medium energy open	36.069728	-121.347261
Mission	NA	Yes	Perennial	Medium energy confined	36.010985	-121.254363
Landfill	1965-2016 *13 km downstream	Yes	Intermittent?	Low energy floodplain	35.971404	-121.213623
MPRC	1965-2016 *8 km downstream	Yes	Intermittent?	Medium energy open	35.934091	-121.162942
Campground	NA	No	Perennial	Medium energy confined	35.991634	-121.365791
Upper Nacimiento	NA	Yes	Intermittent?	Medium energy confined	35.974745	-121.340512
Cultural	NA	Yes	Perennial	Medium energy confined	35.951302	-121.301768

Canyon/ Upper Palisades	NA	Yes	Perennial	Medium energy confined	35.905102	-121.256641
Bridge	1971-2016 *12 km downstream	Yes	Intermittent?	Medium energy confined	35.852199	-121.197605

The Nacimiento and San Antonio Rivers retain natural flow regimes, unimpeded by any reservoirs upstream of our study sites. In all sites we visited, the vegetation was dominated by native woody species such as sycamore, cottonwood, alder, willows and oaks. We noticed that the alder were severely diseased at several sites on the middle sections of both the Nacimiento and San Antonio Rivers including major damage at the Merle Ranch, Mission Confluence on the San Antonio and the "Upper and Cultural sites on the Nacimiento. The disease is likely a fungal pathogen, such as Pytophthora, which has been documented infecting alders in western Oregon.

Since our field trip in April, we have conducted lab work in order to calculate leaf area, wood density, and Carbon13:Carbon12 (C13:C12) ratios for each of our samples. We are interested in C13:C12 ratio in plants because it is a useful measure of plant water use efficiency. We dried and weighed all wood and leaf samples. Once leaf samples were dried, we ground, homogenized and micro-weighed them to 2-3mg in preparation to send them to the University of California Davis Isotope lab for C13:C12 ratio analysis.

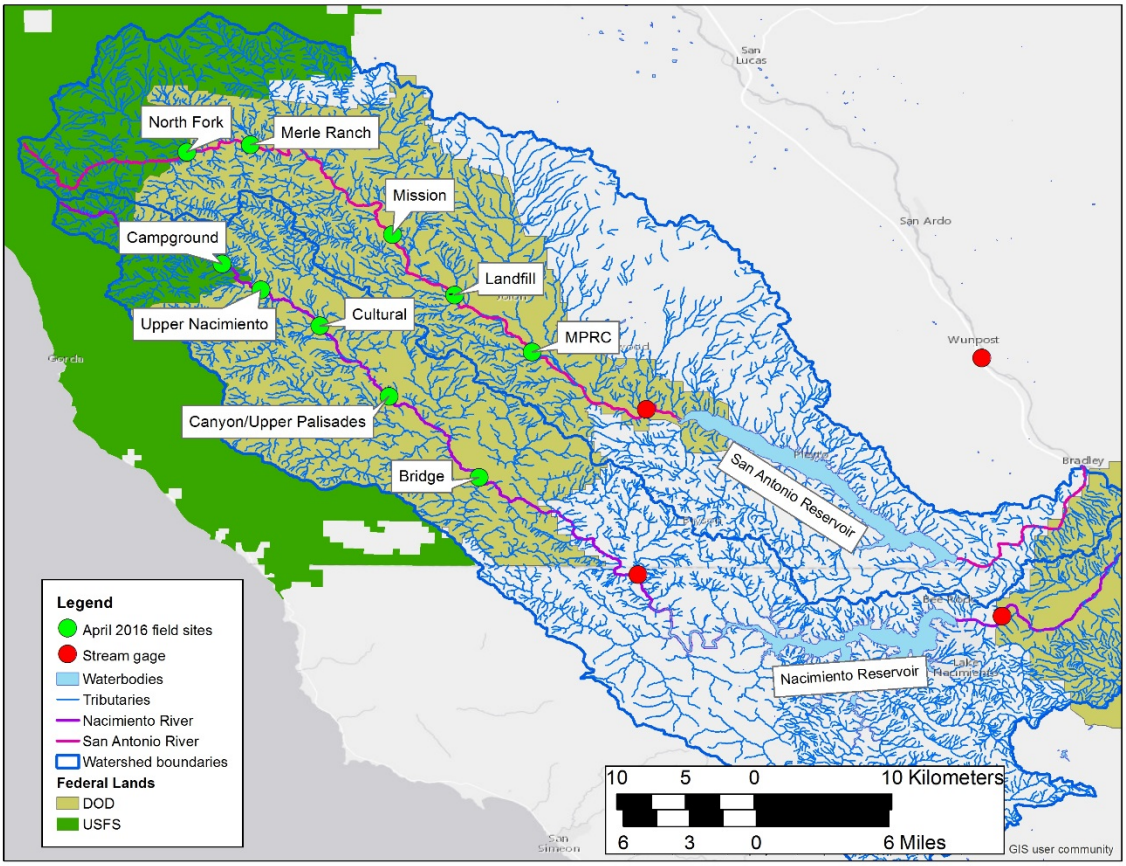

Figure 3.1.3 Field sampling sites visited in April, 2016 along the San Antonio and Nacimiento Rivers through Los Padres National Forest and Fort Hunter Liggett.

We are planning to collect detailed topographic surveys of the San Antonio floodplain at two chosen focal sites: the landfill and north fork sites (Table 3.1.6) in February, 2017. FHL has shared with us recent LiDAR data and the resulting high resolution elevation maps of the base. We will work from these elevation maps to tie in our own detailed surveys of the channel and floodplain. From these detailed surveys and high resolution elevation maps, we will build 2-D hydraulic models which will be the base of our floodplain vegetation modeling under climate change scenarios.

We are also planning to make a final field trip to FHL and LPNF in April, 2017 to do a detailed survey of floodplain vegetation in the Landfill and North Fork sites. We will then link the field-collected vegetation data to the topographic surveys and hydraulic models and hydrologic records to produce floodplain vegetation maps under likely future climate change scenarios.

Our goal is to create informed models of floodplain vegetation based on physical characteristics of the floodplain hydrology that can be used by base managers and Forest Service line officers to understand how floodplain vegetation is expected to change under various climate change scenarios. Further, we seek to develop models that are applicable to other public lands in the

Mediterranean, California Coastal Range Open Woodland-Shrub-Coniferous Forest-Meadow ecoregion, including US Forest Service lands of Los Padres National Forest. These models should help land managers develop vulnerability assessments and incorporate climate change into land management.

Table 3.1.7 Vegetation species list for the Nacimiento and San Antonio Rivers through Fort Hunter Liggett.

Acer macrophyllum	*Lupinus manis*
Aesculus californica	*Melilotis indicus*
Alnus rhombifolia	*Mentha* spp.
Anthriscus caucalis	*Platanus racemosa*
Apocynum cannabinum	*Polygonum amphibium*
Artemisia douglasiana	*Populus fremontii*
Arundo donax	*Potentilla glandulosa*
Baccharis pilularis	*Quercus agrifolia*
Baccharis salicifolia	*Quercus berberidifolia*
Brassica nigra	*Quercus chrysolepis*
Brickellia californica	*Quercus douglasii*
Bromus diandrus	*Quercus lobata*
Calystegia malacophylla	*Quercus wislizeni*
Carduus nutans	*Rosa californica*
Cirsium vulgare	*Rumex crispus*
Clematis ligusticifolia	*Rumex salicifolius*
Cornus glabrata	*Salix exigua*
Datisca glomerata	*Salix laevigata*
Datura spp.	*Salix lasiolepis*
Erigeron phildelphicus	*Salix lucida*
Erigeron spp.	*Salix melanopsis*
Eriogunum viridescens	*Sambucus nigra*
Euthamia occidentalis	*Stachys ajugoides*
Galium aparine	*Thalictrum fendleri*
Heterotheca spp.	*Umbellularia californica*
Hoita macrostachya	*Veronica anagallis-aquatica*
Juglans hindsii	*Vicia* spp.
Lolium perenne	

Fish - We employed two-pass electrofishing for five sites on each river. We used a Smith Root L-24 Backpack Electrofishing Unit with a standard anode (25 cm diameter ring attached to a 2 m pole) and cathode (3.2 m wire cable) following the protocols recommended by the U.S. Fish and Wildlife (U.S. Fish and Wildlife Service. 2000. Principles and Techniques of Electrofishing). For each reach, a 100 m stretch of the river was blocked at the upstream and downstream ends with 5-mm bar mesh block nets unless there was a riffle that would prevent easy passage out of the sampling reach. The operator and two dip-netters electrofished from the downstream end of the site and, using short, intermittent pulses, moved upstream in a zigzag fashion. Fish were

immediately placed in 5-gallon buckets (equipped with an aerator) containing fresh river water stationed at the river bank in the shade, where possible, thus ensuring the same environmental parameters (e.g., temperature, oxygen) as the natural habitat of the fish. All collected fish were identified and enumerated, measured for total length (mm) and biomass (g) and then released back into the river.

A total of six fish species and 21 individuals on the Nacimiento River and eight species and 145 individuals on the San Antonio River were captured and released using backpack electrofishing (Table 3.1.8, Table 3.1.9). Rainbow trout individuals in the Nacimiento River were most likely captured because they were recently stocked into river in Los Padres National Forest a few days prior to our sampling. All of the rainbow trout were between 260-350 mm in length. Invertebrate and plant samples from the 2016 survey are still being processed.

Table 3.1.8 Summary of species and number of individuals captured at each location on the Nacimiento River.

Common name	Scientific name	Above bridge	Campground	Canyon reach	Cultural site	Upper
Sacramento sucker	*Catostomus occidentalis*	1		2	2	
Monterey roach	*Lavinia symmetricus*				1	
Green sunfish	*Lepomis cyanellus*	2		2		
Redeye bass	*Micropterus coosae*	1		1		
Largemouth bass	*Micropterus salmoides*			1		
Rainbow trout	*Oncorhynchus mykiss*		7			1

Table 3.1.9 Summary of species and number of individuals captured at each location on the San Antonio River.

Common name	Scientific name	Land fill	Merle Ranch	Mission crossing	Multi-purpose range crossing	North Fork confluence
Sacramento sucker	*Catostomus occidentalis*	1			4	4
Western mosquitofish	*Gambusia affinis*	22				
Three-spine stickleback	*Gasterosteus aculeatus*	19		6	12	
Monterrey roach	*Lavinia symmetricus*	2	15	17	13	2
Green sunfish	*Lepomis cyanellus*		1			
Rainbow trout	*Oncorhynchus mykiss*					4
Sacramento pikeminnow	*Ptychocheilus grandis*	2				1
Speckled dace	*Rhinichthys osculus*				13	7

3.1.4 Los Padres National Forest

In April, 2016 we made preliminary visits to field sites along the Nacimiento and San Antonio Rivers through Fort Hunter Liggett (FHL) and adjacent Los Padres National Forest (LPNF). We visited ten sites (Figure 3.1.4, Table 3.1.10) and surveyed plants to collect trait data including height, stem diameter, canopy cover and collected leaf and wood samples to determine specific leaf area, wood density, and Carbon13:Carbon12 ratios. We sampled trait data from 96 individual plants covering 55 different plant species on the floodplains and channel margins of the Nacimiento and San Antonio Rivers (Table 3.1.11). Our ten field sites included three distinct geomorphic settings: low energy floodplains, medium energy confined, and medium energy open reaches along the Nacimiento and San Antonio Rivers (from our hydrogeomorphic valley classification (HGVC) mapping).

Table 3.1.10 Site descriptions for ten sites visited in April, 2016 along the San Antonio River (top five sites) and the Nacimiento River (bottom five sites) through Los Padres National Forest and Fort Hunter Liggett.

Site Name	Stream gage record	LiDAR	Hydrology	Valley type	Latitude	Longitude
North Fork San Antonio	NA	No*	Perennial	Medium energy confined	36.064836	-121.388849
Merle Ranch	NA	Yes	Perennial	Medium energy open	36.069728	-121.347261
Mission	NA	Yes	Perennial	Medium energy confined	36.010985	-121.254363
Landfill	1965-2016 *13 km downstream	Yes	Intermittent?	Low energy floodplain	35.971404	-121.213623
MPRC	1965-2016 *8 km downstream	Yes	Intermittent?	Medium energy open	35.934091	-121.162942
Campground	NA	No	Perennial	Medium energy confined	35.991634	-121.365791
Upper Nacimiento	NA	Yes	Intermittent?	Medium energy confined	35.974745	-121.340512
Cultural	NA	Yes	Perennial	Medium energy confined	35.951302	-121.301768
Canyon/ Upper Palisades	NA	Yes	Perennial	Medium energy confined	35.905102	-121.256641
Bridge	1971-2016 *12 km downstream	Yes	Intermittent?	Medium energy confined	35.852199	-121.197605

The Nacimiento and San Antonio Rivers benefit from natural flow regimes, unimpeded by any reservoirs upstream of our study sites. In all sites we visited, the vegetation was dominated by important native woody species such as sycamore, cottonwood, alder, willows and oaks. We noticed that the alder were severely diseased at several sites on the middle sections of both the Nacimiento and San Antonio Rivers including major damage at the Merle Ranch, Mission Confluence on the San Antonio and the Upper and Cultural sites on the Nacimiento. The disease is likely a fungal pathogen, such as Pytophthora, which has been documented infecting alders western Oregon.

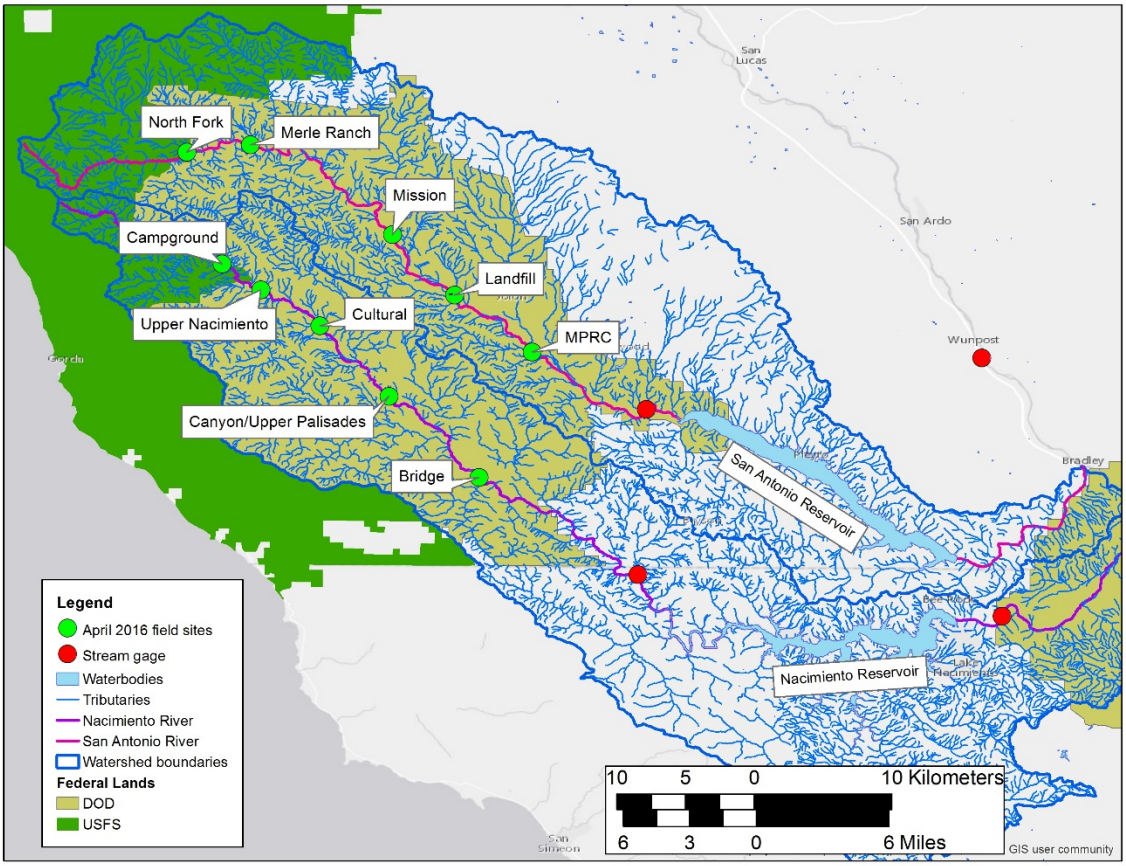

Figure 3.1.4 Field sampling sites visited in April 2016 along the San Antonio and Nacimiento Rivers through Los Padres National Forest and Fort Hunter Liggett.

Since our field trip in April, we have conducted lab work in order to calculate leaf area, wood density, and Carbon13:Carbon12 (C13:C12) ratios for each of our samples. We are interested in C13:C12 ratio in plants because it is a useful measure of plant water use efficiency. We dried and weighed all wood and leaf samples. Once leaf samples were dried, we ground, homogenized and micro-weighed them to 2-3mg in preparation to send them to the University of California Davis Isotope lab for C13:C12 ratio analysis.

We are planning to collect detailed topographic surveys of the San Antonio floodplain at two chosen focal sites: the landfill and north fork sites (Table 3.1.10) in February, 2017. FHL has shared with us recent LiDAR data and the resulting high resolution elevation maps of the base. We will work from these elevation maps to tie in our own detailed surveys of the channel and floodplain. From these detailed surveys and high resolution elevation maps, we will build 2-D hydraulic models which will be the base of our floodplain vegetation modeling under climate change scenarios.

We are also planning to make a final field trip to FHL and LPNF in April, 2017 to do a detailed survey of floodplain vegetation in the Landfill and North Fork sites (Figure 1). We will then link

the field-collected vegetation data to the topographic surveys and hydrologic models to produce floodplain vegetation maps under climate change scenarios.

Our goal is to create informed models of floodplain vegetation based on physical characteristics of the floodplain hydrology that can be used by base managers and Forest Service managers to understand how floodplain vegetation is expected to change under various climate change scenarios. Further, we seek to develop models that are applicable to other public lands in the Mediterranean, California Coastal Range Open Woodland-Shrub-Coniferous Forest-Meadow ecoregion, including US Forest Service lands of Los Padres National Forest. These models should help land managers develop vulnerability assessments and incorporate climate change into land management.

Table 3.1.11 Vegetation species list for the Nacimiento and San Antonio Rivers through Fort Hunter Liggett.

Acer macrophyllum	*Lupinus manis*
Aesculus californica	*Melilotis indicus*
Alnus rhombifolia	*Mentha* spp.
Anthriscus caucalis	*Platanus racemosa*
Apocynum cannabinum	*Polygonum amphibium*
Artemisia douglasiana	*Populus fremontii*
Arundo donax	*Potentilla glandulosa*
Baccharis pilularis	*Quercus agrifolia*
Baccharis salicifolia	*Quercus berberidifolia*
Brassica nigra	*Quercus chrysolepis*
Brickellia californica	*Quercus douglasii*
Bromus diandrus	*Quercus lobata*
Calystegia malacophylla	*Quercus wislizeni*
Carduus nutans	*Rosa californica*
Cirsium vulgare	*Rumex crispus*
Clematis ligusticifolia	*Rumex salicifolius*
Cornus glabrata	*Salix exigua*
Datisca glomerata	*Salix laevigata*
Datura spp.	*Salix lasiolepis*
Erigeron phildelphicus	*Salix lucida*
Erigeron spp.	*Salix melanopsis*
Eriogunum viridescens	*Sambucus nigra*
Euthamia occidentalis	*Stachys ajugoides*
Galium aparine	*Thalictrum fendleri*
Heterotheca spp.	*Umbellularia californica*
Hoita macrostachya	*Veronica anagallis-aquatica*
Juglans hindsii	*Vicia* spp.
Lolium perenne	

3.1.5 Piñon Canyon Manouver Site - Comanche National Grassland

In July 2016 we visited field sites along the Purgatoire River through Comanche National Grassland in Picket Wire Canyon. We visited six sites (Figure 3.1.5, Table 3.1.12) and surveyed plants to collect data on plant traits including height, stem diameter, canopy cover and collected leaf and wood samples to determine specific leaf area, wood density, and Carbon13:Carbon12 ratios. We sampled trait data from 131 individual plants covering 56 different plant species on the floodplains and channel margins of the Purgatoire River (Table 3.1.13). We also collected vegetation composition data at the gage site where we collected occurrence data of plant species in $1m^2$ plots. Bruce Schumacher and Steve Olson were of great help to us, from arranging accommodations and orienting us to the lay of the land, to plant identification and the use of equipment. They enabled us to make the trip very efficient and effective.

Table 3.1.12 Site descriptions for six sites visited in July, 2016 along the Purgatoire River through Comanche National Grassland.

Site Name	Stream gage record	Hydrology	Valley type	Latitude	Longitude
Bunkhouse	NA	Perennial	Medium energy open	37.590151	-103.636232
Gage	1983-2016	Perennial	Medium energy open	37.606733	-103.603624
Arroyo	1983-2016	Perennial	Medium energy open	37.611723	-103.606323
Cemetery	NA	Perennial	Medium energy open	37.635847	-103.578338
Withers	NA	Perennial	Medium energy open	37.646227	-103.559111
Boundary	NA	Perennial	Medium energy open	37.667647	-103.543115

In general, the riparian zone along the Purgatoire River through Comanche National Grassland shows evidence of human and fire impacts, but many important native species are still present. There is evidence of a recent fire in the last ten years with many cottonwood trees showing blackened bark, resprouting, and root suckering. The stream channel is constrained in entrenched meanders throughout the study area with evidence of channel head cutting near the confluence of Bent Canyon just upstream from the Picket Wire Bunkhouse. Much of the herbaceous vegetation on the old floodplain, which is now a post-incision terrace, is weedy with evidence of grazing that occurred during the mid-twentieth century. Amaranth, sunflower, sticky gum weed, non-native grasses and other ruderal, weedy species provide an indication of range degradation. However, the full complement of native woody riparian vegetation is present: cottonwood, peachleaf willow, sandbar willow, hackberry, golden currant and hoptree.

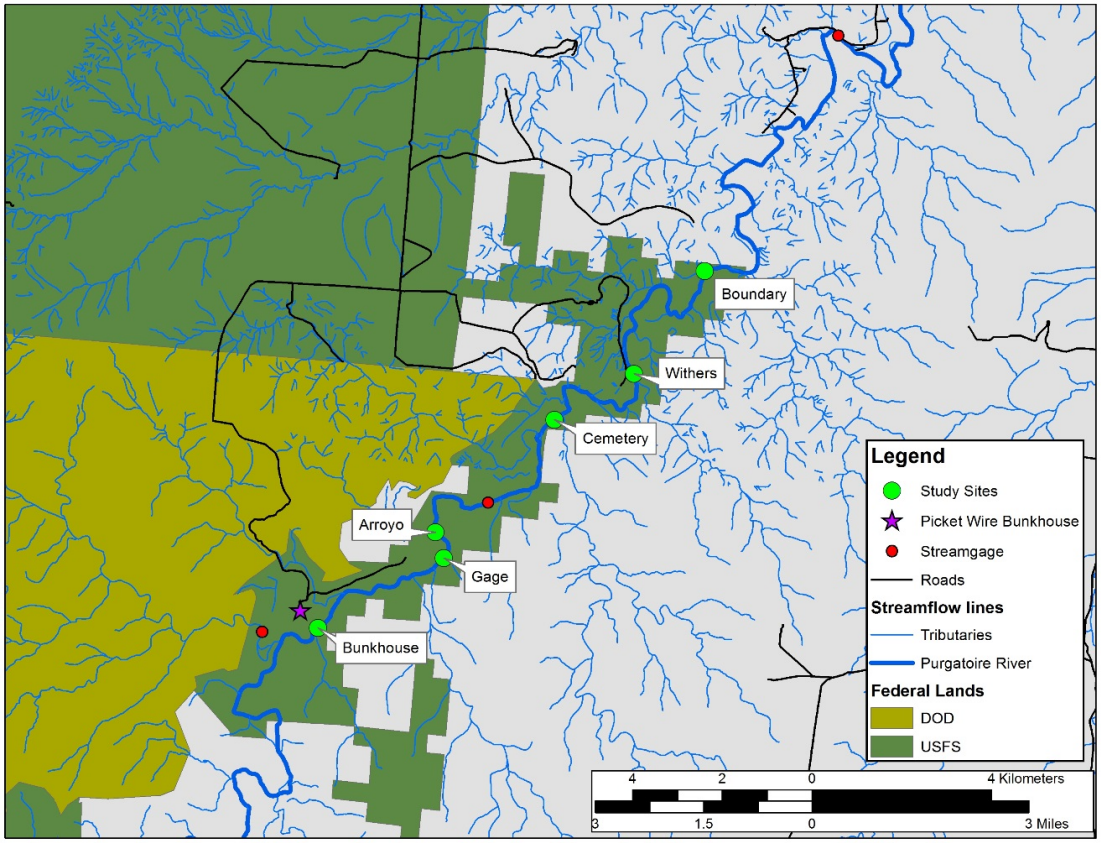

Figure 3.1.5 Field sampling sites visited in July, 2016 along the Purgatoire River through Comanche National Grasslands.

Since our field trip in July, we have conducted lab work in order to calculate leaf area, wood density, and Carbon13:Carbon12 (C13:C12) ratios for each of our samples. We are interested in C13:C12 ratio in plants because it is a useful measure of plant water use efficiency. We dried and weighed all wood and leaf samples. Once leaf samples were dried, we ground, homogenized and micro-weighed them to 2-3mg in preparation to send them to the University of California Davis Isotope lab for C13:C12 ratio analysis.

We are planning to collect detailed topographic surveys of the Purgatoire floodplain at our chosen focal site: the gage site (Table 3.1.12) in 2017. From our detailed surveys we will build 2-D hydraulic models which will be the base of our floodplain vegetation modeling under climate change scenarios. We will then link the field-collected vegetation plot data (gathered and surveyed in July, 2016) to the topographic surveys and hydraulic-hydrologic models to produce floodplain vegetation maps under current and future climate change and water management scenarios.

Our goal is to create informed models of floodplain vegetation based on physical characteristics of the floodplain hydrology that can be used by Forest Service line officers to understand how floodplain vegetation is expected to change under various climate change scenarios. Further, we seek to develop models that are applicable to other public lands in southeastern Colorado and the

southern Great Plains-Dry Steppe ecoregions). These models should help the forest in forest plan revisions, vulnerability assessments, and incorporating climate change into land management.

Table 3.1.13 Vegetation species list for the Purgatoire River Study Sites.

Amaranth spp.	*Mirabilis linearis*
Ambrosia psilostachya	*Mirabilis multiflora*
Amorpha fruticosa	*Muhlenbergia asperifolia*
Apocynum cannabinum	*Oenothera curtiflora*
Asclepias speciosa	*Panicum virgatum*
Asclepias subverticillata	*Pascopyrum smithii*
Bothriochloa laguroides	*Phragmites australis*
Carex spp.	*Physalis longifolia*
Celtis laevigata	*Polygonum lapathifolium*
Cirsium spp.	*Polygonum* spp.
Cleome serrulata	*Polypogon monspeliensis*
Conyza canadensis	*Populus deltoides*
Croton texansis	*Proboscidea louisianica*
Cucurbita foetidissima	*Ptelea trifoliata*
Cynodon dactylon	*Ratibida tagetes*
Eleocharis palustris	*Rhus trilobata*
Elymus canadensis	*Ribes aureum*
Equisetum hyemale	*Rumex* spp.
Ericameria nauseosa	*Salix amygdaloides*
Erigeron spp.	*Salix exigua*
Euphorbia marginata	*Sambucus* spp.
Glycyrrhiza lepidota	*Sarcobatus vermiculatus*
Grindelia inornata	*Schoenoplectus pungens*
Helianthus annuus	*Solidago canadensis*
Juniperus monosperma	*Sphaeralcea angustifolia*
Lactuca serriola	*Tamarix ramosissima*
Lycium pallidum	*Vitis riparia*
Melilotus spp.	*Xanthium strumarium*

3.2 Vital rate estimation

3.2.1 Xeroriparian shrub and hydroriparian tree

Xeroriparian shrub and hydroriparian tree possess similar vital rates in terms of response to flooding, timing of seedset, and other vital rates. We review the literature pertaining to these two guilds and present the relevant data here. For xeroriparian shrub we used chronosequence studies along the upper and lower Colorado River, where stem thinning rate averaged 2,317 (±394) stems ha^{-1} yr^{-1} along the upper Colorado River and 3,257 (±937) stems ha^{-1} yr^{-1} along the lower Colorado River (Merritt and Shafroth 2012). Self-thinning relations were: S = 130,790-2,317(age) and S = 167,781-3,257(age). Stands older than 50 years had average stem densities of 12,300 and 16,800 stems ha^{-1} along the upper and lower Colorado River, respectively. There was no significant difference in the thinning rate between the upper and lower Colorado River (P = 0.1), and the overall thinning rate of xeroriparian shrub was 2,455 ±312 stems ha^{-1} yr^{-1} over the 70 years modeled. The relationship between stand age and xeroriparian shrub stem density (ST) along both upper and lower Colorado River sites was ST = 135,478-2,455(age) (r^2 = 0.27; P < 0.0001). Using data from Horton and Clark (2001) and Shafroth et al. (1998) we estimated the relationship between stage decline and seedling recruitment for xeroriparian shrub as $g(h) = 0.92*\exp[-0.5*((h-1.8)/3.4)^2]$ for $h \geq 0$; 0 otherwise. The shape of this function is similar to that of hydroriparian tree (Lytle and Merritt 2004), but reflects the fact that xeroriparian shrub seedlings are more tolerant of static water levels and rapid water declines than hydroriparian tree seedlings.

Hydroriparian tree and xeroriparian shrub have several similarities in terms of life history attributes and regeneration niche, as well as some important differences. Species in both guilds (e.g., *Populus deltoides* and *Tamarix ramosissima,* respectively) require bare, moist freshly exposed substrate for short-lived aerial or water dispersed seeds to germinate and become established (Merkel and Hopkins 1957, Warren and Turner 1975, Fenner et al. 1984). Flood-created bare patches and areas of fresh sediment deposition are common sites for recruitment; neither guild typically recruit into heavily vegetated or shaded areas (Braatne et al. 1996, Scott et al. 1996, Cooper et al. 1999). Typically, plant establishment occurs as part of the processes of channel narrowing, point bar development due to channel meandering, or overbank deposition of sediment (Scott et al. 1996, Cooper et al. 2003). If viable seeds reach such sites, hydrologic conditions are conducive to seedling survival, and subsequent disturbance does not remove or bury individuals, establishment may occur.

Timing of flowering and seed dispersal phenology differ significantly for the hydroriparian tree and xeroriparian shrub guilds in the climate of the Colorado Plateau and in much of the western U.S. (Warren and Turner 1975, Cooper et al. 1999). In warm climates, xeroriparian shrub may flower as early as its second year of growth and flowering may occur multiple times during the growing season (Merkel and Hopkins 1957, Horton et al. 1960). Older, larger individuals may

produce several hundred thousand seeds during a single season (Merkel and Hopkins 1957). Hydroriparian tree reaches reproductive stage later (5-10 years) and flowers only once per growing season, yet females may produce tens of thousands of seeds per growing season (Karrenberg and Suter 2003). Furthermore, xeroriparian shrub has bisexual flowers, so each individual produces seeds in contrast to dioecious hydroriparian tree, which has a lower ratio of seed producing individuals to individual plants (Warren and Turner 1975).

Our representative species for the hydroriparian guild, *Populus fremontii*, was found to release seeds over a six week period beginning in late-June along the Yampa River (Cooper et al. 1999). By contrast, our representative for xeroriparian shrub, *Tamarix*, began releasing seed in mid-July, seed rain peaked in mid-August, and seeds were still being dispersed in mid-September during the years measured (Cooper et al. 1999). Warren and Turner (1975) found that *Populus* dispersal occurred earlier than *Tamarix*, was of a shorter duration, and had almost ceased by the time the flowering season for *Tamarix* began along two rivers in Arizona, U.S.A.

Tamarix seed density in areas of establishment has been shown to be as high as ~5000 seedlings m^{-2} (Cooper et al. 1999) to 170,000 seedlings m^{-2} in dense *Tamarix* stands (Warren and Turner 1975). In germination trials, *Tamarix* seed viability ranged from 76% at the time of harvest to 40% after four months of cold storage (Merkel and Hopkins 1957), but seed viability in the field lasts only a few weeks (Horton et al. 1960). Laboratory trials indicate that viability ranges from 75% (Moss 1938) to greater than 90% (Van Splunder et al. 1995, Karrenberg and Suter 2003) for various species of *Populus*.

The combination of limited seed viability and differences in the separation in seed release timing of seed release may result in spatial separation in hydroriparian tree and xeroriparian invasive shrub recruitment sites, though mixed stands are not uncommon may occur due to dispersal overlap during the middle of some growing seasons. Hypocotyl extension and primary root growth occur in moist soils and at this stage seedlings are very vulnerable to desiccation. *Populus* seedling root growth rates have been shown to average 0.6-1.3 cm/day, resulting in 72-162 cm of root growth by the end of their first season (Fenner et al. 1984, Mahoney and Rood 1998, Horton and Clark 2001), however, it has been reported that *Populus* seedlings can survive ground water decline rates of 2-4 cm day^{-1} (Mahoney and Rood 1991, Segelquist et al. 1993). These values may more than double in finer soils with higher water-holding retention capacity soils (Cooper et al. 1999). *Populus* root growth and leaf area were found to be highest with steady shallow water tables and declined as a function of water table drawdown rate in rhizopod experiments (Mahoney and Rood 1991). *Tamarix* root growth rates were 1.1 cm d^{-1} in field studies in Arizona, U.S.A. (Merkel and Hopkins 1957). *Tamarix* survival was 86-92% across treatments involving lowering water tables 0, 1, 2, and 4 cm/d, though biomass declined with increasing rates of decline (Horton and Clark 2001). *Tamarix* root growth rate was highest in 1 cm d^{-1}water table drawdowns and *Tamarix* root length averaged 160 cm after 42 days of growth (about double that for *Salix gooddingii*) (Horton and Clark 2001). *Tamarix* seedlings are more tolerant of groundwater declines than are *S. gooddingii* and *Populus*), because it is known to

utilize water from both phreatic sources and unsaturated soils (Everitt 1980, Busch and Smith 1995). Higher drought tolerance may enable *Tamarix* seedlings to persist in dry soils where *Salix* and *Populus* seedlings are unable (Cooper et al. 1999, Horton and Clark 2001).

Seedlings in both guilds are vulnerable to flow-related scour and deposition as well as wind abrasion and dune-burial during the first several months of growth. Due to *Tamarix* seedlings' prostrate growth form in the seedling stage, it may render it be more susceptible than *Populus* to burial (Levine and Stromberg 2001), but may be more resistant to scour due to the high tensile strength of the roots (De Baets et al. 2008). *Tamarix* is more vulnerable to inundation and anoxia in seedling and sapling stages than *Populus* (Bhattacharjee et al. 2006). Sher et al. (2000) and Sher and Marshall (2003) found that *Tamarix* was competitively suppressed by *Populus* mixed stand experiments, suggest that flooding puts native *Populus* at a competitive advantage over *Tamarix*. Degree of shade had no effect on survival of *Populus* seedlings under well-watered conditions, but dramatically effected survival under drought conditions (43% survival in full sun; 0.03% survival in 4% sun) (Cooper et al. 1999). Interspecific competition contributed significantly to mortality over a range of light levels in field experimentation (Cooper et al.1999). Because *Tamarix* maximum aboveground height is less than *Populus*, competition for light and the negative effects of shading remain inhibitive for older age-classes of *Tamarix* (Dewine and Cooper 2008).

3.2.1.1 References

Bhattacharjee, J., J. P. Taylor and L. M. Smith. 2006. Controlled flooding and staged drawdown for restoration of native cottonwoods in the middle Rio Grande Valley, New Mexico, USA. Wetlands 26: 691-702.

Braatne, J. H., S. B. Rood and P. E. Heilman. 1996. Life history, ecology, and conservation of riparian cottonwoods in North America. Biology of *Populus*. R. F. Stettler, H. D. Bradshaw Jr., P. E. Heilman and T. M. Hinckley. Ottawa, ON, Canada, NRC Research Press, National Research Council of Canada: 57-85.

Busch, D. E. and S. D. Smith. 1995. Mechanisms associated with decline of woody species in riparian ecosystems of the southwestern U.S. Ecological Monographs 65: 347-370.

Cooper, D. J., D. C. Andersen and R. A. Chimner. 2003. Multiple pathways for woody plant establishment on floodplains at local to regional scales. Journal of Ecology 91: 182-196.

Cooper, D. J., D. M. Merritt, D. C. Andersen and R. A. Chimner. 1999. Factors controlling the establishment of Fremont cottonwood seedlings on the upper Green River, U.S.A. Regulated Rivers: Research and Management 15: 419-440.

De Baets, S., J. Poesen, B. Reubens, K. Wemans, J. De Baerdemaeker and B. Muys. 2008. Root tensile strength and root distribution of typical Mediterranean plant species and their contribution to soil shear strength. Plant and Soil 305: 207-226.

Dewine, J. M. and D. J. Cooper. 2008. Canopy shade and the successional replacement of tamarisk by native box elder. Journal of Applied Ecology 45: 505-514.

Everitt, B. L. 1980. Ecology of saltcedar- a plea for research. Environmental Geology 3: 77-84.

Fenner, P., W. W. Brady, and D. R. Patton. 1984. Observations on seeds and seedlings of Fremont Cottonwood. Desert Plants 6: 55-58.

Horton, J. L. and J. L. Clark. 2001. Water table decline alters growth and survival of *Salix gooddingii* and *Tamarix chinensis* seedlings. Forest Ecology and Management 140: 239-247.

Horton, J. S., F. C. Mounts and J. M. Kraft. 1960. Seed germination and seedling establishment of phreatophyte species. Research Note 50. Fort Collins, CO., U.S. Department of Agriculture, Rocky Mountain Forest and Range Experiment Station.

Karrenberg, S. and M. Suter. 2003. Phenotypic trade-offs in the sexual reproduction of Salicaceae from flood plains. American Journal of Botany 90: 749-754.

Levine, C. M. and J. C. Stromberg. 2001. Effects of flooding on native and exotic plant seedlings: implications for restoring southwestern riparian forests by manipulating water and sediment flows. Journal of Arid Environments 49: 111-131.

Lytle, D. A. and D. M. Merritt. 2004. Hydrologic regimes and riparian forests: a structured population model for cottonwood. Ecology 85: 2493-2503.

Mahoney, J. and S. Rood. 1991. A device for studying the influence of declining water-table on poplar growth and survival. 8: 305-314.

Mahoney, J. M. and S. B. Rood. 1998. Streamflow requirements for cottonwood seedling recruitment-an integrative model. Wetlands 18: 634-645.

Merkel, D. L. and H. H. Hopkins. 1957. Life History of Salt Cedar (*Tamarix gallica* L.). Transactions of the Kansas Academy of Science 60: 360-369.

Merritt, D. M. and P. B. Shafroth. 2012. Edaphic, salinity, and stand structural trends in chronosequences of native and non-native dominated riparian forests along the Colorado River, USA. Biological Invasions 14: 2665-2685.

Moss, E. H. 1938. Longevity of seed and establishment of seedlings in species of *Populus*. Botanical Gazette 99: 529-542.

Scott, M. L., J. M. Friedman and G. T. Auble. 1996. Fluvial process and the establishment of bottomland trees. Geomorphology 14: 327-339.

Segelquist, C. A., M. L. Scott and G. T. Auble. 1993. Establishment of *Populus deltoides* under simulated alluvial groundwater declines. American Midland Naturalist 130: 274-285.

Shafroth, P. B., G. T. Auble, J. C. Stromberg and D. T. Patten. 1998. Establishment of woody riparian vegetation in relation to annual patterns of streamflow, Bill Williams River, Arizona. Wetlands 18: 577-590

Sher, A. A. and D. L. Marshall. 2003. Seedling competition between native *Populus deltoides* (Salicaceae) and exotic *Tamarix ramosissima* (Tamaricaceae) across water regimes and substrate types. American Journal of Botany 90: 413-422.

Sher, A. A., D. L. Marshall and S. A. Gilbert. 2000. Competition between native *Populus deltoides* and invasive *Tamarix ramosissima* and the implications for reestablishing flooding disturbance. Conservation Biology 14: 1744-1754.

Van Splunder, I., H. Coops, L. Voesenek and C. Blom. 1995. Establishment of alluvial forest species in floodplains - the role of dispersal timing, germination characteristics and water-level fluctuations. Acta Botanica Neerlandica 44: 269-278.

Warren, D. K. and R. M. Turner. 1975. Saltcedar (*Tamarix chinensis*) seed production, seedling establishment, and response to inundation. Journal of the Arizona Academy of Science 10: 135-144.

3.2.2 Aquatic invertebrates

3.2.2.1 Estimating intrinsic rates of population increase

Intrinsic rates of population increase (r) for the three target taxa were tabulated from age-specific fecundity and survival rates from published values using the method of Birch (1948). r was defined as the number of offspring producded by one individual per day, thus measuring the per capita rate of increase over a short time (Gotelli 1998). The parameter values used for this approach, and the resulting estimated intrinsic rates of population increase, are given in Table B1. When information could not be found on the exact taxon of interest, information from a closely related taxon was used. When a range of values were reported, the average was used in the estimation.

3.2.2.2 Example Calculation of Intrinsic Rate of Increase

In order to calculate the estimated intrinsic rate of population increase, total average lifespan, number of eggs laid, and survivorship of life stages or overall survivorship were necessary (Table 3.2.1). Calculations began at the egg stage, and number of individuals were successively reduced by survivorship values until r was estimated. For example, for Fallceon quilleri, calculations began with eggs laid per individual (1850). The value of survivorship of eggs used was 80%, so 1850 was reduced to 1480. This was assumed to be the average number of offspring that survive to larval stage per individual. The value of survivorship of larvae used was 8.9%, so 1480 was reduced to 131.72. This was assumed to be the average number of offspring that survive to the adult stage per individual. The value of survivorship of pre-reproductive adults used was 5%, so 131.72 was reduced to 6.57. This value was divided by the mean duration of lifecycle, 28.5 days, to arrive at an estimated intrinsic rate of population increase of 0.23.

Table 3.2.1 Parameter values used for life-table calculations and resulting estimated intrinsic rates of population increase.

	Mayfly (Fallceon quilleri)	Dragonfly (Progomphus borealis)	Ostracod (Ostracoda)
Egg stage duration (d)	3-34 (18.5)	13 to 56 (34.5)	9 to 86 (47.5)
Egg stage survivorship (%)	70-90 (80)	77.4	-
Larval stage duration (d)	6- 12 (9)	30-180 (105)	21-365 (193)
Larval survivorship (%)	8.9	2.53	-
Adult stage duration (d)	1	30	28-180 (104)

Adult survivorship (pre-reproductive) (%)	1.2-8.8 (5)	78.2	-
Overall survivorship (%)	-	-	40-80 (60)
Mean life cycle duration (d)	28.5	181.5	344.5
Eggs laid per individual	1200-2500 (1850)	1000	8-180 (94)
Estimated intrinsic rate of population increase (r)	0.23	0.08	0.16

Sources: Information used for parameter values were found in Ferguson 1944, Gray 1981, Corbet 1999, Braune et al. 2008, Dole-Olivier et al. 2000, Gandolfi et al. 2001, Werneke and Zwick 2006, and Merritt et al. 2008.
Note: Mean values used in the analyses shown in parentheses.

3.2.2.3 References

Birch, L.C. 1948. The intrinsic rate of natural increase of an insect population. Journal of Animal Ecology 17: 15-26.

Braune, E., Richter, O., Sondgerath, D., and F. Suhling. 2008. Voltinism flexibility of a riverine dragonfly along thermal gradients. Global Change Biology 14: 470-482.

Corbet, P.S. 1999. Dragonflies: Behavior and Ecology of Odonata. Cornell University Press.

Ferguson, E. 1944. Studies on the seasonal life history of three species of freshwater ostracoda. American Midland Naturalist 32: 713-727.

Gandolfi, A., Todeschi, E.B.A., Rossi, V. and Monozzi, P. 2001. Life history in Darwinula stevensoni (Crustacea: Ostracoda) from Southern European populations under controlled conditions and their relationship with genetic features. Journal of Limnology 60: 1-10.

Gotelli, N.J. 1998. A Primer of Ecology, 2nd ed. Sinauer Associates, Inc.

Merritt, R.W., Cummins, K.W., and Berg, M.B. 2008. An Introduction to the Aquatic Insects of North America. Kendall Hunt Publishing Company.

Werneke, U. and Zwick, P. 1992. Mortality of the terrestrial adult and aquatic nymphal life stages of Baetis vernus and Baetis rhodani in the Breitenbach, Germany (Insecta: Ephemeroptera). Freshwater Biology 28: 249-255.

4 Task 4: Forecast ecological effects of changing flow regimes

4.1 Hydraulic and Variable Infiltration Capacity modeling

4.1.1 Hydrograph scenarios

Coastal California rivers are characterized by high flows during winter and early spring months, November to March. Peak streamflow months are driven by low pressure systems moving inland from the Pacific Ocean bringing rain to the coastal ranges, which almost immediately runs off in streamflow. Typical of Mediterranean climates, coastal California summers are hot and dry and the corresponding low flow season is approximately May through October (Figure 4.1.1 and Figure 4.1.2). Climate change projections and hydrologic modeling for California suggest a generally drying climate with more extremes in both wet and dry years. Recent climate modelling efforts show that there is likely to be more extreme flooding in wet seasons, and at the same time, more extreme and prolonged drought in the dry season and across dry years (Yoon et al. 2015, Mallakpour et al. 2018, Swain et al. 2018). Yet, there is still evidence for a drying climate change signal, driven by drier warm season conditions that could result in overall drier conditions (Das et al. 2011). Earlier studies that focused on mean annual flow of California streams found equivocal results for precipitation, with uncertainty in the direction and magnitude of precipitation changes, yet overall climate warming and decreases in mean annual flows (Hayhoe et al. 2004, Maurer and Duffy 2005, Vicuna et al. 2007, Cayan et al. 2008).

Based on current published climate and hydrologic modeling for California, we developed six scenarios for each of our rivers. The first five scenarios represents a percent change in daily discharge from the historic stream flow record, and the sixth scenario is drawn directly from Variable Infiltration Capacity (VIC) model output for an AIB emissions scenario for our rivers obtained from Luce, Wenger and colleagues (Wenger et al. 2010) :
Wetter wet years (increase flows 50%), drier dry years (decrease flows 30%)
All flows decrease 30%
All flows decrease 60%
All flows increase 30%
Reservoir scenario: increase base flows 20%, alter flows during peaks between that exceed the 1-year, by decreasing to 1-year flood levels
VIC late century (2080s) AIB scenario

We used annual Palmer Drought Severity Index for the historic period for each gage record to assign wet and dry years: if the corresponding monthly PDSI value is positive, hydrologic conditions are wetter than average, and when PDSI is negative, hydrologic conditions are drier than average (Figure 4.1.3 and Figure 4.1.4Figure 4.1.3). Scenarios 1-3 percentage decreases and increases are based on current literature on climate change forecasts for California. Yoon and

others (2015) found that both intense drought and intense flooding would increase more than 50%, and Mallakpour and others (2018) found from 0-30% decreases in low flows and from 0-50% increases in high flows. Thus, in our approach for Scenario 1, every flow that fell in a wet PDSI period, flow was increased 50% and for every flow that fell in a PDSI dry period, flow was decreased 30%. Scenario 2 and 3 simulate an over-all drying climate by a moderate amount (scenario 2, 30%) and a more extreme amount (scenario 3, 60%). Scenario 4 is a wet-extreme scenario that has been demonstrated in some model output, although a minority. We use Scenario 4 to demonstrate an opposite end-member hypothesis. Scenario 5 simulates the installation of a dam and reservoir in the headwaters of each stream. Scenario 5 shows typical effects of dam management on rivers: increased base flows and decreased peak flows.

For scenario 6, we obtained daily discharge volumes for 90 years of models runs by the variable infiltration capacity (VIC) model for our study stream reaches for a late-century future A1B emissions (centered on the 2080s) (Wenger et al. 2010). The A1B scenario is analogous to the Representative Concentration Pathway (RCP) scenario 6.0, a "middle-of-the-road" scenario. We transformed discharge volumes (cubic meters) into flow rates (cubic meters per second, cfs) to obtain mean daily discharges, comparable to the historic streamflow record.

Scenario development resulted in five time series based on the historical gage record (Figure 4.1.5 and Figure 4.1.6) and one scenario based on hydrologic model output. Finally, we calculated the flow duration curves calculated from each streamflow record (Figure 4.1.7 and Figure 4.1.8).

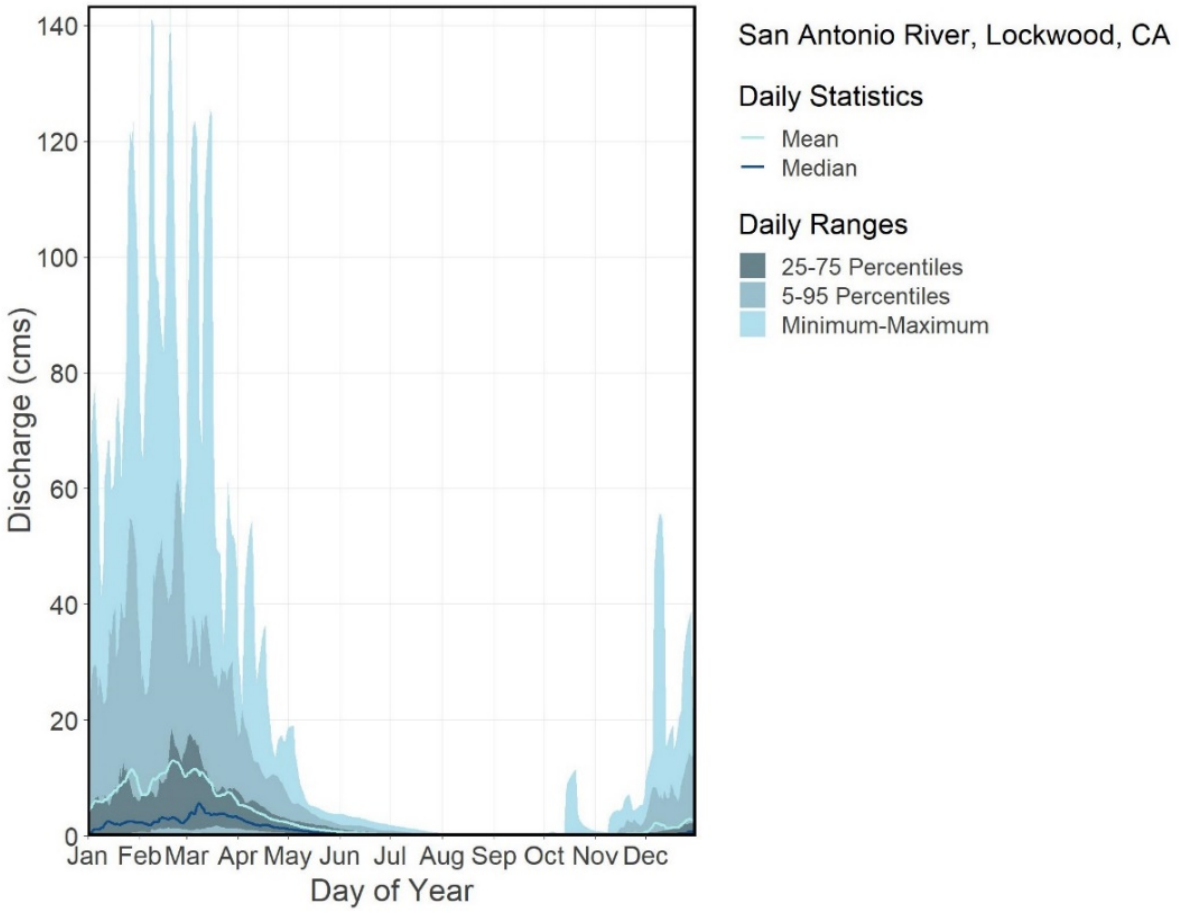

Figure 4.1.1 Mean and median (light and dark blue lines) daily flow statistics calculated from the USGS observed historical stream gage record for the San Antonio River, near Lockwood, CA, water years 1965-2018.

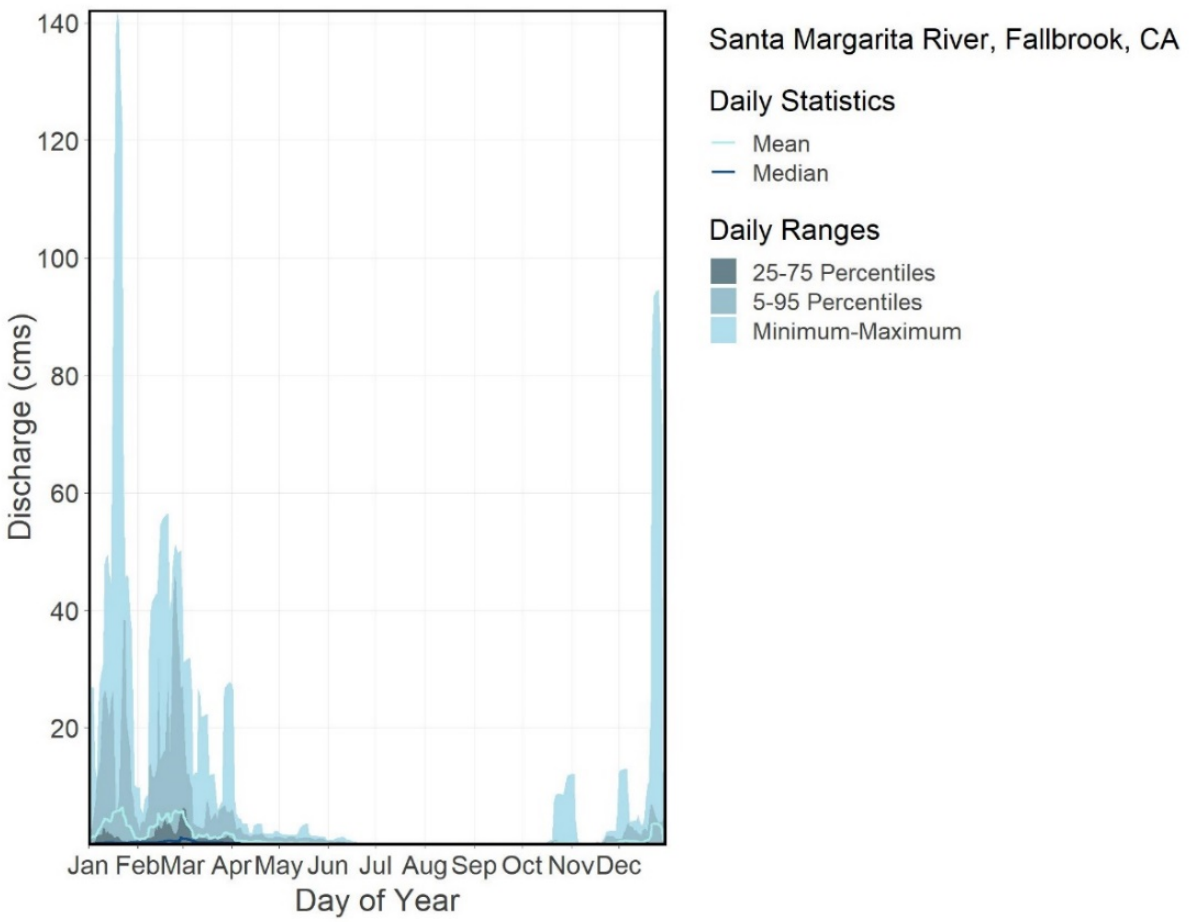

Figure 4.1.2 Mean and median (light and dark blue lines) daily flow statistics calculated from the USGS observed historical stream gage record for the Santa Margarita River, near Fallbrook, CA, water years 1990-2018.

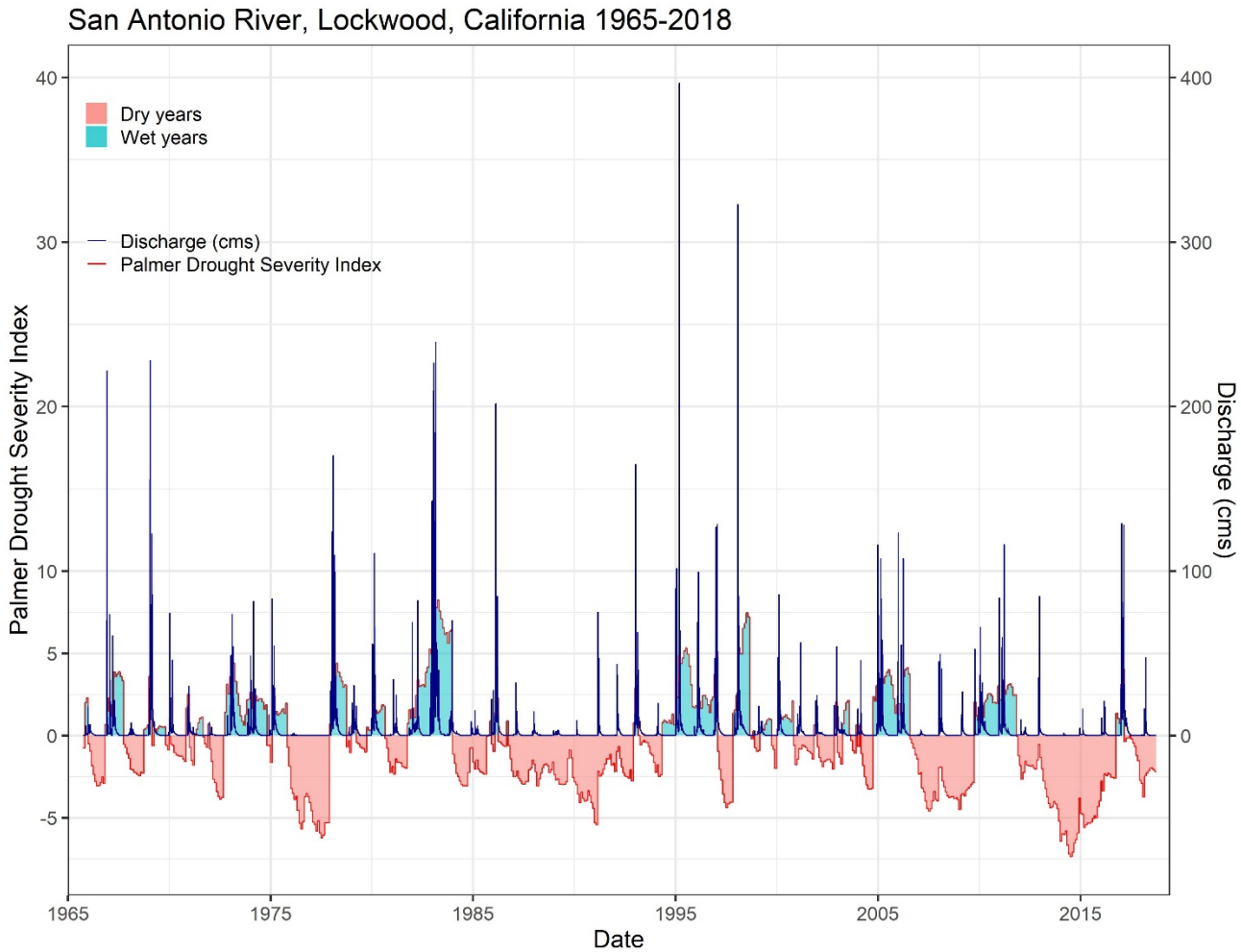

Figure 4.1.3 Time series of Palmer Drought Severity Index (PDSI, left axis) for central coastal California 1965-2018 superimposed on the stream flow record for the San Antonio River near Lockwood, California (Discharge, cms, right axis).

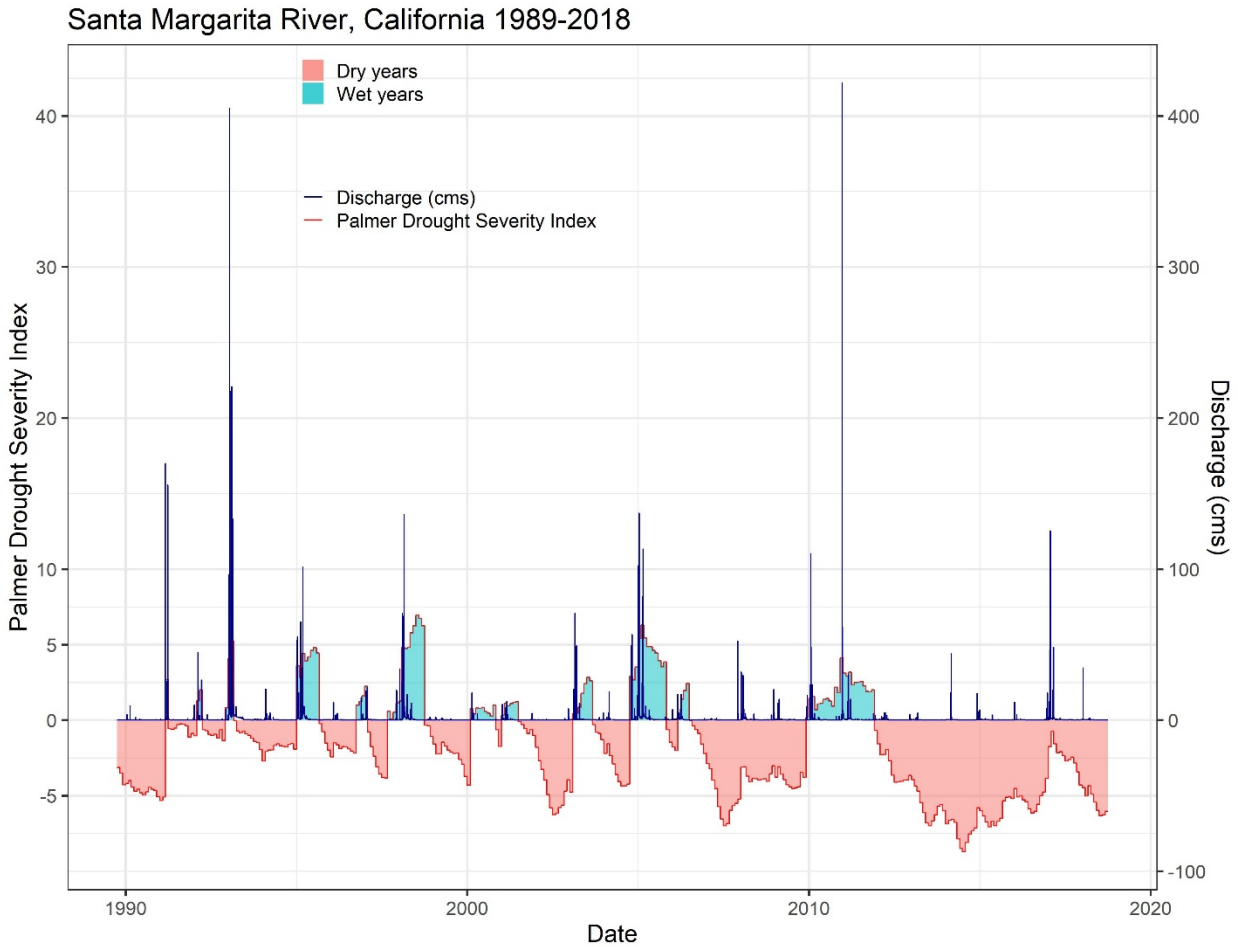

Figure 4.1.4 Time series of Palmer Drought Severity Index (left axis) for southern coast of California 1989-2018 superimposed on the stream flow record for the Santa Margarita River near Fallbrook, California (Discharge, cms, right axis).

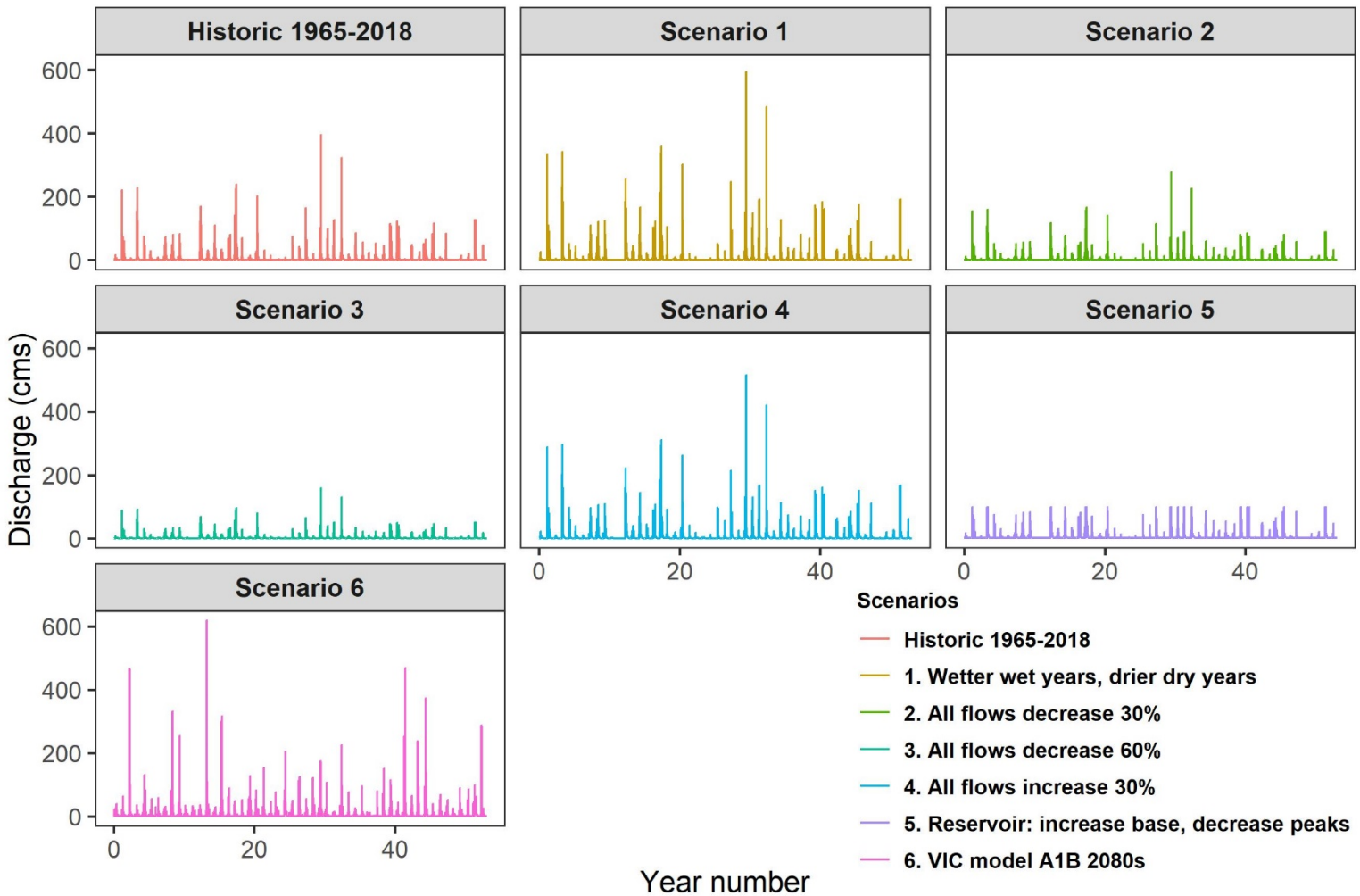

Figure 4.1.5 Daily mean discharge (cms) over time for the San Antonio River, California showing the historic record (top left) and six flow scenarios from left to right: Scenario 1: wetter wet years (increase flows 50%), drier dry years (decrease flows 30%); Scenario 2: All flows decreased 30%; Scenario 3: All flows decreased 60%; Scenario 4: all flows increased 30%; Scenario 5: reservoir-influenced flow with increased base flows (20%), and altered flows during peaks between the 1-year and 5-year flood discharge by decreasing to 1-year flood discharge; Scenario 6: Variable infiltration capacity (VIC) hydrologic model output for AIB late century 2080s emissions scenario.

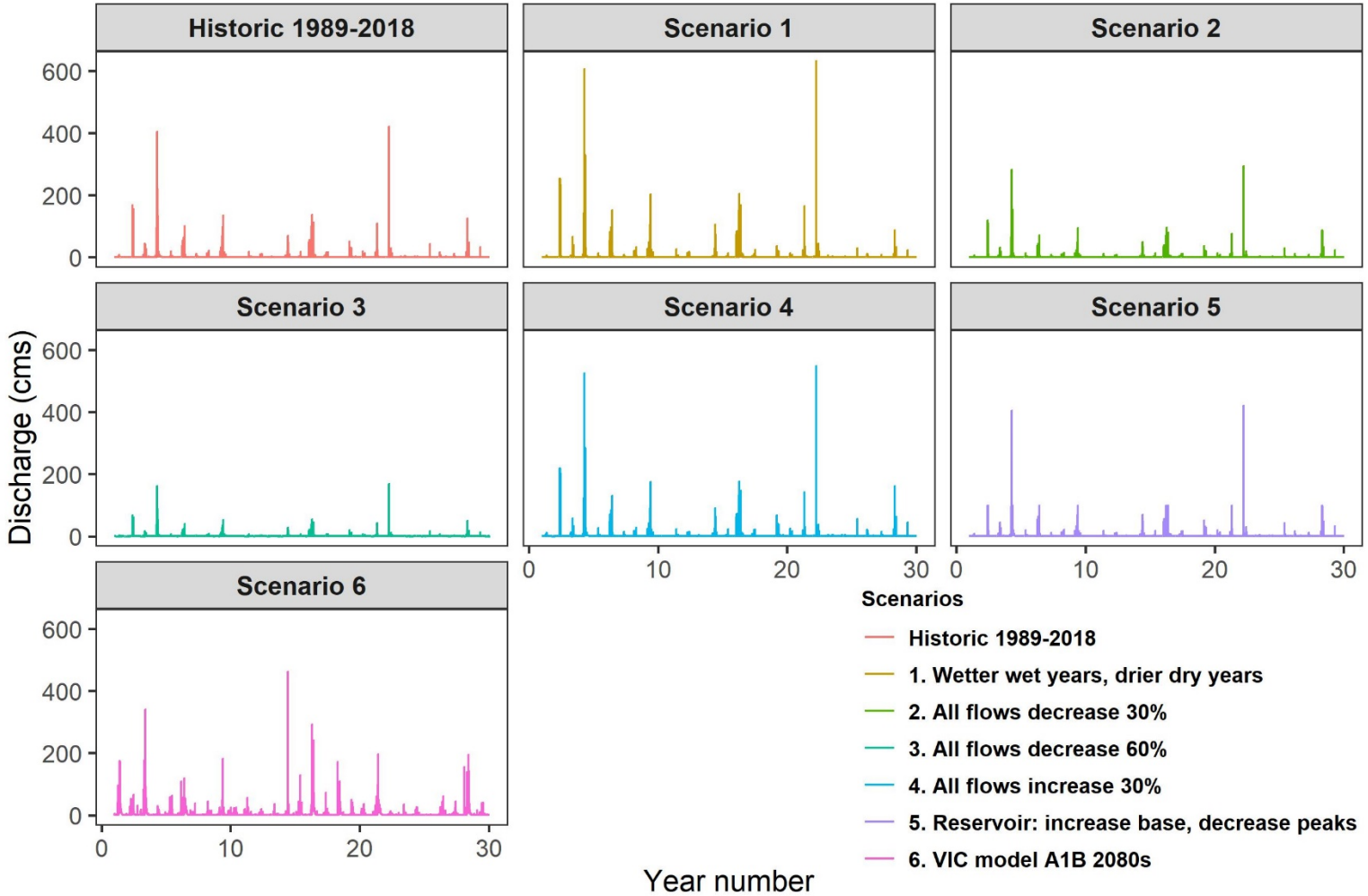

Figure 4.1.6 Daily mean discharge (cms) over time for Santa Margarita River, Fallbrook, California, showing the historic record (top left) and five flow scenarios from left to right: Scenario 1: wetter wet years (increase flows 50%), drier dry years (decrease flows 30%); Scenario 2: All flows decreased 30%; Scenario 3: All flows decreased 60%; Scenario 4: all flows increased 30%; Scenario 5: reservoir-influenced flow with increased base flows (20%), and altered flows during peaks between the 1-year and 5-year flood discharge by decreasing to 1-year flood discharge. Scenario 6: Variable infiltration capacity (VIC) hydrologic model output for AIB late century 2080s emissions scenario.

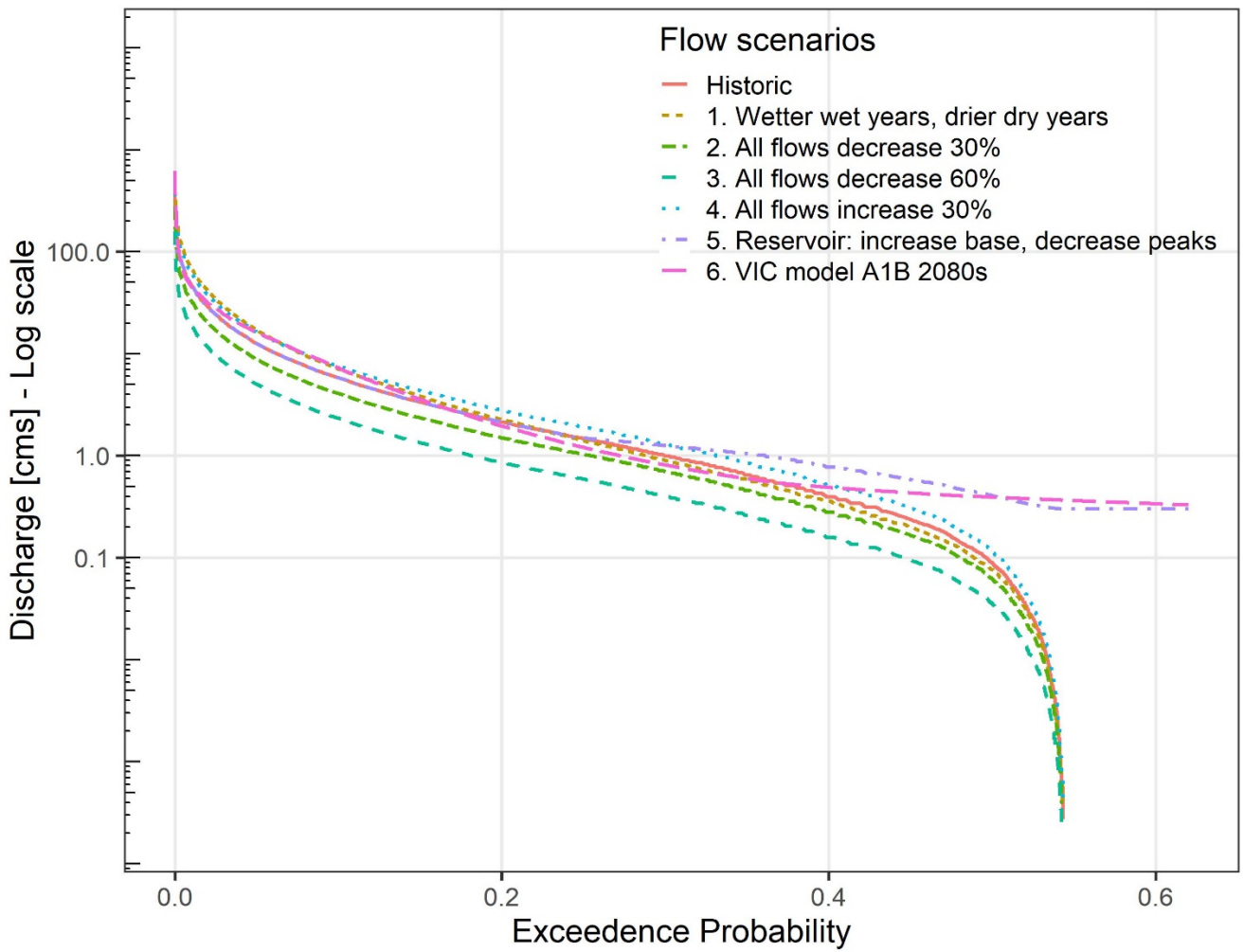

Figure 4.1.7 Flow duration curves for the historical stream gage record (water years 1965-2018) for the San Antonio River near Lockwood, California, and five climate change scenarios: Scenario 1: wetter wet years (increase flows 50%), drier dry years (decrease flows 30%); Scenario 2: All flows decreased 30%; Scenario 3: All flows decreased 60%; Scenario 4: all flows increased 30%; Scenario 5: reservoir-influenced flow with increased base flows (20%), and altered flows during peaks between the 1-year and 5-year flood discharge by decreasing to 1-year flood discharge. Scenario 6: Variable infiltration capacity (VIC) hydrologic model output for AIB late century 2080s emissions scenario.

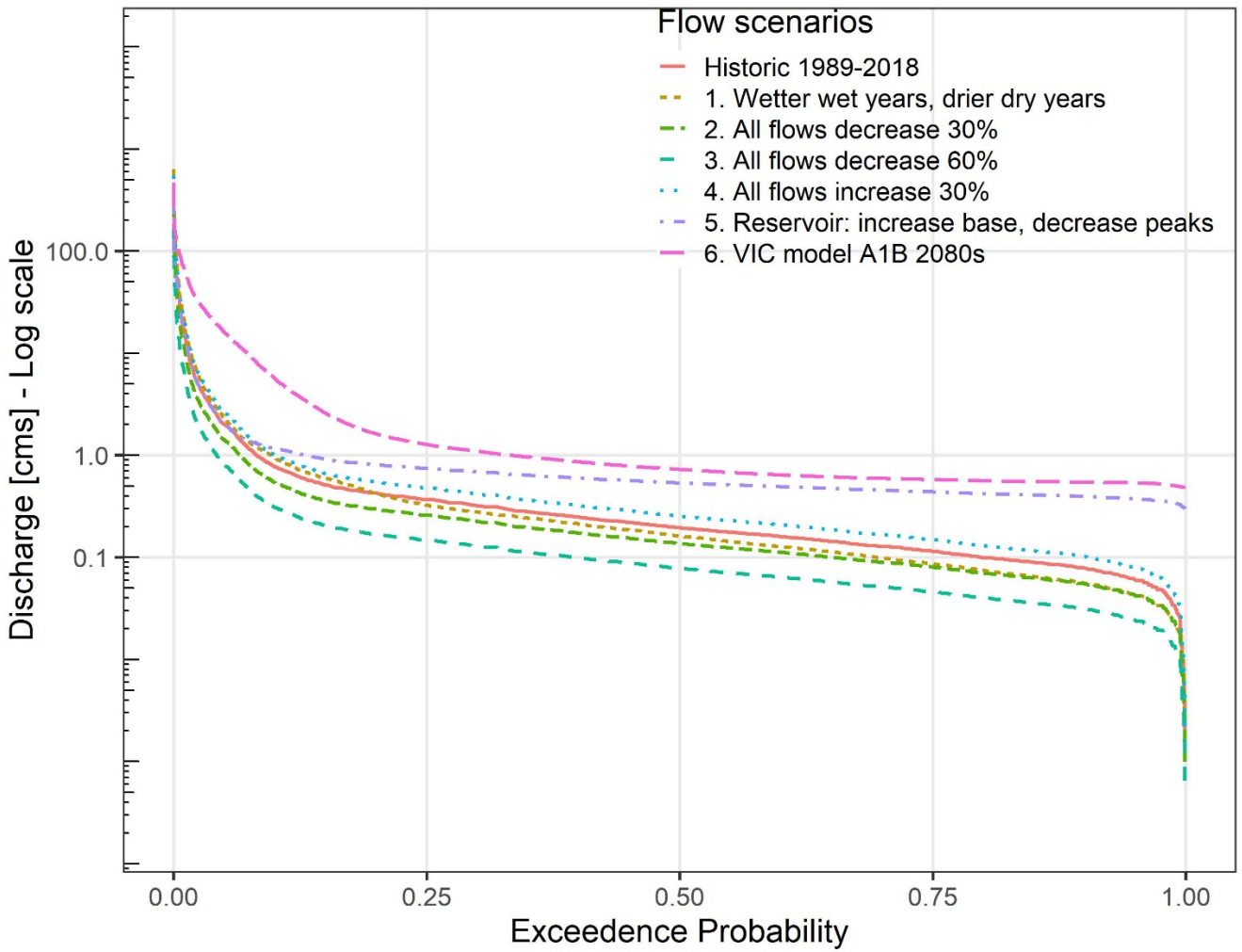

Figure 4.1.8 Flow duration curves for the historical stream gage record (water years 1990-2018) for the Santa Margarita River near Fallbrook, California, and five climate change scenarios: Scenario 1: wetter wet years (increase flows 50%), drier dry years (decrease flows 30%); Scenario 2: All flows decreased 30%; Scenario 3: All flows decreased 60%; Scenario 4: all flows increased 30%; Scenario 5: reservoir-influenced flow with increased base flows (20%), and altered flows during peaks between the 1-year and 5-year flood discharge by decreasing to 1-year flood discharge. Scenario 6: Variable infiltration capacity (VIC) hydrologic model output for AIB late century 2080s emissions scenario.

4.1.2 Hydraulic modeling: Camp Pendleton

After a preliminary visit to sites along the Santa Margarita River through Marine Corps Base Camp Pendleton (MCBCP) in April 2016, we selected the "Fallbrook Bridge" site for intensive study in 2017 (Figure 4.1.9). Fallbrook Bridge is on the northeastern edge of MCBCP where the river enters the base. It is an excellent site for intensive study because it has relatively natural flows with the addition of a major tributary (Sandia Creek) just upstream, it occurs through a medium-confined open valley type which is representative of a majority of valley types along the Santa Margarita through the base, it has relatively easy access, and there are long-term stream gages just upstream of the reach.

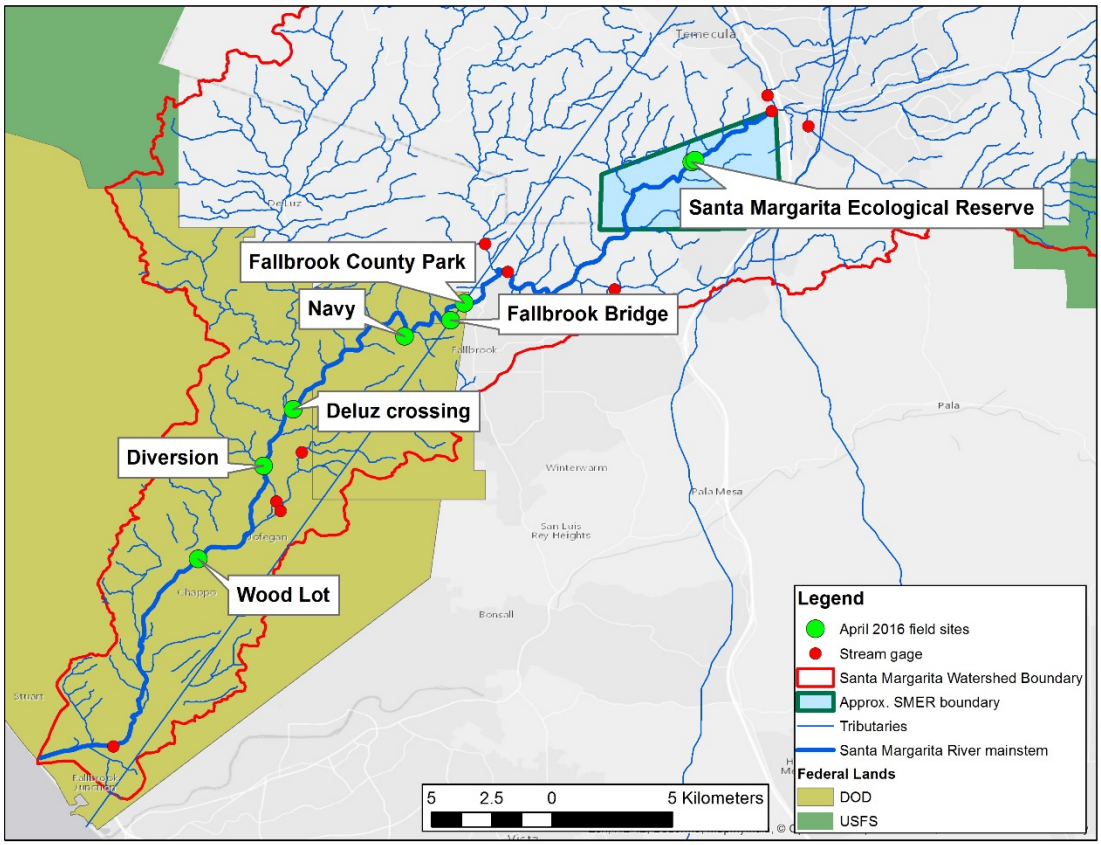

Figure 4.1.9 Field site locations from 2016 sampling along the Santa Margarita River through Camp Pendleton and the Santa Margarita Ecological Reserve. The "Fallbrook bridge" site was selected for intensive sampling.

We made two visits to the Fallbrook Bridge site in 2017: one in February to begin a topographic survey of the floodplain, and one in April to complete the topographic survey and survey the vegetation during spring bloom. We developed two datasets: one consisting of topography points and breaklines representing elevations across our 350

meter reach of river and a second of vegetation abundance and composition within the same stretch of river. From the topography points and lines, we developed an elevation map that will be used as input for a hydraulic model being developed this winter (Figure 4.1.10). The vegetation data collected includes a list of 80 species (Table 4.1.1). The most cover-abundant species within our floodplain reach were willows (*Salix lasiolepis* and *Salix laevegata*) as well as exotic grasses such as *Bromus diandrus* and *Ehrharta erecta* (Table 4.1.2). Other abundant species included woody trees and shrubs such as *Quercus agrifolia*, *Baccharis salicifolia*, *Salix exigua*, and *Platanus racemosa* (Table 4.1.2). We used species' trait information from both field data gathered in 2016 (specific leaf area, wood density, maximum height, water use efficiency) and gathered from the literature (seed weight, rooting depth, growth habit) to classify floodplain plants into plant guilds using a cluster analysis, which resulted in 10 riparian plant guilds (Figure 4.1.11).

In 2018, we will be building 2-D hydraulic models which will be the foundation for our floodplain vegetation modeling under climate change scenarios. We will then link the field-collected vegetation data to the topographic surveys and hydraulic models to produce floodplain vegetation maps under future climate change scenarios.

Our over-arching goal is to create models of floodplain vegetation based on physical characteristics of the floodplain hydrology that can be used by base managers to understand how floodplain vegetation is expected to change under various climate change scenarios. Further, we seek to develop models that are applicable to other public lands across the Mediterranean California Coastal Chaparral Forest and Shrub ecoregion, including U.S. Forest Service lands of the Cleveland National Forest. These models should help land managers develop vulnerability assessments and incorporate climate change into land management and forests plans.

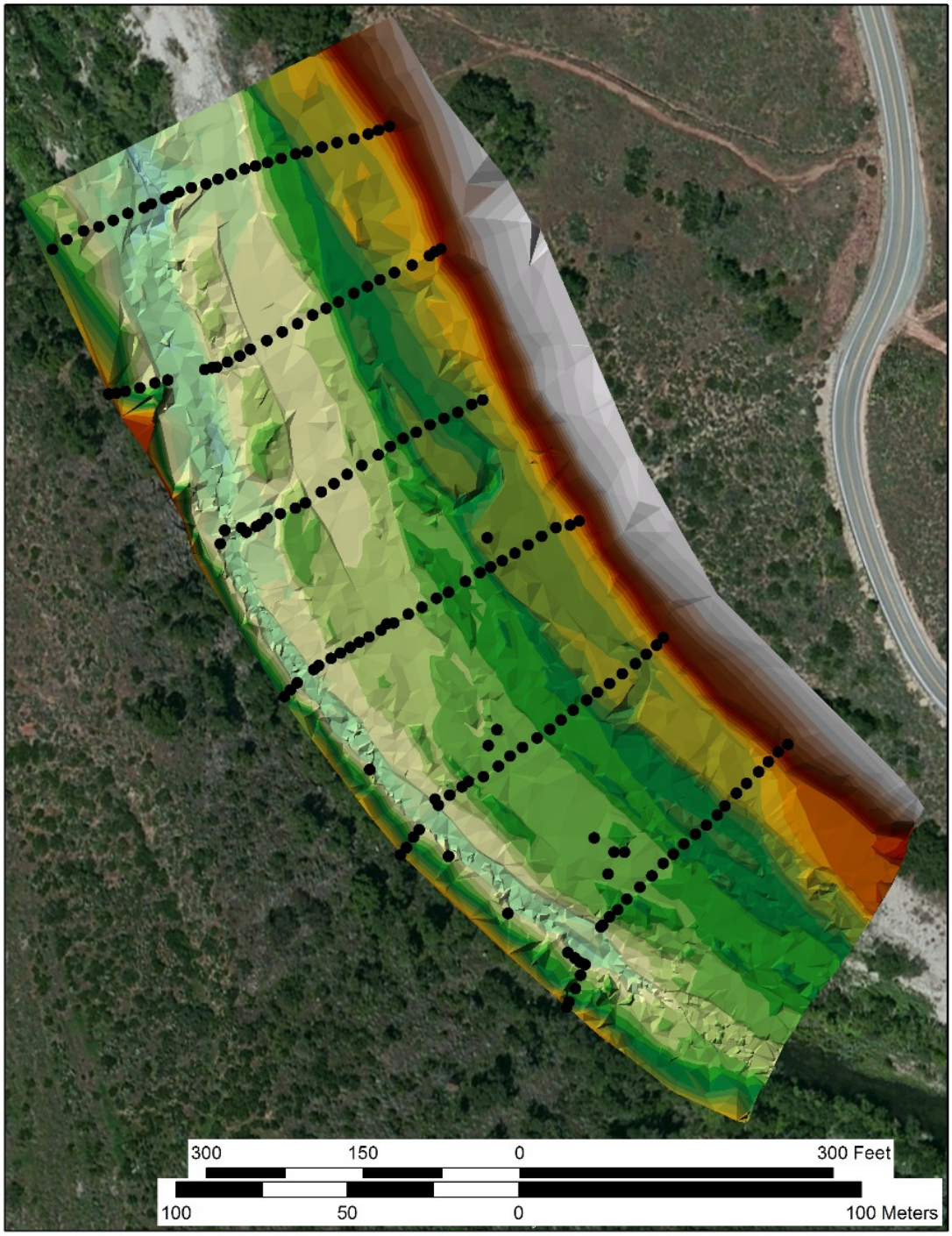

Figure 4.1.10 Surveyed floodplain topography overlain on satellite imagery of the Santa Margarita River near Fallbrook Bridge, California. Color depicts elevation of the survey: blue are low elevations (river channel), greens are moderate elevations on the floodplain, and yellow to orange and red-brown are increasingly high elevations in the uplands. Black dots indicate locations of vegetation survey plots. Flow is from lower right to upper left.

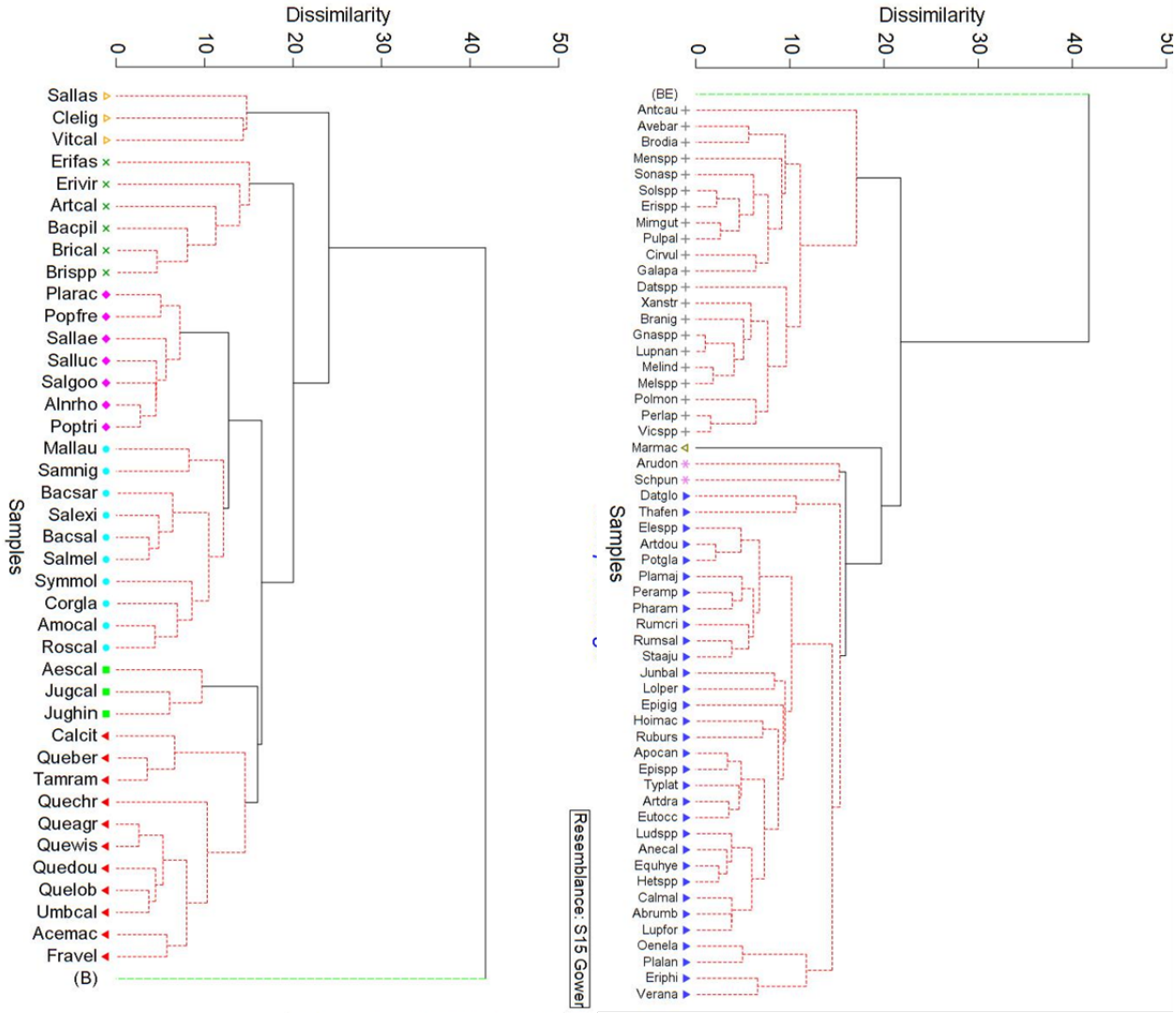

Figure 4.1.11 Cluster analysis ordination plot, grouping species into riparian functional plant guilds depicted by symbols. Yellow triangle: vine/shrubs, green x: xeric shrubs, pink diamond: hydric trees, blue circle: hydric shrubs, green squares and red triangles: drought-tolerant trees, gray x: ruderal generalists, and dark blue triangle: hydric herbaceous.

Table 4.1.1 Species list for plots sampled in April 2017 at the Fallbrook bridge study site.

Allium fimbriatum	*Malosma laurina*
Ambrosia psilostachya	*Marah macrocarpus*
Amorpha fruticosa	*Melica imperfecta*
Anemopsis californica	*Mentha spp*
Artemisia californica	*Nicotiana glauca*
Artemisia douglasiana	*Opuntia engelmannii*
Asparagus asparagoides	*Pentameris airoides*
Avena barbata	*Phacelia cicutaria*
Baccharis salicifolia	*Phalaris aquatica*
Brassica nigra	*Piptatherum miliaceum*

Bromus diandrus	*Plantago lanceolata*
Bromus madritensis ssp rubens	*Plantago major*
Bromus rubens	*Platanus racemosa*
Centaurea melitensis	*Pluchea sericea*
Chenopodium album	*Populus balsamifera*
Claytonia perfoliata	*Populus fremontii*
Clematis ligusticifolia	*Pseudognaphalium biolettii*
Conium maculatum	*Pulicaria paludosa*
Croton californicus	*Quercus agrifolia*
Cynodon dactylon	*Quercus engelmannii*
Cyperus sp.	*Rhamnus ilicifolia*
Diplacus sp.	*Ricinus communis*
Ehrharta erecta	*Rubus ursinus*
Ehrharta longiflora	*Salix exigua*
Eleocharis palustris	*Salix gooddingii*
Equisetum arvense	*Salix laevigata*
Eriogonum fasciculatum	*Salix lasiolepis*
Erodium cicutarium	*Salix lucida*
Festuca myuros	*Salvia apiana*
Fraxinus velutina	*Sambucus nigra*
Galium angustifolium	*Schismus barbatus*
Grindelia sp.	*Schoenoplectus americanus*
Hedypnois cretica	*Silene gallica*
Heteromeles arbutifolia	*Toxicodendron diversilobum*
Hypochaeris glabra	*Trifolium pratense*
Keckiella cordifolia	*Typha latifolia*
Lepidium virginicum	*Urtica dioica*
Logfia californica	*Vicia sp.*
Ludwigia hexapetala	*Vitis californica*
Lupinus sparsiflorus	*Xanthium strumarium*

Table 4.1.2 Species with the most cover in vegetation plots in the Fallbrook Bridge site sampled in April 2017.

Species name	Rank
Salix lasiolepis	1
Salix laevigata	2
Bromus diandrus	3
Quercus agrifolia	4
Salix exigua	5
Ehrharta erecta	6
Baccharis salicifolia	7
Platanus racemosa	8

Schoenoplectus americanus	9
Vitis californica	10
Equisetum arvense	11
Malosma laurina	12
Artemisia douglasiana	13
Toxicodendron diversilobum	14
Piptatherum miliaceum	15
Xanthium strumarium	16
Ambrosia psilostachya	17
Rhamnus ilicifolia	18
Populus balsamifera	19
Salix lucida	20

Figure 4.1.12 Photos of trait sampling and vegetation plot sampling of species on the Santa Margarita River, CA, April 2017.

4.1.3 Hydraulic modeling: Fort Hunter Liggett

After a preliminary visit to sites along the San Antonio and Nacimiento Rivers through US Army Garrison Fort Hunter Liggett (FHL) in April 2016, we selected the "Landfill" site for intensive study in 2017 (Figure 4.1.13). The Landfill site is located in the central

portion of FHL, downstream of the major perennial tributary input of Mission Creek. It is an optimal site for intensive study because it has unimpeded natural flows, it occurs through a medium-energy confined open valley type which is representative of a majority of valley types along the San Antonio and Nacimiento through the base, it has relatively easy access, and there are long-term stream gages just downstream of the reach.

We made two visits to the Landfill site in 2017: one in February to begin a topographic survey of the floodplain, and one in June to complete the topographic survey and survey the vegetation during spring bloom. We developed two datasets: one consisting of topography points and breaklines representing elevations across our 300 meter reach of river and a second of vegetation abundance and composition within the same stretch of river. From the topography points and lines, we developed an elevation map that will be used as input for a hydraulic model being developed this winter (Figure 4.1.14). The vegetation data collected includes a list of 88 species (Table 4.1.3). The most cover-abundant species within our floodplain reach were exotic grasses such as *Bromus diandrus* and *Avena barbata* as well as native trees and shrubs (*Populus fremontii, Platanus racemose*, *Salix laevegata* and *Salix lasiolepis*) as well as exotic grasses such as Bromus diandrus and *Ehrharta erecta* (Table 4.1.4). We used species' trait information from both field data gathered in 2016 (specific leaf area, wood density, maximum height, water use efficiency) and gathered from the literature (seed weight, rooting depth, growth habit) to classify floodplain plants into plant guilds using a cluster analysis, which resulted in 10 riparian plant guilds (Figure 4.1.15).

Our over-arching goal is to create models of floodplain vegetation based on physical characteristics of the floodplain hydrology that can be used by base managers to understand how floodplain vegetation is expected to change under various climate change scenarios. Further, we seek to develop models that are applicable to other public lands across the Mediterranean California Coastal Chaparral Forest and Shrub ecoregion, including U.S. Forest Service lands of the Los Padres National Forest. These models should help land managers develop vulnerability assessments and incorporate climate change into land management and forests plans.

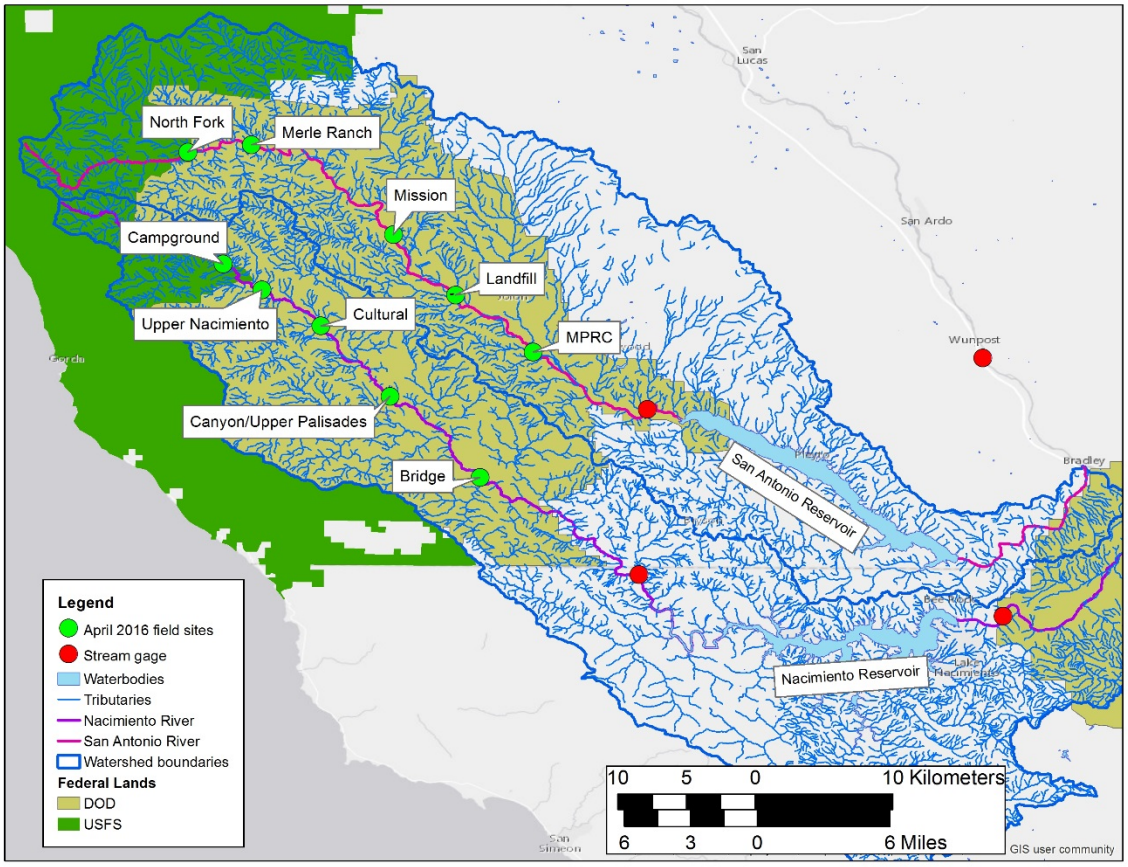

Figure 4.1.13 Field site locations from 2016 along the San Antonio and Nacimiento Rivers through Los Padres National Forest and Fort Hunter Liggett.

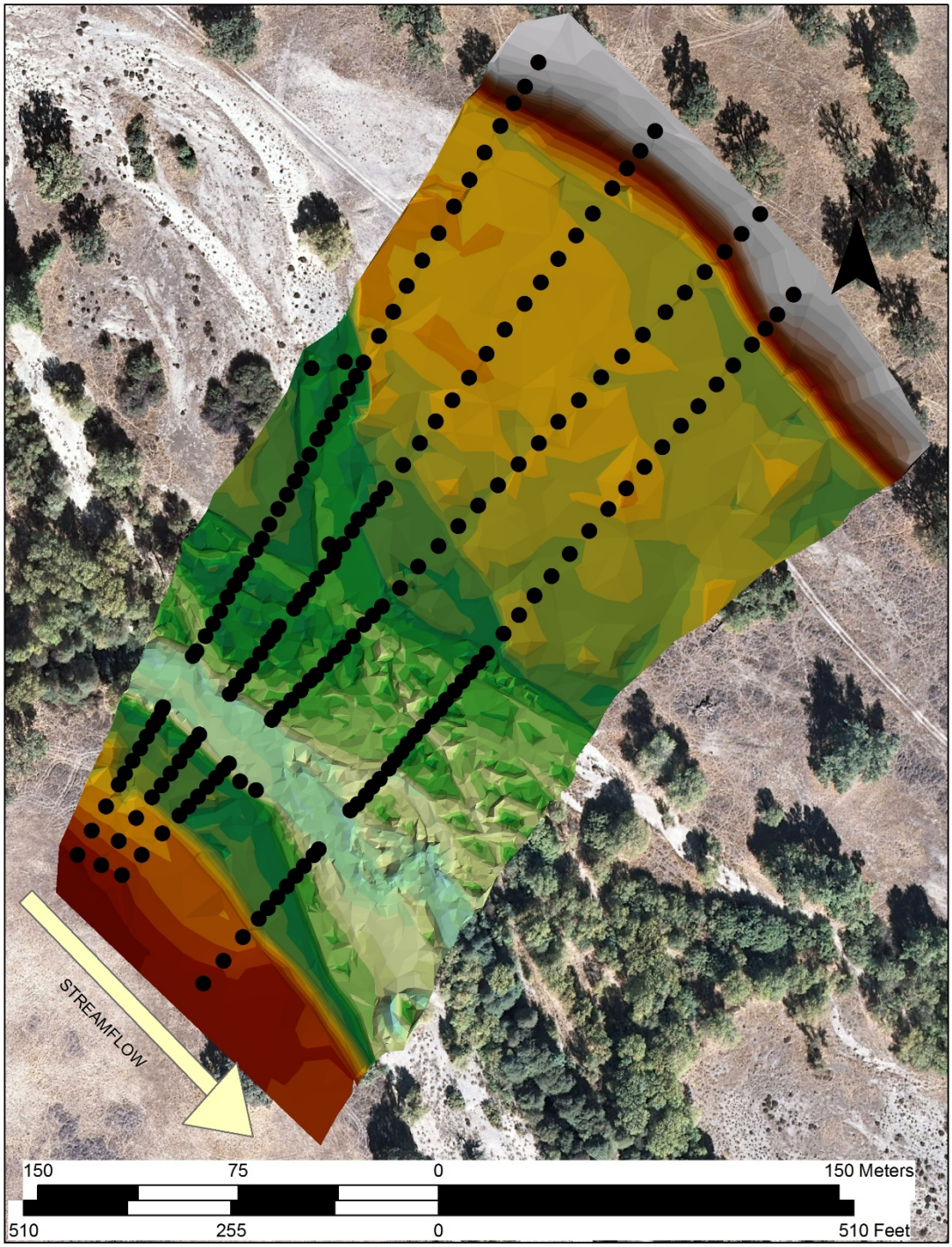

Figure 4.1.14 Surveyed floodplain topography overlain on satellite imagery of the San Antonio River at the Landfill site. Color depicts elevation of the survey: blue are low elevations (river channel), greens are moderate elevations on the floodplain, and yellow to orange and red-brown are increasingly high elevations in the uplands. Black dots indicate locations of vegetation survey plots. Flow is from upper left to lower right.

Table 4.1.3 Species list for plots sampled in June 2017 at the San Antonio Landfill study site.

Acmispon americanum	*Juncus bufonius*
Acmispon strigosus	*Juncus patens*
Agrostis stolonifera	*Lagophylla remosissima*
Alnus rhombifolia	*Lastarriaea coriacea*
Ambrosia acanthacarpa	*Lasthinia sp.*
Amsinkia intermedia	*Lessingia glandulifera*
Amsinkia menzesii	*Linanthus liniflorus*
Anthriscus caulus	*Lolium sp.*
Artemesia dracunculus	*Lupinus bicolor*
Artemisia douglasiana	*Lupinus consinus*
Asclepias eriocarpa	*Lupinus formosus*
Asclepias fasciculata	*Lupinus hirsutissimus*
Avena barbata	*Lupinus succulentus*
Baccharis salicaceae	*Melilotus indicus*
Brassica herschfeldia	*Mentha arvensis*
Brassica nigra	*Mentha piperita*
Bromus diandrus	*Mentha spicata*
Bromus hordeaceous	*Microcarpus californicus*
Bromus rubens	*Mimulus gutattus*
Camissonia contorta	*Nicotiana quadrivalvis*
Carex alma	*Pinus sabiana*
Chenopodium album	*Platanus racemosa*
Chenopodium pratericola	*Poa pratensis*
Chorizanthes douglasii	*Polypogon monspeliensis*
Cirsium occidentale	*Populus fremontii*
Clarkia affinis	*Psuedognaphalium luteoalbum*
Clarkia unguiculata	*Quercus douglasii*
Conium maculatum	*Quercus lobata*
Eleocharis macrostachya	*Ranunculus hebecarpus*
Elymus glaucus	*Rosa californica*
Eriogonum fasciculatum	*Rumex sp.*
Eriogonum gracili	*Salix exigua*
Eriogonum nudum	*Salix laevegata*
Erodium cicutarium	*Salix lasiolepis*
Eryngium vaseyi	*Salix melanopsis*
Euthamia occidentalis	*Sambucus nigra*
Eythranthe guttatus	*Senecio flaccidus*
Festuca perennis	*Silene antirrhina*
Frangula californica	*Stachys ajugoides*
Gallium aparine	*Stipa pulcra*
Heterotheca grandiflora	*Verbena lasiostachys*
Heterotheca oregona	*Veronica anagalis-aquatilus*

Heterotheca sessiflora	*Vulpia octiflora*
Hypochaeris radicata	*Xanthium strumarium*

Table 4.1.4 Species with the most cover in vegetation plots in the San Antonio Landfill site sampled in June 2017.

Species	Rank
Bromus diandrus	1
Populus fremontii	2
Salix laevegata	3
Avena barbata	4
Salix lasiolepis	5
Centaurea solstitialis	6
Bromus rubens	7
Platanus racemosa	8
Erodium cicutarium	9
Bromus hordeaceous	10
Bromus hordeaceous	11
Artemisia douglasiana	12
Melilotus indicus	13
Fuzzy oenothera	14
Baccharis salicaceae	15
Lessingia gladulifera	16
Eleocharis macrostachya	17
Lastarriaea coriacea	18
Eriogonum faiculatum	19
Agrostis stolonifera	20

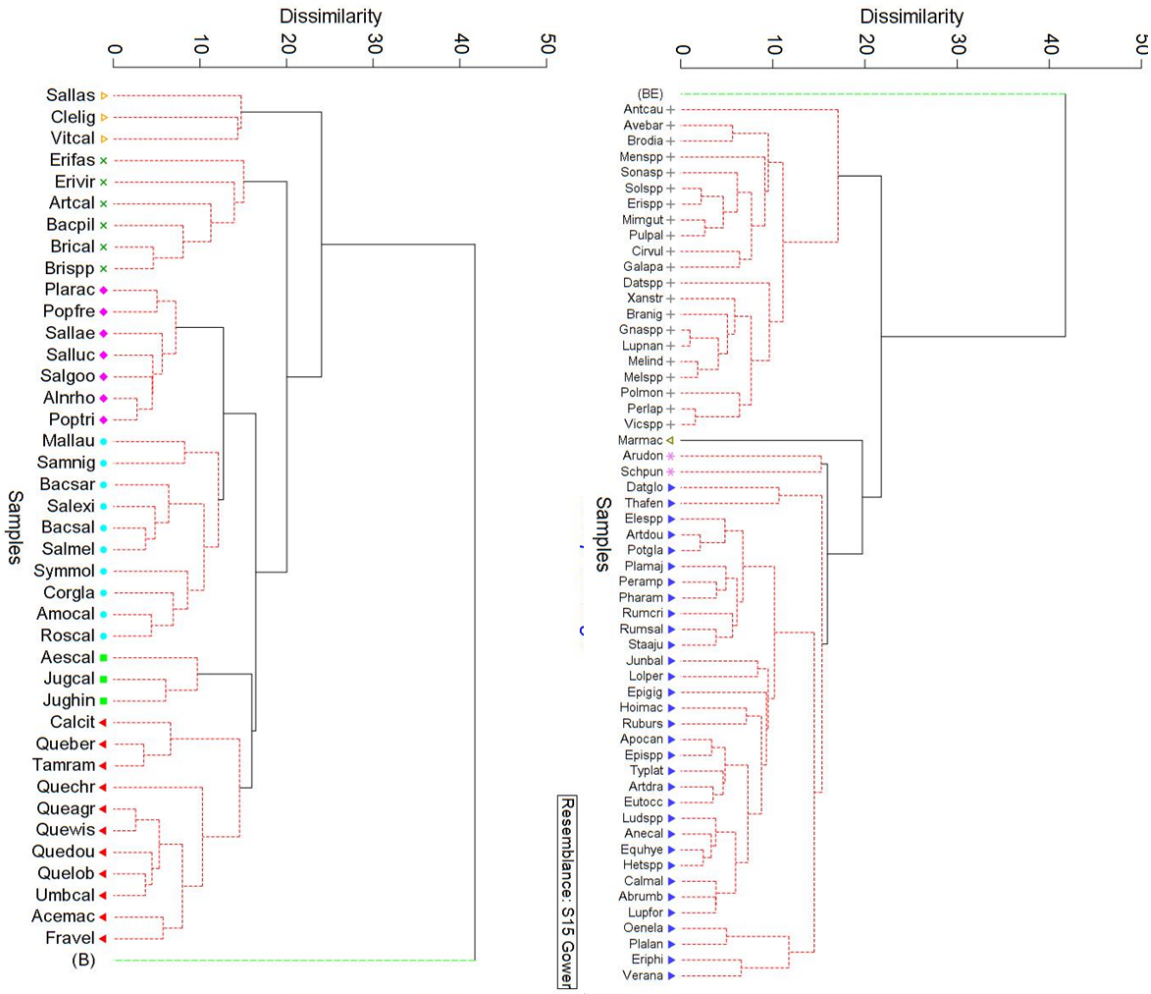

Figure 4.1.15 Cluster analysis ordination plot, grouping species into riparian functional plant guilds depicted by symbols. Yellow triangle: vine/shrubs, green x: xeric shrubs, pink diamond: hydric trees, blue circle: hydric shrubs, green squares and red triangles: drought-tolerant trees, gray x: ruderal generalists, and dark blue triangle: hydric herbaceous.

4.1.4 Hydraulic modeling: Comanche National Grasslands

After an initial visit to sites along the Purgatoire River through Comanche National Grasslands (CNG) in July 2016, we selected the "Gage" site for intensive study in 2017 (Figure 4.1.16). The gage site is an optimal site for intensive study because it is representative of the typical valley type of the Purgatoire through CNG and it has a long-term stream gages just downstream of the reach. We visited the site in November 2017 to complete the topographic survey of the channel and floodplain through the reach. We developed two datasets: one consisting of topography points and breaklines representing elevations across our 350 meter reach of river and a second of vegetation abundance and composition within the same stretch of river. From the topography points and lines, we developed an elevation map that will be used as input for a hydraulic model being developed this winter (Figure 4.1.17). The vegetation data (collected in 2016) includes a

list of 56 species (Table 4.1.5). The most cover-abundant species within our floodplain reach were native shrub willow (*Salix exigua*), native wetland species (eg: *Solidago canadensis, Schoenoplectus pungens, Phragmites australis*) as well as exotic herbs such as Amaranth species (Table 4.1.6).

In 2018, we will build 2-D hydraulic models from our topographic surveys which will be the basis of our floodplain vegetation modeling under climate change scenarios. We will then link the field-collected vegetation plot data (gathered and surveyed in July, 2016) to the topographic surveys and hydraulic-hydrologic models to produce floodplain vegetation maps under current and future climate change and water management scenarios.

Our goal is to create informed models of floodplain vegetation based on physical characteristics of the floodplain hydrology that can be used by Forest Service managers to understand how floodplain vegetation is expected to change under various climate change scenarios. Further, we seek to develop models that are applicable to other public lands in southeastern Colorado and the southern Great Plains-Dry Steppe ecoregions). These models should help the forest in forest plan revisions, vulnerability assessments, and incorporating climate change into land management.

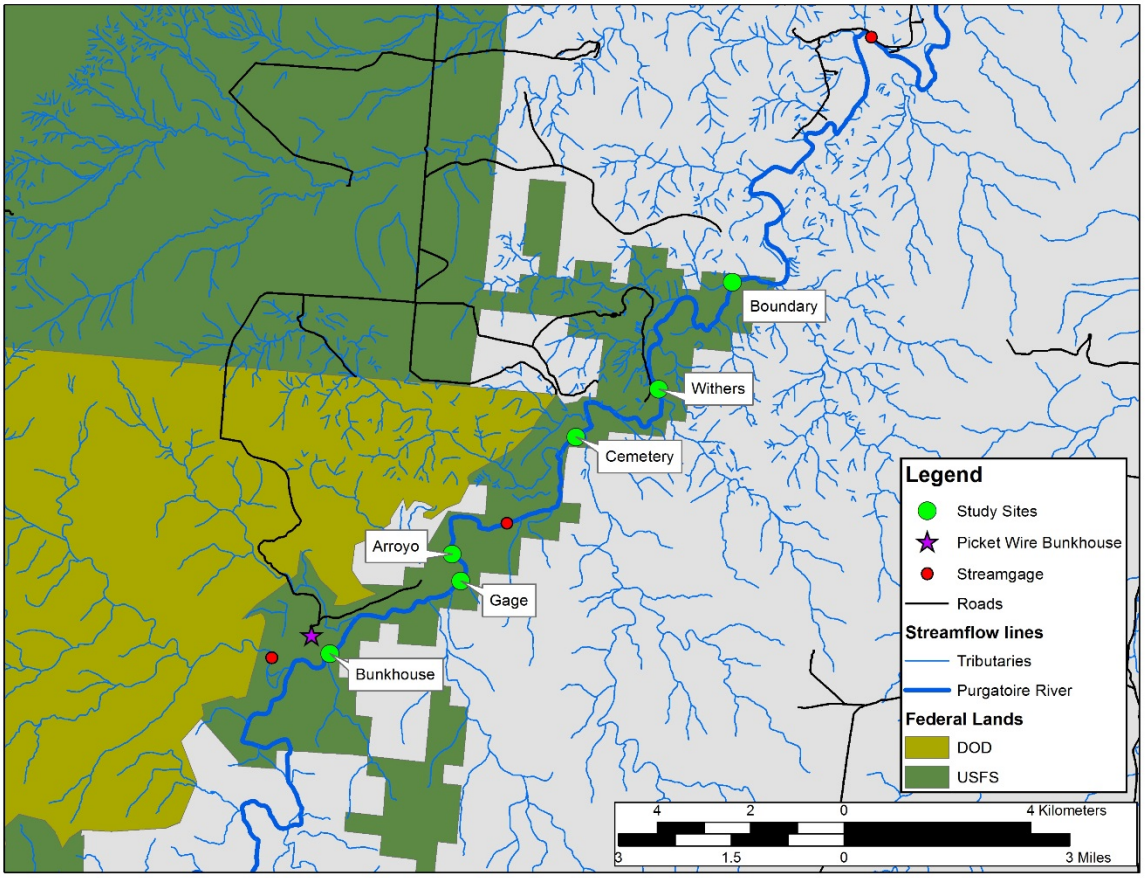

Figure 4.1.16 Field sampling sites visited in July, 2016 along the Purgatoire River through Comanche National Grasslands.

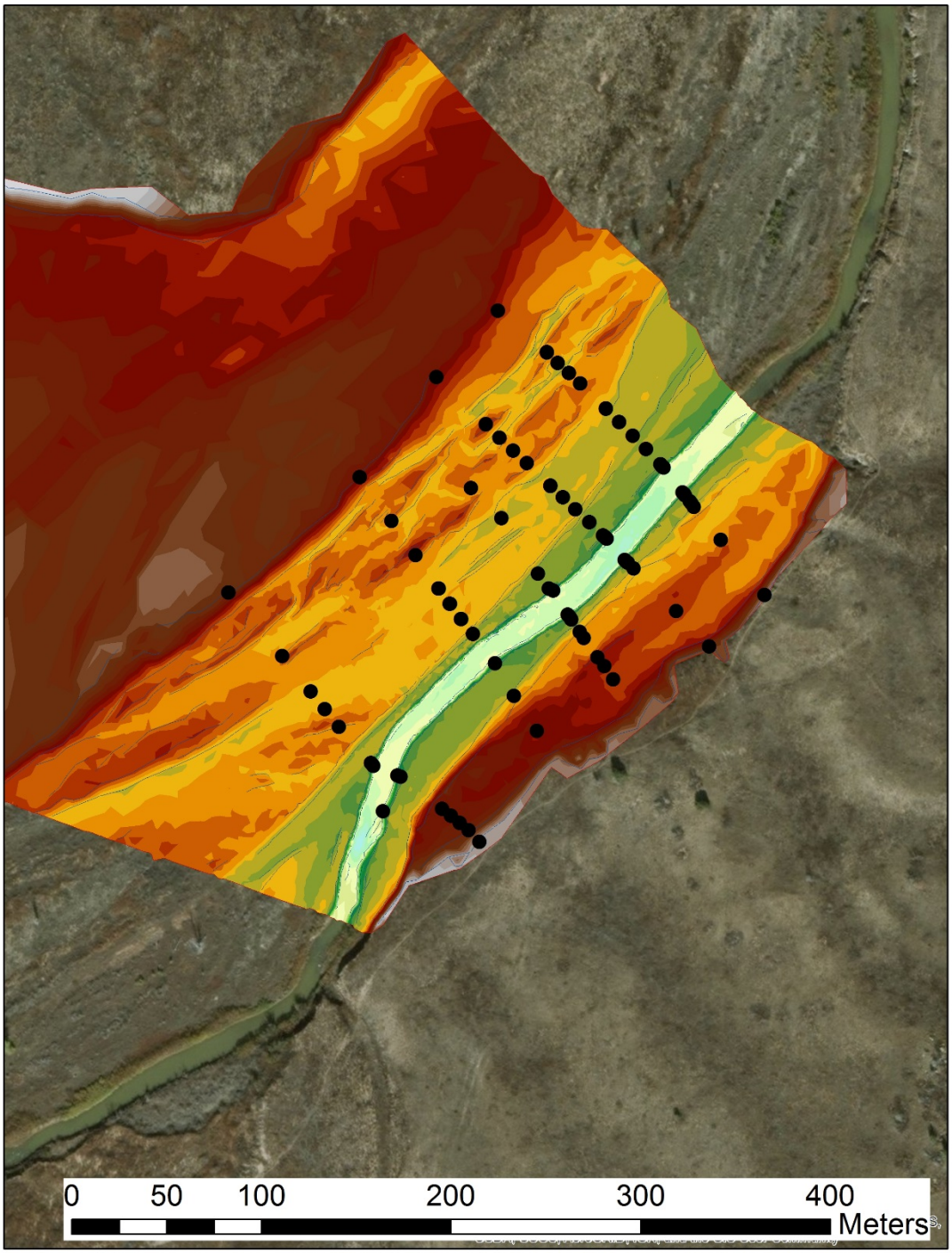

Figure 4.1.17 Surveyed floodplain topography overlain on satellite imagery of the Purgatoire River near the USGS Gage at Rock Crossing. Color depicts elevation of the survey: blue are low elevations (river channel), greens and yellows are moderate elevations on the floodplain, and orange to red-brown are increasingly high elevations in the uplands. Black dots indicate locations of vegetation survey plots. Flow is from lower left to upper right.

Table 4.1.5 Species list for the Purgatoire River Study Sites.

Amaranth spp.	*Mirabilis linearis*
Ambrosia psilostachya	*Mirabilis multiflora*
Amorpha fruticosa	*Muhlenbergia asperifolia*
Apocynum cannabinum	*Oenothera curtiflora*
Asclepias speciosa	*Panicum virgatum*
Asclepias subverticillata	*Pascopyrum smithii*
Bothriochloa laguroides	*Phragmites australis*
Carex spp.	*Physalis longifolia*
Celtis laevigata	*Polygonum lapathifolium*
Cirsium spp.	*Polygonum spp.*
Cleome serrulata	*Polypogon monspeliensis*
Conyza canadensis	*Populus deltoides*
Croton texansis	*Proboscidea louisianica*
Cucurbita foetidissima	*Ptelea trifoliata*
Cynodon dactylon	*Ratibida tagetes*
Eleocharis palustris	*Rhus trilobata*
Elymus canadensis	*Ribes aureum*
Equisetum hyemale	*Rumex spp.*
Ericameria nauseosa	*Salix amygdaloides*
Erigeron spp.	*Salix exigua*
Euphorbia marginata	*Sambucus spp.*
Glycyrrhiza lepidota	*Sarcobatus vermiculatus*
Grindelia inornata	*Schoenoplectus pungens*
Helianthus annuus	*Solidago canadensis*
Juniperus monosperma	*Sphaeralcea angustifolia*
Lactuca serriola	*Tamarix ramosissima*
Lycium pallidum	*Vitis riparia*
Melilotus spp.	*Xanthium strumarium*

Table 4.1.6 Species with the most cover in vegetation plots in the Gage site sampled in July 2016.

Species	Rank
Salix exigua	1
Solidago canidensis	2
Amaranth sp.	3
Schoenoplectus pungens	4
Phragmites australis	5
Apocynum cannabinum	6
Helianthus annuus	7
Ratibida tagetes	8
Glycyrrhiza lepidota	9
Cucurbita foetidissima	10

Amorpha fruiticosa	11
Croton texensis	12
Ambrosia psilostachya	13
Elymus canadensis	14
Conyza canadensis	15
Chamaesyce maculata	16
Erigeron bellidiastrum	17
Proboscidea louisianica	18
Grindelia inornata	19
Salsola collina	20

4.1.5 Literature Cited

Cayan, D. R., E. P. Maurer, M. D. Dettinger, M. Tyree, and K. Hayhoe. 2008. Climate change scenarios for the California region. Climatic Change **87**:21-42.

Das, T., D. Pierce, and D. Cayan. 2011. The importance of warm season warming to western US streamflow changes. Geophysical Research … **38**:L23403.

Hayhoe, K., D. Cayan, C. B. Field, P. C. Frumhoff, E. P. Maurer, N. L. Miller, S. C. Moser, S. H. Schneider, K. N. Cahill, E. E. Cleland, L. Dale, R. Drapek, R. M. Hanemann, L. S. Kalkstein, J. Lenihan, C. K. Lunch, R. P. Neilson, S. C. Sheridan, and J. H. Verville. 2004. Emissions pathways, climate change, and impacts on California. Proc Natl Acad Sci U S A **101**:12422-12427.

Mallakpour, I., M. Sadegh, and A. AghaKouchak. 2018. A new normal for streamflow in California in a warming climate: Wetter wet seasons and drier dry seasons. Journal of Hydrology **567**:203-211.

Maurer, E. P., and P. B. Duffy. 2005. Uncertainty in projections of streamflow changes due to climate change in California. Geophysical Research Letters **32**.

Swain, D. L., B. Langenbrunner, J. D. Neelin, and A. Hall. 2018. Increasing precipitation volatility in twenty-first-century California. Nature Climate Change **8**:427-433.

Vicuna, S., E. P. Maurer, B. Joyce, J. A. Dracup, and D. Purkey. 2007. THE SENSITIVITY OF CALIFORNIA WATER RESOURCES TO CLIMATE CHANGE SCENARIOS. Journal of American Water Resources Association **43**:482-498.

Wenger, S. J., C. H. Luce, A. F. Hamlet, D. J. Isaak, and H. M. Neville. 2010. Macroscale hydrologic modeling of ecologically relevant flow metrics. Water Resources Research **46**.

Yoon, J. H., S. S. Wang, R. R. Gillies, B. Kravitz, L. Hipps, and P. J. Rasch. 2015. Increasing water cycle extremes in California and in relation to ENSO cycle under global warming. Nat Commun **6**:8657.

4.2 Simulated and retrospective hydrograph scenarios: flow regime alteration degrades ecological networks in riparian ecosystems

This analysis was published in *Nature Ecology & Evolution* (Tonkin et al. 2018).

4.2.1 Summary

Riverine ecosystems are governed by patterns of temporal variation in river flows. This dynamism will change due to climate change and the near-ubiquitous human control of river flows globally, which may have severe effects on species distributions and interactions. We employed a combination of population modeling and network theory to explore the consequences of possible flow regime futures on riparian plant communities, including scenarios of increased drought, flooding, and flow homogenization (removal of flow variability). We found that even slight modifications to the historic natural flow regime had significant consequences for the structure of riparian plant networks. Networks of emergent interactions between plant guilds were most connected at the natural flow regime and became simplified with increasing flow alteration. The most influential component of flow alteration was flood reduction, with drought and flow homogenization both having greater simplifying community-wide consequences than increased flooding. These findings suggest that maintaining floods under future climates will be needed to overcome the negative long-term consequences of flow modification on riverine ecosystems.

4.2.2 Introduction

The fundamental human demand for fresh water has resulted in the dramatic transformation of rivers throughout the world[1]. Dams, diversions, and numerous other forms of infrastructure have enabled water flows to be controlled for human utilization, resulting in the dampening or elimination of flooding and other ecologically-important aspects of flow regimes[2,3] (see Table 4.2.1 for definition of the natural flow regime). Such effects threaten riparian ecosystems[4,5] and compromise many functions and services supported by these ecosystems, including the regulation of thermal regimes and water quality, flood attenuation, contribution of carbon to aquatic food webs, and the provision of wood and physical habitat structure along the terrestrial-aquatic interface[6]. These stressors to riparian ecosystems are exacerbated by climate change, which threatens to increase flow intermittency[7] and modify species distributions and interactions via drought intensification in many regions globally[8,9]. What has emerged is a clear need for robust forecasting of how riparian ecosystems will respond to changing flooding and drought conditions over long timescales[10].

Riparian ecosystems have evolved in the context of naturally-recurring cycles of flooding and drought[11]. Thus, alterations to species interactions caused by novel climate and flow

regimes are feared to contribute to the collapse of previously robust and resilient communities[12]. Ecological network theory provides new opportunities to achieve a deeper, more holistic understanding of how organisms interact with each other and their environments[13]. However, while the effects of altered network structure on the functioning of ecosystems has been well explored[14,15], we know less about the effects of environmental change on the structure of ecological networks[16] (but see reference [17]). Despite the potential of network theory to enhance our understanding of how communities are structured, there remains a disconnect between modeling the dynamics of entire communities and the relative roles of individual species or functional groupings of species in these networks[18] and how these roles vary through space and time with various scenarios of environmental change[19].

Table 4.2.1 Glossary of important terms used in the paper.

Category	Term	Definition
General terms		
	Changepoint	A location in the data where the statistical properties of a sequence of observations change.
	The natural flow regime	The recorded historical pattern of floods and drought, characterized by timing, frequency, magnitude, duration and interannual variability in flows[1].
Plant guilds		
	Desert shrub	Drought tolerant, flood-intolerant, upland shrub (e.g. woody *Artemesia* species).
	Hydroriparian pioneer shrub	Flood-adapted, drought-intolerant, phreatophytic species with shrub growth forms and flexible stems that have high water requirements and exist relatively close to the stream channel with similar recruitment requirements to HT (e.g. shrub *Salix* species).
	Hydroriparian pioneer tree	Long-lived, flood-tolerant, phreatophytic tree species that recruit onto bare, moist substrate near the stream channel following floods (e.g. *Populus, Alnus,* and *Eucalyptus* species).
	Mesoriparian meadow species	Facultative phreatophytic species with less restrictive water requirements and tolerance of exposure to brief drought conditions (e.g. wetland grass and forb species).
	Xeroriparian pioneer shrub	Drought-tolerant, facultative phreatophytic plant species that require some flooding for regeneration but whose adults can tolerate periods of extended drought (e.g. *Tamarix* species).
Networks		
	Degree	The number of links connected to the node. These can be broken down into the number of inbound, outbound, and mutual links.
	Keystone node	Nodes that had large effects on the overall network, shown by substantial links out to other nodes. Changes in

	vital rates of these keystone nodes affected a disproportionate number of other nodes in the network.
Mutual node	Nodes that played a key reciprocal role in the network by representing important bidirectional associations akin to compensatory dynamics.
Network	A collection of connected objects (nodes). Connections are formed by links.
Network connectance	The ratio of the number of links in the network to the total number of possible links.
Network link (edge)	A connection between each of the nodes. Links represent emergent competition for space in the riparian landscape. Rather than *in situ* observed interactions, these represent emergent interactions between guilds, arising from the model results, through a shared dependency on finite space. We employed sensitivity analysis to infer interaction strengths within and among guilds, and used these values to build a competitive network[$]. Networks were therefore not defined *a priori*, but arose from population dynamics.
Network node (vertex)	An object in the network. Here a node is a single stage of a given guild. There are six stages for each of the five guilds (30 nodes in total).
Network reciprocity	The proportion of mutual or two-way links, where one node affects another node and is affected in return.
Network robustness	A measure of the tolerance of a network to perturbations, such as extinctions. This is commonly measured by examining the network-wide effects of node deletion.
Passive node	Nodes that had more links in than out and thus responded to, rather than influenced, other nodes in the network.

[$]see Methods for details.

Here, we quantify the community-wide consequences of changing flooding and drought regimes on riparian plant communities. By focusing on five riparian plant guilds (*sensu* reference [20]; groupings of species with similar life histories and vital rates) that constitute riparian assemblages across a wide variety of rivers worldwide, our investigation occurs in western United States but is emblematic of dominant trait syndromes in dryland regions. These guilds encompass hydroriparian pioneer trees (HT), xeroriparian pioneer shrubs (XS), hydroriparian pioneer shrubs (HS), mesoriparian meadow species (MM), and desert shrubs (DS) (Table 4.2.1). Using these dryland riparian plants with empirically-derived biotic information for six stage classes (Figure 4.2.1), we employ a modeling framework based on stochastic, coupled structured population models[10]. The model uses fundamental vital rates to explore ecological futures across a spectrum of possible flow regimes for a snowmelt-driven river in the western US, a region predicted to have a future with reduced runoff and altered flow regimes under climate change[21]. By

combining stage-specific responses of plant guilds with specific attributes of a river hydrologic regime, the model enables a mechanistic approach to understanding the nonstationary effects of climate- and human-driven changes to the flow regime on riparian communities.

We employed network theory as a way to visualize and quantify these consequences, as it provides opportunities to understand how groups of organisms interact with each other under different environmental contexts and allows the exploration of how effects propagate throughout complex systems[13]. Here, riparian plant networks were constructed from models, where we quantified interaction strengths and formed network links by using a novel form of multi-guild sensitivity analysis (also termed 'sensitivity networks'[10]). In these networks, nodes represent life-history stages of different plant guilds, and links between two nodes are formed based on model sensitivity analysis; that is, a link is drawn when a small change in the vital rate of one node (in this case, flood susceptibility) significantly affects the abundance of another node in the network as mediated by competition for finite space. By simulating ecosystems under a diverse range of flow modification scenarios from natural to extreme flooding, drought, and flow homogenization (Figure 4.2.2; see Methods), this work uses network theory to identify alternative potential futures where climate- and human-induced changes lead to significant shifts in the structure of ecological communities.

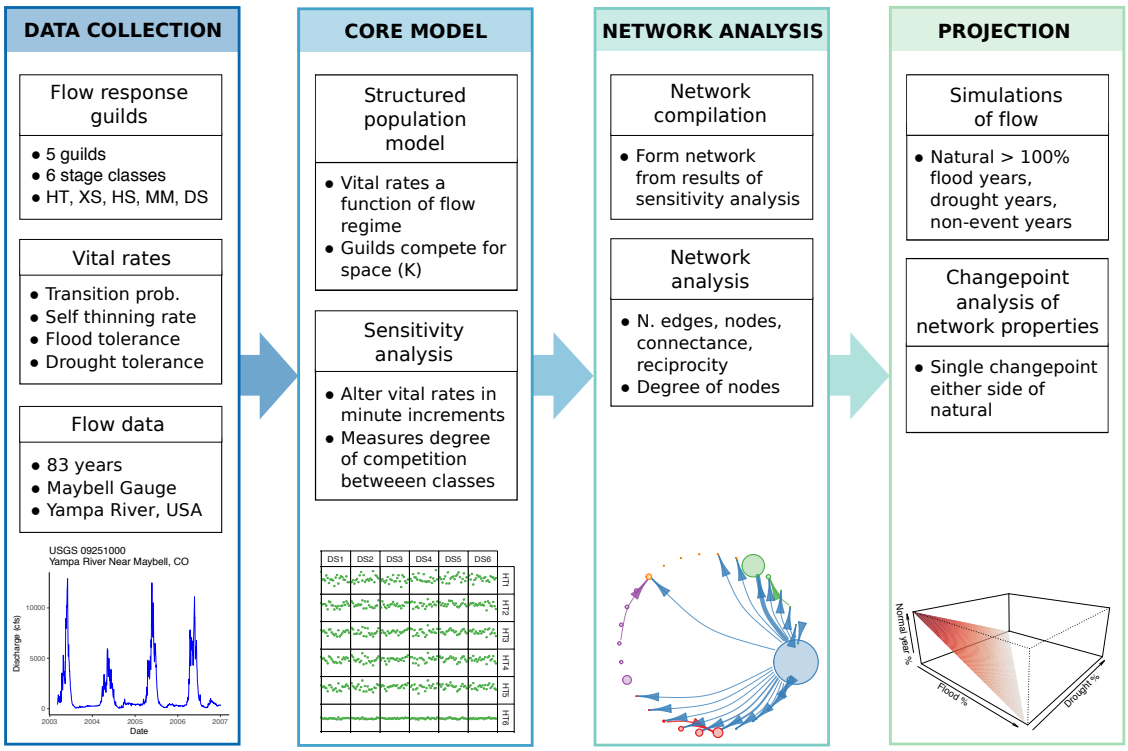

Figure 4.2.1 Conceptual diagram outlining the workflow used in the analysis from data collection to projection. The workflow followed four main steps: data collection (e.g. estimation of guild vital rates from field data and experiments, hydrograph data), model building and analysis (matrix population model, sensitivity analysis), network analysis, and projection and simulation across a range of altered flow regimes. We used iterated sensitivity analysis to quantify interactions between members of the community and form networks. The effects of flow alteration on networks were explored by projecting forward 250 years. See Methods for full details.

4.2.3 Methods

4.2.3.1 Study guilds

We explored population dynamics in five riparian plant guilds that represent riparian assemblages across a wide variety of locations: hydroriparian pioneer tree (HT), xeroriparian pioneer shrub (XS), hydroriparian pioneer shrub (HS), mesoriparian meadow species (MM), and desert shrub (DS) (Table 4.2.1). These guilds represent flow-response guilds[20]: groups of plants with similar morphological and physiological traits and therefore responses to water availability and fluvial disturbance.

4.2.3.2 Experimental design and model structure

We employed a stage-structured coupled stochastic population model to explore scenarios of the flow regime spanning extreme drought to extreme flood frequencies, as well as flow homogenization (Figure 4.2.2). Our approach followed the general modeling framework detailed in Lytle *et al*[10]. The model allows guilds of species that share similar vital rates to simultaneously occupy a dynamic floodplain zone. A guild j is described by a stage-based matrix $\boldsymbol{N}_j(t+1) = \boldsymbol{A}_j(t)\boldsymbol{N}_j(t)$, where $N_j(t)$ is a vector containing stage abundances and $\boldsymbol{A}_j(t)$ is a set of transition matrices that fluctuate according to variation in the hydrograph. Population dynamics of each guild are determined primarily by how their vital rate parameters (mortality, fecundity, self-thinning) are affected by flooding and drought. See Lytle & Merritt[51] for a detailed definitions of vital rate parameters for a subset of the guilds. All analyses were performed in *R* 3.2.3[52].

Each of our study guilds comprised six stage classes from seedling to reproductive adult[10] and are hereafter referred to as network nodes (vertices; n = 30). We obtained vital rates for the five guilds from a variety of sources, including field studies and historical aerial photos[10,51]. While these vital rates were gathered for a specific site and suite of species, the guild approach enables the transferability of modeling approaches between systems and regions.

The model operates at the reach scale, with total potential floodplain habitat, *K*, representing the maximum space available for occupation. Floods, droughts, and senescence can reduce the population size of guilds through interacting with their vital rates, in turn opening space for recruitment in the next cycle. The model keeps *K* constant across years, but changing river dynamics are accounted for broadly through the spatially

implicit nature of the model[51]. That is, the spatially implicit structure allows examining population dynamics without needing an understanding of the spatial dynamics of vegetation or river geomorphology[10,51].

We used 83 years of hydrograph data from the undammed Yampa River near Maybell, Colorado, U.S.A. (U.S. Geological Survey gage number 09251000). Based on river geomorphology, years when peak discharge exceeded 280 m^3s^{-1} were flood years, and years in which floods remained below 210 m^3s^{-1} were drought years. Years falling in between were considered non-event years. Matrix projection was accomplished in annual time steps. To project the model forward in time, a year was drawn at random from the time series and the corresponding flow metrics were calculated for that year (flood decline rate, timing, and whether it was a flood, drought or non-event year). In flood or drought years, all guilds were subject to guild-specific flood or drought mortality, respectively, in addition to baseline transition probabilities. Given the strong role that predictability of temporal environmental fluctuations can have on biodiversity[53], an interesting phenomenon to consider in future expansions of this approach is the role of temporal clustering of river flow regimes that incorporate supra-annual climatic cycles.

4.2.3.3 Sensitivities and network analysis

We used model iterated sensitivity analysis to quantify how small changes in a vital rate (flood susceptibility vital rate, in this case) of one node affects all other nodes within the community. We used iterated sensitivity analysis because it is not possible to obtain an analytical sensitivity from a stochastic, coupled structured population model except under limited circumstances. Iterated sensitivity analysis approximates taking the partial derivative of a population variate with respect to the parameter of interest. This approach differs from those related to the Community matrix (or other Jacobian matrices), where interaction strengths represent functional relationships underlying species interactions and Net Effects matrices (negative inverse of the Jacobian matrix) in turn enable quantitative predictions of effects of perturbations to one species on all others in the matrix[54].

We changed a given vital rate in increments of 0.001 on either side of its actual value for a total of 20 increments. The model was then projected forward 250 years into the future for each iterated step, and population sizes for each node were averaged for the final 100 years (150-250) and recorded. Each of these steps was repeated 1000 times to estimate the repeatability of a given effect. The entire process was repeated for each of the flow alteration scenarios (Figure 4.2.1). We calculated sensitivity as the slope of the regression line between the given vital rate value (20 incremental steps) and the average node population size. Sensitivities were calculated for all pairwise node combinations within the network. This allowed the calculation of standard sensitivities (the response of a guild

to a change in one of its own vital rates) as well as cross-guild sensitivities (the response of one guild to a change in a vital rate of another guild, as mediated by competition for available space). For example, changes in abundance of a guild, as a result of increased susceptibility to flooding, can have a cascading effect through the ecosystem by opening space for another guild to establish after a recruitment event. Considering this is a hydrograph-driven model and the fact that these riparian plants are inherently linked to floods, the choice of the flood susceptibility vital rate was clear, but other vital rates could also be used to form network links when examining other systems or particular management objectives.

Cross-guild sensitivities were used to create ecological networks, where we quantified the effects of changes to each node's vital rate on abundances of all others in the river reach (also termed 'sensitivity networks'[10]). A link (edge) was created between two nodes only where a clear linear relationship was present. These interactions emerge through indirect competition for space on the landscape as each guild occupies a portion of *K*, the total amount of riparian habitat available to all guilds in a given riparian reach. Occupying space makes it unavailable for new recruitment for another guild, thereby affecting each other's population dynamics. We used a cutoff of $R^2 \geq 0.30$ and $P < 0.01$ for sensitivities to be included as links. Thus, while a species may still be present in a community, it was not included as a node in a network if it had no interactions meeting this criterion. For specific relationships discussed in the text, we also calculated 95% confidence intervals on the simulated data to determine differences in abundances of particular guilds under differing flow regimes. We compiled networks using the 'graph.data.frame' function in the igraph *R* package[55].

We analyzed network properties by calculating the number of nodes and links, their connectance (the ratio of the number of links to the maximum possible number of links), and reciprocity (the proportion of mutual links; where there is a two-way relationship). Depending on the scenario, stage classes of particular guilds may have been present in very low abundances during the final 100-year data collection period, and potentially only briefly. Thus, while we included all nodes in the graphs for visualization, we calculated metrics on networks with unconnected nodes (i.e. where there were no sensitivity relationships that met our criteria) removed. That is, we considered non-linked nodes as non-members for this purpose. Therefore, missing nodes are those that are no longer linked with any other nodes in the network, based on our criteria of a significant interaction, and node number can drop below 30, despite lack of local extinctions. We also examined the degree (number of links connected to the node, or how well connected that node is in the network) of each guild stage class in the model. We calculated links out from a node and into a node, as well as bidirectional links.

Networks were compiled for the full suite of flow scenarios spanning from the natural flow regime to 100% drought years, 100% flood years, and 100% non-event years. Thus, the entire process of model runs, network building, and network analysis described above was repeated at each flow regime scenario (Figure 4.2.1). Vital rates were held constant across all flow regime scenarios (i.e. our goal was to simulate ecological rather than evolutionary dynamics), but hydrograph parameters were allowed to vary across an array of flow regime scenarios. For this analysis, we explored the sensitivity of networks to changes in one vital rate at time; we did not explore the possibility of multiple vital rates changing simultaneously. To simulate increased flood (or drought) frequency, we successively changed two of the 83 gauge years so that eventually all of them became flood (or drought) years (42 iterations in total for the 100% drought to flood scenario). To simulate flow homogenization due to damming, we successively changed year types, starting at natural flow regime frequency, until all of them became non-event years. Although our simulations were limited to modification of the frequency of floods and droughts, the core matrix model incorporates and varies other aspects of the natural flow regime depending on the year drawn from the flow vector (duration, timing, and interannual variability; magnitude is fixed as a threshold function). Thus, it is also possible to examine the network-wide effects of shifts in the timing and duration of floods using this approach.

To examine whether thresholds existed in network properties with altered flow scenarios, we tested for changepoints in the data. These represent precise locations in the ordered data series where the statistical properties of a sequence of observations change. We searched for single changepoints in the mean ('cpt.mean' function) moving from the natural flow regime through to extreme flood, drought, and non-event scenarios using the changepoint *R* package[56]. To do this, we used the 'at most one change' (AMOC) method and the MBIC (modified bayesian information criterion) penalty.

4.2.4 Results and Discussion

Changing flow conditions led to substantial shifts in riparian network properties according to the modeling results, including the number of nodes and links, network connectance, and reciprocity (see Table 4.2.1 for definitions). Here, nodes represent the six life-history stages of the five plant guilds, and links represent a significant cross-guild sensitivity (small changes in a vital rate of one node significantly alters abundance of another through a shared dependency on finite space). Therefore, links were not defined *a priori*, but arose through population dynamics resulting from the models. Increasing the frequency of drought years relative to flood years led to a simplification of ecological networks (Figure 4.2.2, Figure 4.2.3). By contrast, increasing flood year frequency (the frequency of years over the time series that were defined as flood, rather than drought or non-event years) had a less pronounced effect on network completeness and connectance.

The greatest simplifications (with significant changepoints, which represent locations in the data where the statistical properties of a sequence of observations change; Table 4.2.1) were observed for the number of nodes with increased drought, and the number of links with both increasing drought and flood years (Figure 4.2.3).

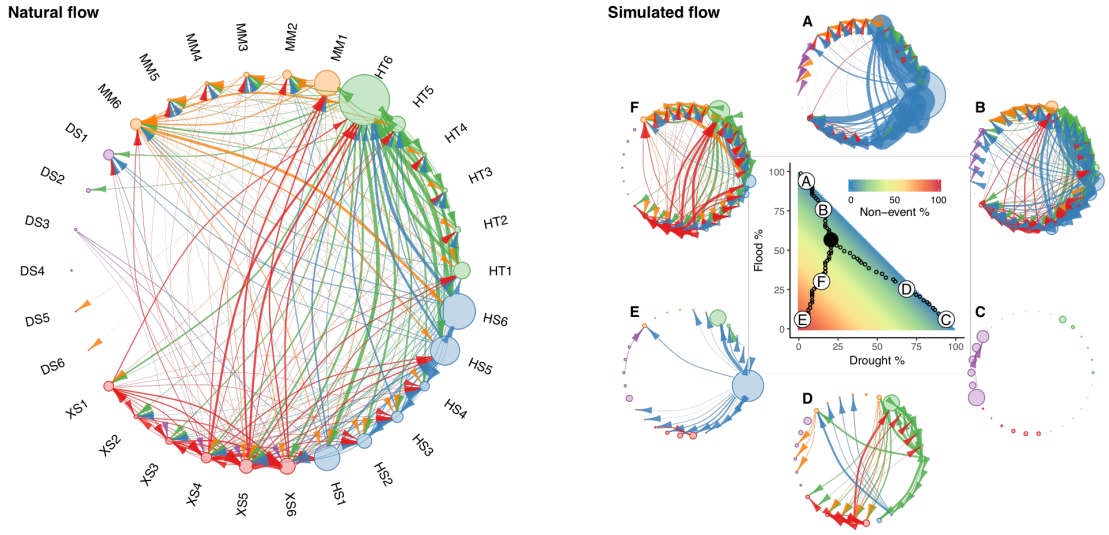

Figure 4.2.2 Examination of riparian plant networks across a spectrum of possible flow regime futures. Left panel represents the network simulated according to the natural flow regime. Nodes on the outside of the circle represent the 30 members of the network (5 guilds, 6 stage classes; color coded by guild; size scales with abundance), and links represent significant interactions (see Table 4.2.1; width = relationship strength; color matches source node; links are directional). Node order is consistent across networks and all nodes are shown, even if unconnected. The labels on the nodes represent the guild and its stage class (HT = hydroriparian pioneer trees; XS = xeroriparian pioneer shrubs; HS = hydroriparian pioneer shrubs; MM = mesoriparian meadow species; DS = desert shrubs). Right panel demonstrates examples of networks at a range of altered flows. Scenarios A-F represent the position of networks in this flow-space and correspond to the letters in the central flow-space graph (e.g. 'A' is an extreme flood scenario and 'C' extreme drought). Three year types are possible in the model: flood, drought and non-event (flow homogenization) and we run scenarios from the natural flow regime (56.6% flood years) to the extremes of these year-types, as shown in the flow-space plot. All simulated scenarios (open circles on the flow-space) are shown in relation to natural flow regime (filled circle). See online Supplementary Information for the complete range of networks (directional and bidirectional) and Methods for details.

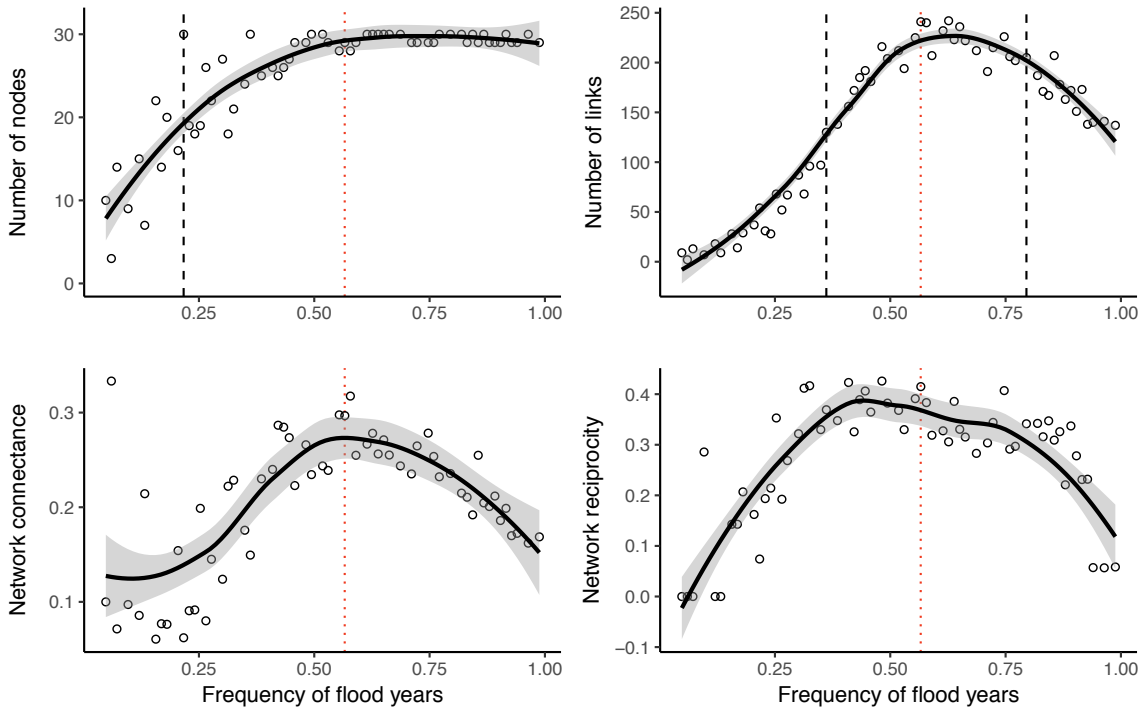

Figure 4.2.3 Summary metrics of full ecological networks spanning the spectrum of flow extremes from extreme drought to flood. See Table 4.2.1 for definitions of terms. Network metrics were calculated only on nodes that were connected; i.e. isolated nodes in Figure 4.2.2 were not incorporated into networks, but unconnected does not mean extinct. Trend lines represent locally weighted smoothing (LOESS) fits, accompanied by 95% confidence intervals (shaded area). The natural flow regime is shown as the dotted line. Dashed lines represent significant changepoints in the series. We limited the search for changepoints to a maximum of one per scenario (i.e. natural flow regime to each of the three extreme flows). Each point represents an approximately 1.5% change in the frequency of flood and drought years. 'Flood years' are years when the peak discharge exceeds 280 m^3s^{-1}. See online Supplementary Information for homogenization scenario results.

Networks were most connected for hydrographs (a record of river discharge over time) similar to the natural flow regime (Table 4.2.1), likely due to the fact that species comprising these guilds had evolved under these flow conditions[11]. Although the number of nodes in networks peaked near the natural flow regime and plateaued with increasing floods, network connectance and reciprocity declined at high flood year frequencies (Figure 4.2.3). High network connectance and reciprocity indicate the existence of compensatory population dynamics, which confer resilience to flood or drought disturbances[22] and can stabilize communities in the presence of perturbations[23]. This demonstrates that if one community member experiences a decline in a vital rate or density through external stressors, others (not experiencing such decline) will respond by taking its place, a beneficial phenomenon for overall biodiversity and ecosystem functioning. Network connectance also influences the stability of communities in ways that affect the long-term persistence of particular community types[14,24–26]. Connectance plays a fundamental role in the maintenance of biodiversity, with highly connected

communities being more robust to species losses in food webs[15] and more resistant to invasion by non-native species[27]. Losses of interactions can also be precursors to future biodiversity loss[28]. Therefore, the simplification of networks, particularly with increasing drought, which is predicted to increase widely over the next century[29], may predispose networks to collapse[12]. In sum, the highly-connected networks that we observed under natural flow regime conditions could represent communities that are evolutionarily-optimized to the flow components associated with such natural or historic conditions.

Flow homogenization (i.e. stable base-flow and reduced flood events, often the result of dam operations) caused network simplification similar to that observed under drought scenarios, reflecting the central role of floods in dryland rivers (Figure 4.2.2). Flow homogenization considerably influences the resident biota of rivers[30], and can directly affect the riparian community through reduced water availability, changes in the timing of availability, and lack of flood scouring necessary for seedling recruitment[31]. Preserving or restoring key components of the natural flow regime, such as flooding, should therefore be a high priority for river managers. Our results and mechanistic modeling approach, which can be tailored for target species, complements an existing literature on experimental flows[32]. Together, these provide the tools required for managers to design prescribed flow releases to maximize the benefits for target species or overall emergent community properties, such as our metric of network connectance.

The natural flow regime has been severely modified in many river systems through human activities such as dam construction and management for hydropower and water storage and diversion, but components of the flow regime are expected to shift under even the most conservative of climate change scenarios[7,33]. The results of our drought and homogenization scenarios indicate how influential these environmental changes can be on the organization of river-dependent communities. By incorporating riparian plant guilds that occur in dryland river systems worldwide[34,35], these results apply beyond our study system. The particular relevance of the results to dryland regions explains why scenarios involving elevated flood frequency were less problematic than the outcomes involving reduced flooding. Although increasing flood frequency is just one of many predicted changes for the study region, our results help to demonstrate the importance of preserving floods in dynamic river systems. In less water-scarce regions, increased flood frequency and magnitude (disturbance rather than water availability) may cause more dramatic shifts in riparian ecosystems[36,37]. Thus, the widespread nature of flow-altering dams[4], the pervasive threat of future damming worldwide[3], and the adaptation of many riverine organisms to specific attributes of the natural flow regime[11], highlight the concerning nature of the demonstrated network-wide effects of flow modification on these individual species, communities, and riparian ecosystems overall.

The role of individual nodes within networks revealed guild-specific responses to altered flow conditions. By examining how guild interactions (links in the network) changed in response to hydrology, we identified three distinct node types based on their degree (number of links per node) within the network. Rather than defining interactions *a priori*, guild interactions emerged from the model via sensitivity analysis, as a direct result of a shared dependency on finite space. *Keystone nodes*[18,28,38] were those that had large effects on the overall network, shown by substantial numbers of links outbound to other nodes (Table 4.2.1, Figure 4.2.4). *Mutual nodes* played a key reciprocal role in the network, by harboring many bidirectional links, akin to compensatory dynamics[22]. By contrast, *passive nodes* were those that responded to, rather than influenced, other nodes in the network through receiving many inbound links (Table 4.2.1). Keystone nodes were most prevalent in reproductive guild stages, and non-reproductive stages tended to function as passive nodes, having little influence on other stages or guilds.

Adult hydroriparian pioneer trees and xeroriparian pioneer shrubs functioned as keystone nodes at or near the natural flow regime, and declined with both increasing and decreasing flood frequency. Hydroriparian pioneer shrubs, on the other hand, are the dominant riparian guild in many temperate and mesic regions globally[39–41] and became keystone nodes at high flood frequency scenarios (Figure 4.2.4). Thus, the model identified critical hydrologic thresholds where alteration to river hydrology caused a change in the identity of the keystone riparian guild. Hydropriparian trees (e.g. poplars, alder, river red gum) and hydroriparian shrubs (e.g. willow species) are critical components of riparian plant communities and riparian habitats worldwide. These flood-adapted, phreatophytic woody species provide ecosystem services such as habitat for riparian wildlife, flood mitigation and bank stabilization, modification to microclimate conditions by cooling and increasing humidity, and nutrient cycling[40]. In riparian ecosystems globally, there are woody species, both trees and shrubs, which perform keystone roles in riparian communities, including black poplar (*Populus nigra*) in Europe, river red gum (*Eucalyptus camaldulensis) in Australia, and cottonwood species (Populus spp.) in North America*[42–44]. With loss of native hydroriparian shrubs and trees due to changes in flow regimes, there are often shifts to more xeric and upland species and decreases in riparian habitat quality and complexity[34,45,46]. These effects, however, largely depend on the baseline hydrologic setting of a river[47].

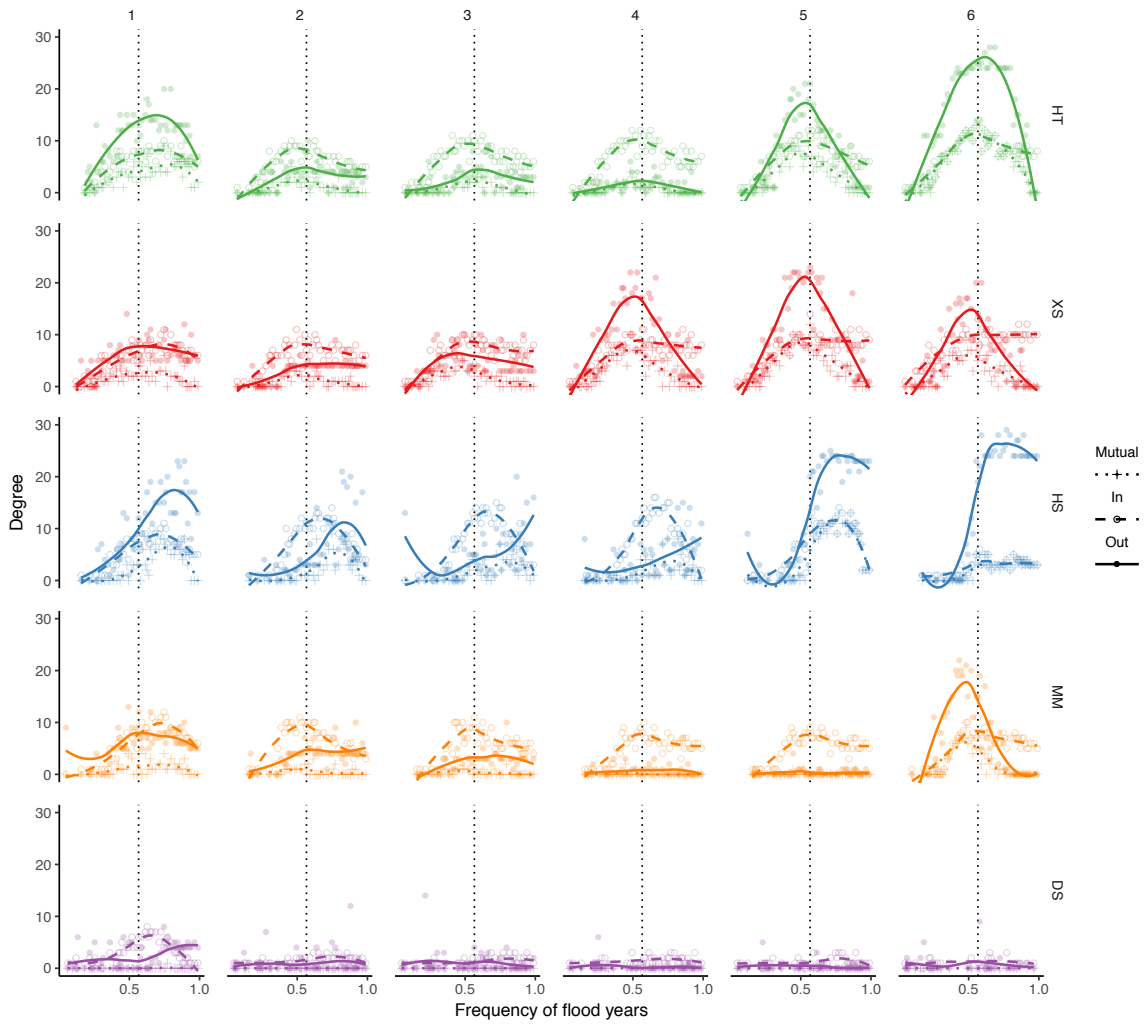

Figure 4.2.4 Degree (number of links connected to the node) of each network node in relation to flow-state. All five guilds (as rows), each with six stage classes (as columns 1-6) are shown. Scenarios were run from 100% drought years to 100% flood years (through the natural flow regime, indicated as the dotted line). Inward, outward, and mutual relationships are shown. Trend lines represent locally weighted smoothing (LOESS) fits. Each point represents an approximately 1.5% change in the frequency of flood and drought years. 'Flood years' are years when the peak discharge exceeds 280 m3s-1. See online Supplementary Information for homogenization scenario results. HT = hydroriparian pioneer trees; XS = xeroriparian pioneer shrubs; HS = hydroriparian pioneer shrubs; MM = mesoriparian meadow species; DS = desert shrubs.

The model was sensitive to scenarios where small changes to the flow regime led to substantial reorganization of networks and shifts in the stage-specific ecological role of guilds. Network connectance has been shown to be generally well-conserved and insensitive to changing environmental conditions in ecological networks[48]. However, we observed changes in network connectance across the spectrum of flow regime scenarios. Under the increased-drought scenario, relatively small increases in drought frequency led to increases in the number of outbound links for xeroriparian pioneer shrubs, particularly

for reproductive stages (stages 4-6; Figure 4.2.4). However, the overall relative space occupied by all stage classes increased similarly for xeroriparian pioneer shrubs (20.7 to 24.1% of *K*; 95% CIs [17.1, 24.3] and [20.9, 27.4], respectively) and hydroriparian pioneer trees (33.4 to 36.7% of *K*; 95% CIs [29.8, 36.9] and [33.5, 39.8], respectively) with a small shift to drier conditions from the natural flow regime (56.6% to 45.7% flood years). Increasing drought frequencies can lead to loss of the unique ecosystem structure and services that distinguish riparian ecosystems from surrounding uplands. Due to available space opening up in increasingly flood-free conditions, the degree of each node was lower than more natural or flood dominated conditions, which was true even for the drought specialist desert shrub. Increased flood frequency, however, shifted the community towards guilds more tolerant of wet conditions, with stages five and six of flood-tolerant hydroriparian pioneer shrubs being keystone nodes in flood-dominated conditions. The overall space occupied by all hydroriparian pioneer shrub stages reflected this dominance when moving from natural flow conditions to slightly wetter conditions (63.8% flood years; 43.1 to 51.0% of *K*; 95% CIs [34.8, 51.4] and [43.6, 58.4], respectively). By contrast, the desert shrub guild played little role in any network other than being a passive responder, dominating only under the most severe drought conditions in response to the decline of other river-dependent guilds[49]. Such terrestrialization has been demonstrated in response to groundwater depletion linked to streamflow alteration in a number of studies[49,50].

4.2.5 Conclusions

Network connectance declined with increasing flow alteration. River-dependent communities have evolved over millennia and have been tailored by natural selection to the volume and seasonal variability in natural flow regimes[11]. Examining how ecological networks change across a spectrum of environmental conditions, we show that moving even modestly away from this natural flow regime can have detrimental effects on the organization of ecological networks, and conversely, how minor adjustments in managed flow regimes may restore necessary flow components for riparian ecosystem functioning (Figure 4.2.3). Highly connected networks represent communities that are optimized at these conditions, having evolved mechanisms to enable persistence in the face of a wide variety of perturbations including and beyond flow regime dynamics. Connectance has implications for community stability[14,24–26], robustness[12,15], and resistance to invasion[27]; and here indicates the presence of compensatory dynamics stabilizing aggregate community properties[23]. Being able to explore and visualize the consequences of a changing environment on the structure and emergent properties of highly complex ecological communities, and identify and predict the specific environmental conditions that enable a particular guild to perform a keystone role in the community, highlights the benefits of the mechanistic and network-based approach employed in the present study.

Keystone status is affected by changes to the natural flow regime. Removing floods, in particular, led to a loss of keystone status of hydroriparian pioneer trees. Loss of keystone guilds leads to changes in fundamentally important ecosystem services, such as habitat provision for riparian wildlife, flood mitigation and bank stability, microclimatic regulation, and nutrient cycling[40]. Conversely, under scenarios of increased flooding the keystone status of hydroriparian pioneer tree was replaced by hydroriparian pioneer shrub. Because these two guilds have different edaphic requirements and ecological roles, it is important to predict which guilds will function in a keystone role under future flow regime scenarios. Thus, our network analysis facilitates proactive management for species and life stages of interest under future scenarios.

Floods are fundamental to the maintenance of complex ecological networks. Floods, despite their negative effects on human infrastructure, are associated with many beneficial and necessary processes that enhance the diversity of riverine systems and the robustness and resilience of ecological networks. Although much focus has been on drought, flow homogenization (due to damming) may be equally detrimental to riparian communities. Therefore, managers should strive to preserve or restore natural flow dynamics, particularly floods, as a vital driver of the ecology of rivers[32]. Through connecting flood and drought distributions directly to complex multi-guild networks, our modeling approach highlights the consequences of future climates on riparian networks. Such a mechanistic modeling approach allows us to forecast the nonstationary effects that climate change is expected to impose on future river flow regimes, and equips managers seeking to mitigate these impacts by enabling detailed projections of potential flow futures.

4.2.6 Acknowledgements

We thank N. LeRoy Poff, Albert Ruhi, and members of the OSU Integrative Biology journal club for comments on earlier versions of the manuscript. Dinosaur National Monument supported the research that led to the vital rate data. Funding was provided in part by the U.S. Department of Defense (SERDP RC-2511) and the U.S. Department of Agriculture Forest Service.

Code availability. The core matrix model in *R* is available on figshare (http://dx.doi.org/10.6084/m9.figshare.4652608). Sensitivities can be calculated from this script using an iterative outer loop as detailed in the Methods.

Data availability. All data required to run the model, including the flow hydrograph from the Yampa River and guild vital rates, is available on figshare (http://dx.doi.org/10.6084/m9.figshare.4652608).

4.2.7 References

1. Poff, N. L. *et al.* The natural flow regime. *Bioscience* **47,** 769–784 (1997).
2. Nilsson, C., Reidy, C. A., Dynesius, M. & Revenga, C. Fragmentation and flow regulation of the world's large river systems. *Science* **308,** 405–408 (2005).
3. Zarfl, C., Lumsdon, A. E., Berlekamp, J., Tydecks, L. & Tockner, K. A global boom in hydropower dam construction. *Aquat. Sci.* **77,** 161–170 (2014).
4. Poff, N. L., Olden, J. D. J., Merritt, D. M. & Pepin, D. M. Homogenization of regional river dynamics by dams and global biodiversity implications. *Proc. Natl. Acad. Sci.* **104,** 5732–5737 (2007).
5. Flanagan, N. E., Richardson, C. J. & Ho, M. Connecting differential responses of native and invasive riparian plants to climate change and environmental alteration. *Ecol. Appl.* **25,** 753–767 (2015).
6. Naiman, R. J. & Décamps, H. The ecology of interfaces: riparian zones. *Annu. Rev. Ecol. Syst.* **28,** 621–658 (1997).
7. Reynolds, L. V., Shafroth, P. B. & Poff, N. L. Modeled intermittency risk for small streams in the Upper Colorado River Basin under climate change. *J. Hydrol.* **523,** 768–780 (2015).
8. Lu, X. *et al.* Drought rewires the cores of food webs. *Nat. Clim. Chang.* **6,** 875–878 (2016).
9. Ledger, M. E., Brown, L. E., Edwards, F. K., Milner, A. M. & Woodward, G. Drought alters the structure and functioning of complex food webs. *Nat. Clim. Chang.* **3,** 223–227 (2012).
10. Lytle, D. A., Merritt, D. M., Tonkin, J. D., Olden, J. D. & Reynolds, L. V. Linking river flow regimes to riparian plant guilds: a community-wide modeling approach. *Ecol. Appl.* **27,** 1338–1350 (2017).
11. Lytle, D. A. & Poff, N. L. Adaptation to natural flow regimes. *Trends Ecol. Evol.* **19,** 94–100 (2004).
12. Strona, G. & Lafferty, K. D. Environmental change makes robust ecological networks fragile. *Nat. Commun.* **7,** 1–7 (2016).
13. Ings, T. C. *et al.* Ecological networks - beyond food webs. *J. Anim. Ecol.* **78,** 253–269 (2009).
14. Thebault, E. & Fontaine, C. Stability of ecological communities and the architecture of mutualistic and trophic networks. *Science* **329,** 853–856 (2010).
15. Dunne, J. A., Williams, R. J. & Martinez, N. D. Network structure and biodiversity loss in food webs: robustness increase with connectance. *Ecol. Lett.* **5,** 558–567 (2002).
16. Poisot, T., Stouffer, D. B. & Gravel, D. Beyond species: Why ecological interaction networks vary through space and time. *Oikos* **124,** 243–251 (2015).
17. Thompson, P. L. & Gonzalez, A. Dispersal governs the reorganization of ecological networks under environmental change. *Nat. Ecol. Evol.* **1,** 162 (2017).

18. Stouffer, D. B., Sales-Pardo, M., Sirer, M. I. & Bascompte, J. Evolutionary conservation of species' roles in food webs. *Science* **335,** 1489–1492 (2012).
19. Poisot, T., Stouffer, D. B. & Gravel, D. Beyond species: why ecological interactions vary through space and time. *Oikos* **124,** 243–251 (2015).
20. Merritt, D. M., Scott, M. L., Poff, N. L., Auble, G. T. & Lytle, D. A. Theory, methods and tools for determining environmental flows for riparian vegetation: riparian vegetation-flow response guilds. *Freshw. Biol.* **55,** 206–225 (2010).
21. Milly, P. C. D., Dunne, K. A. & Vecchia, A. V. Global pattern of trends in streamflow and water availability in a changing climate. *Nature* **438,** 347–350 (2005).
22. Gonzalez, A. & Loreau, M. The causes and consequences of compensatory dynamics in ecological communities. *Annu. Rev. Ecol. Evol. Syst.* **40,** 393–414 (2009).
23. Brown, B. L., Downing, A. L. & Leibold, M. A. Compensatory dynamics stabilize aggregate community properties in response to multiple types of perturbations. *Ecology* **97,** 2021–2033 (2016).
24. Allesina, S. & Tang, S. Stability criteria for complex ecosystems. *Nature* **483,** 205–208 (2012).
25. Mougi, A. *et al.* Diversity of interaction types and ecological community stability. *Science* **337,** 349–51 (2012).
26. May, R. M. Will a large complex system be stable? *Nature* **238,** 413–414 (1972).
27. Baiser, B., Russell, G. J. & Lockwood, J. L. Connectance determines invasion success via trophic interactions in model food webs. *Oikos* **119,** 1970–1976 (2010).
28. Aizen, M. A., Sabatino, M. & Tylianakis, J. M. Specialization and rarity predict nonrandom loss of interactions from mutualist networks. *Science* **335,** 1486–1489 (2012).
29. Dai, A. Drought under global warming: A review. *Wiley Interdiscip. Rev. Clim. Chang.* **2,** 45–65 (2011).
30. Bunn, S. E. & Arthington, A. H. Basic principles and ecological consequences of altered flow regimes for aquatic biodiversity. *Environ. Manage.* **30,** 492–507 (2002).
31. Rood, S. B., Goater, L. A., Mahoney, J. M., Pearce, C. M. & Smith, D. G. Floods, fire, and ice: disturbance ecology of riparian cottonwoods. *Can. J. Bot.* **85,** 1019–1032 (2007).
32. Olden, J. D. *et al.* Are large-scale flow experiments informing the science and management of freshwater ecosystems? *Front. Ecol. Environ.* **12,** 176–185 (2014).
33. Rood, S. B. *et al.* Declining summer flows of Rocky Mountain rivers: Changing seasonal hydrology and probable impacts on floodplain forests. *J. Hydrol.* **349,** 397–410 (2008).

34. Stromberg, J. C. & Merritt, D. M. Riparian plant guilds of ephemeral, intermittent and perennial rivers. *Freshw. Biol.* **61,** 1259–1275 (2016).
35. Aguiar, F. C., Cerdeira, J. O., Martins, M. J. & Ferreira, M. T. Riparian forests of Southwest Europe: Are functional trait and species composition assemblages constrained by environment? *J. Veg. Sci.* **24,** 628–638 (2013).
36. Gurnell, A. M., Bertoldi, W. & Corenblit, D. Changing river channels: The roles of hydrological processes, plants and pioneer fluvial landforms in humid temperate, mixed load, gravel bed rivers. *Earth-Science Rev.* **111,** 129–141 (2012).
37. Hupp, C. Hydrology, geomorphology and vegetation of Coastal Plain rivers in the south-eastern USA. *Hydrol. Process.* **14,** 2991–3010 (2000).
38. Lewinsohn, T. & Cagnolo, L. Keystones in a tangled bank. *Science* **335,** 1449–1451 (2012).
39. Friedman, J. M. *et al.* Dominance of non-native riparian trees in western USA. *Biol. Invasions* **7,** 747–751 (2005).
40. Kominoski, J. S. *et al.* Forecasting functional implications of global changes in riparian plant communities. *Front. Ecol. Environ.* **11,** 423–432 (2013).
41. Rivaes, R. P. *et al.* Modeling the evolution of riparian woodlands facing climate change in three European rivers with contrasting flow regimes. *PLoS One* **9,** e110200 (2014).
42. Doody, T. M. *et al.* Quantifying water requirements of riparian river red gum (Eucalyptus camaldulensis) in the Murray-Darling Basin, Australia – implications for the management of environmental flows. *Ecohydrology* **8,** 1471–1487 (2015).
43. Kath, J., Le Brocque, A., Leyer, I. & Mosner, E. Hydrological and land use determinants of Eucalyptus camaldulensis occurrence in floodplain wetlands. *Austral Ecol.* **39,** 643–655 (2014).
44. Guilloy-Froget, H., Muller, E., Barsoum, N. & Hughes, F. M. R. Dispersal, germination, and survival of Populus nigra L. (Salicaceae) in changing hydrologic conditions. *Wetlands* **22,** 478–488 (2002).
45. Middleton, B. A. & Souter, N. J. Functional integrity of freshwater forested wetlands, hydrologic alteration, and climate change. *Ecosyst. Heal. Sustain.* **2,** e01200 (2016).
46. Andersen, D. C. & Cooper, D. J. Dams, floodplain land use, and riparian forest conservation in the semiarid upper Colorado River basin, USA. *Environ. Manage.* **40,** 453–475 (2007).
47. Belmar, O., Bruno, D., Martínez-capel, F., Barquín, J. & Velasco, J. Effects of flow regime alteration on fluvial habitats and riparian quality in a semiarid Mediterranean basin. *Ecol. Indic.* **30,** 52–64 (2013).
48. Tylianakis, J. M., Tscharntke, T. & Lewis, O. T. Habitat modification alters the structure of tropical host-parasitoid food webs. *Nature* **445,** 202–205 (2007).
49. Merritt, D. M. & Bateman, H. L. Linking stream flow and groundwater to avian

habitat in a desert riparian system. *Ecol. Appl.* **22,** 1973–1988 (2012).
50. Shafroth, P. B., Auble, G. T., Stromberg, J. C. & Patten, D. T. Establishment of woody riparian vegetation in relation to annual patterns of streamflow, Bill Williams River, Arizona. *Wetlands* **18,** 577–590 (1998).
51. Lytle, D. A. & Merritt, D. M. Hydrologic regimes and riparian forests: a structured population model for cottonwood. *Ecology* **85,** 2493–2503 (2004).
52. R Core Team. *R: A language and environment for statistical computing*. (2015).
53. Tonkin, J. D., Bogan, M. T., Bonada, N., Ríos-Touma, B. & Lytle, D. A. Seasonality and predictability shape temporal species diversity. *Ecology* **98,** 1201–1216 (2017).
54. Novak, M. *et al.* Characterizing species interactions to understand press perturbations: what is the community matrix? *Annu. Rev. Ecol. Evol. Syst.* **47,** 409–432 (2016).
55. Csardi, G. & Nepusz, T. The igraph software package for complex network research. *InterJournal, Complex Syst.* 1695 (2006).
56. Killick, R. & Eckley, I. A. Changepoint: An R Package for Changepoint Analysis. 1–18 (2011).

4.3 Synthesis: Cross-taxon analysis of riparian vegetation, fish, and invertebrates

4.3.1 Summary

Overcoming the physical limits of dam operations under nonstationarity will require creative approaches to flow management and modeling approaches that forecast the effects of management actions on multiple ecosystem components simultaneously. Using a novel multispecies modeling approach, we investigated the cross-ecosystem effects of environmental flow regimes designed for specific ecosystem outcomes. We reveal tradeoffs associated with flow regimes targeting riparian vegetation, fishes, and invertebrates. The different frequencies associated with each flow regime in some cases caused non-target ecosystem components to become locally extirpated within 50 years. By incorporating multiple flow frequencies, the natural flow regime enabled a balanced but sub-optimal response of the three ecosystem components (mean 72% of designer flow). Although returning to a natural flow regime may not be possible in highly managed rivers, novel flow regimes must incorporate diverse frequencies inherent to such a regime and accomodate the sometimes conflicting requirements of different taxa at different times.

4.3.2 Introduction

Dams and other types of human infrastructure have modified river hydrology globally and continue to do so at an unprecedented rate (Grill et al. 2019). Alteration of river flows comes at a major cost for the biota that inhabit freshwater and riparian (hereafter "river") ecosystems (Bunn and Arthington 2002, Tonkin et al. 2018), threatening the countless ecosystem services they provide (Auerbach et al. 2014). Maintaining functional river ecosystems under uncertain hydroclimatic futures presents a major management challenge for both existing and planned dam projects (Horne et al. 2019, Palmer and Ruhi 2019, Tonkin et al. 2019), requiring the consideration of flow prescriptions that target the health of downstream ecosystems (Acreman et al. 2014).

Environmental flows are increasingly used to help minimize the detrimental effects of dam management on river biota (Poff and Matthews 2013, Yarnell et al. 2015). Designer environmental flows range from single events designed to achieve a specific goal, such as a flood for mobilizing sediment, to entire flow regimes designed to accommodate multiple ecosystem needs (Acreman et al. 2014). In practice, most environmental flow programs target a few important species or a particular component of the river ecosystem, such as recruitment of riparian vegetation or spawning of native fish (Olden et al. 2014) without directly considering secondary effects on other components of the ecosystem. This presents the question: Does flow management designed to benefit one important

component of the river simultaneously protect other ecosystem components, or does it involve ecological tradeoffs that compromise other ecosystem components?

Calls for holistic ecosystem approaches to support sustainable riverine management continue to mount, yet robust quantitative models to underpin such efforts remain scarce (Poff and Olden 2017). Here, we examined the responses to designer flows targeting three ubiquitous but distinct components of river ecosystems: riparian vegetation, fishes, and aquatic invertebrates. Using a mechanistic, multispecies modeling approach that links population dynamics and hydrology, we designed flow regimes to maximize management outcomes for each of the three ecosystem components. The modeling approach permitted us to simultaneously design flows for a single ecosystem component as well as quantify the associated synergies or tradeoffs across other ecosystem components. These approaches enable an assessment of the potential ecological benefits or deficits of designer flow prescriptions at the ecosystem scale.

4.3.3 Methods

Management targets. Using species common to the Colorado River Basin of the southwestern United States, we defined management targets that natural resource managers often seek to maximize downstream from large dams. These outcomes relate to three components of a river-riparian (hereafter "river") ecosystem: cottonwood tree coverage as a percent of riparian carrying capacity, native fish species biomass as a percent of total carrying capacity (including nonnative fishes), and abundance of terrestrially-available benthic invertebrates (hereafter "aquatic invertebrates"). Cottonwood is an important native riparian tree that suffers from the effects of flow regime modification and competition with nonnatives such as tamarisk (Merritt and Poff 2010). Native fish species are a focal management target because they face an uncertain future resulting from altered hydrology and impacts from nonnative species (Chen and Olden 2017). Terrestrially-available aquatic invertebrates serve as aquatic prey for fish and, upon emergence as winged adults, as terrestrial prey for birds, bats, lizards and other riparian animals (Baxter et al. 2005). Using these targets, coupled with mechanistic population models, we identified flow regimes that maximized the value of each ecosystem component and explored tradeoffs in achieving positive outcomes across all three components by projecting the flow time-series for up to 200 years into the future. We also examined a natural flow regime scenario using a hydrograph derived from a large free-flowing river supporting riparian vegetation, fish and aquatic invertebrate assets (upper Verde River, Arizona, USA) and quantified the community-wide population responses across ecosystem components.

Modeling frameworks. We modeled the three ecosystem components using three independent existing models parameterized using empirical data. Riparian vegetation and

fishes were modeled using a novel application of coupled, stage-structured matrix population models projected at annual time steps (Lytle et al. 2017, Rogosch et al. 2019). Informed by empirical data from a variety of sources, these models link the flow regime directly with population dynamics in a coupled framework that enables an understanding of whole-community dynamics and can incorporate stochasticity by taking random draws from a sequence of river flow year types. Floods and droughts interact with vital rates, affecting population sizes, which opens vacant space (vegetation) or biomass (fish) for recruitment during the next year if conditions are met. Both models have demonstrated a strong ability to recover known patterns on the landscape via tests against empirical data (Lytle et al. 2017, Rogosch et al. 2019).

The plant community comprised five taxa with six stage classes from seedling to reproductive adult: cottonwoods (*Populus deltoides*), tamarisk (*Tamarix ramosissima*), willow (*Salix exigua*), meadow grasses, and sagebrush (*Artemisia tridentata*). These taxa are representative of dominant groups across dryland regions. The fish community comprised three native species to the southwest USA (each with three stage classes): desert sucker (*Catostomus clarki*; CACL), Sonora sucker (*Catostomus insignis*; CAIN) and roundtail chub (*Gila robusta*; GIRO); and four non-native species (each with three stage classes): yellow bullhead (*Ameiurus natalis*; AMNA), green sunfish (*Lepomis cyanellus*; LECY), smallmouth bass (*Micropterus dolomieu*; MIDO), and red shiner (*Cyprinella lutrensis*; CYLU).

Benthic invertebrates, which experience population dynamics at intra-annual timescales, were modeled using a novel form of the continuous logistic growth model that enables carrying capacity (K) to fluctuate through time (McMullen et al. 2017). Carrying capacity, in this case, responds to flood events. For flood-adapted species, carrying capacity is highest immediately post-flood. The magnitude of a flood pulse determines the magnitude of change in K, and this relationship can be modeled for events of any magnitude and for multiple, repeated events. Contrary to the fish and riparian plant models, this model operates on individual populations in that the populations do not share a finite resource such as space or biomass: each population has its own carrying capacity. We modeled three invertebrate taxa: a fast life-cycle, flood-adapted mayfly, *Fallceon* spp. (Ephemeroptera: Baetidae); a slow life-cycle, flood-adapted dragonfly *Progomphus* spp. (Odonata: Gomphidae); and a flood-averse ostracod seed shrimp (Crustacea: Ostracoda).

Vital rates for all species included in the models were obtained from independent sources in the literature and from field studies. Vital rates included stage-specific mortality rates in response to flow events for fish and riparian plants, and population growth rates and flow-specific mortality rates for aquatic invertebrates.

Hydrograph details. Although our approach was simulation-based (with parameterizations from field data) in a generalized river in the southwestern United States, we used a real flow regime to generate a natural hydrograph vector. To do this, we sourced a 45-year (1964-2008) historical hydrograph from the upper Verde River (USGS gauge number 09503700) near Paulden, Arizona. All three groups were modeled from this one central flow regime in our natural flow regime scenario, enabling a comparison of community dynamics across the whole ecosystem.

Flow design. We searched flow parameter space for optimal sequences of flow events that maximized each of the management targets associated with riparian plants, native fishes, and aquatic invertebrates. For riparian plants and fishes, this search for an optimal flow design followed a series of steps that incrementally adjusted the frequency of particular year-types. The resulting prescribed flow regime for riparian vegetation consisted of a spring flood every six years, preceded by a drought year, with a series of non-event years in between (Figure 4.3.1). These floods occurred within the spring window that enabled cottonwood and tamarisk to recruit (synchronized with seed release). The resulting prescribed flow regime for native fish percentage consisted of a spring flood every year. In contrast to the plant and fish models, the invertebrate models operates in continuous time. Because the aquatic invertebrates we modeled do not compete directly with each other for a resource such as space or food, we modelled the the three taxa independently so that each species had its own carrying capacity, which we scaled to 100. We sought to maximize the average value of the two terrestrially-available target taxa (i.e. % of K) over the 20-year evaluation period. The resulting scenario that maximized the target was four small pulses per year, below the threshold of a flood in either the fish or riparian models. Therefore, the invertebrate prescription results in 100% of years being non-event years for the non-target taxa.

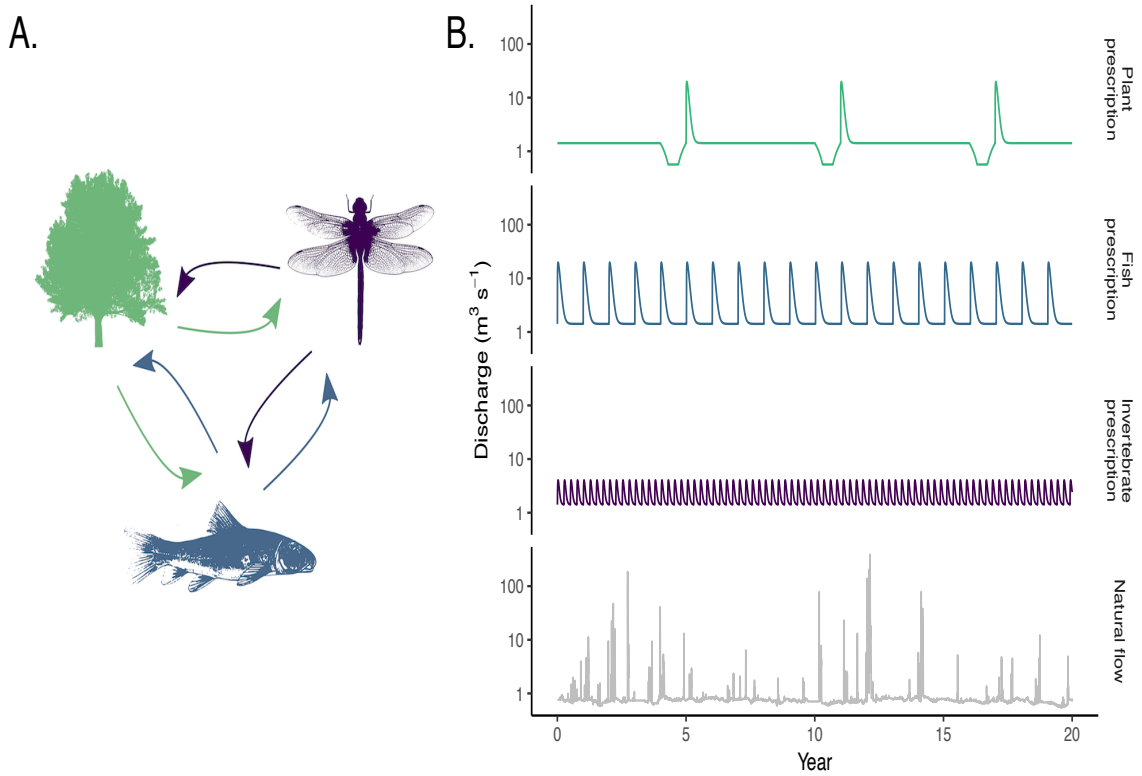

Figure 4.3.1 The modeled ecosystem components and flow regimes. A. The three ecosystem components examined: riparian plants (target: % cottonwoods), fish (target: % native species), and benthic invertebrates (target: % terrestrially-available taxa). B. A schematic of the three flow regimes designed for each target ecosystem component. The plant and fish models are based on year-types and the invertebrate model responds to individual flow events, thus the 'hydrographs' are for visual purposes only (e.g. the plant prescription shows a single large flood event every 6 years, preceded by a drought year). The bottom panel represents the historical hydrograph taken from the Verde River, Arizona, USA. Note the logarithmic scale on the y-axis.

4.3.4 Results and discussion

We identified specific flow regimes that were highly beneficial to populations of each targeted ecosystem component—cottonwoods, native fishes, and aquatic invertebrates—by maximizing their average population sizes through time (Figure 4.3.2). These designer flow regimes, optimized separately for each ecosystem target, always outperformed the historical natural regime for the intended ecosystem component, suggesting that artificially-imposed flow regimes can in some instances generate greater population sizes than the natural flow regime. This finding is consistent with recent studies targeting native fish abundance in the San Juan River, United States, and fisheries yield in the Mekong River Basin (Chen and Olden 2017, Sabo et al. 2017).

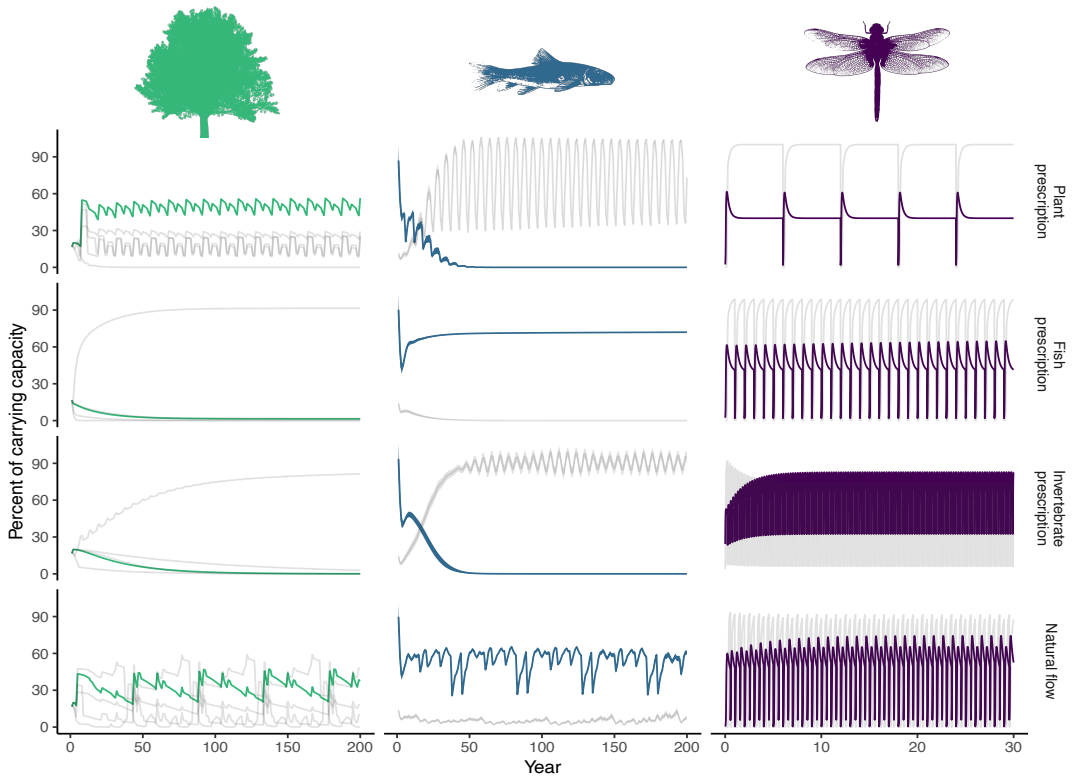

Figure 4.3.2 Results of simulations for target and non-target taxa, both within and among ecosystem components. Target taxa (plants: % cottonwood; fish: % native species; invertebrates: % terrestrially-available taxa) are shown as the colored lines and non-target taxa as grey. For plants, the four grey lines represent the four non-target plant taxa individually. For fish, the single grey line represents the four non-native fish species combined (the band around the line represents 2 standard errors around the mean of 100 iterations). For invertebrates, the grey line represents the non-target taxa (ostracods). Model evaluation discarded the first ten years as a burn-in period.

However, our results highlight that a narrow management focus on a single taxonomic group, as is commonly the case for environmental flow efforts, may come at a cost for other components of the ecosystem (Figure 4.3.3). Each scenario had at least one major losing ecosystem component: cottonwoods declined in the fish-prescribed flows (7% of natural flow %*K*), native fish abundance declined in the vegetation-prescribed flows (5% of natural flow %*K*), and both vegetation (10% of natural flow %*K*) and native fishes (6% of natural flow %*K*) declined in the invertebrate-prescribed flows. Thus, major ecological deficits appear to accompany environmental flow regimes that target a single ecosystem outcome.

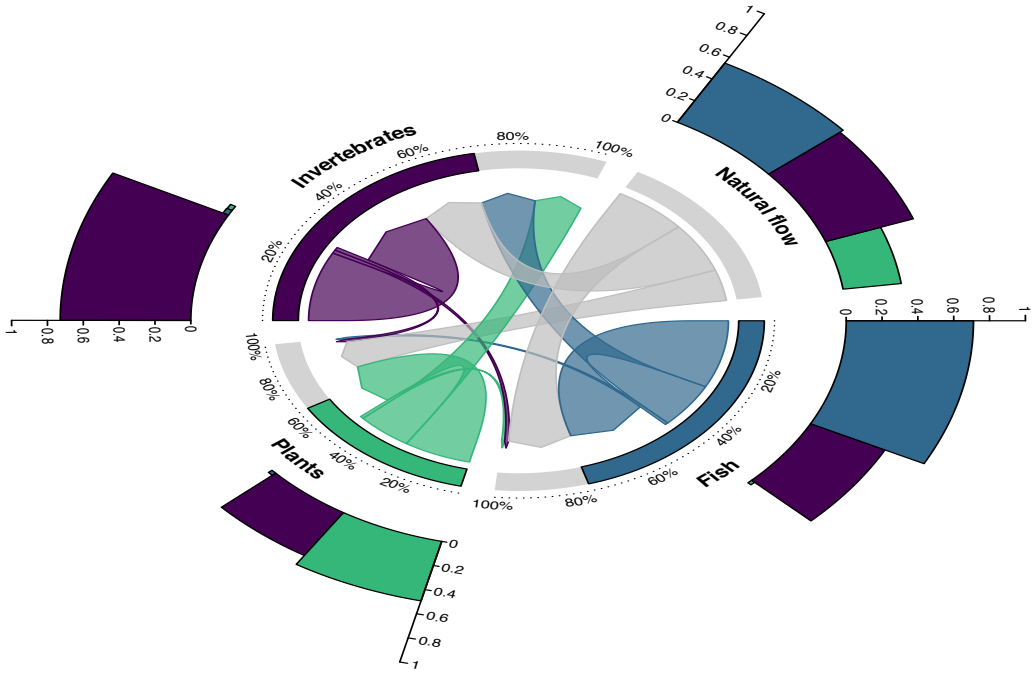

Figure 4.3.3 The ecosystem-wide effects of designer and natural flow regimes. Each of the four figure sectors represents a particular flow regime and/or ecosystem component: the natural flow regime and three designer flow regimes (riparian vegetation, fishes, and invertebrates). The effects of designer flow regimes on each component are shown, both targeted (arrow returns to same figure sector; e.g. fish to fish) and non-targeted (arrow from one sector to another; e.g. fish to plants), as well as the natural flow regime. Arrow widths correspond to the relative effects of a particular flow scenario (source of arrow) on all other components (arrow endpoint; larger equal more positive responses). These values are shown as proportions of maximum in the outermost bars (1 = maximum; e.g. native fish biomass 100% of carrying capacity). For instance, when designing flows to most benefit native fishes, fish respond strongly (large arrow and outer bar) but plants perform poorly (small arrow and bar). The bar tracking the circumference of the center arrows represents the difference between the natural and prescribed flow for the group in that sector (given in percentage). For example, under the natural flow regime, fish achieve 77% of the biomass achieved under the designer flow.

Each designer flow regime had a characteristic temporal frequency, reflecting the varying biology of the three ecosystem components: approximately decadal or half-decadal timescale flow events for riparian vegetation, annual or near-annual for fishes, and intra-annual for invertebrates. Cottonwood thrive under regimes with large recruitment floods approximately every six years followed by growth years (i.e. non-event years), with a drought year included to limit population growth of drought-intolerant competitor species (Lytle et al. 2017). Native fishes prosper under flow regimes with more frequent and reliable (i.e. annual) spawning floods and no drought (Rogosch et al. 2019). Thus, bigger floods are beneficial for vegetation and fishes, but the timescale of response differs. By

contrast, the pulses required for maintaining aquatic invertebrates are insufficiently large to exert a positive benefit for native fishes or cottonwood; this taxonomic group responds best to flow regimes comprising many regular small pulses to maintain shallow riffle habitat. Without regular small pulses (larger pulses may also be incorporated), slower-water specialist invertebrates, many of which do not have a terrestrial lifecycle phase, become dominant (McMullen et al. 2017). In summary, various temporal frequencies are thus fundamental aspects of a flow regime designed for the benefit of an entire ecosystem—a characteristic of the historical natural flow regime that is essential for the vitality of rivers (Fig. [fig:flows]) (Poff et al. 1997, Naiman et al. 2008, Tonkin et al. 2019). Administering such ecosystem-level designer flows may be challenging if single sensitive (threatened, endangered, or red listed) species provide the impetus (legal mandate) for implementation of designer flows.

Contrary to the designer flow regimes, the natural flow regime scenario resulted in species persistence for all ecosystem components, although population sizes were never as large as those achievable under designer flow regimes (vegetation: 66% of designer flow; fishes: 77%; invertebrates: 72%) (Figure 4.3.3). We attribute this to the fact that most natural flow regimes exhibit an array of hydrologic events at multiple temporal frequencies (from intra-annual to inter-decadal), thereby satisfying the ecological needs of diverse biological groups with sometimes conflicting requirements. Most dam operations fail to provide this diverse portfolio of flows that are important for recruitment, migration, spawning and juvenile rearing across a broad array of taxa (Palmer and Ruhi 2019). Organisms have evolved life histories to capitalize on natural cycles of flooding and drought (Lytle and Poff 2004). However, the evolutionary fine-tuning, and potential for rapid evolution, of entire ecosystems to the natural flow regime remains an important topic of inquiry, as does the interaction among the different ecosystem components that we have yet to consider (e.g. invertebrates are a food source for fish, plants provide organic matter for invertebrates). Maintaining these cycles is fundamental to the maintenance of diverse and resilient communities into the future (Tonkin et al. 2018). Flooding also plays a critical role in maintaining functional river geomorphology by creating and maintaining critical off-channel habitats, and mobilizing sediment, woody debris and essential nutrients (Yarnell et al. 2015). Whether maintaining such variability is possible with environmental flows remains to be seen given the rapidly shifting state of river flows worldwide (Poff and Olden 2017, Poff 2018, Tonkin et al. 2019).

Interannual variability in flows that are supported by natural flow regimes enables the persistence of multiple species across diverse taxonomies. Simply put, some flows benefit particular suites of species in certain years to the detriment of others, but gains made during these periods enable their persistence and coexistence with other species,

often through unfavorable periods, over long time-scales (Ruhí et al. 2016, Tonkin et al. 2017). Through time, the full dynamism of river hydrology accommodates higher temporal diversity, emphasizing the importance of taking a functional whole-regime approach to designing and prescribing environmental flows (Yarnell et al. 2015). In long-lived species, such as riparian vegetation, desired outcomes may only manifest in response to flow prescriptions that operate over multiple years or decades. Bottomline: plants and animals are committed to long-term flow regimes; humans similarly need to be committed to long-term flow management.

The mechanisms that produced undesired non-target outcomes were specific to each ecosystem component. For fishes, native species were forecast to become locally extirpated within approximately 50 years due to a complete lack of flood recruitment events reflected in the invertebrate flow prescription, and or a combination of droughts with too-infrequent flood events reflected in the riparian flow prescription, both of which allowed non-native fishes to dominate the community. This finding is supported by empirical research in the American Southwest (Ruhí et al. 2016, Chen and Olden 2017, Rogosch et al. 2019). Cottonwoods collapsed in response to native fish-prescribed flows due to phreatophytic, flood-tolerant willow species dominating at high flood frequencies. In response to a lack of recruitment flood events under the invertebrate flow prescription, cottonwoods were replaced by non-riparian upland species such as sagebrush, representing a loss of riparian trees and shrubs that comprise essential and high quality habitat for diverse terrestrial fauna (Merritt and Bateman 2012). The target invertebrates exhibited much greater fluctuations in population abundance than fish or vegetation. Both the fish and riparian prescriptions did not meet the needs of the aquatic invertebrates due to a lack of regularly-spaced pulses required to maintain open habitat for the two target taxa: a flood-resilient mayfly *Fallceon* spp. (Ephemeroptera: Baetidae), and a flood-resistant dragonfly *Progomphus* spp. (Odonata: Gomphidae) (McMullen et al. 2017). These clear tradeoffs reflect situations where flows are targeted not for an entire community response (e.g. community evenness), but a specific component of each community. Different outcomes may be apparent with alternative ecological targets, but the important implication of this research is that narrowly targeting individual ecological outcomes with specific flows may have broader ecosystem-wide negative impacts.

Different frequencies of response to flows among taxa presents unique challenges when setting out to optimally manage rivers in an environmental flows context. Experimental flood programs have in some cases demonstrated benefits to non-target ecosystem components (e.g. River Spöl, Switzerland: (Robinson et al. 2018); Bill Williams River, USA: (Shafroth et al. 2010)). However, the potential ecosystem-wide impacts of narrowly prescribed flow regimes emphasizes the need to consider entire ecosystems as the ultimate management goal, rather than focus on single physical (e.g. sediment) or

biological (e.g. fish) outcomes (Olden et al. 2014). Considering whole-ecosystem integrity will inevitably require mimicking some functional components of natural hydrologic variability (Yarnell et al. 2015), most notably the presence of multiple frequencies and magnitudes of flow events over extended timescales. However, hydroclimatic nonstationarity, where the envelope of variability in which a river flow regime fluctuates no longer remains fixed (Milly et al. 2008), means returning to the inherently dynamic natural flow regime as a management target may no longer be the most beneficial option (Acreman et al. 2014, Poff 2018, Tonkin et al. 2019). Overcoming the physical limits of dam operations under nonstationarity, therefore, requires creative approaches to flow management (Poff and Olden 2017) and a coherent modeling approach that forecasts the effects of management actions on multiple ecosystem components simultaneously.

The unprecedented magnitude at which river flows are being altered across the developing world, combined with the already large proportion of dammed rivers in the developed world, puts into question the long-term sustainability of freshwater ecosystems (Poff and Matthews 2013, Grill et al. 2019). Environmental flow regimes targeting single ecological outcomes may help to alleviate some of these detrimental effects, but we urge caution in their application due to the potential of unintended collateral impacts on other components of the ecosystem. How can entire ecosystems be better considered in modern day flow management strategies? We assert that designing flows for the benefit of entire ecosystems requires long-term perspectives that embrace hydrologic dynamism involving critical flow events that occur at multiple temporal frequencies. While returning to the historical natural flow regime is an increasingly distant option in highly managed rivers in a nonstationary world (Tonkin et al. 2019), environmental flows must remain founded on the principles of the natural flow regime paradigm.

4.3.5 Acknowledgements

Funding was provided in part by the US Department of Defense (SERDP RC-2511) and the US Department of Agriculture Forest Service. JDT is supported by a Rutherford Discovery Fellowship administered by the Royal Society Te Apārangi (RDF-18-UOC-007).

4.3.6 References

Acreman, M., A. H. Arthington, M. J. Colloff, C. Couch, N. D. Crossman, F. Dyer, I. Overton, C. A. Pollino, M. J. Stewardson, and W. Young. 2014. Environmental flows for natural, hybrid, and novel riverine ecosystems in a changing world. Frontiers in Ecology and the Environment 12:466–473.

Anderson, K. E., A. J. Paul, E. McCauley, L. J. Jackson, J. R. Post, and R. M. Nisbet. 2006. Instream flow needs in streams and rivers: The importance of understanding ecological dynamics. Frontiers in Ecology and the Environment 4:309–318.

Auerbach, D. A., D. B. Deisenroth, R. R. McShane, K. E. McCluney, and N. L. Poff. 2014. Beyond the concrete: Accounting for ecosystem services from free-flowing rivers. Ecosystem Services 10:1–5.

Baxter, C. V., K. D. Fausch, and W. Carl Saunders. 2005. Tangled webs: Reciprocal flows of invertebrate prey link streams and riparian zones. Freshwater Biology 50:201–220.

Bunn, S. E., and A. H. Arthington. 2002. Basic principles and ecological consequences of altered flow regimes for aquatic biodiversity. Environmental Management 30:492–507.

Caswell, H. 2001. Matrix Population Models: Construction, Analysis, and Interpretation. Page 710. Sinauer Associates, Inc., Sunderland, MA, USA.

Chen, W., and J. D. Olden. 2017. Designing flows to resolve human and environmental water needs in a dam-regulated river. Nature Communications 8:2158.

Cooper, D. J., D. M. Merritt, D. C. Andersen, and R. A. Chimner. 1999. Factors controlling the establishment of fremont cottonwood seedlings on the upper Green River, USA. Regulated Rivers: Research & Management 15:419–440.

Grill, G., B. Lehner, M. Thieme, B. Geenen, D. Tickner, F. Antonelli, S. Babu, P. Borrelli, L. Cheng, H. Crochetiere, H. E. Macedo, R. Filgueiras, M. Goichot, J. Higgins, Z. Hogan, B. Lip, M. E. McClain, J. Meng, M. Mulligan, C. Nilsson, J. D. Olden, J. J. Opperman, P. Petry, C. R. Liermann, L. Sáenz, S. Salinas-Rodríguez, P. Schelle, R. J. P. Schmitt, J. Snider, F. Tan, K. Tockner, P. H. Valdujo, A. van Soesbergen, and C. Zarfl. 2019. Mapping the world's free-flowing rivers. Nature 569:215–221.

Horne, A. C., R. Nathan, N. L. Poff, N. R. Bond, J. A. Webb, J. Wang, and A. John. 2019. Modeling flow-ecology responses in the anthropocene: Challenges for sustainable riverine management. BioScience nil:nil.

Lytle, D. A., and N. Poff. 2004. Adaptation to natural flow regimes. Trends in Ecology & Evolution 19:94–100.

Lytle, D., D. Merritt, J. Tonkin, J. Olden, and L. Reynolds. 2017. Linking river flow regimes to riparian plant guilds: A community-wide modeling approach. Ecological Applications 27:1338–1350.

Mahoney, J. M., and S. B. Rood. 1998. Streamflow requirements for cottonwood seedling recruitment – an integrative model. Wetlands 18:634–645.

McMullen, L., P. De Leenheer, J. Tonkin, and D. Lytle. 2017. High mortality and enhanced recovery: Modelling the countervailing effects of disturbance on population dynamics. Ecology Letters 20:1566–1575.

Merritt, D. M., and H. L. Bateman. 2012. Linking stream flow and groundwater to avian habitat in a desert riparian system. Ecological Applications 22:1973–1988.

Merritt, D. M., and N. L. R. Poff. 2010. Shifting dominance of riparian *populus* and *tamarix* along gradients of flow alteration in western North American rivers. Ecological Applications 20:135–152.

Milly, P. C. D., J. Betancourt, M. Falkenmark, R. M. Hirsch, Z. W. Kundzewicz, D. P. Lettenmaier, and R. J. Stouffer. 2008. Stationarity is dead: Whither water management? Science 319:573–574.

Naiman, R. J., J. J. Latterell, N. E. Pettit, and J. D. Olden. 2008. Flow variability and the biophysical vitality of river systems. Comptes Rendus Geoscience 340:629–643.

Olden, J. D., C. P. Konrad, T. S. Melis, M. J. Kennard, M. C. Freeman, M. C. Mims, E. N. Bray, K. B. Gido, N. P. Hemphill, D. A. Lytle, L. E. McMullen, M. Pyron, C. T. Robinson, J. C. Schmidt, and J. G. Williams. 2014. Are large-scale flow experiments informing the science and management of freshwater ecosystems? Frontiers in Ecology and the Environment 12:176–185.

Olden, J. D., N. L. Poff, and K. R. Bestgen. 2006. Life-history strategies predict fish invasions and extirpations in the Colorado River Basin. Ecological Monographs 76:25–40.

Palmer, M., and A. Ruhi. 2019. Linkages between flow regime, biota, and ecosystem processes: Implications for river restoration. Science 365:eaaw2087.

Poff, N. L. 2018. Beyond the natural flow regime? Broadening the hydro-ecological foundation to meet environmental flows challenges in a non-stationary world. Freshwater Biology 63:1011–1021.

Poff, N. L., J. D. Allan, M. B. Bain, J. R. Karr, K. L. Prestegaard, B. D. Richter, R. E. Sparks, and J. C. Stromberg. 1997. The natural flow regime. BioScience 47:769–784.

Poff, N. L., and J. H. Matthews. 2013. Environmental flows in the anthropocence: Past progress and future prospects. Current Opinion in Environmental Sustainability 5:667–675.

Poff, N. L., and J. D. Olden. 2017. Can dams be designed for sustainability? Science 358:1252–1253.

R Core Team. 2017. R: A language and environment for statistical computing. R Foundation for Statistical Computing, Vienna, Austria.

Robinson, C. T., A. R. Siebers, and J. Ortlepp. 2018. Long-term ecological responses of the River Spöl to experimental floods. Freshwater Science 37:433–447.

Rogosch, J., J. Tonkin, D. Lytle, D. Merritt, L. Reynolds, and J. Olden. 2019. Increasing drought favors nonnative fishes in a dryland river: Evidence from a multispecies demographic model. Ecosphere 10:e02681.

Ruhí, A., J. D. Olden, and J. L. Sabo. 2016. Declining streamflow induces collapse and replacement of native fish in the american southwest. Frontiers in Ecology and the Environment 14:465–472.

Sabo, J. L., A. Ruhi, G. W. Holtgrieve, V. Elliott, M. E. Arias, P. B. Ngor, T. A. Räsänen, and S. Nam. 2017. Designing river flows to improve food security futures in the Lower Mekong Basin. Science 358:eaao1053.

Shafroth, P. B., A. C. Wilcox, D. A. Lytle, J. T. Hickey, D. C. Andersen, V. B. Beauchamp, A. Hautzinger, L. E. McMullen, and A. Warner. 2010. Ecosystem effects of environmental flows: Modelling and experimental floods in a dryland river. Freshwater Biology 55:68–85.

Tonkin, J., M. Bogan, N. Bonada, B. Rios-Touma, and D. Lytle. 2017. Seasonality and predictability shape temporal species diversity. Ecology 98:1201–1216.

Tonkin, J., D. Merritt, J. Olden, L. Reynolds, and D. Lytle. 2018. Flow regime alteration degrades ecological networks in riparian ecosystems. Nature Ecology and Evolution 2:86–93.

Tonkin, J., N. Poff, N. Bond, A. Horne, D. Merritt, L. Reynolds, J. Olden, A. Ruhi, and D. Lytle. 2019. Prepare river ecosystems for an uncertain future. Nature 570:301–303.

Yarnell, S. M., G. E. Petts, J. C. Schmidt, A. A. Whipple, E. E. Beller, C. N. Dahm, P. Goodwin, and J. H. Viers. 2015. Functional flows in modified riverscapes: Hydrographs, habitats and opportunities. BioScience 65:963–972.

5 Task 5: Technology transfer

5.1 Web tools

Prepared as separate document, “Web tools for riparian and aquatic population monitoring, RC-2511”.

5.2 Guild occurrence maps

In riverine systems, the relationships of plants to water availability and fluvial disturbance are governed by evolutionary traits imparting varying levels of resistance and resilience to plant species. Thus, grouping species based on similarities and differences in functional traits, by identifying plant “functional guilds”, is a valuable way to model riparian plant distributions. By moving beyond the taxonomic level, functional guilds of plants are especially helpful for forecasting how plant distributions and communities will change and shift under various environmental conditions and at different spatial scales.

To understand riparian plant distributions across a floodplain, we used a functional guild approach to plant distribution modeling. We identified plant traits related to moisture acquisition, disturbance tolerance, and growth strategies, measured these traits in the field for 165 species at study sites in California: The San Antonio River, Fort Hunter Ligget (Figure 5.2.1), and the Santa Margarita River, Camp Pendleton, California. We then grouped species into guilds with similar trait values, using ordination and cluster analysis (Figure 5.2.2, Table 5.2.1).

We constructed a reach-scale 2-dimensional hydraulic model of the San Antonio River (Figure 5.2.3). We routed a range of 75 incremented streamflows from the lowest baseflow (0.31 cubic meters per seconc (cms)), to the 500 year flood (1011 cms) through the 2-D hydraulic model to map inundating discharges across the floodplain. We then extracted flow duration from long-term streamflow records and mapped flow duration across the floodplain. We then modeled riparian species distribution across the floodplain using flow duration on the San Antonio River, to predict guild distribution probabilities using logistic regression models (Figure 5.2.4). The resulting models predict short-term guild probability in 2-dimensional space, based on current floodplain topography and current streamflow hydrology (Figure 5.2.5 – 5.2.9).

San Antonio River

Figure 5.2.1 The location of the San Antonio River in Central Coastal California.

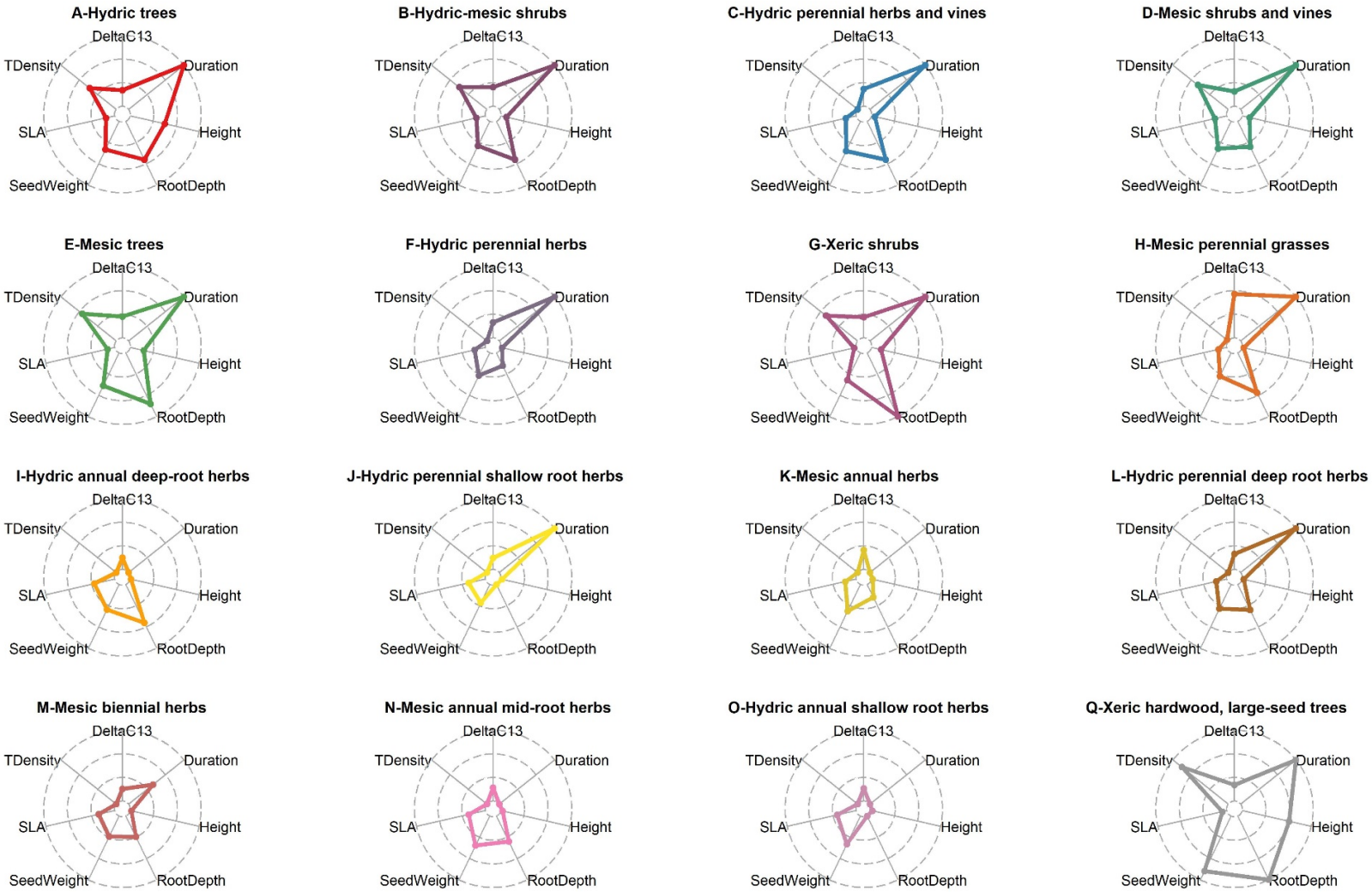

Figure 5.2.2 Mean trait values of seven functional traits for each of 16 riparian plant streamflow-response guilds for coastal California Rivers.

Table 5.2.1 Description of riparian plant – streamflow response guilds from cluster analyses on plant stream-flow response trait values.

Guild Code	Name	Mediod/centroid species	Hydro-Disturburbance-Competitive descriptive name
A	A-Hydric trees	*Salix lucida*	Mesic-Prone-Dominant
B	B-Hydric-mesic shrubs	*Amorpha fruiticosa*	Mesic-Prone-Mid
C	C-Hydric perennial herbs and vines	*Equisetum hyemale*	Hydric-Inter-Inferior
D	D-Mesic shrubs and vines	*Symphoricarpos mollis*	Mesic-Inter-Mid
E	E-Mesic trees	*Celtis reticulata*	Xeric-Inter-Mid
F	F-Hydric perennial herbs	*Epilobium spp.*	Hydric-Prone-Inferior
G	G-Xeric shrubs	*Tamarix ramossissima*	Xeric-Prone-Mid
H	H-Mesic perennial grasses	*Apocynum cannibatum*	Mesic-Prone-Inferior
I	I-Hydric annual deep-root herbs	*Melilotus indicus*	Hydric-Tolerant-Inferior
J	J-Hydric perennial shallow root herbs	*Stachys ajugoides*	Hydric-Prone-Inferior
K	K-Mesic annual herbs	*Erigeron spp.*	Hydric-Prone-Inferior
L	L-Hydric perennial deep root herbs	*Carex nudata*	Hydric-Prone-Inferior
M	M-Mesic biennial herbs	*Plantago lanceolata*	Hydric-Prone-Inferior
N	N-Mesic annual mid-root herbs	*Datura spp.*	Hydric-Tolerant-Inferior
O	O-Hydric annual shallow root herbs	*Persicaria lapathafolia*	Hydric-Tolerant-Inferior
Q	Q-Xeric hardwood, large-seed trees	*Quercus engelmannii*	Xeric-Tolerant-Dominant

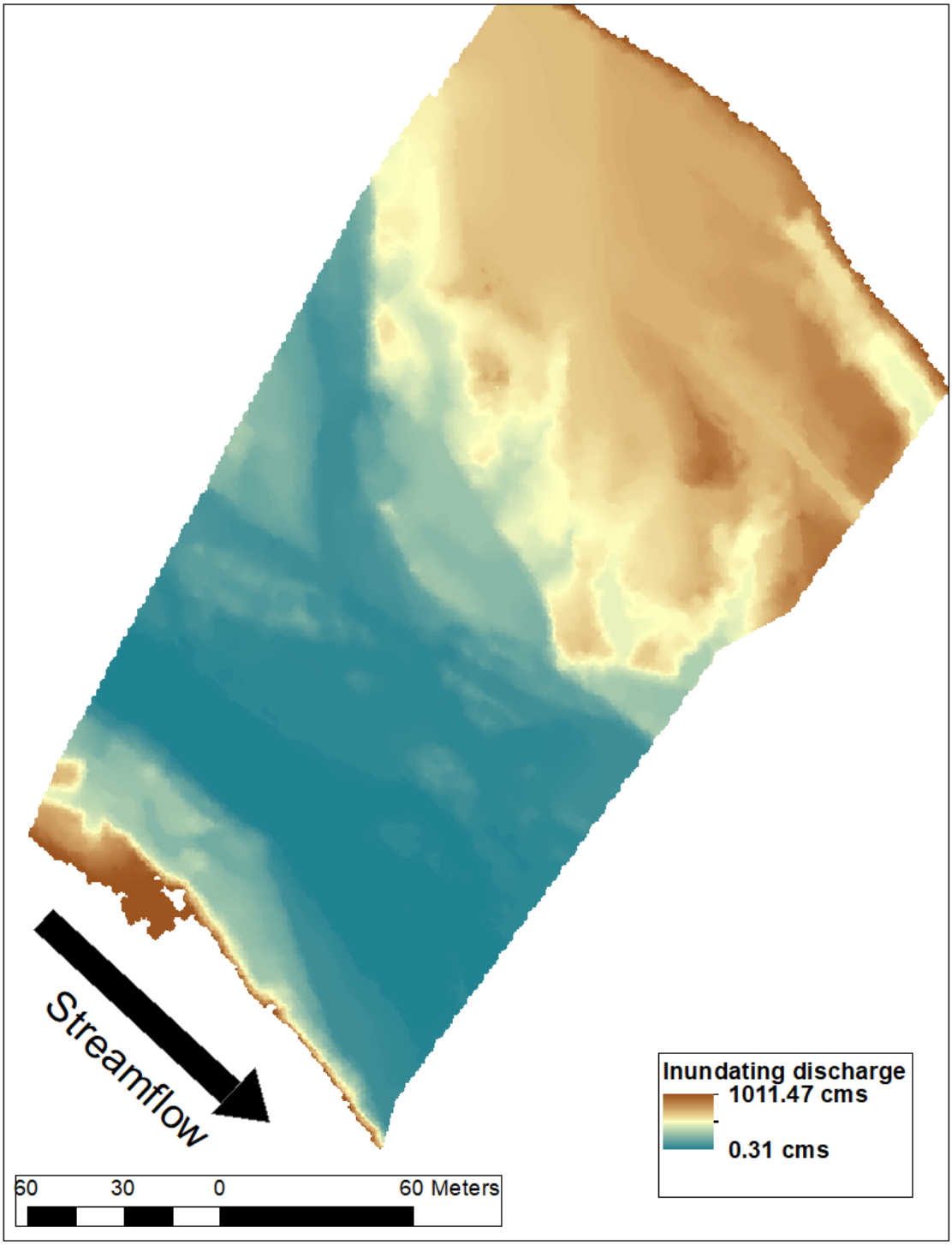

Figure 5.2.3 Inundation map from 2-dimensional hydraulic modeling of the San Antonio River, California.

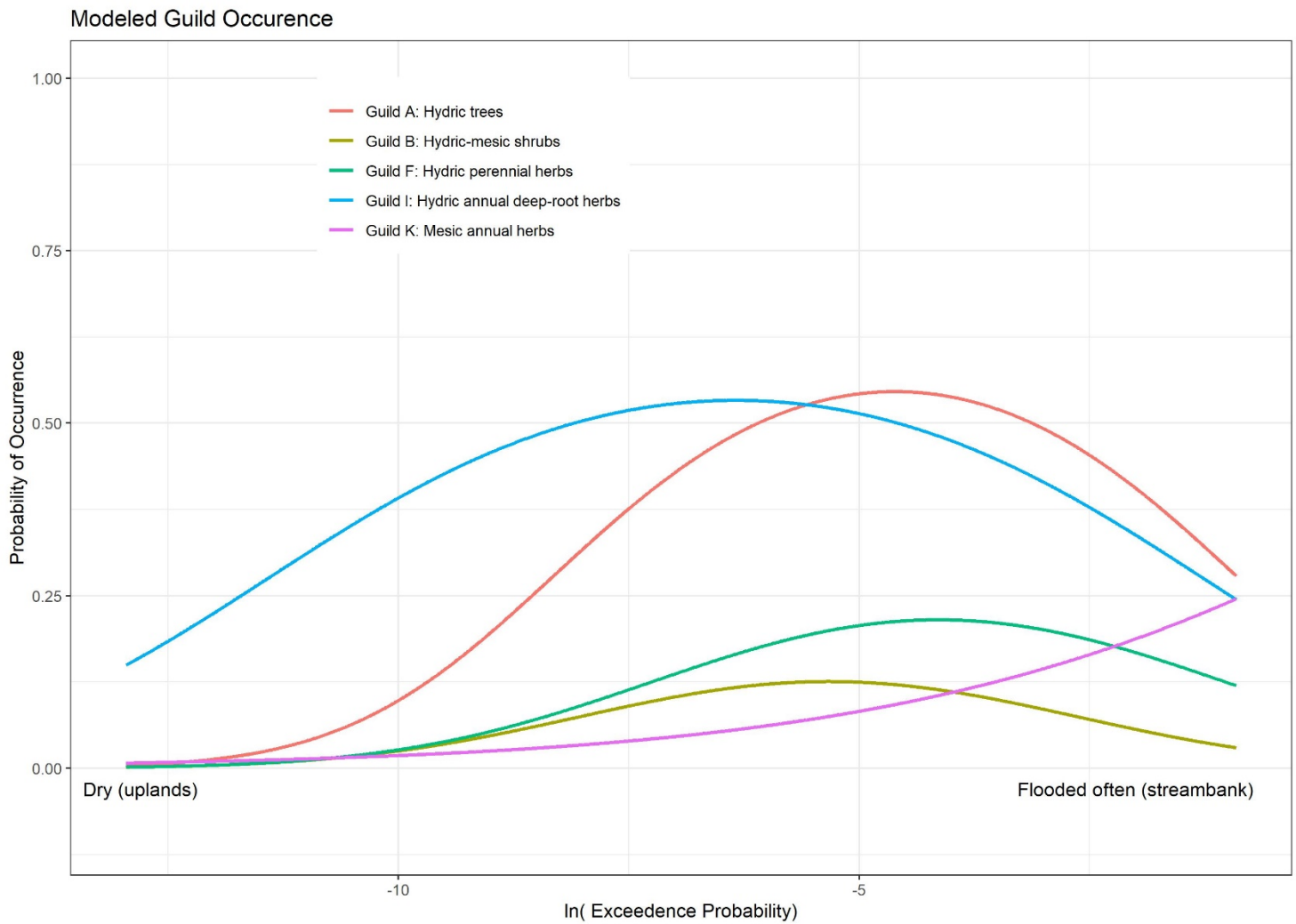

Figure 5.2.4 Probability of occurrence for five example guilds on the San Antonio River, California, across a gradient of flow exceedance probability (x-axis) from upland dry areas (left side) to wetter, frequently flooded areas by the river bank (right side).

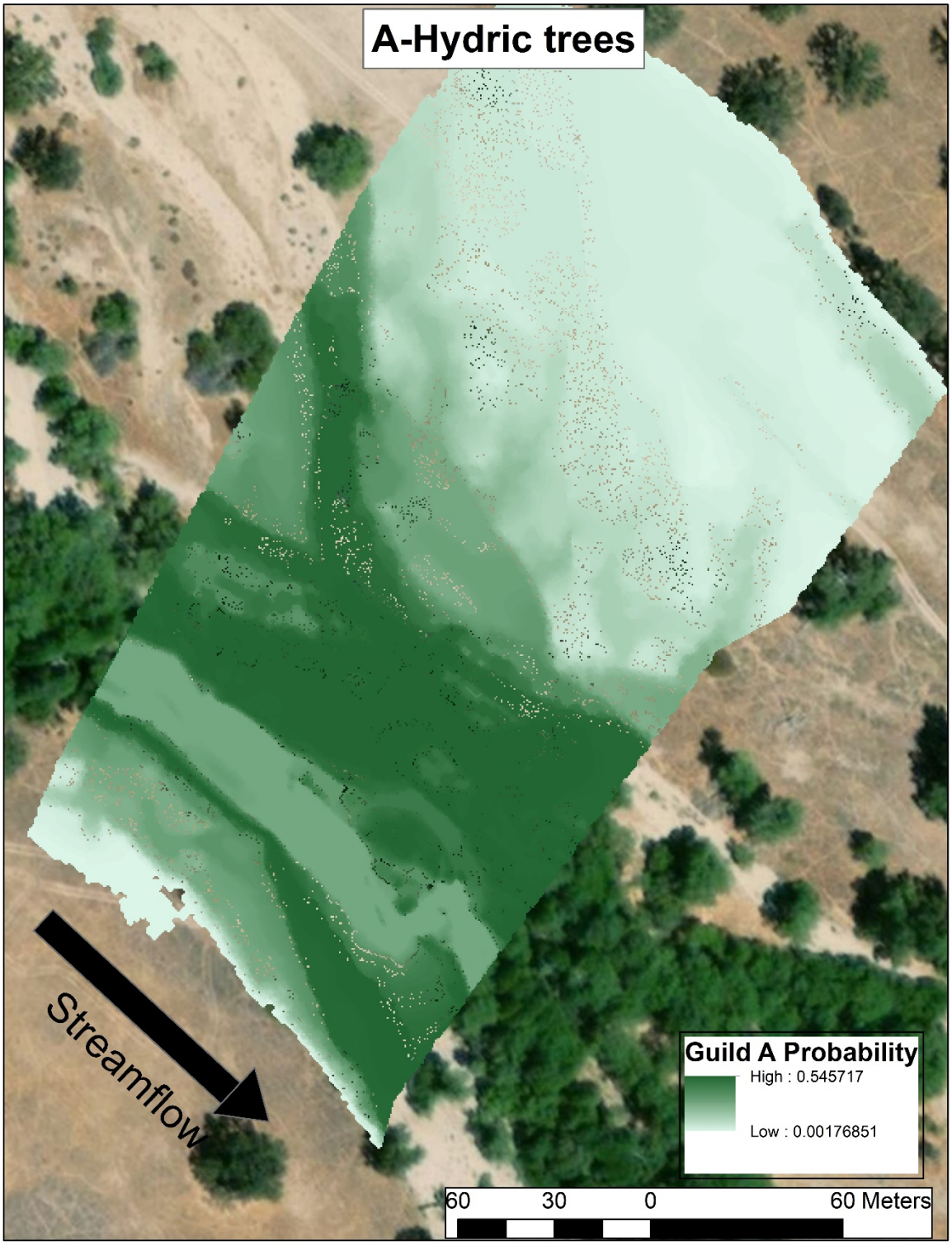

Figure 5.2.5 Hydric trees - Guild distribution models projected on to the floodplain of the San Antonio River, Fort Hunter Ligget, California

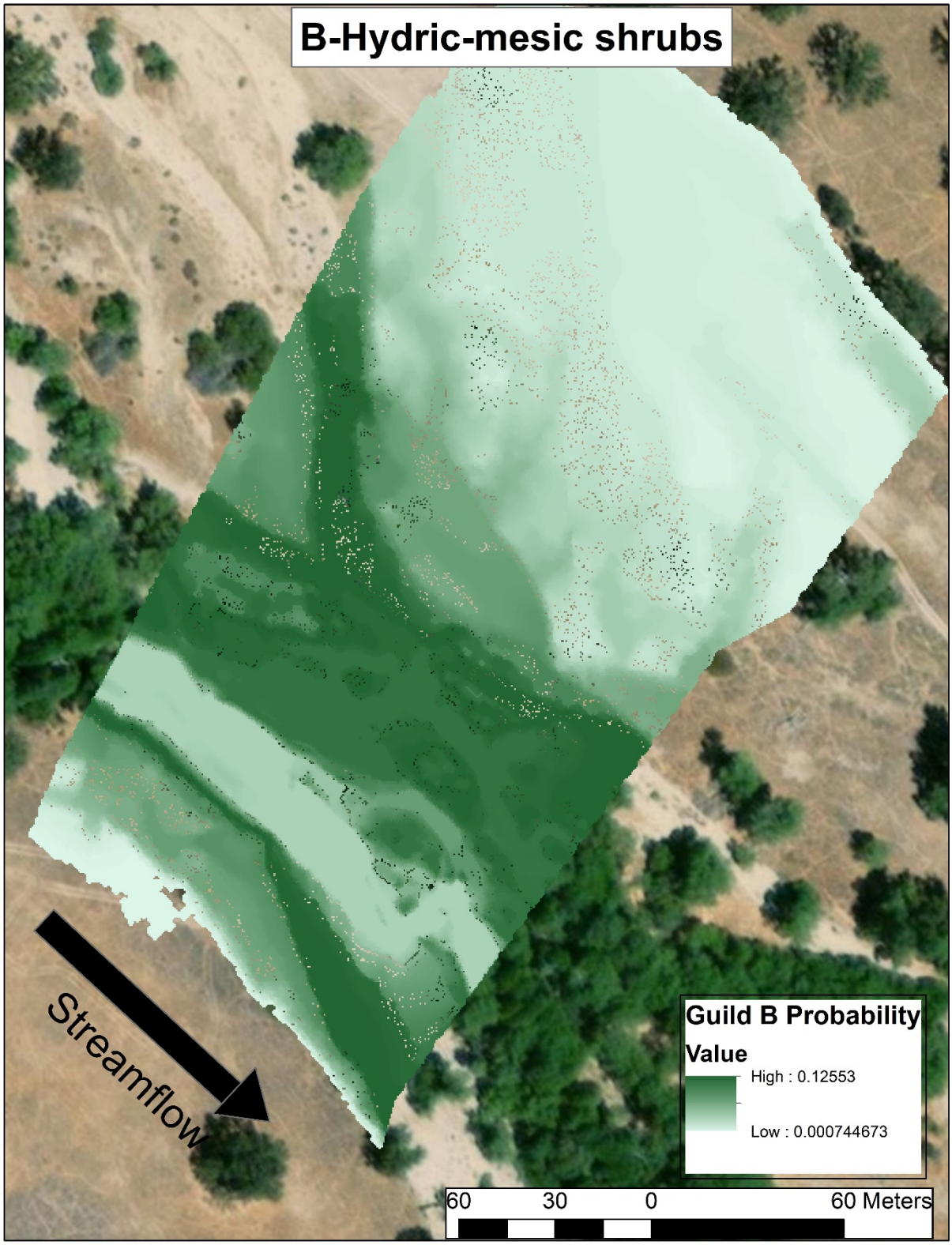

Figure 5.2.6 Hydric mesic shrubs - Guild distribution models projected on to the floodplain of the San Antonio River, Fort Hunter Ligget, California

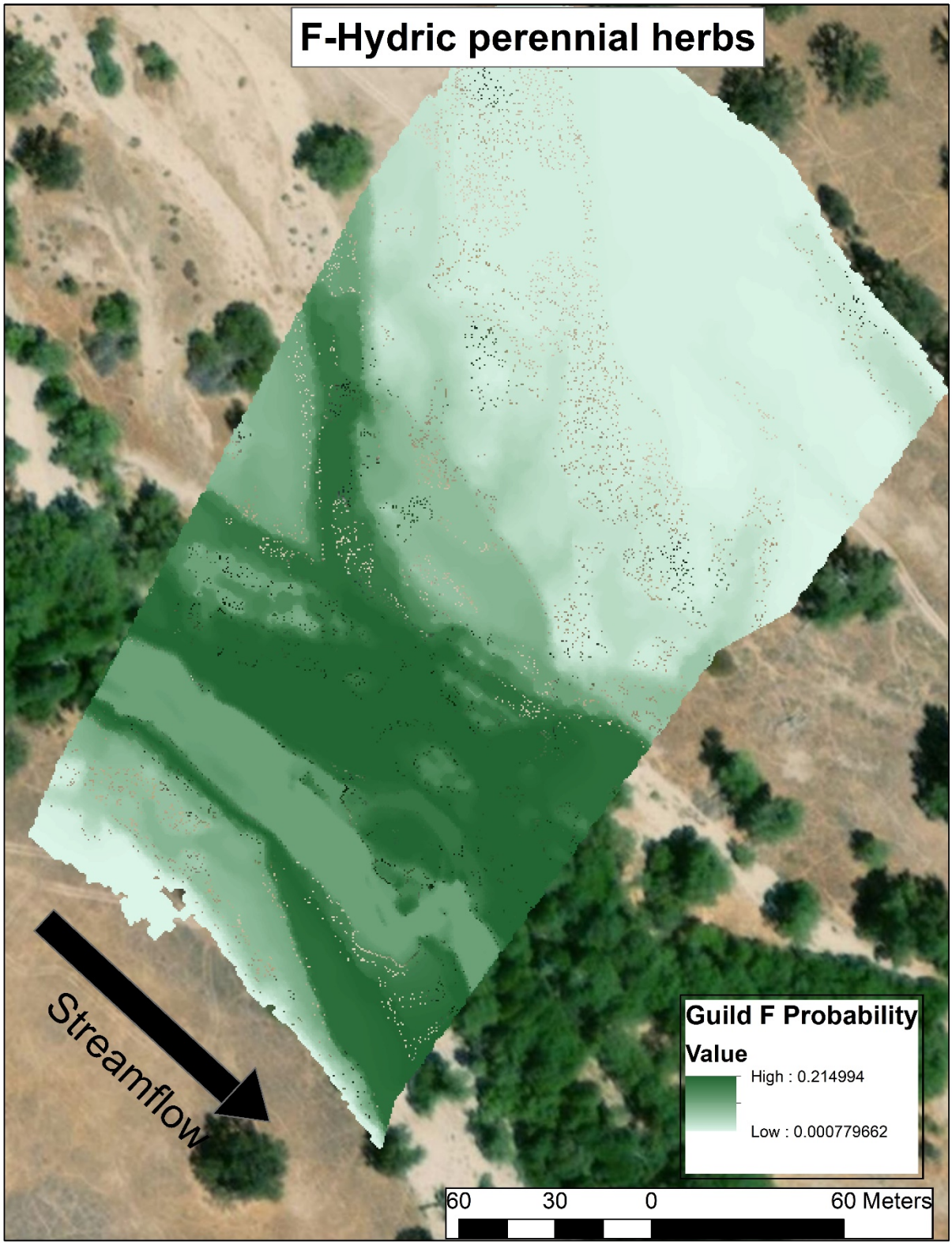

Figure 5.2.7 Hydric perennial herbs - Guild distribution models projected on to the floodplain of the San Antonio River, Fort Hunter Ligget, California

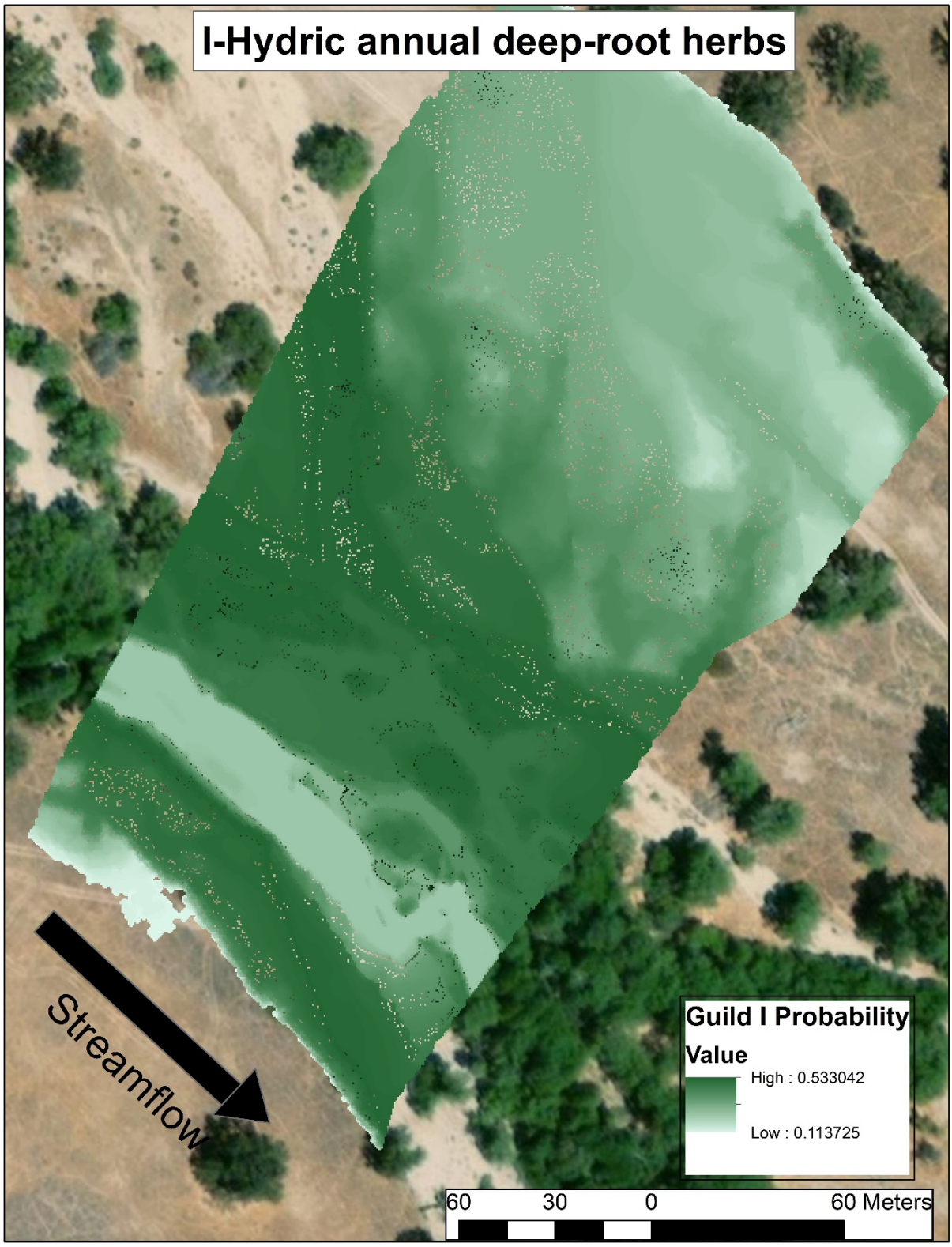

Figure 5.2.8 Hydric annual deep-root herbs - Guild distribution models projected on to the floodplain of the San Antonio River, Fort Hunter Ligget, California

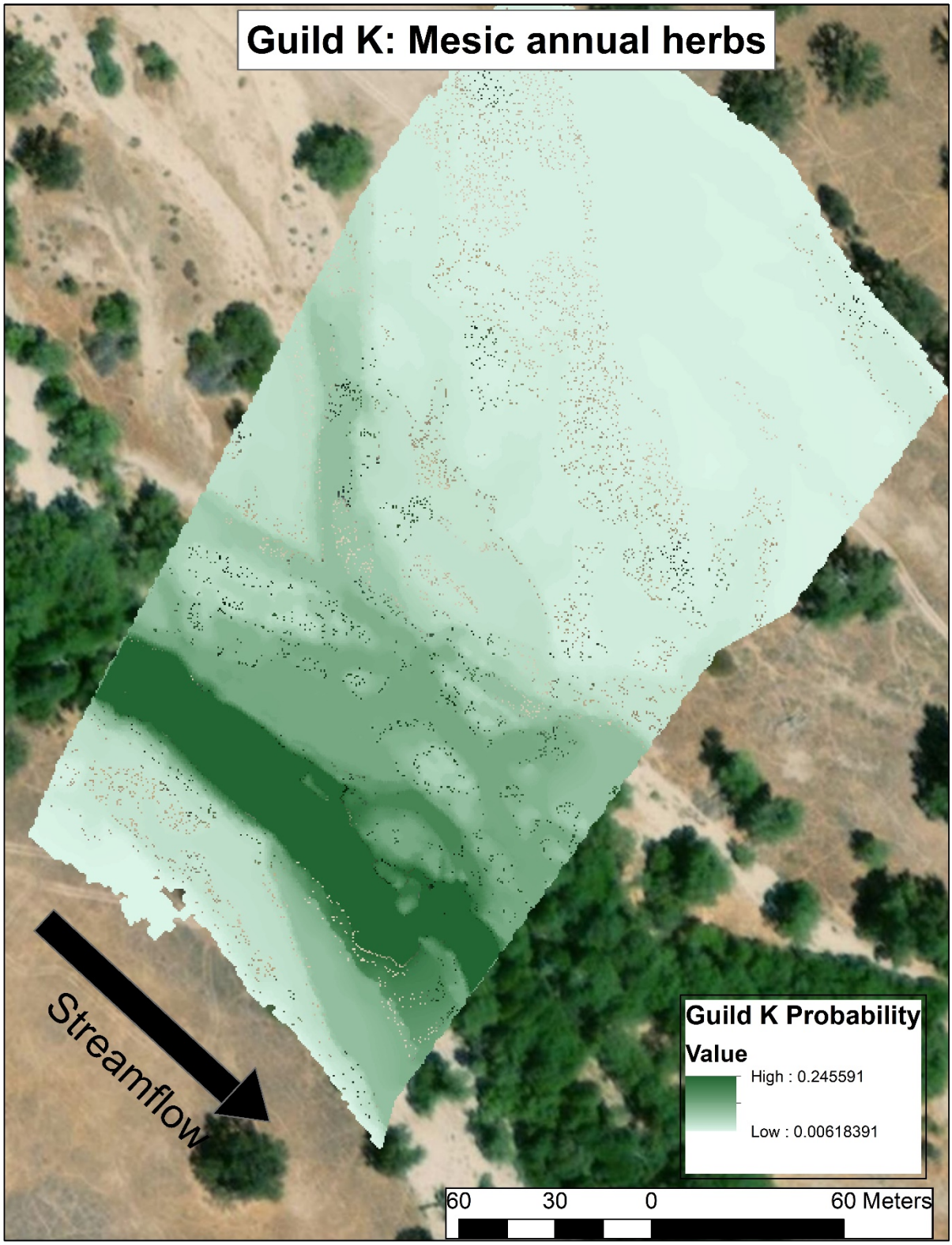

Figure 5.2.9 Mesic annual herbs - Guild distribution models projected on to the floodplain of the San Antonio River, Fort Hunter Ligget, California.

5.3 Professional summary: Managing rivers for resilience

From a Comment in *Nature*, 18 June 2019 (Tonkin et al. 2019).

5.3.1 Introduction

In January 2019, millions of fish died in Australia's Murray-Darling Basin. The region was experiencing some of the driest and hottest weather on record, causing severe water shortages for people living there as well. Such harsh conditions will become more common as the world warms. Iconic and valuable species like the Murray cod (*Maccullochella peelii peelii*) --- Australia's largest freshwater fish --- could vanish.

Rivers are struggling around the world. In Germany and Switzerland, a heatwave in 2018 killed thousands of fish (https://www.bbc.com/news/world-europe-45102093) and blocked shipping on the Rhine (https://www.nytimes.com/2018/11/04/world/europe/rhine-drought-water-level.html). The recent multi-year drought in California[1] has restricted water supplies and devasted trees, fish and other aquatic life. Extended dry spells are destroying many more riparian forests and wetlands across the American Southwest.
What should river managers do? They cannot look to tools of old. Traditional river management aims to restore ecosystems to states that they no longer hold – before they were degraded by human development and climate change. And models are often based on past correlations that do poorly looking into the future for how species may respond to unprecedented changes. A different approach is called for.

Rivers must be managed adaptively ---- to enhance resilience and limit risk to maintain water supplies and avoid devastating population crashes. Researchers must develop forecasting tools that project how key species, life stages and ecosystems respond to environmental changes. This will mean moving beyond simply monitoring the state of ecosystems to establishing the biological mechanisms that underpin their survival.

5.3.2 Model process

Today, river managers track properties like species diversity and population abundance and compare them to historical averages. If they spot troubling declines in populations they can intervene, by altering the amount of water released from dams for instance. Yet, by the time such trends are detected, they can be impossible to arrest.

Moreover, ecosystems are not stationary. When conditions change, so do they. For example, in the American west, native cottonwoods (*Populus* spp.) are valuable long-lived trees that anchor river banks and offer habitats to many species. They are finely tuned to seasonal flood patterns, releasing their seeds in early summer when river flows

peak. The seeds take root in moist ground after the floods recede[2]. But if that flood is delayed even by a few days, the seeds fall on dry ground and die. Drought-tolerant species, such as salt cedar (*Tamarix ramosissima*), which disperse seed over a longer period of time, move in. Replacing native trees with non-native shrubs dramatically alters habitat conditions for many native flora and fauna.

Mechanistic or 'process-based' models can follow and predict these changes. They consider how rates of survival, reproduction and dispersal vary with environmental conditions. For example, modelling the impacts of changes in flood timing on mortality and population growth of aquatic invertebrates has shown how the numbers of dragonflies (*Progomphus borealis*) and mayflies (*Fallceon quilleri*) in a dryland river vary with different patterns of dam releases[3].

Process-based models can be tailored to life stages of populations, whole communities of species and sequences of events[4]. They can identify tipping points and bottlenecks. For example, models have identified the early juvenile stage of coho salmon (*Oncorhynchus kisutch*) in the northwestern United States is particularly sensitive to summer droughts. The salmon spawn in streams flowing into coastal rivers and may spend a couple of years in fresh waters before moving to the sea. Juveniles may not survive or find it hard to travel downstream when river levels are low[5].

By bringing together whole communities, models can consider trajectories of change not only for their constituent species but also for how these species interact under different hydrologic conditions[6]. For example, a drier future with fewer and smaller floods has been projected to reorganise and simplify the network of interactions between riparian plant species in dryland river systems of the southwest US[6]. Such projected changes could reduce the buffering capacity of communities to future climate change and their ability to resist invasions by alien species.

Armed with this information, managers are able to intervene before a problem arises. For example, in wet years, conservationists in the Pacific Northwest can find and support habitats crucial to rearing juvenile salmon. They can manage water flows in dry years to enable them to migrate. Similarly, in Australia, releasing more water from dams in Autumn could limit the time rivers experience no flow to protect the eggs of Murray cod[7]. Or in dryland rivers of the US Southwest, flow releases from reservoirs could be prescribed to protect important species.

But rivers also need to be managed for people. Allocating scarce water resources is always contentious. Policymakers, water resource engineers, conservation practitioners and ecologists need to work together to decide how much water should be diverted to

people, agriculture and industry, and how much is needed to protect ecosystems during drought, for example. Modelling the impacts of different interventions would help planners to assess the ecological risks more fully.

Some river basins are beginning to be managed adaptively --- different management practices are tried, learned from and updated as needed. For example, in Australia, both state (e.g. https://www.water.vic.gov.au/planning-and-entitlements/victorias-entitlement-framework/the-water-act) and federal (https://www.mdba.gov.au/basin-plan-roll-out/basin-plan/developing-basin-plan) agencies periodically reassess and rebalance how water resources are allocated, to allow for emerging climate trends, new information, and new assessment tools to be considered. Similarly, the California Bay-Delta Update Plan proposes to revisit relationships between target species, water flows and water quality every 5 years, adjusting flows as necessary (https://www.waterboards.ca.gov/waterrights/water_issues/programs/bay_delta/comp_review.shtml).

But adaptive management may not achieve conservation targets acting alone. Far-term forecasts of responses to interventions will help foresee outcomes that may not be obvious when examining responses to one-off events. By narrowing the number of justifiable interventions, modelling can save time, money and disruption. Coupling flexible and adaptive approaches to process-based models would also help stakeholders and managers choose which features of ecosystems to maintain, or justify costly interventions such as major engineering works, or weigh trade-offs to build resilience under increasing climatic uncertainty[8].

5.3.3 Obstacles to implementation

Process-based models are already used in fisheries and conservation. They have shown conservationists that it is more effective to protect juvenile loggerhead sea turtles from marine bycatch than to protect eggs on the beach, for example[9]. And they help guide the management of wetland habitats in the US for the endangered Everglades snail kite, whose fledglings are susceptible to droughts[10].

But they are rarely used in river management. The main reason is lack of data. Data on the basic biology of species are costly for scientists and state agencies to gather. Measuring fecundity or survivorship, for example, entails monitoring populations in the field over years, and thus requires long-term commitment to funding of data collection. Such data are often reserved for endangered or commercially valuable species.

Simplifying models may help in the interim. Species with similar life histories or characteristics may respond similarly to changing river conditions. Studies of one could

inform models and management in other places. For instance, *Populus deltoidies* (Plains cottonwood) in North America, *Eucalyptus camaldulensis* (river red gum) in Australia, and *Populus euphratica* (Euphrates poplar) in North Africa and Eurasia are all riparian trees that have similar hydrological requirements and drought tolerances, sharing shallow roots, furrowed bark that resists flood scour, and the ability to sprout after being buried by sediment. Analytic methods might also be developed to extrapolate across gaps in datasets.

5.3.4 Next steps

River scientists and managers should take the following 4 steps:

Collect data on mechanisms. We call for a new global focus on gathering natural history data on the responses of riverine biodiversity to changes in river flow. This will take greater observational and experimental effort than standard monitoring programmes but will improve forecasts.

Estimates of fecundity and survivorship at various life stages will require monitoring in the field. Other information, like flood-induced mortality rates, might be gathered through natural and lab-based experiments. Data from different sources should be able to be combined, including species traits, population abundances across life stages, and remote sensing data about ecosystems on wider scales[4].

We urge local, state and federal agencies, as well as researchers, NGOs, and other organisations to make existing data available for synthesis. Facilities for hosting the data already exist, such as the COMPADRE and COMADRE global databases of population models of hundreds of plant and animal species (https://www.compadre-db.org). Organisations such as the Alliance for Freshwater Life, World Wildlife Fund, and Group on Earth Biodiversity Observatory Network should rally global funding bodies to support data collection.

Describe key processes in models. Scientists need to better articulate the relationships between ecosystem attributes and water flow patterns in process-based models. Unlike extrapolation from observed trends, process-based models connect population dynamics to individual flow events, allowing managers to forecast the effects of entirely novel flow regimes such as those produced by climate change. This mechanistic approach isolates critical population bottlenecks or processes that mediate population responses to flow variability in the future, including how well different life-stages of plants reproduce or survive under flood or drought conditions, the flow conditions and timing required for fish to reproduce, or the growth rates of insect populations after different size flood events[3-5,7]. By building up from the component parts of population responses to flow

events, rather than correlating emergent population responses with average flow patterns, more specific information can be relayed to decision makers tasked with managing rivers experiencing rapid change.

Focus management on bottlenecks. Targeted interventions to avoid populations collapsing during extreme flows is likely to be a cornerstone of managing for river resilience. Accordingly, dam managers need to focus on the most vulnerable or responsive life stages, not just population abundance. Sadly, as extreme flow events become more common, scientists and managers will have the opportunity to empirically observe population collapses and thus help calibrate the models.

Support adaptive management with robust predictions. Confidence may influence managers' willingness to deal with varying levels of risk. Model predictions should thus quantify the level of trust that can be placed on them. Scientists must present uncertainties in forecasts clearly. Models should be tested by hindcasting (predicting past or present-day population size, for example), and uncertainty in model inputs should be traced through to the outputs. The knowledge gaps that matter most when trying to improve model accuracy should be identified. The models should be regularly updated, tested and improved as new data arrive.

Freshwater biodiversity is disappearing on our watch (see http://www.livingplanetindex.org). Climate change is amplifying the pressures on river ecosystems already imposed by urbanisation, invasive species, pollution and more. As the biodiversity crisis deepens (see IPBES global assessment report; https://www.ipbes.net), we must transform how we model and manage rivers to safeguard the services they provide to humanity.

5.3.5 References

1. Diffenbaugh, N. S., Swain, D. L. & Touma, D. Anthropogenic warming has increased drought risk in California. *Proceedings of the National Academy of Sciences* ***112***, 3931-3936 (2015).
2. Mahoney, J. M. & Rood, S. B. Streamflow requirements for cottonwood seedling recruitment – an integrative model. *Wetlands* ***18***, 634-645 (1998).
3. McMullen, L. E., De Leenheer, P., Tonkin, J. D. & Lytle D. A. High mortality and enhanced recovery: modelling the countervailing effects of disturbance on population dynamics. *Ecology Letters* ***20***, 1566-1575 (2017).

4. Lytle, D. A., Merritt, D. M., Tonkin, J. D., Olden, J. D. & Reynolds, L. V. Linking river flow regimes to riparian plant guilds: a community-wide modeling approach. *Ecological Applications* ***27***, 1338-1350 (2017).

5. Ohlberger, J., Buehrens, T. W., Brenkman, S. J., Crain, P., Quinn, T. P. & Hilborn, R. Effects of past and projected river discharge variability on freshwater production in an anadromous fish. *Freshwater Biology* ***63***, 331-340 (2018).

6. Tonkin, J. D., Merritt, D. M., Olden, J. D., Reynolds, L. V. & Lytle, D. A. Flow regime alteration degrades ecological networks in riparian ecosystems. *Nature Ecology & Evolution* ***2***, 86-93 (2018).

7. Yen, J. D. L., Bond, N. R., Shenton, W., Spring, D. A. & Mac Nally, R. Identifying effective water-management strategies in variable climates using population dynamics models. *Journal of Applied Ecology* ***50***, 691-701 (2013).

8. Poff, N. L., Brown, C. M., Grantham, T. E., Matthews, J. H., Palmer, M. A., Spence, C. M., Wilby, R. L., Haasnoot, M., Mendoza, G. F., Dominique, K. C. & Baeza, A. Sustainable water management under future uncertainty with eco-engineering decision scaling. *Nature Climate Change* ***6***, 25-34 (2016).

9. Crouse, D. T., Crowder, L. B. & Caswell, H. A stage-based population model for loggerhead sea turtles and implications for conservation. *Ecology* ***68***, 1412-1423 (1987).

10. Beissinger, S. R. Modeling extinction in periodic environments: Everglades water levels and snail kite population viability. *Ecological Applications* ***5***, 618-631 (1995).

6 Task 6: Submit technical reports to SERDP

6.1 Interim report

Completed and accepted 3/23/2018.

6.2 Final report

This document.

6.3 Web tools

Prepared as separate document, “Web tools for riparian and aquatic population monitoring, RC-2511”.